Elucidating the nature of bonding in mechanical pulps

A Dissertation Submitted by

Lauri K. Lehtonen

M.S. 1999, University of Helsinki

This Thesis is in Partial Fulfillment of the Requirements from the
Institute of Paper Science and Technology
for the Degree of Doctor of Philosophy
Atlanta, Georgia

To my wife Sanna,

Mä lykkään purteni laineillen
ja järven poikki sen ohjaan
ja lasken salmia saarien
tuon pienen poukaman pohjaan.

Ja rannalla lahden tyynen sen
on tuoksuva tuomilehto,
koti peippojen, kerttujen keväisten
ja laulujen, tuoksujen kehto.

Mut varjossa lehdon vilppahan sen
on neitonen tummatukka,
mun leppäkerttuni keväinen,
mun lauluni, lempein kukka.

Eino Leino 1897

Abstract

Bond strength is classically characterized into two separate factors; area of the bond and specific bond strength. This separation is especially important in pulps that lack strength properties, and are specifically used for their optical properties, such as mechanical pulps. In this research the applicability of the Ingmansson and Thode method for distinguishing between specific bonded area and specific bond strength in mechanical pulps is studied. It is shown that the rigid, non-collapsable, nature of the mechanical pulp can be overcome by press drying the sheets until they approach their 50% relative humidity moisture content, ultimately producing extended tensile strength to scattering coefficient relationships. Mechanical pulps have been assumed to operate in a domain where fiber failure can be considered insignificant, and the bonded area to tensile strength relationship is linear. In this study it was shown that most commercial pulps operate in a significant fiber failure domain. However, it is shown that pure fines and fines rich mechanical pulp better follow a linear bonded area to tensile strength relationship rather than a non-linear (significant fiber failure) model, suggesting that only the fiber fraction undergoes fiber failure and the finer fractions predominantly bond failure. The Ingmansson and Thode method relies on the use of scattering coefficient as a measure of specific surface area. It is shown that scattering coefficient is an accurate estimate of mechanical pulp specific surface area at a constant wavelength of light, provided that the wavelength used to measure scattering coefficient is above the significant absorption limit. It is shown that the middle and fines fractions bond to a lesser degree in a mixed sheet than they do as a homogeneous pure sheet at a constant pressing level, indicating that the pressing force is predominantly transferred through the fiber fraction. However, the overall deviation from the linear addition model, where the mixture scattering coefficient is dictated by the individual components of the sheet is small (4.8%). It is also shown that the total unbonded specific surface area (S_o) follows a linear addition model, which consequently results in that the relative bonded area (RBA) by definition is intrinsically non-linear as a function of the sheet composition. It is shown that the consolidation mechanisms associated with the press drying at elevated temperatures and wet pressing at room temperature are significantly different. Wet pressing produces a mechanical pulp sheet with higher scattering coefficient at constant density or tensile strength. These are explained with a shift in pore size distribution of fines.

TABLE OF CONTENTS

List of Figures

List of Tables

Introduction

Throughout the 20th century there has been a significant research effort to develop methods to estimate the Relative Bonded Area in chemical pulp fiber based papers. This is due to the belief that stresses in a paper sheet are borne through the bonded areas between fibers, and bonds are solely responsible for the internal cohesion in paper.

Bond strength has been classically characterized into two separate factors; area of the bond and specific bond strength (total bond strength divided by the bonded area) [1]. For practical purposes it is of interest to separate these two factors, since changes in bonded areas not only affect the strength properties of paper but are also reflected in the optical properties of the sheet, whereas changes in the specific bond strength only affect the strength properties of the sheet. Specific bond strength describes the efficiency of the bonded area to produce bonding strength. This parameter is especially important in pulps that lack strength properties, and are specifically used for their optical properties, such as mechanical pulps. Although often left out of the debate over bond strength, mechanical pulps represent a significant market segment that would benefit from an increase in specific bond strength, and where functional methods used with chemical pulps are often ineffective.

Mechanical pulps are extremely heterogeneous in nature, with a particle size distribution that varies from the nanometer scale to several millimeters in length [2]. This heterogeneity is assigned to be the largest contributing factor to the special characteristics of these pulps, where very high scattering properties are obtained simultaneously with almost adequate strength properties [3-6]. This indicates that the total unbonded specific surface area and the total specific bonded area of the sheet are high. If we consider the mechanical pulping process in terms of fiber development, most of the energy is spent on creating specific surface area (Figure 1). Subsequently, during web formation part of this enormous amount of surface area, bonds and enhances strength properties of these pulps. However, at the same time a significant part of surface area remains unbonded, leaving the sheet with a high effective specific surface area, that contributes to the scattering properties of the sheet [7]. There are numerous indications that wood species, process intensity, and process configuration influence the development of bonded and unbonded areas of mechanical pulps [7-17].

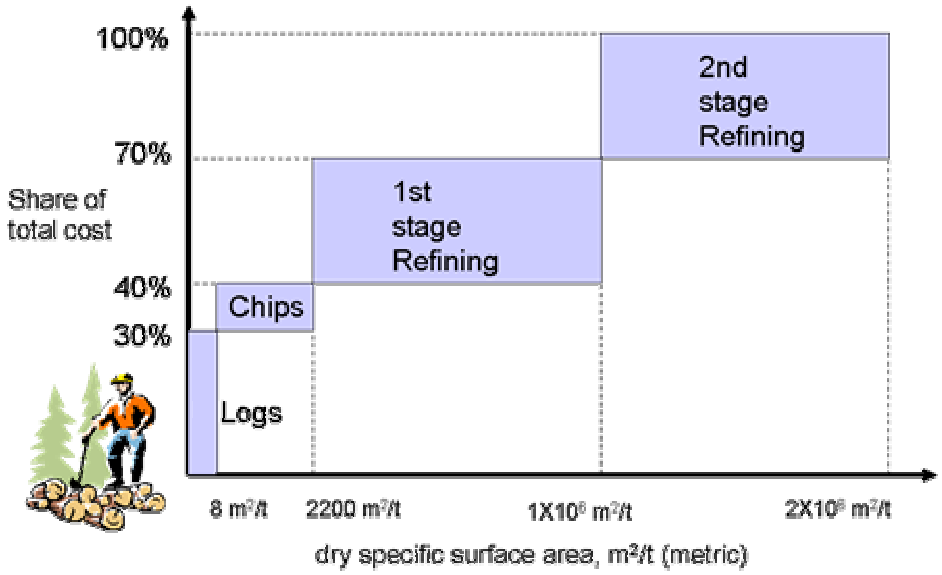

Figure 1. Estimated dry specific surface area (collapsed fiber wall) creation in mechanical pulping. Share of cost data from [18], specific surface area estimation partially based on [19, 20]

However, due to the lack of methods to quantify the amount of bonded area and total unbonded area in mechanical pulps, the above mentioned research areas have rarely been approached.

Literature review

Mechanical pulps and their papermaking potential

Mechanical pulps are used in papermaking for their favorable cost to quality ratio. The specific positive quality factors are high opacity, surface smoothness, and good sheet formation. The low cost is mainly due to the high yield (95-98%) from wood to pulp. However, there are two main limiting factors why mechanical pulps cannot be used as the primary raw material for all paper grades. The first one is related to the light absorption properties, i.e. lower brightness, and photo yellowing of these pulps, which can be partially overcome by sufficient coating of the base sheet. The second and most important factor is the limited strength of mechanical pulps. The low strength ultimately restricts the use of these pulps in paper grades. Either a sufficient amount of reinforcement fiber or higher basis weight is needed to obtain the necessary sheet strength, to ensure the runnability of the web in the paper machine, coating operations, and eventually in printing machine [21].

The favorable papermaking properties of mechanical pulps can be assigned to the heterogeneous nature of the pulp. Due to the character of the pulping process various sizes and shapes of particles are created, which creates a sheet with a smooth surface, and a porous structure [22, 23]. The limited strength properties are often related to the poor bonding of the sheet, short fiber length, limited fiber strength due to the cell wall damage induced during processing, and ultimately the high lignin content of the mechanical pulp fibers [7, 19, 21, 24-27]. The poor bonding potential should be emphasized, since chemical pulp with the same wet specific surface area would bond so well that the sheet would have extremely low opacity and porosity, but tremendously high tensile strength.

The papermaking potential of mechanical pulps for various grades is determined by several factors, related to the properties of pulp particles and their interactions during sheet consolidation [2, 7, 28, 29]. These particle properties and interaction characteristics vary significantly depending on the process type, wood raw material and the amount of energy applied in the process [3-6, 8-10, 12, 13, 21, 30-38].

Mechanical pulp development in refining

The variation in the quality of mechanical pulps is due to a triangle of interrelationships, wherein the pulp quality is dependent on the process type, raw material characteristics and the amount of energy applied. The process can also be characterized in a broad sense as the intensity at which the energy is applied, defined here as specific energy per bar impact *(refining rotational speed, plate configuration, temperature, pressure)*. However, all the variables are interdependent; specific energy consumption at a constant property (*such as strength or freeness*) depends on the raw material and process [7, 8, 10, 13]. Furthermore, different process intensities affect the energy consumption as well as fiber separation and development [10, 12, 14, 26, 29, 36, 39]. In other words, it is impossible to keep two parameters constant while changing the third.

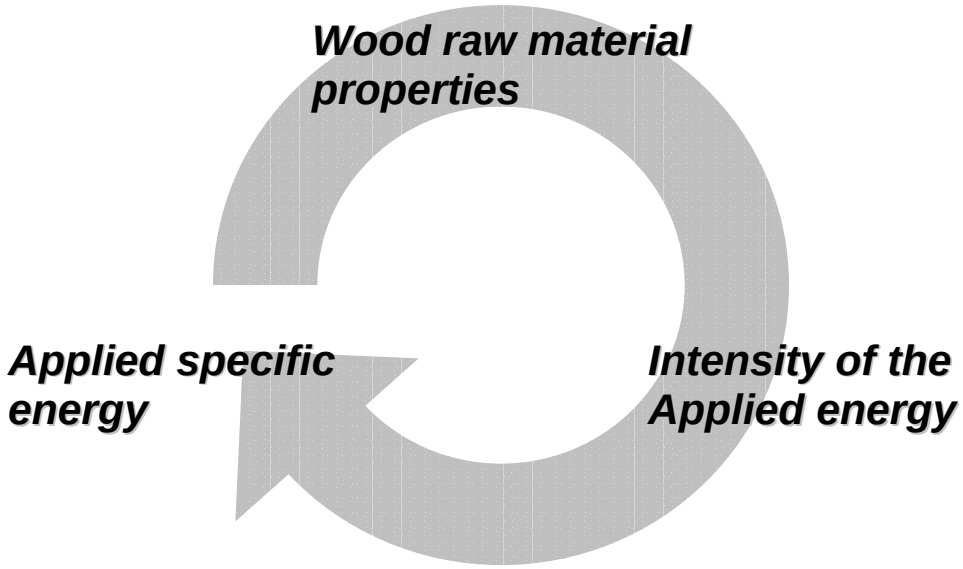

Figure 2. Interdependence of specific energy consumption, intensity, and wood raw material properties.

This triangle of relationships is best understood in the light of the currently used models that describe the wood breakdown to various particles, while keeping in mind that process intensity and wood species significantly affect the wood breakdown at constant energy consumption [40]. Here two of the most significant models are described.

Comminution theory

In mechanical pulping, the defiberization process and particle size reduction was first successfully modeled using a first order comminution model [41, 42]. Comminution models assume that the size reduction proceeds through a progressive breakdown pathway from chips to fiber, and eventually to broken fiber particles (Figure 3). It has been shown that the fiber size reduction follows a first-order kinetic model as a function of specific energy [41]. Although effective in describing the particle size reduction mechanism, and the effect of wood characteristics on the fiber length reduction [40], the comminution model is still a simplified description of the mechanical defiberization process. It neglects the contribution from energy that is consumed in fiber wall delamination, internal fibrillation and quality development of various fractions. Hence the model is limited in describing the produced pulp quality sufficiently beyond the particle size distribution.

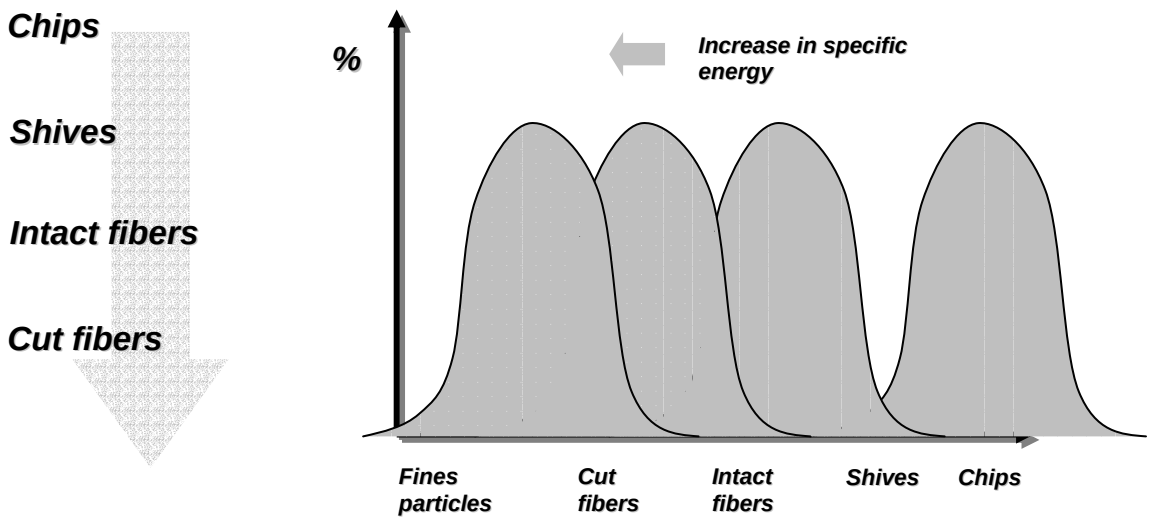

Figure 3. Schematic illustration of comminution mechanism in refining.

Karnis model

Karnis observed an apparent increase in fines content without any significant change in the average fiber length of the fiber fraction [11]. Consequently he proposed two distinct different mechanisms for fiber development in mechanical pulping, wherein either the shortening of the fibers *(traditional comminution)* or the peeling of the cell wall dominates [11]. The peeling mechanism was then related to fiber fraction coarseness reduction and a simultaneous increase in fines content as a function of specific energy consumption. Today cell wall peeling is usually associated with properly executed TMP refining, whereas fiber shortening is seen as the dominating mechanism in groundwood production. However, both mechanisms are believed to occur simultaneously in all mechanical pulping processes to some degree.

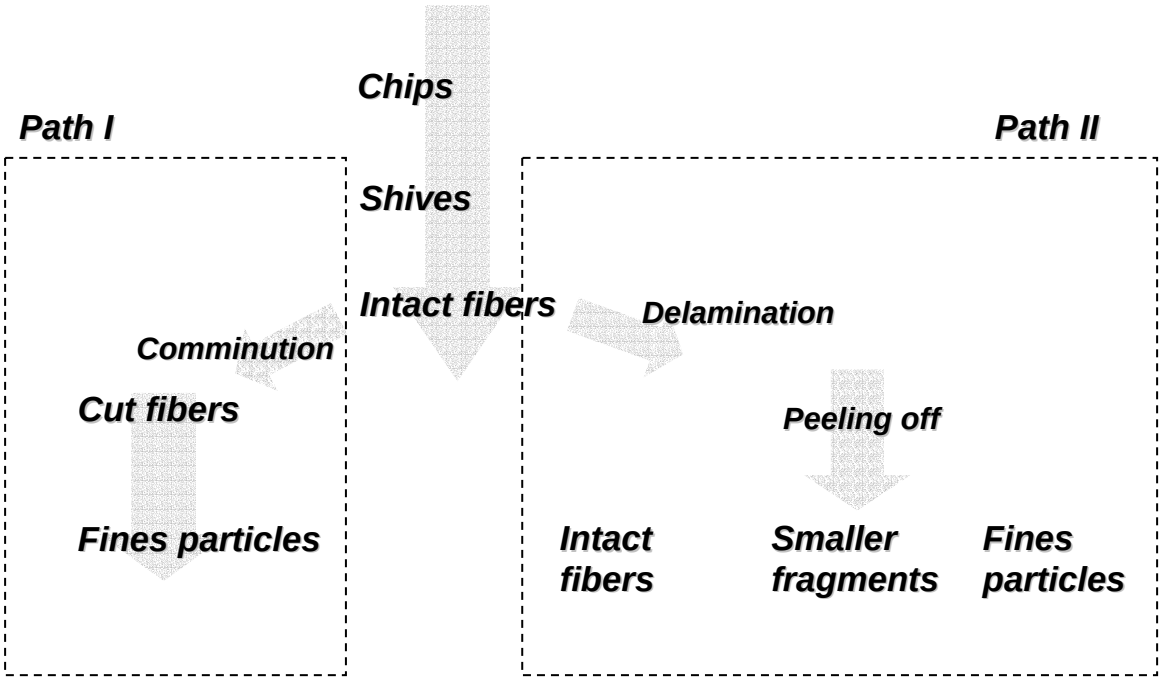

Figure 4. Two paths of fiber development in mechanical pulping, according to [11].

The delamination of the fiber wall is an important mechanism in the development of mechanical pulp properties, affecting the size, shape and chemical characteristics of mechanical pulp particles.

Delamination

As mentioned earlier, mechanical pulp refining reduces the coarseness of the fibers *(R48 or R50 Bauer McNett fraction)* by peeling the material of the cell wall [9, 11, 26, 43], while progressively increasing the fines content [44] and the fines specific sediment volume [45]. The development of these properties are all a function of specific energy consumption and the latter effect has been shown to correlate with the fibril content of the fines [30]. This peeling effect can be extensive, resulting in the delamination of a large portion of the cell wall and generation of significant amount of fines from the S_1 and S_2-layer of the cell wall. Due to the varying distribution of lignin, hemicellulose and cellulose in the cell wall layers, the peeling effect exposes fragments containing progressively higher concentrations of cellulose and hemicellulose. Thus, the bulk lignin content of fines decreases as the fibril content (*material peeled from the S_2-layer*) of the fines is increased [30]. This mechanism is illustrated in Figure 5.

The specific energy consumption and process intensity affect the severity of the peeling, as well as fiber cutting. In addition to the process intensity and applied energy, the initial wood fiber characteristics affect the pulp fiber characteristics, formation of the fines, as well as their quality [9, 10, 13, 21, 26, 44]. The amount of fines created during the process is usually assigned to the energy absorption per fiber in the refining. It is believed that large fibers (springwood fibers with low cell wall thickness and large diameter) experience higher intensities due to the lower number of fibers between refiner bars, and are preferentially cut in the process, creating a larger amount of finer particles [9, 26]. It has also been shown that summerwood fibers or wood with slower growth rate, nominally thicker cell wall, are more prone to unraveling of the cell wall during refining, which then creates fines with higher specific sediment volume (fibril content) [10, 26, 46].

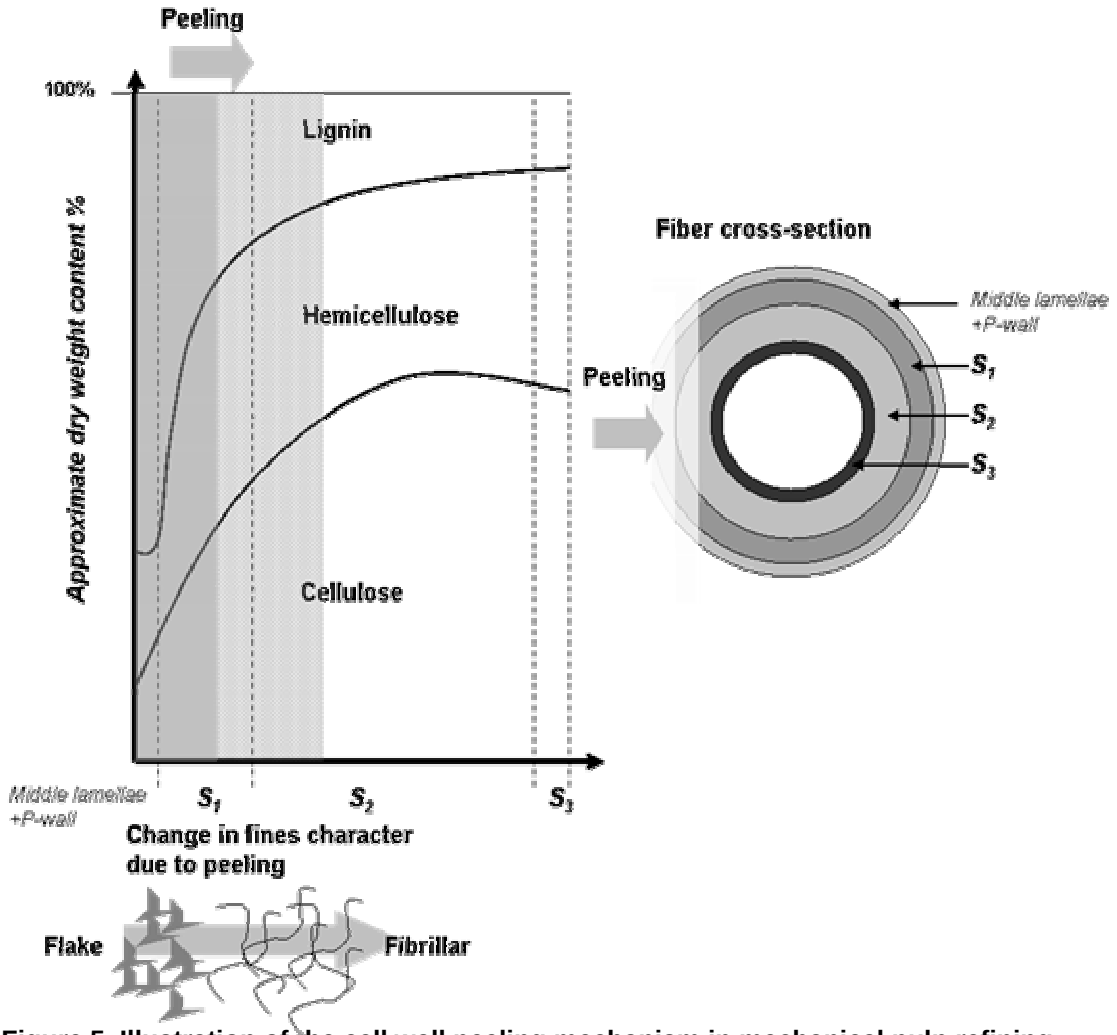

Figure 5. Illustration of the cell wall peeling mechanism in mechanical pulp refining.

Nature of the heterogeneity in mechanical pulps

Due to the comminution and delamination character of the mechanical pulping process and the variability of the raw material, there is significant diversity in the properties of the particles created during the mechanical defiberization of the wood matrix.

The traditional methods for characterizing mechanical pulp particle size distributions include various microscopical methods, and sieve size based classification methods, including the widely used Bauer-McNett classification method. Microscopy based methods traditionally lack the ability of the Bauer-McNett classifier to detect small fines particles [47]. In this study the Bauer-McNett classifier is used to characterize the heterogeneity of mechanical pulps, due to the limitations regarding optical fines detection. The Bauer-McNett classifier has the ability to segregate particles into an unlimited number of size classes, although each class represents a distribution of particle sizes. However, the traditional simple classification of mechanical pulps includes usually four classes: long fibers, short fibers, middle fraction and fines. The so called middle fraction in mechanical pulps is a mixture of broken fiber like particles and broken cell wall material similar to fines [2]. The middle fraction has special properties and significantly contributes to the properties of mechanical pulps, but it is morphologically similar to that of a mixture fibers and fines [48]. In addition, (especially the TMP's with 2-stage reject refining systems) modern mechanical pulps increasingly have a u-shaped Bauer-McNett fraction distribution with significantly lower middle fraction content. Thus, throughout this study the emphasis is on the characteristics of mechanical pulp fiber and fines, and particularly on thermo-mechanical pulp.

Fiber characteristics

The fibers in mechanical pulps are often characterized as the fraction retained on the 14, 28 or 48 mesh screens of the Bauer McNett [2]. This classification corresponds to length weighted fiber lengths varying from 1.36 mm to 2.9mm depending on the screen used [49]. The fiber fraction classified this way normally has a large portion of sound fibers, and a significant portion of cut and split fibers. In the whole, the material can be

characterized as fiber, having fairly intact cell wall structure, and tubular shape (Figure 6).

The fiber characteristics of mechanical pulps are mainly a reflection of the fiber properties of the wood. It has been shown that the pulp fiber length and fiber cross-sectional characteristics have a significant correlation with the length and cross-sectional dimension of fibers in the wood [9, 10, 14, 44]. Due to the mechanical demeanor of the process (high yield – 98%), there is no significant alteration of the chemical character of the fiber from wood to pulp with respect to material properties. The high lignin content in the fiber cell wall results in a rigid and uncollapsible fiber fraction when the sheet is formed at normal temperatures (below the glass transition temperature of lignin) [50]. This rigidity results in a sheet structure that is very porous with low density and low strength [5, 51], shown in Figure 6.

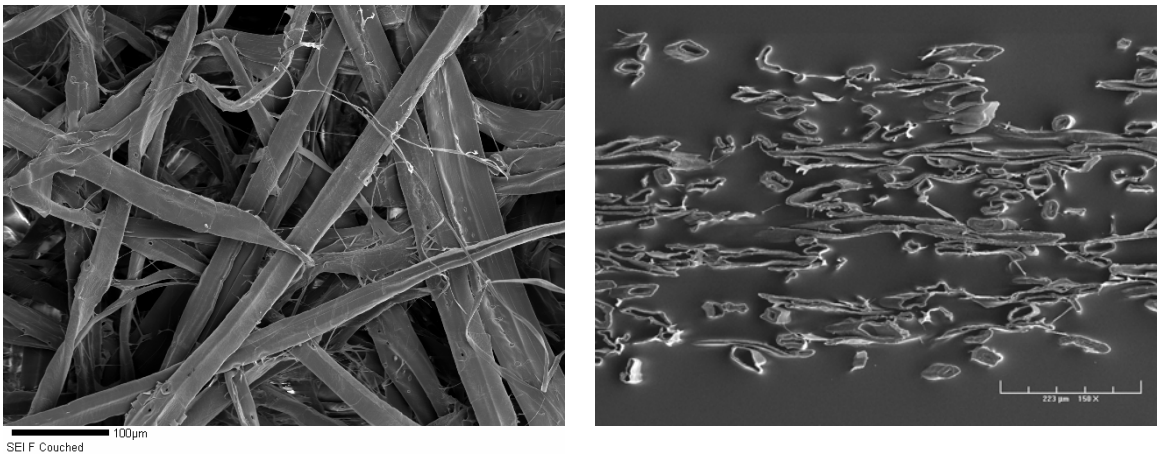

Figure 6. SEM surface (left) and cross-section (right) images of Norway spruce TMP R48 fiber fraction handsheets (no pressing).

The cross-sectional dimension of the fiber fraction in mechanical pulping can be altered through cell wall thickness reduction by peeling, which manifests itself as a decrease of fiber coarseness [11, 26]. This reduction in coarseness affects the moment of inertia of the fiber, making it more flexible and collapsible [11, 26, 32], and thus more readily responsive to the Campbell effect. In addition to cell wall thickness reduction there is a significant cell wall destructive element involved in mechanical pulping. This has been mainly observed as fiber splitting [12, 45], and cell wall fibrillation [7, 52, 53]. In addition

it has been shown that there is a significant variation in mechanical pulp fiber flexibility at a constant fiber moment of inertia [32]. The cell wall destruction in mechanical pulps is often considered to be similar to that of chemical pulp, traditionally characterized as fiber internal fibrillation through refining. The main effect is the increase in fiber flexibility. This is also expected to increase the fiber fractions response to Campbell's effect. However, lately it has been shown that changes in mechanical pulp fiber flexibility caused by refining are primarily determined by the fiber moment of inertia rather than elastic modulus [54].

Characteristics of fines

Fines are critical to the properties of mechanical pulps because the weight fraction of fines may account for up to 40% of the whole pulp in high quality printing papers. The fines material is usually defined as the fraction passing through a 200 mesh screen in the Bauer-McNett apparatus. Alternately the P100 fraction has been used as the fines fraction. The difference in the particle character between P200 and P100 is not very significant.

The peeling mechanism by which fines are likely created and the heterogeneous lignin distribution in the wood cell wall results in bulk lignin content and surface lignin contents that are higher for fines than that of fibers [30, 55]. However, in mechanical pulps the fines are not a homogeneous fraction, but consist of pieces of fiber and "debris", such as fragments of the middle lamellae and cell wall, bordered pits and ray cells. The first ones to report the significant differences in the fines quality were Brecht and Klemm [56] *(Schleimstoff and Flourstoff)*, followed by Forgacs [7], who showed that a good estimate of the ribbon-like and chunky material in the pulp could be obtained from measurements of the specific surface area (or freeness) of the middle fraction. Later the differences in specific surface area due to the morphological variations were related to the microscopical shape of the material (fibrillar shape vs. flake shape). Luukko [30] was able to characterize fines quality by their shape. He defined the quality of the fines with an image analysis method, which measured the fibrillar content of the fines. This was then further correlated with several pulp characteristics. Lately Sundberg [57] classified TMP fines into 5 different fractions, and confirmed the earlier results of Luukko, showing

that fibril type fines particles have lower lignin content and higher cellulose content than ray cells and flake type particles. Similar results were also obtained for groundwood pulp fines by Kleen [55]. From these studies two underlying fines quality characteristics that have specific effects on the properties of mechanical pulp sheet can be derived:

- Particles with high specific surface area and higher lignin content, mainly originating from the outer layers of the fiber wall and middle lamellae. These particles have a flake type shape character and contribute to the scattering properties (free dry surface area – unbonded area) of the sheet, with less significant contribution to strength properties (bonding).
- Particles with very high specific surface area, lower lignin content due to the origin (S_1 and S_2 -layers) and fibrillar shape contribute to the strength properties (bonding) with lesser contribution to the scattering coefficient (unbonded area).

The quantity of the fines has several effects on paper properties. Studies independent of refining effect, wherein fines were added to fiber fraction, clearly show the significance of fines in mechanical pulps [3-6]:

- Increase in tensile index (maximum 40-50% in fines content)
- Increase in tear index (maximum in 20–25% fines content)
- Decrease in surface roughness
- Increase in scott bond
- Decrease in freeness
- Increase in light scattering

The significant contribution of fines to all properties of mechanical pulp based paper is traditionally explained by the high specific surface area of the fines particles. The high specific surface area contributes significantly to the Campbell effect, thus consolidating (bonding) the otherwise very stiff, lignin-rich, mechanical pulp fiber matrix [1, 28]. There is a significant increase in fiber collapse as fines are added into the sheet [28]. In addition fines themselves bond readily losing 80-90% of their initial specific surface area

[58]. However, a large amount of the initial specific surface area of fines remain unbonded in the paper web and significantly contribute to the scattering coefficient of paper made from mechanical pulps (Figure 7).

The variable character of the fines in mechanical pulps is likely the most significant factor differentiating the behavior of these pulps from chemical pulps. In lignin-free chemical pulps it is generally accepted that the fines created during refining collapse completely upon drying and thus solely add to the bonded area of the network [59, 60]. Conversely, the fines of mechanical pulps do not collapse completely upon drying, which is then observed as a change in the dry total unbonded specific surface area of the paper. This is the primary reason why refining cannot be used as a means to induce bonding in mechanical pulps without significantly changing other properties of the finished sheet. The creation of uncollapsable fines through refining alters the total unbonded specific surface area of the sheet. Due to this peculiar character, fines fulfill various structural functions in a mechanical pulp sheet. Fines can act as short fibers, fill interstices and bridge gaps between fibers, coat fiber surfaces but do not facilitate fiber bonds, or coat fiber surfaces and facilitate fiber-to-fiber bonds [23].

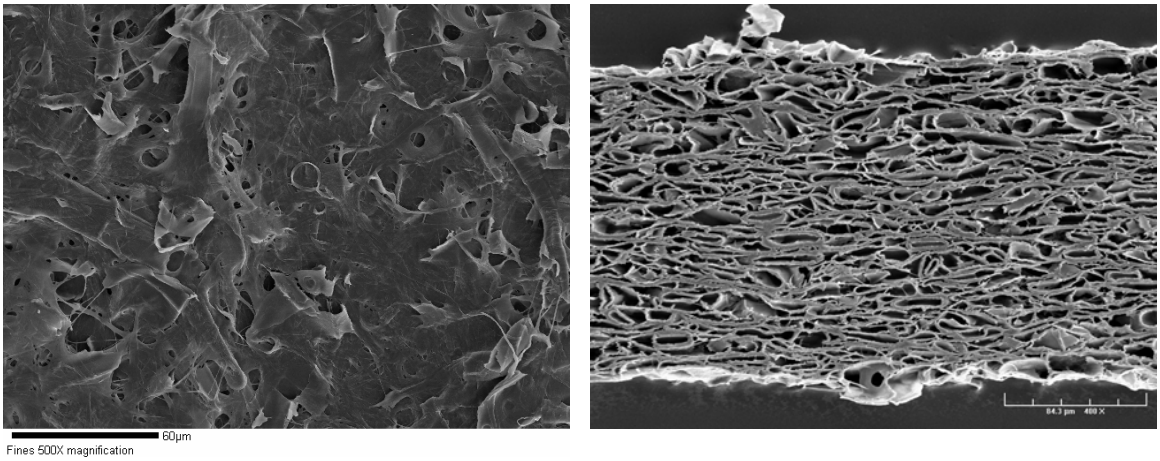

Figure 7. SEM surface (left) and cross-section (right) images of Norway spruce TMP P200 fines fraction handsheets.

Strength theories

In this study it is of particular interest to be able to use a theoretical basis for relating bonded area to tensile strength. This would allow the use of a scientifically sound method to extrapolate to zero bonding and ultimately to obtain a measure for the total dry unbonded area of the sheet. Previous investigations of tensile strength and tear strength of mechanical pulps are reviewed as appropriate.

There are several empirical and theoretical paper structure models that explain the strength properties of the paper sheet as a function of fiber and sheet consolidation characteristics with reasonable accuracy. However, only two approaches are traditionally considered to have some level of validity in understanding the behavior of heterogeneous structures such as mechanical pulps. The first one is an empirical pulp characterization model derived by Forgacs [7], and the second is the theoretical approach of Shallhorn and Karnis [24]. Both of these models indicate that there are only two common factors describing the mechanical pulp sheet strength (these models will be introduced later in detail):

- Fiber length parameter
- Bonding parameter

The existence of only two common factors is supported by the research by Strand [61, 62]. Strand used factor analysis to explain the variation in mechanical pulps. Pilot plant mechanical pulps from various pulping processes, specific energy consumptions and raw materials were used. Two common factors explaining 92% of the total variation were found. These were assigned to the bonding potential and fiber length of the pulp. Later these results were confirmed in an industrial setting [62].

Further evidence of the existence of only two factors explaining the variability of mechanical pulp is supported by the research of Andersson [37, 38], who showed that the tensile strength of various mechanical pulps can be explained with z directional tensile strength (bonding) and fiber length.

Contrary to mechanical pulps, Howard *et al.* [63] found that the variation of chemical pulp properties required three common factors, which explained 99.6 % of the total variation. These common factors were interpreted to describe the following structural properties:

- Factor 1 of bonding
- Factor 2 of length/fines
- Factor 3 of defects – curls and kinks

Factor analysis (or Principal Component Analysis) uses linear relationships to find correlations between variables. However, in paper and pulp most of the variables are not linearly correlated. Thus, when factor analysis is used it is probable that an excessive number of factors are needed to explain the whole variability. Evidence of this was provided by Karrila [64], who used the same data as Howard [63], and nonlinear (neural network tools) relationships between various variables. He was able to show that 99% of the variability within chemical pulps in refining can be explained with only two common factors, however he did not try to characterize the factors.

In conclusion, neglecting the limitations of the factor analysis, the significant differences between the mechanical pulp models and chemical pulp models can be assigned to the third common factor that exists within the chemical pulps but seems to be undefined for mechanical pulps. In chemical pulps this third factor is related to the strength of fibers. This implies that mechanical pulps might operate mainly in a domain where fiber breaking is negligible, and that fiber strength does not contribute to the properties of mechanical pulp sheets.

In the following section the empirical models that are used to explain the strength properties of mechanical pulps are reviewed. Then two distinctly different theoretical (or semi-empirical) models are presented and discussed (Shallhorn-Karnis model and Page equation). These two particular models were selected due to their fundamental differences in accounting for fiber failure in the low bonding regime.

Empirical strength models

The use of empirical models in the characterization of mechanical pulps is largely done in order to reduce the number of measured parameters needed for quality control purposes. The methods used in the extraction of these parameters often rely on statistical methods, such as multivariate regression analysis or factor analysis, both often using linear relationships. Thus, the models often lack accuracy, but provide insight to the total amount and the nature of the factors needed to explain the properties of mechanical pulps.

The first significant contribution to the understanding of mechanical pulp strength properties was the extensive research by Forgacs [7]. He used mechanical pulps from several wood species with different process types, and specific energy consumptions, to find the significant pulp characteristics which would explain mechanical pulp sheet properties. Two primary parameters were identified: a fiber length factor (L-factor) and a shape (S-factor) factor. The shape factor was characterized using the hydro-dynamically measured specific surface area of the middle fraction (P48-R100 mesh). The length factor was determined as the mass proportion of fiber retained on the 48 mesh screen on the Bauer-McNett classifier. Forgacs was able to obtain very high correlation coefficients for tear and tensile strength properties using these two parameters. However, L and S factors have been investigated by several others and were found to be insufficient in explaining the strength properties of mechanical pulps [65], especially in the case of thermo-mechanical pulps [66].

The S-factor in Forgacs' model is related to the bonding potential of the pulp solely based on the assumption that wet specific surface area has a direct correlation with the true bonding ability of the pulp. However, it is not known, due to the surface coverage of lignin and extractives of these pulps, whether all the specific surface area is capable of bonding. Andersson [37, 38] accounted for this contribution using z-directional tensile strength (ZDT) to explain the true bonding potential of the pulps. Using two factors, the average fiber length and the ZDT, Andersson was able to explain most of the variability of various commercial mechanical pulps.

Shallhorn-Karnis model and modifications

There are several sheet strength predictive models in which fibers are assumed to be embedded in a matrix with shear bond strength [24, 67, 68]. The Shallhorn-Karnis model [24] is of particular interest because it was developed to explain the tensile strength and tear resistance of mechanical pulps. The Shallhorn-Karnis theory of the tensile properties of mechanical pulp is based on concepts of composite structures. The theory considers paper as a continuum and makes three fundamental assumptions:

A) *All the fibers experience the same forces*

B) *Fiber geometry is uniform, and fiber strength as well as the bond strength distributions are uniform*

C) *All the fibers are oriented perpendicular to the tensile fracture line*

The model uses fibers of uniform size all aligned in the direction of the stress, and fibers are differentiated into two separate groups: fibers which pull-out in the breaking zone, and fibers which break. Because fiber pull-out and breaking is assumed to occur simultaneously, the pull-out force is added to the breaking force. The redistribution of stresses in the sheet during loading is not considered. Also the matrix does not contribute to the strength of the sheet. The models were developed for two different cases.

1. The ultimate tensile strength per unit cross-section for a sheet in the low bonding regime, where fiber strength is grater than the bond strength ($\tau<\tau c$):

$$T = \int_0^{l/2} (2N/l)(2\pi r\tau x)dx = N\pi r\tau l/2 \qquad \textbf{Equation 1}$$

2. The ultimate tensile strength per unit cross-section for a sheet in the higher bonding regime, where fiber strength is lower than bond strength ($\tau > \tau c$):

$$T = \int_0^{\sigma r/2\tau} (2N/l)(2\pi r\tau x)dx + \int_{\sigma r/2\tau}^{l/2} (2N/l)\sigma\pi r^2 = N\pi r^2\sigma(1-\sigma r/2\tau l)$$

Equation 2

Where N = number of fibers per unit cross-sectional area of the crack

l = fiber length

r = fiber radius

x = embedded length

τ = shear strength per total fiber surface area

σ = fiber strength per cross-sectional area of the fiber

Retulainen [69] slightly modified the equations derived by Shallhorn and Karnis. He adopted the term relative bonded area (RBA) to account for the known fact that all surface area is not bonded area, specific bond strength (τ changed to b) and changed fiber radius to fiber width (w). Fs is the fiber strength.

1. For $\tau<\tau c$

$$T = Nw(RBA)bl/2 \qquad \textbf{Equation 3}$$

2. For $\tau>\tau c$

$$T = NFs(1-\frac{Fs}{2l(RBA)wb}) \qquad \textbf{Equation 4}$$

In order to overcome the Shallhorn-Karnis model assumption that all fibers are aligned in the direction of the applied stress and account for number of fibers involved in carrying stress, Karenlampi [70] further developed the model to include the number of fibers in the breaking zone, and applied the model to a to randomly oriented sheet.

N = sheet basis weight / coarseness * width of the breaking zone

$$T = \frac{8}{9}\int_0^{l/2}(2/l)\int_0^{\pi}(2Nr\tau x\sin^4\theta)d\theta dx = \frac{Nr\tau l}{6} \qquad \textbf{Equation 5}$$

The Shallhorn-Karnis tear resistance model is based on an assumption that a negligible amount of energy is consumed in fiber breaking, and all energy consumed is due to fibers being pulled out from the matrix. The maximum tear index is an indication of the domain where the fracture mechanism changes from fiber pull-out to fiber failure. Again, two different cases were constructed:

1. For ($\tau<\tau c$)

$$W = \int_0^{l/2}(2N/l)(\pi r\tau x^2)dx = N\pi r\tau l^2/12 \qquad \textbf{Equation 6}$$

2. For ($\tau>\tau c$)

$$W = \int_0^{\sigma r/2\tau}(2N/l)(\pi r\tau x^2)dx = N\pi r^4\sigma^3/12l\tau^2 \qquad \textbf{Equation 7}$$

The modeled relationships based on the Shallhorn Karnis equations were constructed for two cases and are depicted in Figure 6, the cases are:

1. Decreasing the amount of fiber (adding fines)
2. Decreasing the fiber length

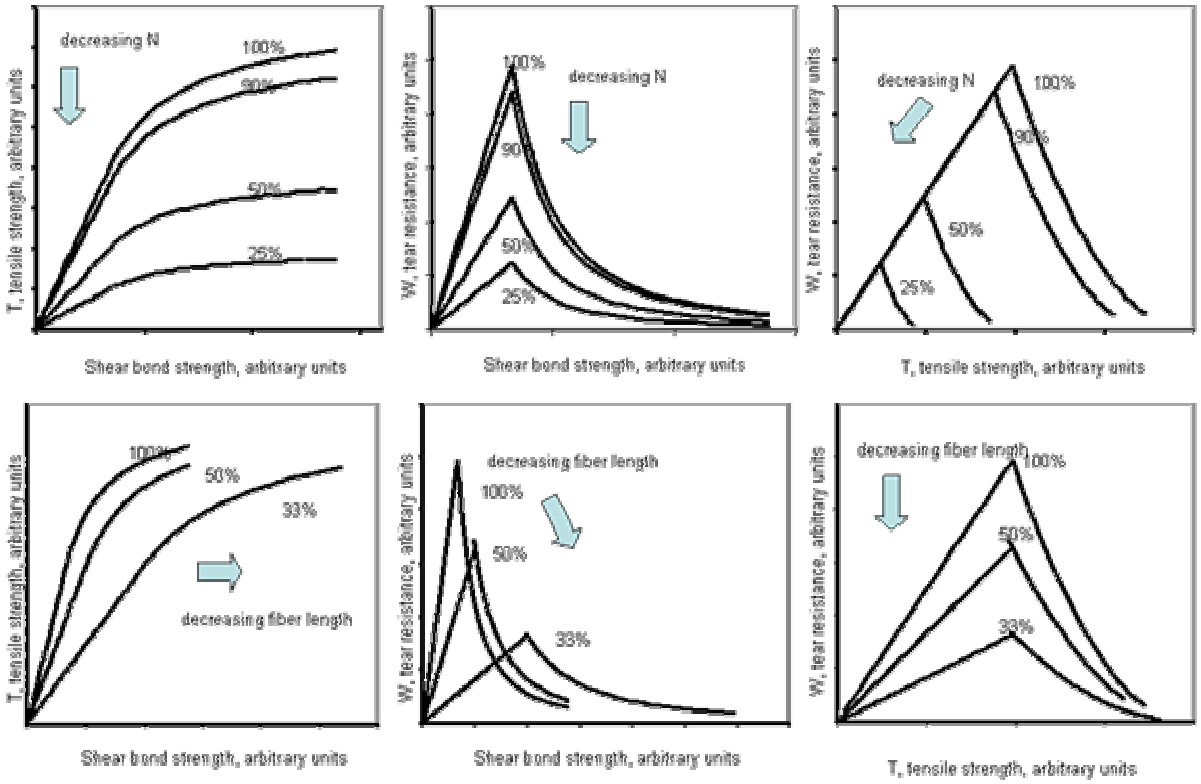

Figure 8. Shallhorn-Karnis model [24] predictions for tensile strength (T) and tear resistance (W), at various shear bond strengths (τ), fiber lengths (l), and number of fibers in the breaking zone (N). Redrawn based on equations 1,2,6 and 7.

Page Equation

Although not originally developed for heterogeneous structures, the Page equation [60] still provides additional insight regarding the theoretical framework involved in micro-mechanistic approaches of understanding paper strength. The observations that led to the semi-empirical equation of Page involved two fundamental studies. In 1958 Van den Akker et al. [71] showed that a significant portion of fibers break under tensile load, and when bonding is increased by means of wet pressing or strength additives more fibers break. These results were later confirmed by Helle in 1963 [72], however he stated that for high freeness pulp almost all fibers pulled out in tensile. In 1961, Page showed that during straining of the sheet the load is taken by progressively fewer fibers crossing the rupture line due to the failure of bonds at the ends of fibers [73]. Thus, in 1969 Page writes :"As the point of failure [of the sheet] is approached, more bonds fail in the rupture region and the remaining fibers take more of the sheet load until the fibers lying in the direction of loading reach their rupture strain. At this point, catastrophic failure of paper occurs." This led him to postulate the first premise, where tensile strength of the sheet is determined by bonding and fiber strength:

$$\frac{1}{T} = \frac{1}{Z} + \frac{n_p}{n_f Z} \qquad \textbf{Equation 8}$$

,where T = tensile strength of the strip expressed as breaking length

Z = finite-span tensile strength of the strip expressed as breaking length if no bond breakage had occurred

n_f = number of fibers crossing the rupture zone that take the load at failure and then break

n_p = number of fibers crossing the rupture zone that pull out intact due to prior bond breakage and hence carry no load at failure

The second premise relates the number of fibers that fail to the number that are pulled out intact. Page assumes a direct proportionality between fibers breaking to pulling out and fiber strength to bond strength.

$$\frac{n_p}{n_f} = \frac{Z}{B}$$ **Equation 9**

Using these two premises, Page derives an equation that describes the tensile strength of paper with three factors: fiber length, fiber strength and bond strength. Bond strength can be further divided into two separate factors, bonded area and shear bond strength.

$$\frac{1}{T} = \frac{9}{8Z} + \frac{12g}{bL\alpha}$$ **Equation 10**

,where Z = zero span tensile strength

g = acceleration due to gravity

b = shear bond strength per unit bonded area

L = fiber length

α = bonded area

Fiber failure in the low bonding regime

The premises of Page equation are mostly from observations that were derived from research done with highly bonding fibers. Thus, the Page equation describes a condition where fiber failure already occurs at very low bonding levels, and gradually becomes more significant when bonding is increased. This is not likely to apply to comparatively poorly bonded mechanical pulp sheets.

For low bonding sheets, such as mechanical pulps, Kallmes [74] and Shallhorn and Karnis [24] have suggested that there is a critical bonding level where the failure transitions from pure bond failure to fiber failure. Kallmes derived this critical bonding level to be where the tensile strength to zero span tensile strength ratio is 4/9, and demonstrated it with data from the original work of Ingmansson and Thode [59]. Shallhorn and Karnis [24] showed using mechanical pulps that, at constant fiber length, the tensile strength of the sheet is a linear function of wet specific surface area or specific filtration resistance (bonding) of the pulp, indicating that the fiber failure is constant or insignificant. In addition, the empirical works of Forgacs [7], Mannstrom [33, 34] , Andersson [38] and Strand [61, 62] indicate that mechanical pulps mostly operate in a domain where fiber breakage can be considered negligible, and that mechanical pulp properties can be explained with two independent factors; fiber length and bonding.

The significance of this fundamental difference regarding the fiber failure at low bonding regime is illustrated in Figure 9, where an imaginary plot of the Ingmansson and Thode method is presented. In order to get an estimate of the total unbonded specific surface area (S_o) using the Ingmansson and Thode method, an equation is needed to relate bonded area to tensile strength. For low bonding sheets, where it is likely that fiber failure has no contribution to the sheet failure mechanism, the Page equation results in an underestimation of the total unbonded specific surface area. Whereas, a linear model extrapolation results in a significantly higher total unbonded specific surface area and specific bonded area.

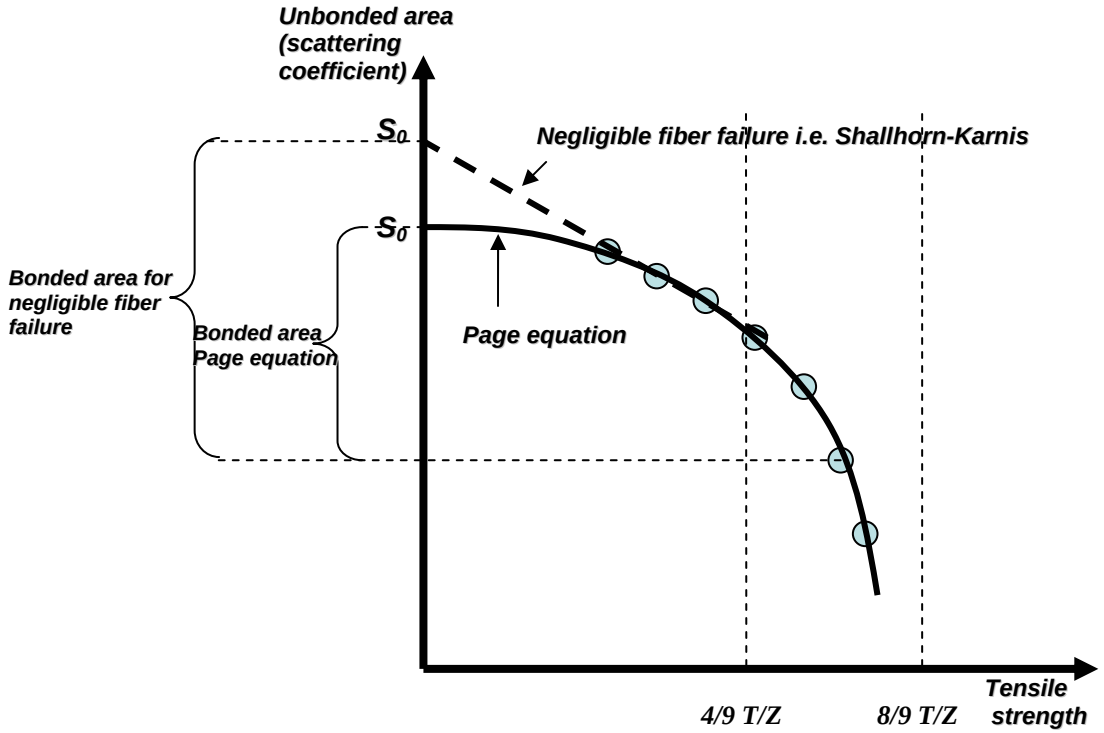

Figure 9. Schematic illustration of the difference between Page equation and negligible fiber failure models.

Mohlin's work has been critical of the use of only two factors to explain the strength of mechanical pulps [75]. In 1979 she stated: "The data used as the basis of these conclusions were mainly obtained for pulps intended for use in newsprint, i.e. pulps with relatively high freeness. For the low freeness mechanical pulps needed for other printing papers, two variables are no longer sufficient for the characterization of the pulps." There are indications that a third factor (fiber strength) also exists in mechanical pulps that would confirm Mohlin's early suspicions. Lindholm [76] has shown that when comparing artificial mechanical pulp blends at the same fiber length and Scott bond (bonding strength), the tensile strength varies significantly depending on the type of long fiber used. Using Lindholm's data, Mohlin showed [77] that at constant fiber length, with the addition of fines, the tear strength progresses through a maximum. Retulainen [27] was able to show that a significant portion of mechanical pulp fibers break during tensile test by using dyed fibers. However, Buchanan and Washburn [78] observed with SEM that there was no fiber breakage for the long fibers in the tensile fracture zone of groundwood pulps. However, as the bonding was increased by lowering the freeness

(down to CSF 79) an increased number of the secondary fiber elements were observed to break in tensile failure.

The existence of a third factor at higher levels of bonding does not contradict the earlier suggestions of a linear relationship between bonding and tensile strength in the low bonding regime. The existence of a third factor at higher levels of bonding simply introduces curvature into the tensile bonding relationship as a sufficient level of bonding is achieved.

Fiber strength in mechanical pulps

Fiber strength in chemical pulps has been shown to be governed by three dominant factors: secondary wall fibril angle, structural defects and cellulose content [79-81]. Due to the significant variability of these factors between single pulp fibers the tensile breaking stresses are shown to lie in a wide range between 40-130 kg/mm^2 [82-84]. Single fiber strength studies of mechanical pulps are scarce. McDonough [85] was able to show that the mean single fiber strength of mechanical pulp fibers range from 55 to 114 kg/mm^2 depending on the fraction the fibers were from. The single fiber strength was observed to decrease with the Bauer-McNett screen mesh size, as well as with decreasing temperature, indicating a strong fiber defect effect on the strength properties of the single fibers.

Fiber strength in chemical pulps is traditionally measured using a zero-span tensile strength apparatus. The use of zero span tensile strength was initially suggested in 1925 by Hoffman [86], and extensively developed by Clark [87, 88] and Boucai [89]. In zero span tensile testing a strip of paper is clamped between two jaws separated with a near zero distance and the strip is then strained in tensile. It has been shown empirically that zero span tensile strength correlates linearly with single fiber strength [71, 90], is very sensitive to fiber chemical and mechanical degradation, and is significantly affected by fiber curl [91]. Van den Akker [71] has shown theoretically and experimentally that for a defect free, completely straight fibers all aligned in the stress direction, the fiber strength is related to zero span according to the following relationship:

$$\phi = \frac{8}{3} A \rho g Z \qquad \textbf{Equation 11}$$

where A is the average fiber cross-section, ρ is the density of the fibrous material, g is the acceleration due to gravity and Z is the zero span tensile strength of the sheet.

There are indications that, at low bonding levels the zero span tensile strength is bonding dependent, but at higher bonding levels this dependency is nonexistent [89, 92]. The reason for this is not fully understood, but it has been assumed that either a fiber slippage occurs when the sheet is not sufficiently bonded or that the zero span is

increased due to the reduction in sheet caliper at higher bonding levels [93]. However, opposite views have also been presented [94], and concise summary of the subject can be found in [95]. Indications of bonding dependant zero-span tensile strength behavior have also been observed in mechanical pulps. Karnis [96] measured the zero span tensile strength of mechanical pulps with various fines contents, and observed no change in zero span tensile strength up to 40% of fines content, even though the zero span tensile strength of fines is significantly less than that of fibers. It is possible that significant bonding enhancement by fines contributes to this result. In general the zero-span tensile strength of mechanical pulps is in the range of 10 to 12 kilometers, whereas in chemical pulps it has been shown to range anywhere from 10 to 22 kilometers [97]. These differences are generally in agreement with the effect of cellulose content on fiber strength [81].

Bonding

Fiber bonding is responsible for stress transfer between structural elements in paper, and thus the key to the internal cohesion of paper. Nearly all mechanical interactions between fibers during papermaking take place through fiber bonds. The number and area of bonds affect most of the functional properties of paper, *ie*. optical, mechanical, thermal and electrical properties. [1]

Bonding can be considered to be a general term for the three different types of generally accepted bonds formed in the matrix between fibers.

1. Chemical bonds (chemical bonding theory, hydrogen bonding theory)
2. Intermolecular van der Waals bonds (adsorption theory)
3. Entanglements of polymer chains (diffusion theory, mechanical interlocking theory)

The formation of bonds begins as solid content increases during the paper making process. Initially surface tension forces govern the consolidation by pulling particles together as water is progressively removed from the matrix, this is generally known as the *Campbell effect* [98]. Current understanding is that there is a gradual change from the Campbell effect to the concurrent final bonding mechanism (often referred as hydrogen bonding) above 50% solids content, at which level a significant increase in sheet modulus is traditionally observed. During this later stage of drying, ligno-cellulosic particles (fibers and fines) shrink laterally and possibly cause shear stresses in the bonded regions, which are frequently identified microscopically as *microcompressions* [99]. The lateral fiber shrinkage effect on the bonding zone connects the fiber properties to the ultimate bond strength, because the fiber wall character is responsible for the stress distribution caused in the bond by transverse shrinkage. However, the shrinkage potential of mechanical pulp fibers is smaller than that of chemical pulp fibers [1].

If the bonded area and bond strength are directly proportional, the quality of bonding and fiber bonds can be described by the specific bond strength (SBS) concept, as defined by Retulainen [1]:

Specific bond strength = Strength of a bond / Area of a bond

Specific bond strength has been determined directly through individual fiber-fiber bonding tests [82, 83, 100, 101], as well as indirectly from fiber network sheets [60, 102-105] (using micromechanical models, or z-directional tests). The results vary significantly depending on the method used. The concept of specific bond strength is not very well understood, because the measured specific bond strength has been shown to be loading mode dependent [103].

RBA –Relative Bonded Area

Relative bonded area, RBA, is the fraction of the total surface area involved in bonding. RBA is defined as the ratio of bonded area to total dry surface area of the material, in the following manner:

$$RBA = (S_o - S)/ S_o \qquad \textbf{Equation 12}$$

, where S_o is the totally unbonded surface area of the fibers, and S the unbonded area at certain bonding degree. There are two unquantifiable parameters in this definition: the total unbonded surface area of the material and the surface area of the material in a bonded stage. Traditionally (chemical pulps) several different approaches have been taken to measure both of these parameters, here only the most significant contributions that are relevant for mechanical pulps are reviewed. [1]

Direct methods for estimating RBA

All direct methods for determining RBA of paper are based on light microscopy or SEM imaging, and image analysis [51, 73, 106]. The pioneering work of Yang et al [51] and Eusufzai [106], focused on analyzing the perimeter length of fiber cross-sections and the bonded length of fiber cross sections from paper SEM image cross-sections. Aside from the work intensive nature of the image analysis based method, the approach has been shown to be useful in determining RBA in chemical pulp based papers. This is mainly due to the fact that fibers are clearly visible and separable from each other. However, for

mechanical pulps the methods are not as straight forward due to the heterogeneous nature of the pulp, where fibrous elements are not readily discernible, as seen in Figure 10 .

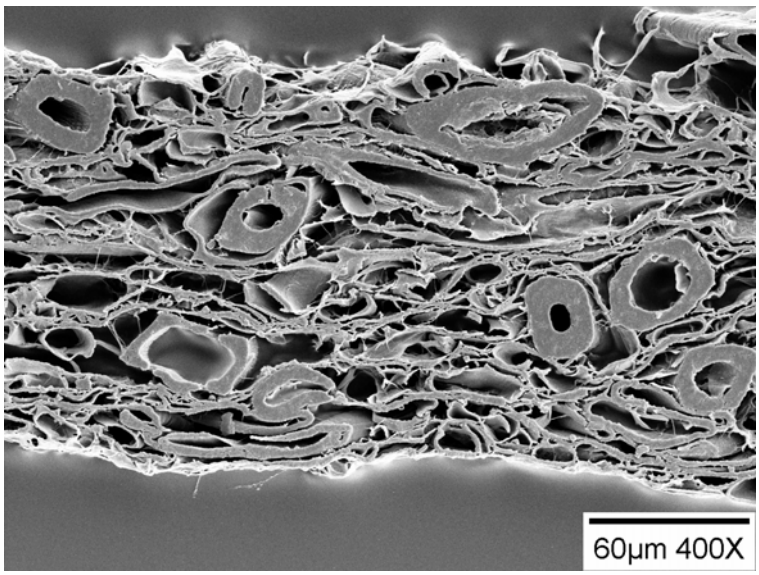

Figure 10. Southern pine TMP (110 CSF) cross-section SEM image

Indirect methods for estimating RBA

The first attempt to obtain a measurement of the relative bonded area on paper (RBA) was made by Parsons [107], who used a solvent replacement technique to produce a sheet with low bonding in order to estimate the total dry unbonded specific surface area of the sheet. The sheet was formed by soaking spruce sulphite pulp several times in acetone and forming the sheet eventually in *n*-butyl alcohol. The ultimate goal in the solvent replacement technique is to prevent surface tension forces from pulling the fibers into close contact and eventually bonding. Parsons' work was followed by investigations by Ratliff [108], Keeney [109], and Leech [110]. In these studies, the final solvent was usually benzene used to solve the problem of poor formation on Parsons' unbonded sheets. Later Haselton [111] used a gas adsorption technique (BET) to show that in the solvent exchanging method fiber is left in an expanded condition, when compared

drying from water method. This produces unbonded dry specific surface areas that are grossly in error. This was later confirmed by Rennel for solvent-exchange dried fibers [112]. Rennel's work also indicates that in freeze-drying and spray-drying fibers remain in a swollen state producing specific surface areas higher than what can be expected from the Ingmansson-Thode approach.

Ingmanson and Thode [59] suggested that the problem with solvent exchange could be circumvented by plotting specific scattering coefficient against tensile strength, and extrapolating to zero tensile strength in order to obtain a fully unbonded scattering coefficient from a water formed sheet. They used refining and wet pressing to increase the tensile strength of spruce sulphite pulp. In their data, refining and wet pressing produced a similar scattering-tensile relationship, allowing them to conclude that the fibril structure of chemical pulps collapses completely on the surface of the fiber. Thus, refining produces results similar to wet pressing. However, later Swanson and Steber [113] showed that the fibrillar structure created in refining does not collapse completely upon drying and that beating indeed develops non-collapsible surface area. This was supported by Luner *et al.* [114] finding that, when using high yield pulps (up to 19.0% lignin content), beating produced different scattering-tensile relationships at different wet pressing levels. Later Rennel also showed the same behavior using a large variety of different pulps, including mechanical pulps [115]. Ultimately, using unbonded (spray-dried) fiber sheets and nitrogen absorption techniques, Hartler showed that the dry-fiber specific surface area of chemical pulp fibers does not remain constant during the beating process [116]. For high yield and mechanical pulps, the spray dried unbonded dry specific surface area increases with additional beating [115].

Although described by Van Den Akker [117] as a crude method for estimating RBA in pulps, wet pressing and the Ingmansson-Thode approach still remains as the only indirect method that is believed to produce a meaningful measure of RBA in chemical pulps [118].

The use of scattering coefficient as a measure of specific surface area of paper

Davis was the first to state that the scattering coefficient should be proportional to the specific surface per unit mass of the material [119]. The first to attempt to prove this was made by Parsons [107] using a modified silvering method similar to the Clark method [120]. In Clark's method, the fibers are coated with a uniform layer of silver by boiling fibers in aqueous ammoniacal silver, and the area of this silver coating can be determined chemically. The measurement depends upon the catalytic decomposition of hydrogen peroxide by contact with the silver surface. The calibration curve for absolute specific surface area is made with small squares of cellophane that have a known area. Using the silvering method Parsons was able to obtain unique linear relationships between silvering specific surface areas and specific scattering coefficients of fractionated sulphite and groundwood pulps. However, chemical pulp fines did not fall in line with rest of the chemical pulp data. Interestingly, mechanical pulp fines were in line with rest of the fractions. Using the same method Ratliff showed that each pulp produces unique and significantly different scattering coefficient specific surface area relationships [108].

The use of gas adsorption (nitrogen) in determining specific surface area and relating it to specific scattering coefficient of paper was first introduced by Haselton in 1954 [111, 121]. Haselton found a linear correlation between scattering coefficient and nitrogen adsorption specific surface area of sulphite pulps that had been refined and wet pressed to different levels of bonding. The correlation obtained by Haselton showed a linear slope of 0.045. The wavelength used in the scattering coefficient measurement was 600 nm. Later Rennel [115] confirmed the linear relationship between scattering coefficient and nitrogen gas adsorption specific surface area (the wavelength used in scattering measurements was not mentioned) for various pulps wet pressed and refined to different levels of bonding. In his data, all pulps produced unique relationships between scattering coefficient and gas adsorption specific surface area. Swanson and Steber [113] also observed that each type of pulp has a unique nitrogen adsorption vs. scattering relationship. Their results did approach a similar value of 0.044 for the linear slope at higher wavelengths of light (650nm), which was similar to Haselton's result. Rennel [122] also obtained a similar linear relationship using cylindrical model fibers of glass, when

the diameters of the glass fibers remained larger that 1 micrometer, or the specific surface area was below approximately 1.5 m^2/g. Van den Akker [113], and Page [123] have made an interesting observation that 0.044 is approximately the value which would be expected by application of Fresnel's law of reflection to a diffusely reflecting body of randomly oriented fibers. This was later confirmed as an accurate approximation using the Stokes approach for layered paper structure [124].

There are indications that the cross-sectional shape of the fiber affects the measured scattering coefficient. The effect of the particle shape on the scattering coefficient at constant specific surface area was studied first by Arnold [125], who showed that the light scattering coefficient was greater for dog-bone shaped fibers than circular ones. The effect of fiber shape on scattering efficiency was confirmed by Rennel [122], who showed that each shape represented a unique nitrogen adsorption specific surface area vs. light scattering relationship (at 557 nm wave length of light and a specific surface area range between 0.2 m^2/g to 0.37 m^2/g), using model glass fibers with variable cross-sectional shapes. The reason for this type of behavior was attributed to the possible variable pore size distribution in the sheet by stating "It should be borne in mind, however, that the determinations of the light-scattering coefficient and surface area (BET) are not concerned with the same thing. The former applies to surfaces down to a distance about 500-600 Å, whereas the nitrogen molecule, which measures 3.6 Å, record nearly all surfaces – even those not scattering light." However, it is not known whether the shape effect is actually an intrinsic effect or is directly related to the pore size distribution (scattering efficiency of small pores) of the sheet.

Since pore size distribution appears to have a significant impact on the light scattering of paper, significant amount of research has been conducted in order to understand this relationship. Microporosity, measured with mercury intrusion porosimetry, considers paper to be a continuous solid phase containing air voids that are the light scattering elements. It provides an application for studying the effect of pore size distribution on scattering coefficient. Using this approach, Alince *et al.* [126, 127], Fineman *et al.* [128] , and Rundlof *et al.* [129], have shown that there is a correlation between the void surface area of the sheet and scattering coefficient of paper. However, the correlation is better when void pores smaller than 100-200nm are excluded from the data. Interestingly, the relationship between the total area of pores above 200nm and the scattering coefficient

from Alince et al. [126] produces a linear correlation following the approximate slope of 0.045, up to approximately 1.5 m^2/g mercury intrusion specific surface area, after which slight curvature appears. This indicates that the minimum optically effective pore sizes are in the range of 200nm, confirming the earlier statement by Rennel. However, the mercury intrusion results are not in agreement with the BET nitrogen adsorption results. In both methods similar slopes between scattering coefficient and specific surface area were detected (0.044-0.045). The detection ability of the nitrogen adsorption method is related to the size of the nitrogen molecule, and thus pores down to the size of 4.3 Å should be detected [113]. Due to the fact that mercury does not wet fibers, a positive pressure is needed to force the penetration of mercury into the pore structure. In order to detect nanometer scale pores, significantly high pressures (up to 60 000psi) are needed. It has been stated that these high pressures could possibly lead to structural changes in the material under investigation [129, 130]. Thus, it is possible that the low correlation between specific surface area measured by mercury intrusion and light scattering coefficient beyond the 100-200nm pore size, is due to the potentially destructive nature of the mercury intrusion method.

It has been shown that the Kubelka-Munk scattering coefficient is significantly reduced at high levels of light absorption [131-133]. This effect is known as the NAM anomaly [133] or Foote effect [131]. It is not clear whether this decrease in scattering coefficient at higher absorption is an intrinsic error in the theory or an actual physical material property. When the decrease in scattering coefficient at high absorption has been considered to be a material property, the scattering decrease has been explained to be a combination of two phenomena: the influence of the absorption on the surface reflectivity of the cell wall and the absorption of light internal to the cell wall [132]. However, it has also been shown using a discrete ordinate radiative transfer (DORT) model that there is an intrinsic error in the Kubelka-Munk model at high absorption levels, explaining roughly 20% of the decrease in scattering coefficient [134]. It needs to be recognized that when scattering coefficient is to be used as a measure of bonded area in paper, the wavelength of light used in the measurement should be chosen such that the scattering is not affected by the strong absorption [135].

Mechanical pulp sheet consolidation through wet pressing and press drying

Mechanical pulp fibers are rigid at temperatures below the glass transition temperature of lignin. Thus, when wet pressing is used to induce consolidation in mechanical pulp sheets the increase in density obtained is limited. It has been demonstrated that even high pressing pressure can not overcome this behavior [50]. It is unknown whether this phenomenon is due to the rebound of the fibers to their original shape, or if the fibers resist the induced pressure and remain uncollapsed under pressure. Mechanical pulp fibers with fines respond better to wet pressing than the fiber fraction alone, resulting in reduction in scattering coefficient following wet pressing [136]. This behavior has been attributed to the ability of the fines to reduce fiber rebound when they are brought into close contact and a significant amount of water is removed from the sheet [28].

The rigidity of mechanical pulp fibers can be overcome by press drying the sheet at elevated temperatures [50, 137-141]. The effective temperature has been shown to be close to 100 ^{o}C, strongly indicating that the lignin in the fiber restricts the collapsibility of the fiber [141]. The efficiency of press-drying consolidation is dependent on the initial moisture content of the sheet, because water acts as plasticizer, and prolongs the effective time needed to dry the sheet [141, 142]. The induced fiber collapse is permanent, assuming that the press drying is prolonged so that the sheet is dried under load. Back and Norberg [143] showed that in pressing an Asplund pulp, there was a significant springback of the pulp pad depending on the pad moisture content and temperatures used in pressing. At a pad moisture ratio of 0.50 the springback decreased from 44% at about 10 ^{o}C to 27% at about 90 ^{o}C. At a pad moisture content of 0.80, the springback decreased from 18% at about 10 ^{o}C to virtually nil at 90 ^{o}C.

Press drying of lignin rich pulps increases the strength properties of the sheet by increasing inter-fiber bonding [144]. At low pressing pressures the most significant strength enhancements are seen in the wet strength properties of the sheet. This has been attributed to flow of hemicelluloses and lignin, with lignin covering the hemicellulose bonds making them more hydrophobic, and thus more resistant to water [139, 145]. However, in order to induce lignin flow it is essential that the lignin glass

transition temperature of 90-110 ºC is exceeded by 60-70 ºC. This has been shown to apply in case of spruce CTMP, where no significant alterations in the fiber surface chemistry were observed using ESCA, when the pulp sheets were pressed below 140 ºC [146]. In addition to the flow of lignin and hemicellulose during the heat treatment of wood there is a significant redistribution of extractives on the surfaces of the material [147]. However, Nordman and Levlin [148] showed that this temperature induced redistribution of extractives has no effect on the bonding characteristics of groundwood pulp.

Based on studies by Gupta and Goring it is believed that lignin surfaces on fibers do not present any bonding ability at temperatures below their softening temperatures [25, 149]. When the temperature is raised to the softening temperature of lignin, the lignin surface bonds readily [25]. There are several possible mechanisms that can explain lignin bonding, ranging from polymer cross-linking and mechanical interlocking to polymer diffusion [150-153]. Mechanical pulp fibers and fines have a significant portion (~65%) of the total specific surface area covered by lignin and extractives [55]. In other words, half of the specific surface area cannot be bonded at temperatures below the softening temperature of lignin, but can be bonded when the temperature is raised above the glass transition temperature of lignin.

Interestingly, the studies where wet pressing and press drying are used to induce consolidation in mechanical pulps indicate that press drying is an extension of wet pressing with respect to sheet bonding. Seth et al. [144, 154] showed that wet pressed and press dried (180 °C) mechanical pulp sheets followed the same scattering coefficient to tensile strength ratio when the sheets were densified using variable pressures. This indicates that even though the bonding mechanisms of wet pressing and press drying are believed to be different, the bonded area to tensile strength relationship is not affected. However, this is not true if density is considered as the measure of bonding in the sheet. At constant sheet density, the press dried sheets have higher strength properties and lower scattering coefficient than wet pressed sheets. This observed “bonding” without consolidation is pronounced for TMP pulps, is observed in newsprint production [155], and is almost non-existent within kraft pulps [144, 154]. Poirier *et al.* [156] showed that when a TMP sheet is dried with superheated steam,

there is significant drop in scattering coefficient with subsequent increase in tensile strength, but without significant change in bulk (or density). In addition, they observed a significant decrease in fibrillation of the steam dried sheets as observed in SEM. Thus, it seems that bonding without consolidation can be at least partially attributed to the structural collapse of fines and fibrils.

Mechanical pulps are heterogeneous structures, where the range of particle size varies from fairly sound wood fiber particles with lengths of 2 mm and width of approximately 50 µm to small fines particles with size distributions anywhere from the nanometer scale to several hundred microns in length [2]. Due to this heterogeneity, there can be a large distribution of bonded area, i.e. the bonded area of the fine particles, bonded area of the fibers, and a range of everything in between. When an approach to measure bonded area similar to that used in chemical pulps is used to determine the total unbonded specific surface area (S_o) of the mechanical pulp sheet, it is unclear whether the pressing procedure induces bonding of all the fractions homogenously, or whether some structures experience less bonding due to the structure of the sheet.

Problem analysis

Mechanical pulps are mainly used for their favorable cost to quality ratio. The important quality parameters are related mainly to the heterogeneous nature of the pulp, where the high specific surface area fines particles assist in producing a sufficiently consolidated sheet with a porous structure, smooth surface and a high scattering coefficient.

In mechanical pulping most of the energy is consumed in specific surface area creation through fiber cutting, or fiber peeling, ultimately creating fines and fibers of various characteristics. Depending on the raw material, process type, and specific energy consumption, these particles have different ability to consolidate into a heterogeneous sheet, and ultimately create cohesion between particles through bonding.

Bonding is the key to the internal cohesion of paper. Nearly all mechanical interactions between fibers during papermaking take place through fiber bonds. Bonding is traditionally characterized into two separate factors: bonded area, and the strength of bonds per unit bonded area. This separation is especially important for pulps where the strength to unbonded surface area ratio is considered as one of the key product parameters, determining the ultimately quality and paper making potential of the pulp, as is the case in mechanical pulps. However, currently there are no applicable measurement methods that are able to separate bonded area from specific bond strength in mechanical pulps.

Ingmansson and Thode used refining and wet pressing to induce bonding in handsheets, and performed an extrapolation to zero tensile strength to obtain a totally unbonded specific surface area of dry fibers from light scattering. Later it was shown by many that refining creates significant amount of additional specific surface in high yield pulps altering the dry total unbonded area of the sheet. This prevents the use of refining as a bonding inducer. Today, although considered as a crude method for obtaining a measure of bonded area, currently the Ingmansson and Thode method is the most accepted method in assessing bonded area and specific bond strength in paper.

It has been shown that bonding in mechanical pulps cannot be significantly increased using the wet pressing procedure that is used for chemical pulps. This limitation can be

attributed to the stiff nature of the mechanical pulp fibers, and to the high lignin coverage of mechanical pulp, which reduces the surface available for bonding. Press drying at elevated temperatures has been shown to facilitate fiber collapse in lignin rich structures, and also induce lignin-lignin bonding when the temperature is brought close to the glass transition temperature of lignin. Also there are indications that wet pressing and press drying are similar in terms of mechanical pulp specific bond strength. Thus press drying is a possible approach to extend the bonding to strength relationship in mechanical pulps to increase the accuracy of the extrapolation to zero bonding when using the Ingmansson and Thode method.

A significant amount of research has been done to describe the bonded area to tensile strength relationship of chemical pulps. Today, the most widely used theoretical equation (actually semi-empirical) to extrapolate to zero tensile strength (using the Ingmansson and Thode wet pressing method to obtain an unbonded dry surface area of fibers), is the Page equation. The Page equation was initially derived for homogeneous structures, which were significantly well bonded. Thus, the equation assumes progressive fiber breaking even at low bonding levels, which results in a non-linear bonded area tensile strength relationship. For mechanical pulps, the tensile strength has been characterized empirically with high accuracy using only two factors: fiber length and a bonding indicator. This indicates that for these low bonding structures, fiber breaking is negligible, and also that the tensile strength bonded area relationship might be linear. This results in an underestimation of the bonded area when using the Page equation. However, due to the limitation of inducing bonding by wet pressing in mechanical pulps it is uncertain whether either of these approaches is applicable.

In summary:

1. Bonded area and specific bond strength are important characteristics in assessing the paper making potential of mechanical pulps, but there are no methods for measuring these properties in mechanical pulps.
    a. However, it is not clear what is the definition of bonded area, RBA or specific bond strength in heterogeneous pulps
2. The Ingmansson and Thode wet pressing procedure is a possible method for being able to measure these parameters, however, wet pressing is not sufficient to produce

significant amount of bonding in lignin rich mechanical pulps to enable accurate extrapolation to zero tensile strength. This can be possibly overcome by using press drying at elevated temperatures.

   a. However, pressing of heterogeneous structures might collapse and bond some fractions more than others, which then make the interpretation of the increase in tensile strength difficult.
   b. It is not known if the fiber properties (fiber strength), or bond properties (specific bond strength, shear bond strength) are altered during press drying.

3. The use of scattering coefficient as a measure of unbonded area in a mechanical pulp sheet is questionable due to
   a. The existence of particles smaller than certain fraction of the wavelength of light that possible facilitate bonding in mechanical pulp sheets but cannot be detected using light
   b. The increase in absorption coefficient due to the press drying procedure possibly alters the scattering ability of the material so that the scattering coefficient is reduced significantly due to the change in absorption coefficient.
4. In mechanical pulps there is no sound theoretical method that relates bonded area to tensile strength in order to extrapolate to zero tensile strength to obtain the total unbonded dry specific surface area of the sheet.
   a. It is not known whether fiber strength is a limiting factor for low bonded sheets.
   b. Thus it is unclear whether the specific bonded area tensile strength relationship is linear, or possible similar to the approach of Page equation, where fiber breaking is assumed to occur already at low bonding regions.

Thesis structure

In this thesis the problems identified in the problem analysis were approached using a multitude of research methods (Table 1). Each separate chapter in the results and discussion section is an independent publication, some of them published, submitted or to be modified for a journal publication. Thus each chapter can be read without reading the whole thesis. In each chapter parts of the literature review was used in the introduction sections.

Table 1. Objectives of the different publications

Research problem	*Chapter 1*	*Chapter 2*	*Chapter 3*	*Chapter 4*	*Chapter 5*	*Chapter 6*
1	X	X	X	X		
2		X	X	X		
3			X		X	
4	X					X

Chapter 1 is an initial study on the applicability of the Ingmansson and Thode method in mechanical pulps, and is the introductory chapter for the rest of the results and discussion section. The concept of using press drying to induce bonding in mechanical pulps is introduced. In chapter 1 the effect of time, temperature and pressure on bonding and sheet consolidation is examined. Also the response of individual mechanical pulp fractions to press drying is studied. The objective is to show how far the scattering-tensile strength relationship can be extended using press drying. The difference using the non-linear Page equation and a linear model to extrapolate to zero bonding is elucidated. Also, the shortcomings and possible problems related to the press drying assisted Ingmansson and Thode method are discussed. These are then approached in the following chapters.

In chapter 2 the problem of using scattering coefficient as a measure of specific surface area in mechanical pulps is approached using mercury porosimetry and nitrogen adsorption (BET) measurements with scattering coefficient measurements at various wavelengths of light. Also the interdependence of scattering coefficient and absorption coefficient is researched. The main objective is to find the highest absorption coefficient

(or wavelength) below which scattering coefficient is not significantly reduced. It is shown that scattering coefficient at a constant wavelength of light is an accurate approximation of the specific surface area in mechanical pulps independent of sheet composition. However, in order to avoid the significant absorption effect and obtain accurate scattering coefficient measurements the wavelength of light should be above 600 nm.

The homogeneity of the pressing procedure is approached in chapter 3. This is done by examining the additivity of scattering coefficient as a function of sheet composition at various wet pressing (23 °C) and press drying (120 °C) levels. A ternary approach is used. It is shown statistically that scattering coefficient does not strictly follow a linear addition rule. However, the deviation from the linear additivity is small (4.8%), and it is concluded that scattering coefficient follows a linear model as a function of the sheet composition.

Chapter 4 elucidates the meaning of relative bonded area (RBA) in heterogeneous structures. Due to the findings in chapter 2 and 3 it is reasonable to assume that specific bonded area in mechanical pulps also follows a linear addition rule as function of sheet composition. This results in and RBA that, by definition, is intrinsically non-linear. It is proposed that specific bonded area rather than RBA is used to describe area involved in bonding.

Throughout the study wet pressing is used in parallel with press drying believing that press drying would be an extension of the wet pressing in terms of scattering-tensile relationship. However, this is not true. Wet pressing in most cases produces higher scattering coefficient at constant density or tensile strength. In Chapter 5 the different collapse mechanisms associated with wet pressing and press drying are approached using mercury intrusion porosimetry pore size distribution data, handsheet physical testing data and SEM imaging. It is shown that the significantly higher scattering coefficient at constant density in wet pressing is caused by the different pore distribution of the fines fraction. It is also shown that the difference in pore size distribution in wet pressed and press dried fines did not alter the scattering-tensile strength relationship of pure fines sheets, suggesting that the total unbonded specific surface area (S_o) is not altered in press drying. This results in that at constant fines bonded area ($S-S_o$) press

dried fines sheet has significantly lower density than the wet pressed fines. It is suggested that in a mixed sheet where fibers are present this increases the distance between the fibers and is likely to decrease the stress transfer efficiency between them, which is then observed as a decrease in specific bond strength. However, at higher pressing pressure the wet pressing and press drying scattering-tensile curves united, indicating that at higher densities the stress transfer efficiencies approach each other.

Chapter 6 focuses on the significance of fiber failure in mechanical pulps. The regime where the dominant mechanism of paper failure transitions from negligible fiber failure to significant fiber failure is believed to be at the maximum tear index. Press drying and wet pressing are used to increase bonding. It is indirectly shown that most mechanical pulps operate in significant fiber failure domain. The domain transitions from negligible to significant fiber failure in the range of 30-40 Nm/g of tensile strength or 0.3-0.45 bonding index (tensile strength divided by zero span tensile strength). The significance of the fiber failure in terms of bonded area – tensile strength relationship is discussed.

Experimental materials and methods

Pulps used in this study

The preliminary research was done using a commercially available News grade southern pine TMP, with a freeness of 110 CSF. The southern pine (approximately 80% *Pinus taeda*) sample was collected from the storage tower before bleaching. The fraction mixing studies were done using two commercially available Thermo-Mechanical Pulps (TMP). Both pulps were from the same species (Norway spruce- *Picea abies*), but were refined to two distinctly different freenesses. The first one was a printing and writing grade TMP (35 CSF), and the second one a newsprint grade TMP (110 CSF). Both Norway spruce samples were collected from the disc filter prior to bleaching tower. The basic properties of the pulps are shown in Table 2.

Table 2. Basic properties of pulps used in the study

Grade **Species**	**Southern pine TMP** News *80% Pinus taeda*	**Norway spruce TMP** LWC *Picea abies*	**Norway spruce TMP** News *Picea abies*
CSF, mL	110	35	110
Bauer-McNett			
R28	33.80%	28.87%	44.45%
R48	17.90%	22.26%	11.76%
R100	7.60%	6.99%	7.29%
R200	1.20%	6.23%	4.63%
P200	39.50%	35.65%	31.87%
FQA, LW fiber length, mm	1.52	1.442	1.68
Tensile index, Nm/g	26.55	51.09	34.33
Scattering coefficient, m^2/kg	58.50	67.09	61.52

Bauer-McNett Fractionation

Pulp fractionation was conducted using a modified method, where 30 O.D. grams of pulp was fractionated for 45 minutes. In the Bauer-McNett apparatus 14, 28, 48 and 200 mesh screens were collected. The fiber retained on 14, 28 and 48 mesh screens was combined. In addition all the excess water passing the 200 mesh screen was collected

into a 55 gallon barrel. After the initial fractionation, in order to obtain a fines free fiber fraction, the combined R14, R28 and R48 fiber fraction was refractionated using the same procedure as described earlier.

Figure 11. Bauer-McNett apparatus

The fiber length analysis was done using the Fiber Quality Analyzer (FQA) for each pulp and Bauer-McNett fraction separately. The results for each fraction are shown in Table 3. Light microscope images of the fractions are shown in Figures 12-14 for the newsprint grade Norway spruce TMP (110 CSF).

Table 3. FQA fiber length and curl of fractions

		FQA Fiber length,mm			FQA Curl
Pulp	Fraction	Arithmetic	LW	WW	Arithmetic
Southern pine TMP	R28	2.05	2.42	2.72	0.043
110 CSF	R48	1.28	1.62	1.95	0.032
	R100+R200	0.492	0.703	1.026	0.03
Norway spruce TMP	>R48*	1.49	2.03	2.47	0.045
35 CSF	P200	0.105	0.151	0.369	0.089
Norway spruce TMP	>R48*	1.9	2.555	3.13	0.0495
110CSF	R200	0.283	0.4905	0.732	0.037
	P200	0.1055	0.147	0.3625	0.1245

* includes R14 R28 and R48

Figure 12. Fiber fraction (>R48) of the Newsprint grade TMP (110 CSF)

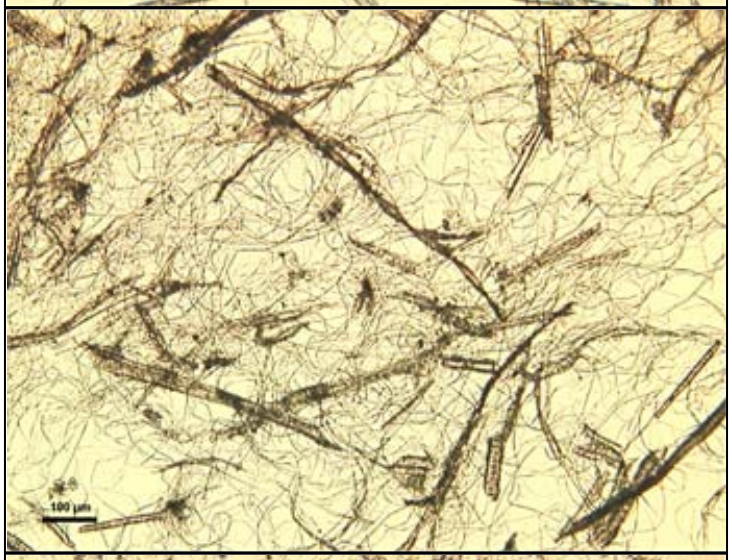

Figure 13. Middle fraction (R200) of the Newsprint grade TMP

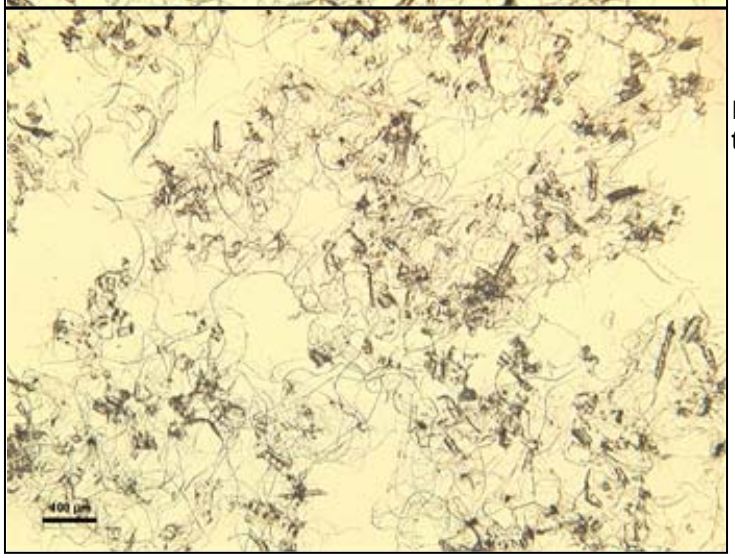

Figure 14. Fines fraction (P200) the Newsprint grade TMP

Fiber cross-sectional dimensions of the long fiber fractions were determined using the FQA and light microscopy. Fiber widths and cell wall thickness were measured using a half automated system existent at the Institute of Paper Science and Technology. Approximately 1% dispersed solution of dyed fibers was placed on a glass slide, and individual fibers were then characterized using 400X magnification. At least 200 fibers per sample were measured. The measurements included fiber widths, cell wall thicknesses, their distributions, as well as calculated parameters, such as runkel ratio and fiber perimeter.

Table 4. Cross-sectional properties of the fiber fractions, FQA coarseness and light microscopy fiber width and cell wall thickness

		Coarseness	Light microscopy	
Pulp	Fraction	mg/m	Width, um	Wall thickness, um
Norway spruce TMP 35 CSF	>R48*	0.224	4.72	37.14
Norway spruce TMP 110CSF	>R48*	0.251	5.14	38.28

* includes R14 R28 and R48

Fines collection

The excess water passing the 200 mesh screen was collected into a 55 gallon drums. These drums were then left to stand untouched for the fines to settle onto the bottom of the barrel. This initial settling lasted 3 days, after which the excess water was removed using a low pressure pump. Every barrel yielded approximately 10 O.D. grams of fines at a consistency of 0.5-1.5 g/L. After the initial settling the fines slurry was collected into a tall barrel with a small diameter, and the barrel was stored in a cold room at a 4 °C temperature for 24 hours, after which the fines, due to reduced mobility had settled more, the excess water was removed again. Ultimately a consistency of between 4 and 5 g/L was obtained. Throughout the study a total of 52 fines collection runs were done.

Figure 15. Fines settling

The fines content in the fiber (R48) and fines (P200) mixed sheets was determined using the DDJ Tappi standard T 261 cm-00. For sheets with middle fraction mixed in, the contents of various fractions were estimated based on the initial mixing.

Handsheet forming

Handsheet were formed using a standard British handsheet mold with recirculated white water and a 150 mesh screen. Before each collected sample set a number of handsheets were formed in order to attain an appropriate level of fines in the recirculation to keep the fines content of the sheets constant. In most cases the number of handsheets was 8 before the samples could be taken. Fines handsheets were formed on a dense glass fiber filter paper (Whatman 934 AH), which was placed on top of the wire in the standard British handsheet mold.

Figure 16. Standard British handsheet mold with recirculation

Wet pressing

Wet pressing of the sheets was done immediately after the sheets were formed. A standard hydraulic press was used to press individual handsheets between a stack of blotter papers and a chrome plate of the other side of the handsheets. All wet pressed handsheets were pressed for 1 minute using variable pressures. Pressure was calculated based on the area of the handsheet and the load at pressing.

Press drying

Initial press drying (Southern pine TMP and Printing and Writing grade Norway spruce TMP studied) was conducted using a standard Carver press with heated platens on both sides. In the initial studies the handsheets were stored in sealed plastic bags between blotters in a cold room at 4 °C for 24 hours prior to pressing. Later an automated press was designed to better control the pressing procedure. This enabled an immediate press drying of the sheets after the sheets were formed. The press drying was done using a compiled sandwich that consisted of a felt, wetted blotter paper, smooth filter paper, handsheet, chrome plate and a filter paper. The purpose of the sandwhich was to provide a route for the steam to escape, as well as prolong the time at higher moisture content and temperature for more efficient glass transition effect to occur. All handsheets were pressed until they were dry. The pressing time depended on furnish used, and

varied between 3 minutes (100% R48 fiber sheets) and 6 minutes (100% P200 fines sheets). Platen temperature was varied.

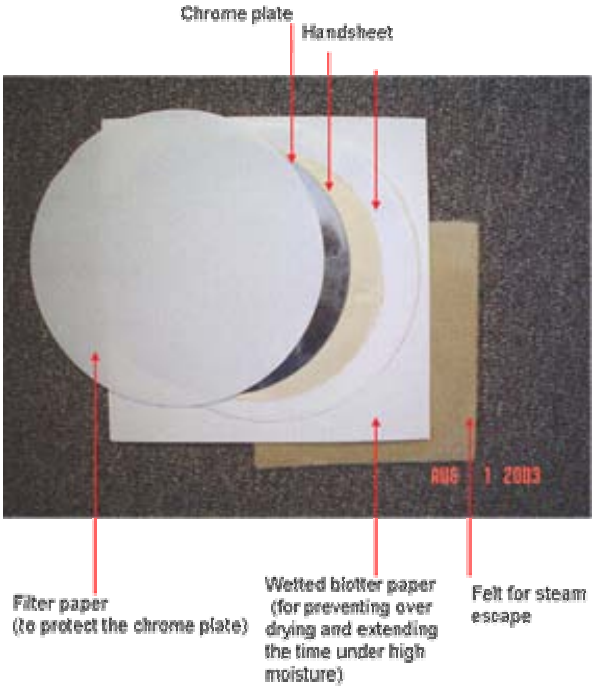

Figure 17. Compiled sandwich used in press drying

Figure 18. Press drying apparatus

Testing

All testing was performed at 50% Relative humidity and all sheets were preconditioned at 20% relative humidity.

Strength properties

Tensile strength testing for the Southern pine TMP was performed according to the Tappi standard T 494. The Norway spruce pulps were measured using a modified method, where the strip width was 15 mm, strip length only 5.08 cm (2 inches), and strain velocity was set at 0.5 inches/minute. The short span length was used to minimize the amount of flaws in the 100% fines (P200) sheets. The strain rate was reduced in order to produce enough data points for a good stress-strain curve. Tensile testing was done using an Instron tester with mounted iron clamps.

Zero span tensile testing was done using a Pulmac zero span tensile tester. The span length was set to 0 and the clamp pressure to 80 psi.

Tear resistance was measured using a pendulum type Elmendorf tear apparatus, using 4 sheets in one tear test. The procedure followed the Tappi T414 method.

Z-direction tensile strength was measured using the STFI ZDT tester, and followed the Tappi standard T 541 procedure.

Scattering coefficient

Scattering coefficients were measured according to the Tappi T1214 standard, at 572 nm wavelength and 15° angle. This method was chosen in order to avoid the effect of high adsorption coefficient on the scattering measurement, as well as to avoid the surface gloss effect on the measurement.

The UV/vis spectra were recorded on a Perkin-Elmer Lambda 900 UV/vis spectrometer equipped with a diffuse reflectance and transmittance accessory (PELA-1000). The accessory is essentially an optical bench that includes double-beam transfer optics and a six-inch integrating sphere. Background corrections were recorded using a Labsphere SRS-99-020 standard. Reflectance data were measured over a black and a white background with known reflectance values. For each sample and background, an

average of five measurements was utilized to determine both the light scattering (*s*) and light absorption (*k*) coefficients. The absorption and scattering coefficients were calculated from the reflectance data by means of the Kubelka-Munk. Data were collected from 300 to 800 nm.

BET nitrogen adsorption and mercury intrusion porosimetry

BET was measured at Micromeritics, Norcross, Georgia, U.S.A., using the TriStar 3000 nitrogen absorption surface area equipment. The nitrogen gas partial pressure was changed by altering the helium/nitrogen mixture. All the samples were degassed at 60ºC. Mercury intrusion porosimetry specific surface area measurements were performed also at *Micromeritics,* using the AutoPore IV equipment. The intrusion pressure and pore size was related using the Washburn equation. Since the Washburn equation is based on cylindrical capillaries with circular openings, the specific surface area based on the voidal pore structure was calculated using a cylindrical pore model assumption. The pressure range used in the mercury porosimetry was between 1.3 - 60.000 psi, corresponding to a pore diameter range from 150 um to 4nm.

Ultrasonic in-plane and out-plane testing

Wave propagation at ultrasonic frequencies provides a method for non-destructive analysis of paper moduli. The method is based on the dependency of the velocity of the ultrasound on the elastic stiffness of the material, according to the following equation:

$$V = \left(\frac{C}{\rho} \right)^{1/2}$$

,where

V= ultrasound propagation velocity (m/s)
C= elastic stiffness constant (N/m^2)
ρ= density of the material (kg/m^3)

The measurements of all nine orthotropic elastic stiffness constant was first shown by Mann et al.[157], and later developed and refined for out-of-plane elastic stiffness constant by Habeger et al [158] .

In this research the in-plane longitudinal (C_{11}) and shear moduli (C_{66}) were tested using an automated IPST ultrasonic in-plane robot tester. The Poisson ratios were also calculated based on the in-plane longitudinal and shear moduli. Also out-of plane longitudinal modulus (C_{33}) was measured using a different tester, where two piezoelectric transducers facing each other on opposite sides of the sample are used to launch a pulse through the sheets and to record the transmitted signal. The incident pulse has a frequency close to 1 MHz. Soft neoprene interfaces are used to reduce the variability caused by the heterogeneous sample surface. The transit time through the sheet is obtained by cross-correlating the transmitted pulse through it with a reference pulse obtained from a material with known elastic properties (thin aluminum shim).

Figure 19. IPST ultrasonic modulus robot.

Cross-sectional sample preparation and Scanning Electron Microscope (SEM imaging)

Cut handsheets were embedded into epoxy resin using the mixing procedure shown in Table 5. The resulting epoxy stub was then polished using 6 different grit sizes (120, 320, 800, 1200, 2400 and 4000). The first three coarse grinding was done using a grinding machine, and the last three were polished by hand.

Table 5. Preparation of Spurr resin

Ingredients	ml
ERL 4206 (VCD	9.2
DER 736	8.25
NSA	25.5
DMAE	0.3

After polishing the stub was etched for 5 minutes in a solvent consisting of 4 grams of KOH pellets in 20 ml of 100% methyl alcohol and 10 ml of propylene oxide. After etching the samples were thin film cold coated. The cross-sections of the sheets were analyzed using secondary electron image.

Fines bromination and SEM imaging of brominated fines fiber mixed sheets

30 O.D. grams of 35 CSF Norway spruce TMP P200 fines was halogenated with bromine. Then brominated fines were mixed in with the R48 fiber fraction obtained from the same pulp (10%, 25% and 45% P200 fines in R48 fiber sheet) and inspected in SEM. No allowance was made for the weight of the bromine in the treated fines. Bromination was done following the procedure described by de Silveira *et al.* [159]. 10 mL of liquid Bromide (Br_2) was added into 30 O.D. grams of fines. The bromination was conducted at room temperature letting the bromide react for 2 hours, by mixing every 5 minutes. After 2 hours of bromination the fines were washed 6 times using a dense glass fiber filter paper (Whatman 934 AH). The total bromine content of the fines was 7.3% by weight, measured using a method described below.

The total Bromine content of the halogenated fines was determined by combusting the paper in an oxygen bomb, washing the bomb with water after combustion and quantifying bromide ion by capillary ion analysis. The sample was combusted using a Parr Bomb. The sampling technique used was chosen because we expected to find a trace amount of bromine in the sample. The entire handsheet was cut into small pieces and weighed into 3 separate stainless steel crucibles. 2 ml of water was placed in the bomb, the sample and fuse wire were then placed into the bomb and it was charged with oxygen. To minimize the nitrate formed the oxygen was vented from the bomb to flush out air (nitrogen) and then the bomb was refilled. The bomb was then placed in a water bath and the sample ignited. Once the water bath reached an equilibrated temperature the bomb was removed and vented. A small amount of water was used to rinse the sampling crucible and the next aliquot was placed in the bomb and combusted in the same manner. This was repeated for a total of 3 burns. All combustion products were collected in the same bomb; it is not rinsed between samples. After all combustions were completed the bomb was rinsed and collected to a known volume. This solution was then analyzed using Electrophoretic Capillary Ion Analysis, against a calibration curve for bromide ion. The sample was diluted as necessary to keep the peaks of interest in the calibration range.

Cross sectional samples of the brominated fines (P200) and fiber (R48) mixed sheets were prepared using a method, where small pieces of cut handsheets (3mm X 10 mm) were embedded in an epoxy polymer of low viscosity. The resulting capsules were trimmed and cut using a microtome (diamond blade) in order to produce a sufficiently smooth surface for imaging. Then the cut capsules were mounted on a carbon stub, and the stub with the capsule was carbon coated with ultra thin carbon layer using evaporated carbon (Figure 20). These stubs were then analyzed using backscattered electron imaging.

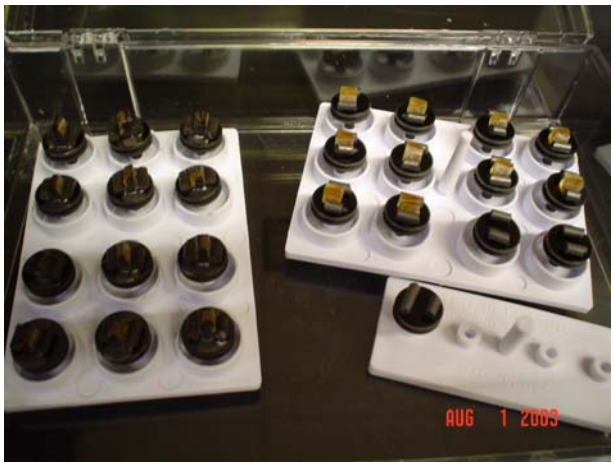

Figure 20. Carbon coated cross-section capsules of brominated fines (P200) and fiber (R48) mixed sheet samples.

Results and discussion

Chapter 1: Study of the applicability of the Ingmansson and Thode method using press-drying to increase bonding in mechanical pulps

Abstract

In mechanical pulps two factors are generally adequate to describe the properties of these pulps. These factors are bonding and fiber length. Bonding has been traditionally described with two separate variables: bonded area and specific bond strength. For practical purposes it is important to separate these two variables, because bonded area affects the optical and strength properties, whereas specific bond strength is only reflected in the strength properties of the sheet. In chemical pulps the Ingmansson and Thode method is traditionally used to distinguish between these two parameters. However, in mechanical pulps wet pressing does not induce enough bonding in order to determine these parameters. In this paper the problem is circumvented by using press drying to induce bonding. It is shown that efficient bonding increase of mechanical pulp can be achieved by press drying the sheets until they approach their 50% relative humidity moisture content. The use of higher temperatures decreases the time to dry the sheet, and thus the time to produce the bonded sheet. The use of elevated pressing pressures in press drying significantly induces bonding in all the fractions in mechanical pulps, and ultimately produces extended tensile strength scattering coefficient relationships, similar to those of Ingmansson and Thode method in chemical pulps. Two approaches were used to separate specific bond strength from specific bonded area (Page equation and linear model). Although fundamentally different, both approaches fit the data well. The problems related to the applicability of Ingmansson and Thode method in mechanical pulps is discussed.

Introduction

In terms of fiber development, in mechanical pulping most of the energy is consumed in the creation of specific surface area, and is created though fiber separation, cutting and peeling, always creating a significant amount of very high specific surface area fine particles [2, 11, 16, 26, 160]. This created specific surface area significantly helps the consolidation of the sheet in drying through the Campbell's forces [98]. However, it has been shown that not all specific surface area created in the process is similar in quality,

but the papermaking characteristics are specific to each raw material, process configuration and specific energy consumption level [2, 8, 9, 13, 26, 28, 30, 56, 161, 162].

Generally mechanical pulps can be characterized using two principal components [7, 61, 62]. These components have been identified to be related to the fiber length of the pulps and bonding of the sheet. Traditionally the bonding of mechanical pulps has been characterized using z-directional strength testing [38], or from a pulp slurry using specific surface area measurements of various fractions [7, 19]. Bonding can be separated into two independent variables: bonded area and specific bond strength [1, 60]. This separation has been often strongly criticized, mainly due to several observations that relate bonding strength to the fiber properties, indicating that specific bond strength is not an intrinsic bond characteristic, but rather a description of the fiber-bond-fiber system [1]. For practical purposes the separation of bonded area from specific bond strength is important, due to the fact that bonded area affects both strength and optical properties, where specific bond strength, by definition, has no effect on the optical properties. This is especially important for pulps that are used for their optical properties but lack strength, i.e. mechanical pulps.

The Ingmansson and Thode [59] wet pressing method is the most widely used method in chemical pulps for determining bonded area [104, 118]. In the method the sheet strength is increased using wet pressing. At the same time the scattering coefficient decreases, which is shown to correlate with nitrogen absorption specific surface area, indicating an increase in bonded area. In order to determine the total unbonded free area of dry fibers, which is needed in determining the bonded area, the scattering coefficient is extrapolated to zero tensile strength (zero bonding). Although considered as crude method, it still remains the only readily applicable method for estimating bonded area in chemical pulps [117, 118]. In mechanical pulps this subject has been rarely approached, and thus the understanding related to the significance of bonded area and specific bond strength is nowhere close to that of chemical pulps. In order to rise to the level of understanding comparable to where the paper physics community is in chemical pulp structures, it is essential that research should be directed to the understanding of bonding in these heterogeneous mechanical pulp structures. The logical approach is

then to use the Ingmansson and Thode method, which is fairly well understood by the paper physics community.

However, traditional wet pressing does very little to the mechanical pulp sheet, leaving it fairly uncollapsed and porous, indicating that the bonding can not be sufficiently increased [50, 143]. This can be attributed to the high lignin content of these pulps. The fiber wall in mechanical pulps fibers has a significant amount of lignin [2], which is not plasticized under normal temperatures [149], and thus the fibers cannot be sufficiently collapsed in wet pressing. Also surfaces of all the particles in the pulp have a significant proportion of their total area covered by lignin [55], which has been shown not to form adhesive properties at temperatures below their softening temperature [25]. This implies that the bonding of mechanical pulps can be significantly increased when higher temperatures are used in pressing.

Press drying has been shown to increase collapse of fibers and increase bonding in lignin rich pulps, observed as significant reduction in scattering coefficient and increase in tensile strength [50, 148]. Thus, it is of interest to increase bonding of mechanical pulps using a modified Ingmansson and Thode method, where higher temperatures are used to plasticize the material that is to be bonded, as is the case in chemical pulps.

In this paper a series of experiments with variable pulps and pressing methods were collected into one large publication. Thus, this publication serves as a starting point for guiding the direction of further research on understanding the applicability of the Ingmansson and Thode method in mechanical pulps. The main objective of this paper was to study the applicability of press drying to obtain Ingmansson and Thode method type scattering coefficient-tensile strength relationships in mechanical pulps. Here the effect of time, temperature and pressure was elucidated in order to select the optimum pressing conditions for press drying of mechanical pulps. Also fundamental aspects of bonding-tensile strength relationship in mechanical pulps were studied using two distinctly different approached: negligible fiber failure model (linear) and significant fiber failure model (Page equation).

Experimental

Time, temperature and pressure study: A commercial printing and writing grade (35 CSF) Norway spruce TMP was hot-disintegrated according to the Tappi standard (T-262). Handsheets were made using a standard British handsheet mold with white water recirculation. Sheets were pressed at various temperatures, pressures and pressing times directly after couching. The pressing was conducted between cintered porous metal plates (Mott corporation, 1/8 inch thick, 2 µm average pore size), using an automated press equipped with two heated platens. Scattering coefficient was measured using the Tappi (T 1214 sp-98) standard with 572 nm wavelength. Tensile strength was measured using the Tappi (T 494) standard, but with the exception of a reduced span length of 2 inches and reduced strain velocity. This adjustment was done to minimize the effect of faulty strip edges due to strip cutting. The 0.5 inches/min strain velocity was used, in order to be able to gather enough data points (20 points/sec) to produce a sound stress-strain curve.

Pulp fractions study: A commercial Southern pine 120 CSF Newsprint TMP pulp was used in the study. Pulp was fractionated using the Bauer McNett classifier with 28, 48, 100 and 200 mesh screens. 20 grams of pulp was fractionated at one time using 30 minute fractionation time. R100 and R200 were later combined. P200 fraction was not collected. All handsheets were wet pressed at 60 psi for 5 minutes before testing. Press drying was done using a standard Carver press with installed heated platens on both sides. Platen temperature of 130 °C was used, and sheets were pressed for 3 minutes. Press drying was conducted using a sandwich of felt, wet blotter, mechanical pulp handsheet, chrome plate and filter paper. Fiber length was measured using FQA fiber analyzer. Tensile strength was measured using Instron tensile tester according to the Tappi standard T-494. Scattering coefficient was measured using a Technodyne brightness analyzer using x-filter, at 580nm wavelength, in order to avoid the high absorption effect on scattering coefficient. Zero span tensile strength was measured using a Pulmac zero span tensile tester. SEM imaging was done from cross-sections from a different batch of Southern pine TMP (110 CSF) pulp from the same mill. Pressing was conducted as described earlier. The cross-sectional handsheet strips were mounted in standard epoxy, then polished using progressively smaller sandpaper grain sizes, and eventually etched.

Freeze drying study: A commercial hot-disintegrated Southern pine 120 CSF Newsprint TMP pulps was used in the study. Prior to press drying handsheets were not wet pressed, but only couched. Press drying was done using a standard Carver press with installed heated platens. Platen temperature of 130 °C was used, and sheets were pressed for 3 minutes. Press drying was conducted using a sandwich of felt, wet blotter, mechanical pulp handsheet, chrome plate and filter paper. Wet pressing was conducted using a pressing pressure of 60 psi and pressing time of 5 minutes. Wet pressed sheets were restraint dried. Freeze drying was conducted at -72 °C for 24 hours.

Results

The effect of temperature on the scattering coefficient and tensile strength

Temperature, time and pressing pressure effect studies were conducted with the objective to determine the optimum pressing conditions for obtaining a maximum extension of the scattering coefficient - tensile strength relationship.

The effect of pressing temperature on the bonding development of mechanical pulp was studied using a Norway spruce highly refined (35 CSF) TMP. Sheets were pressed at 49 psi for 180 seconds, and the tensile strength and scattering coefficient was determined (Figure 21). There was a significant decrease in scattering coefficient and increase in tensile strength at temperature above of 100 ^{o}C, which then leveled off as a temperature of 120 ^{o}C was reached.

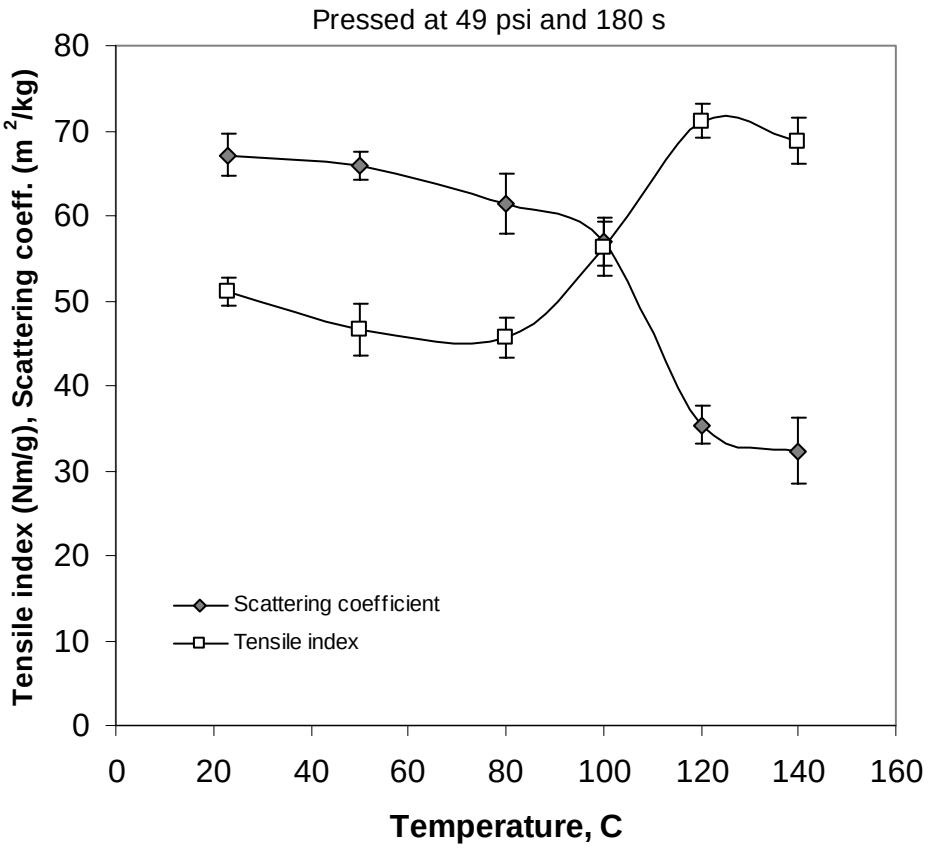

Figure 21. Tensile strength and scattering coefficient of Norway spruce TMP (35 CSF) pressed at 49 psi and 180 seconds using a range of press platen temperatures.

This significant increase in bonding, which manifested itself as the increase in tensile strength and decrease in scattering coefficient, was caused by the drying of the sheet during pressing, as shown in Figure 22. The bonding began to develop as the sheets were dried under pressure below 5 g/g moisture content. At a temperature of 120 °C the sheet was completely dried under pressure, eventually producing a sheet with very high bonding. After the sheet was completely dry, the increase in temperature from 120 °C to 140 °C did not have any significant effect on bonding.

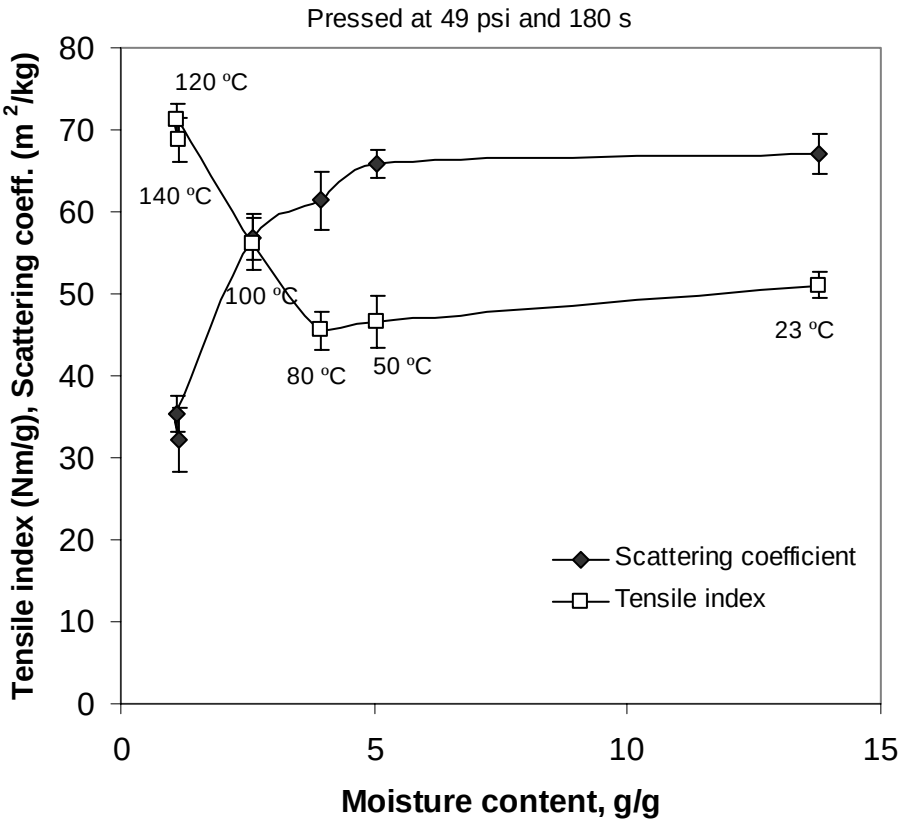

Figure 22. Tensile strength and scattering coefficient of Norway spruce TMP (35 CSF) pressed at 49 psi and 180 seconds using a range of press platen temperatures. Plotted as a function of the sheet moisture content (gram water/gram of fiber) after pressing.

The effect of pressing time on the scattering coefficient and tensile strength

The effect of time was studied by pressing Norway spruce TMP (35 CSF) pulp handsheets at 100 °C and 163 psi for 90, 190, 300 and 510 seconds. The bonding began to significantly develop after 200 seconds of pressing, eventually reaching a maximum approximately at 300 seconds, beyond which the bonding was not significantly affected (Figure 23). The obtained minimum scattering coefficient (t-test p=0.998) and maximum tensile strength (t-test p=0.656) were the same as were obtained using the same pressing pressure but higher temperatures (120 °C) and shorter time (180 seconds). Thus, the bonding development at constant pressing pressure was

independent of temperature when temperatures above 100 °C were used and the sheet was completely dried under load.

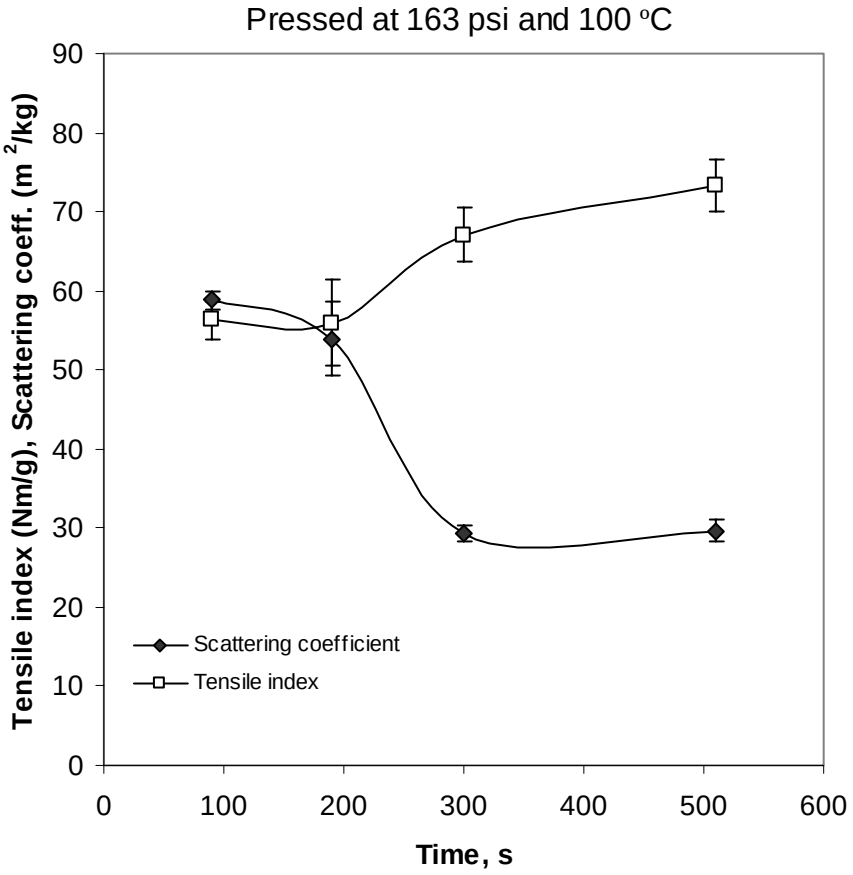

Figure 23. Tensile strength and scattering coefficient of Norway spruce TMP (35 CSF) pressed at 163 psi and 100 °C using variable pressing times.

The effect of time on the bonding development was caused by the drying of the sheet (Figure 24). Significant increase in bonding was achieved as the sheets were pressed to a moisture content of approximately 1.6 g/g, which was significantly lower than in the temperature effect series, where the bonding started to develop already at 5 g/g moisture content. This can be explained by the different pressing pressures used in the two studies. In the time effect study higher pressing pressures were used, which created a sheet with higher initial bonding.

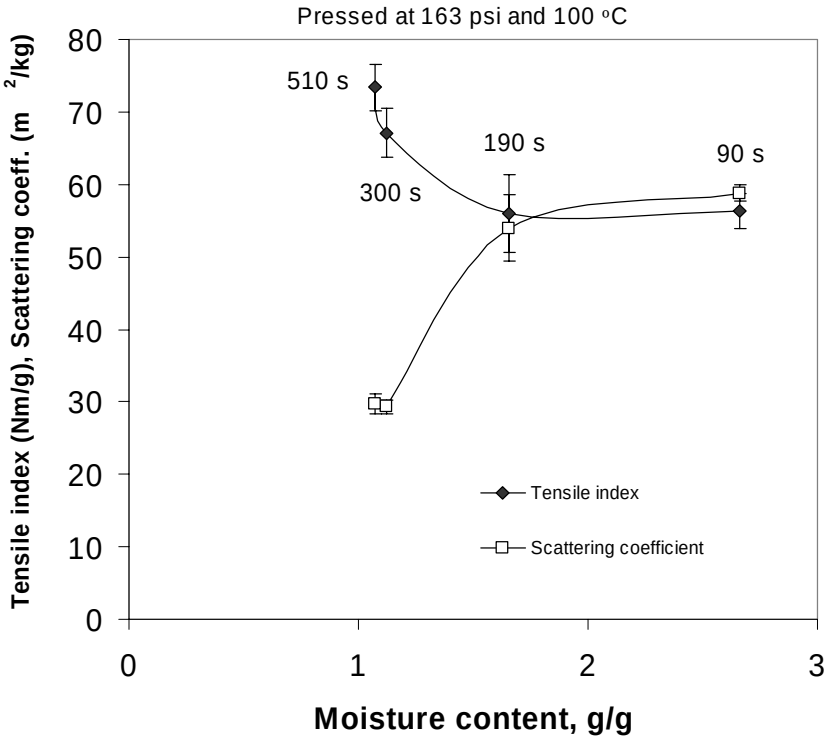

Figure 24. Tensile strength and scattering coefficient of Norway spruce TMP (35 CSF) pressed at 163 psi and 100 °C using variable pressing times. Plotted as a function of sheet moisture content (gram water/ gram fiber) after pressing.

The effect of time and temperature on the bonding development compared at a constant moisture content after pressing

The time and temperature affected the drying of the sheet during pressing. Here the effect of time and temperature was studied independent of the drying effect by plotting the scattering coefficient and tensile strength as a function of sheet moisture content after pressing for sheets pressed at constant pressure but various temperatures and times. Scattering development was independent of time and temperature, as shown in Figure 25, where the scattering coefficient of sheets pressed at 163 psi using variable pressing times and temperatures plotted on a single curve as a function of sheet moisture content after pressing.

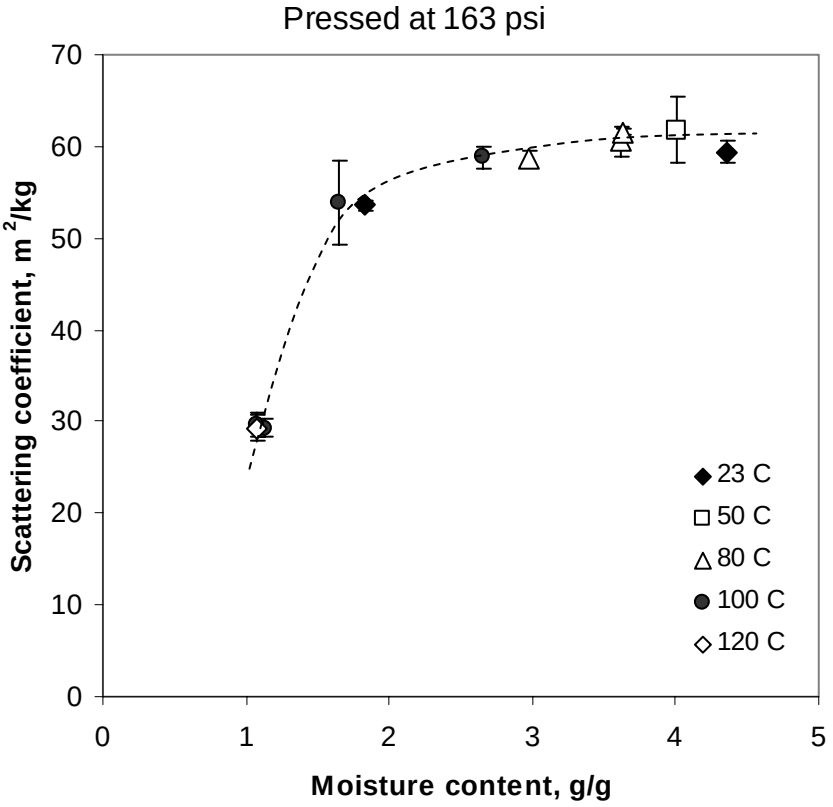

Figure 25. Scattering coefficient of Norway spruce TMP (35 CSF) pressed at 163 psi using variable pressing times and temperatures. Plotted as a function of the sheet moisture content (gram water/ gram fiber) after pressing. Pressing time and temperature were varied.

Tensile strength development as a function of sheet moisture content after pressing was dependent on the pressing temperature (Figure 26). Sheets pressed at 23 °C had slightly higher tensile strength at a constant end moisture content of the sheet after pressing than sheets pressed at elevated temperatures. However, the temperature dependency of the tensile strength decreased as the sheets were pressed to lower moisture content by using longer pressing times, eventually converging into a common tensile strength.

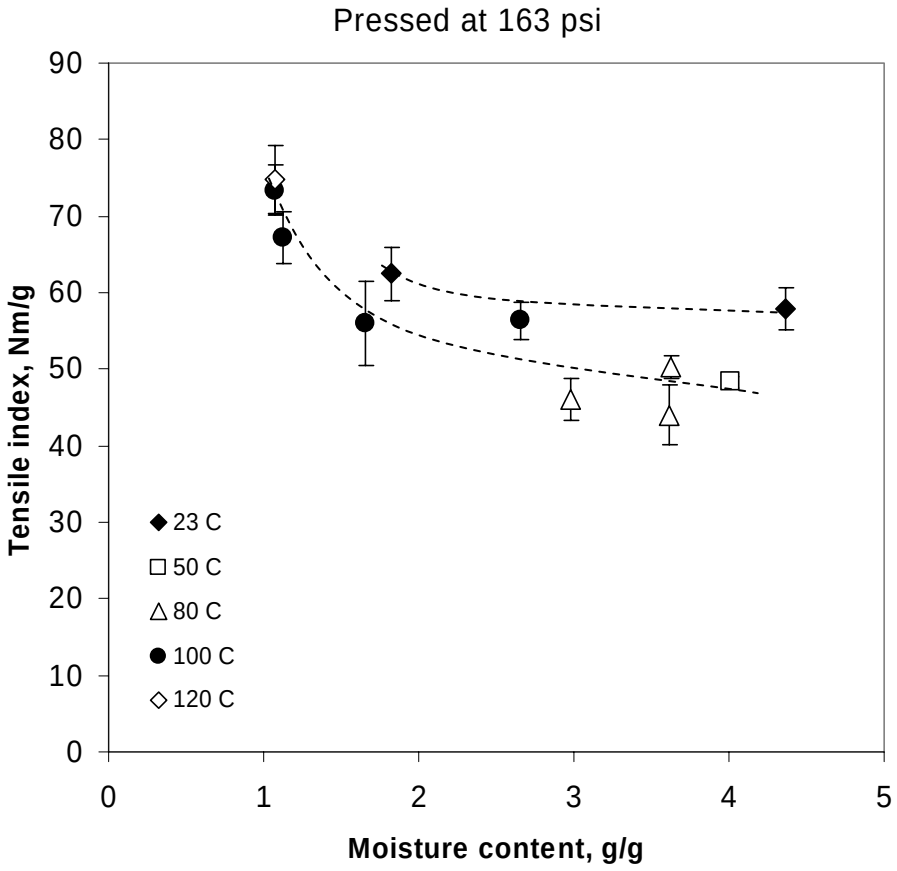

Figure 26. Tensile strength of Norway spruce TMP (35 CSF) pressed at 163 psi using variable pressing times and temperatures. Plotted as a function of sheet moisture content (gram water/ gram fiber) after pressing. Pressing time and temperature were varied

The lower tensile strength of sheets pressed at higher temperatures, above 50 ^{o}C, compared at constant sheet end moisture content after pressing was explained by the difference in the consolidation mechanism of the sheets at various temperatures. Figure 27 depicts the density development as a function of the sheet moisture content after pressing. Sheets pressed at 23 ^{o}C and constant pressing pressure had higher densities at constant moisture content, producing a more consolidated sheet. This was likely due to the lower surface tension of water at higher temperatures, which reduces the Campbell's forces.

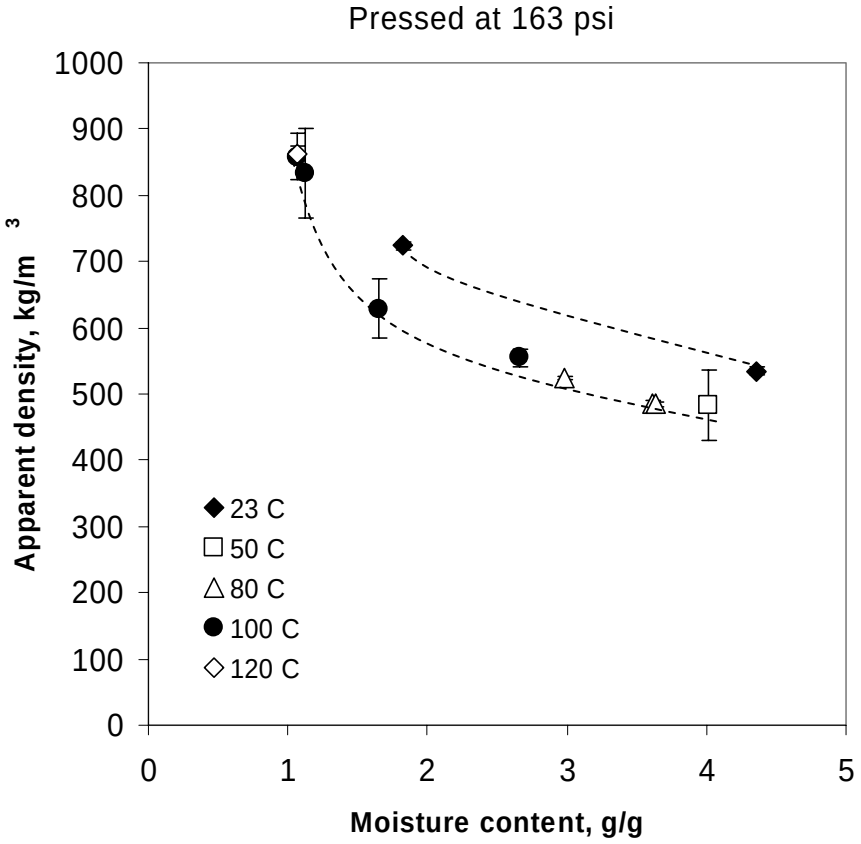

Figure 27. Apparent density of Norway spruce TMP (35 CSF) pressed at 163 psi using variable pressing times and temperatures. Plotted as a function of sheet moisture content (gram water/ gram fiber) after pressing. Pressing time and temperature were varied.

The effect of pressing pressure on the scattering coefficient and tensile strength

The effect of pressing pressure independent of sheet moisture content after pressing was studied using a pressing temperature of 120 °C and pressing sheets for 180 seconds. This resulted in that all sheets were dried under a pressing load. The pressure was varied between 0 and 330 psi. The increase in tensile strength was associated with a consistent decrease in scattering coefficient, showing a very sensitive response to the applied pressing pressure (Figure 28). Ultimately the tensile strength was maximized at a pressing pressure of approximately 163 psi.

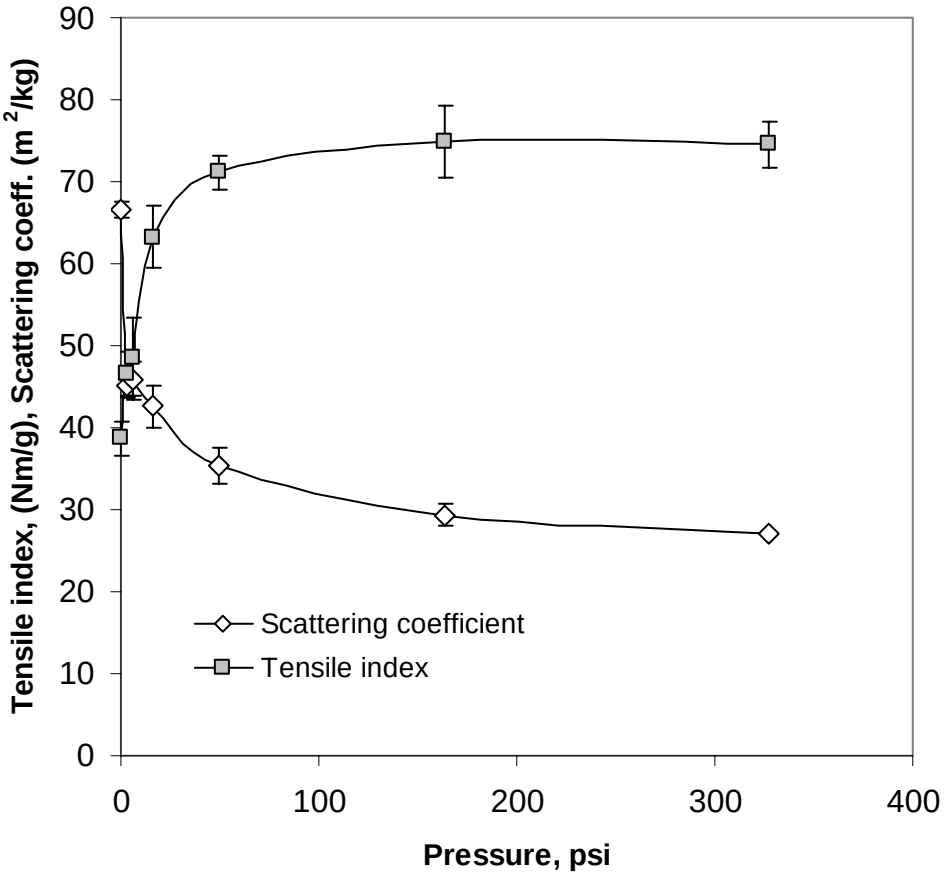

Figure 28. Tensile strength and scattering coefficient of Norway spruce TMP (35 CSF) pressed at 120 °C and 3 min using variable pressing pressures.

Bonding development of mechanical pulp fractions in relation to whole pulp bonding

Whole pulp TMP showed efficient response to variable press drying pressure, ultimately producing sheets with significantly higher bonding, which manifested itself as increased tensile strength and decreased scattering coefficient. In order to examine the effect of pressing pressure on the various sheet components (pulp fractions) a Southern pine Newsprint grade TMP (110 CSF) pulp was fractionated using a Bauer-McNett apparatus into a long fiber (R28), short fiber (R48) and middle fractions (R200). The pressing response of individual fractions was compared to the response of the whole pulp. Figure 29 depicts how all individual fractions reduce scattering coefficient as a function of

pressing pressure. In addition, the scattering coefficient reduction for all fractions showed similar response to the pressing pressure at high pressing pressures as the whole pulp, indicating a homogenous bonded area development of all fractions in the whole TMP pulp. At low pressing pressures the reduction in scattering coefficient of the whole pulp was more due to the reduction of scattering of the middle fraction (R200), and possibly also fines (Figure 29).

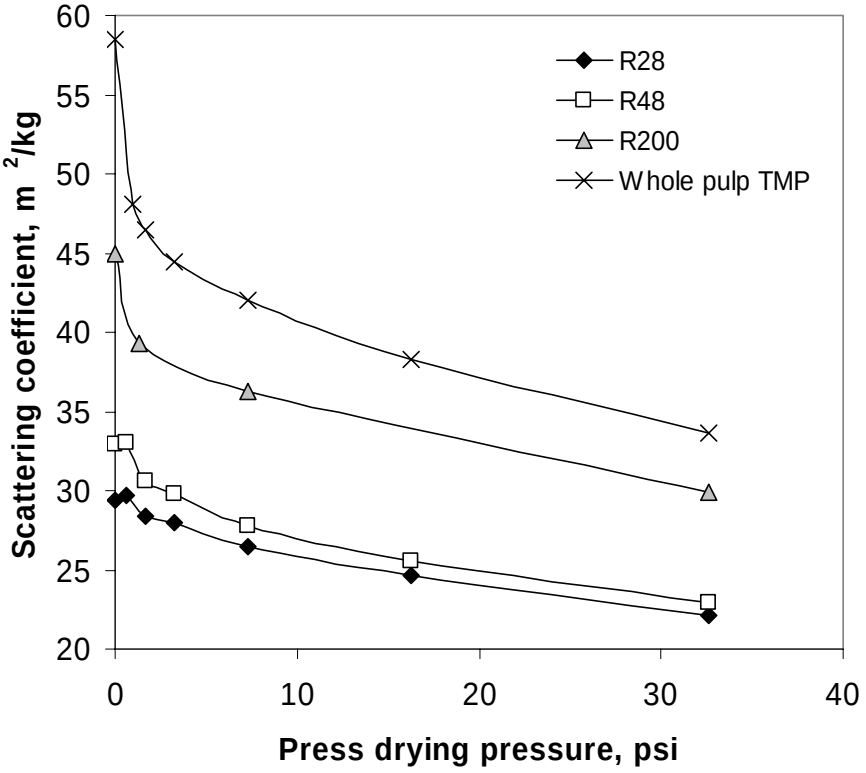

Figure 29. Whole TMP pulp and TMP fractions scattering coefficient as a function press-drying pressure. Platen temperature 120 °C.

Homogeneous bonding increase of all fractions was further supported by the increase in tensile strength as a function of pressing pressure (Figure 30). All fractions increased tensile strength following the shape of the tensile strength increase of the whole TMP. The long fiber fraction (R28) showed slightly slower tensile strength development from the rest of the fractions as a function of the pressing pressure at the low pressing pressure range. This was likely due to the stiff demeanor of the long fiber fraction.

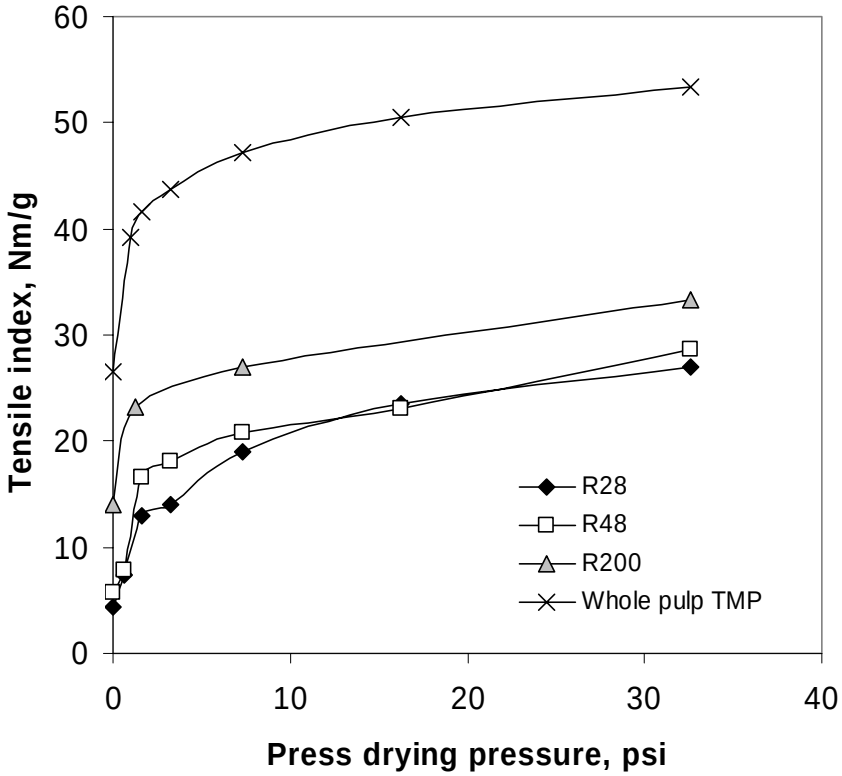

Figure 30. Whole TMP pulp and TMP fractions tensile strength as a function press-drying pressure. Platen temperature 120 °C.

Sheet collapse in press drying

The cross-sectional SEM images of whole pulp Southern pine TMP revealed a significant consolidation of the sheet in z-direction as the press drying pressure was increased. In Figure 28 it was shown that the whole pulp TMP significantly decreased its scattering coefficient as a function of pressing pressure. Comparing the wet pressed Tappi standard sheet in Figure 31 with the low pressure press dried sheet in Figure 32, there was a significant decrease in scattering coefficient and increase in tensile strength without a significant change in caliper. This further reinforces the earlier observation (Figure 27) of an altered consolidation mechanism when pressed above the glass transition temperature of lignin, which is possibly due to the efficient middle and fines fraction bonding ability at higher temperatures as shown in Figure 29. Ultimately, at high press drying pressures there was an almost full collapse of the sheet (Figure 35).

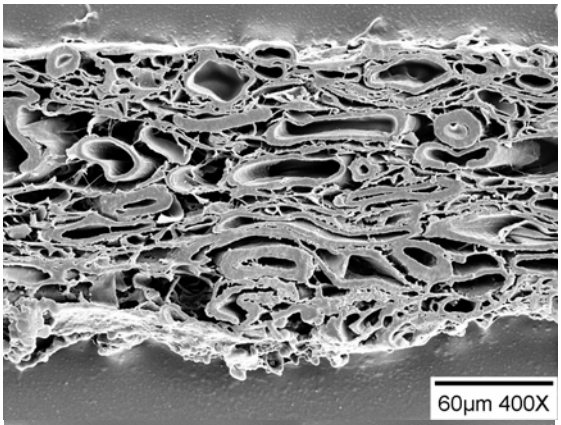

Figure 31. Tappi standard sheet

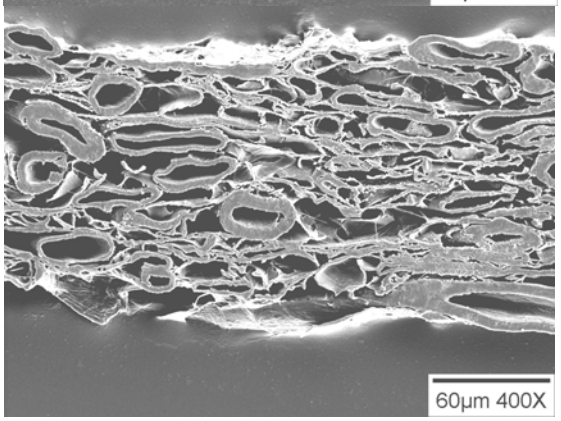

Figure 32. Tappi standard sheet hot pressed at 130 °C for 3 minutes, 0.8 psi pressure

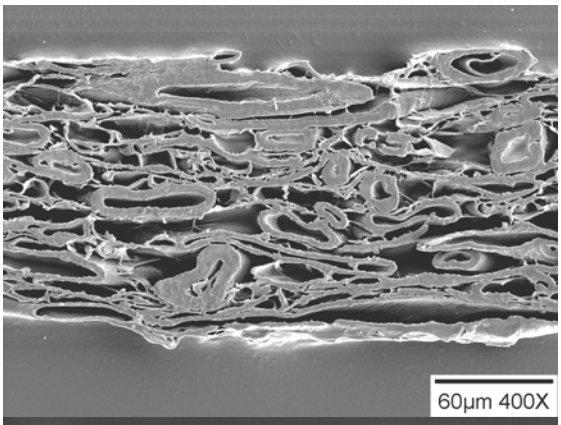

Figure 33.Tappi standard sheet hot pressed at 130 °C for 3 minutes, 1.6 psi pressure

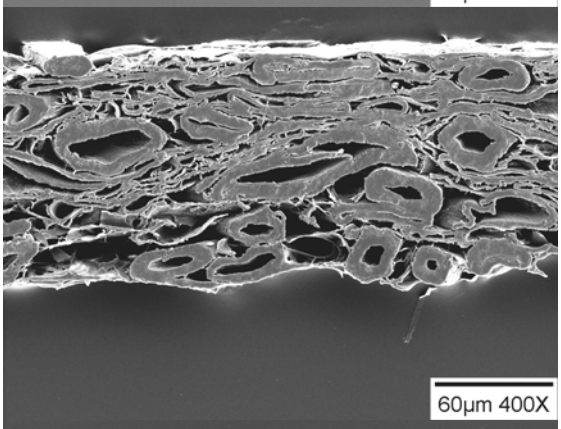

Figure 34 .Tappi standard sheet hot pressed at 130 °C for 3 minutes, 8.2 psi pressure

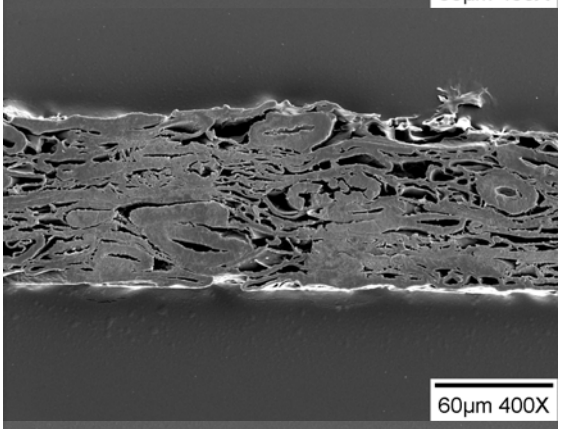

Figure 35.Tappi standard sheet hot pressed at 130 °C for 3 minutes, 32.6 psi pressure

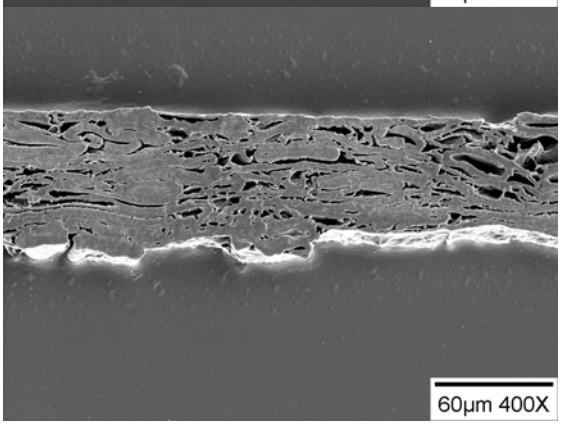

Figure 36.Tappi standard sheet hot pressed at 130 °C for 3 minutes, 65.2 psi pressure

Scattering coefficient and tensile index relationship

As was shown earlier all the fractions followed the logical increase in tensile strength as the scattering coefficient was decreased by using higher press drying pressures. The result was that when scattering coefficient was plotted against tensile strength similar relationships were obtained as when using the Ingmansson and Thode method for chemical pulps. These scattering vs. tensile strength relationships were plotted in Figure 38 -Figure 40, using a linear model and the Page equation to explain the data. The use of a linear model assumes a linear relationship between bonded area and tensile strength. This assumption is correct in light of the Shallhorn-Karnis equation [24] for negligible fiber failure during the sheet fracture in tensile test. However, the introduction of a fiber failure mechanism results in curvature in the scattering vs. tensile index relationship, where additional bonded area has less impact on the tensile strength at high levels of bonding, as more fibers are broken in the fracture zone. This type of behavior was seen for R28 and R48 fiber fractions. Another plausible explanation for the non-linear behavior of the fiber fraction is derived from the morphology of the fibers. In fiber fraction roughly half of the scattering surface area is located in lumens, which do not add to the bonded area. However, as fibers are collapsed these lumens reduce scattering surface area without contributing to the bonding or to tensile strength. In whole TMP pulp there are also fiber lumens present, but their contribution to the total surface area is only a fraction of that in a pure fiber sheet. Thus it is expected that the slight nonlinearity observed in whole TMP is not so much due to the lumen collapse as it due to a possible fiber failure mechanism.

The negligible fiber failure, linear relationship, was supported by the plot in Figure 37, where a whole pulp Southern pine TMP pulp sheets were press dried, Tappi standard pressed and freeze dried at -72 °C and the tensile strength was plotted against the scattering coefficient. All the various pressing types plotted on a common line. In addition the tensile strength at zero scattering coefficient was 71.26 Nm/g, which was in the proximity of the 8/9 of the measured zero span tensile strength (73.06 Nm/g). The resulting S_o was 102.7 m^2/kg, which translates into 2.28 m^2/g specific surface area, using Haselton's conversion factor of 0.045. This is in the proximity of the highly refined total unbonded specific surface area of mechanical pulp obtained by Rennel [115].

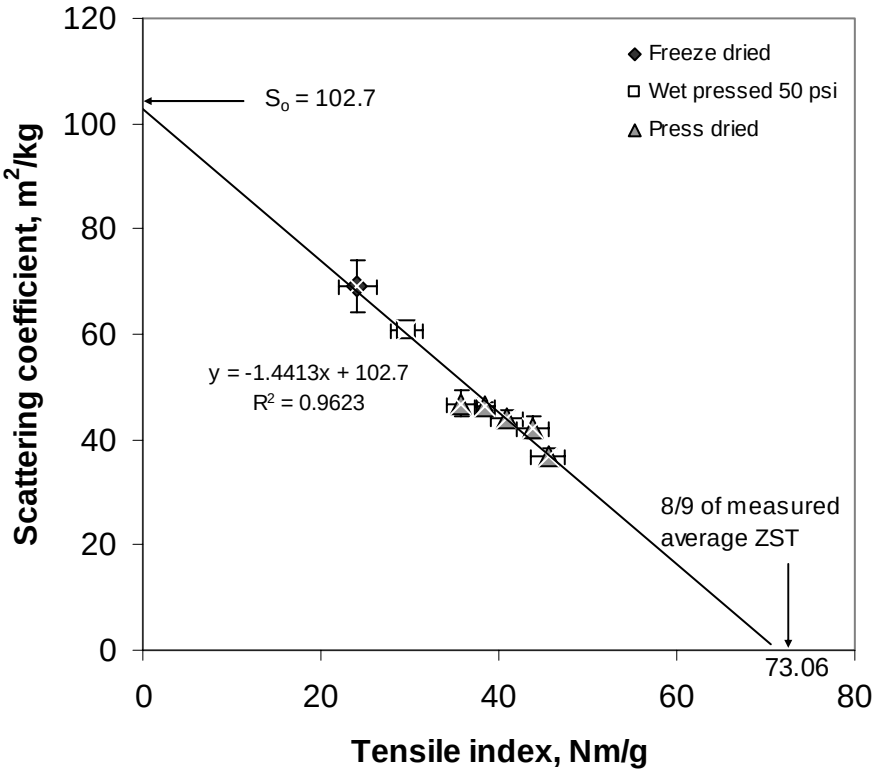

Figure 37. Tensile strength vs. scattering coefficient of Southern pine TMP (110 CSF) press dried (130 °C), wet pressed (23 °C) and freeze dried (-72 °C) to various levels of bonding.

Applying Page equation and linear model to separate specific bond strength and specific bonded area in mechanical pulps

Here two fundamentally different approaches were used to separate specific bond strength from specific bonded area. The first approach assumes a fiber failure to occur at low bonding (Page equation), whereas the second neglects the fiber failure mechanism throughout the whole bonding range (Linear model). These two approaches can be considered as the two extremes in the bonded area-tensile strength relationship, where the fiber failure neglecting approach produces a linear relationship and the significant fiber failure approach regime produces a non-linear relationship.

The semi-empirical Page equation [60], which was originally developed based on observations from homogeneous chemical pulps, provides a tool where a fiber failure mechanism is included in the bonded area tensile strength relationship even at low bonding levels. One form of the equation can be written as follows:

$$\frac{1}{T} = \frac{9}{8Z} + \frac{12g}{bL\alpha} \qquad \textbf{Equation 13}$$

where T is the tensile strength (in kilometers), Z zero span tensile strength, b specific bond strength, L arithmetic fiber length and α is the bonded area per gram of fibrous material.

Considering a domain where fibers do not break in the fracture the equation can be written as [163]:

$$T = \frac{bL\alpha}{12g} \qquad \textbf{Equation 14}$$

The term g (acceleration due to gravity) can be omitted from both equations if a specific stress (Nm/g) is considered for terms T and Z.

In order to be able to use the equations 12 and 13, a coefficient is needed to convert scattering coefficient to specific surface area. Haselton [111] measured BET nitrogen absorption specific surface areas of wet pressed and refined chemical pulps at various levels of bonded area. He was able to show a linear correlation between scattering coefficient and specific surface area with an approximate slope of 0.045 (m^2/g vs. m^2/kg), passing very close to the origin. This has been later confirmed by Scallan and Borch [124, 164]. Rennel [115], has shown that the conversion factor of Haselton is also a close approximation for mechanical pulps.

Using the conversion provided by Haselton the scattering data was converted into specific surface areas. Then least squared Page equation fit and a linear fit were done for each individual fraction and whole pulp, letting the total unbonded specific surface area and specific bond strength float, using both equations 12 and 13.

In Figure 38 -Figure 40 the linear and Page equation models are presented for each fiber fraction individually, as well as for the whole pulp. Summary of the results are shown in Table 6.

Table 6. Page equation and linear equation based total unbonded specific surface area (S_o), specific bond strength and R^2 of the models.

Pulp	Page equation			Linear model		
	S_o m^2/g	Specific bond strength dynes/cm^2 $X10^7$	R^2	S_o m^2/g	Specific bond strength dynes/cm^2 $X10^7$	R^2
R28	0.696	1.174	0.941	0.720	0.753	0.912
R48	0.792	1.387	0.952	0.826	0.884	0.926
Whole pulp	1.473	3.758	0.970	1.850	0.837	0.986

The use of non-linear models instead of linear models had very little impact on the total variance explained (R^2). In fact the linear models predicted the tensile strength of whole pulp better than the non-linear Page equation fit. The major differences between the models were seen in the total unbonded specific surface area (S_o) and specific bond strength. The total unbonded specific surface areas predicted by the Page equation were lower than those of linear model, especially in whole TMP. Linear models predicted a fairly constant specific bond strength for all the fractions including the whole pulp, whereas the Page equation fit predicted significantly higher specific bond strength for the whole pulp than for the long (R28) and short (R48) fiber fractions. However, the specific bond strength values obtained here using Page equation or linear models were not in agreement with the literature values. For example Thorpe *et al.* [165] reported shear bond strength of 2.9 dynes/cm^2X10^7 for southern pine TMP fibers bonded at 110°C.

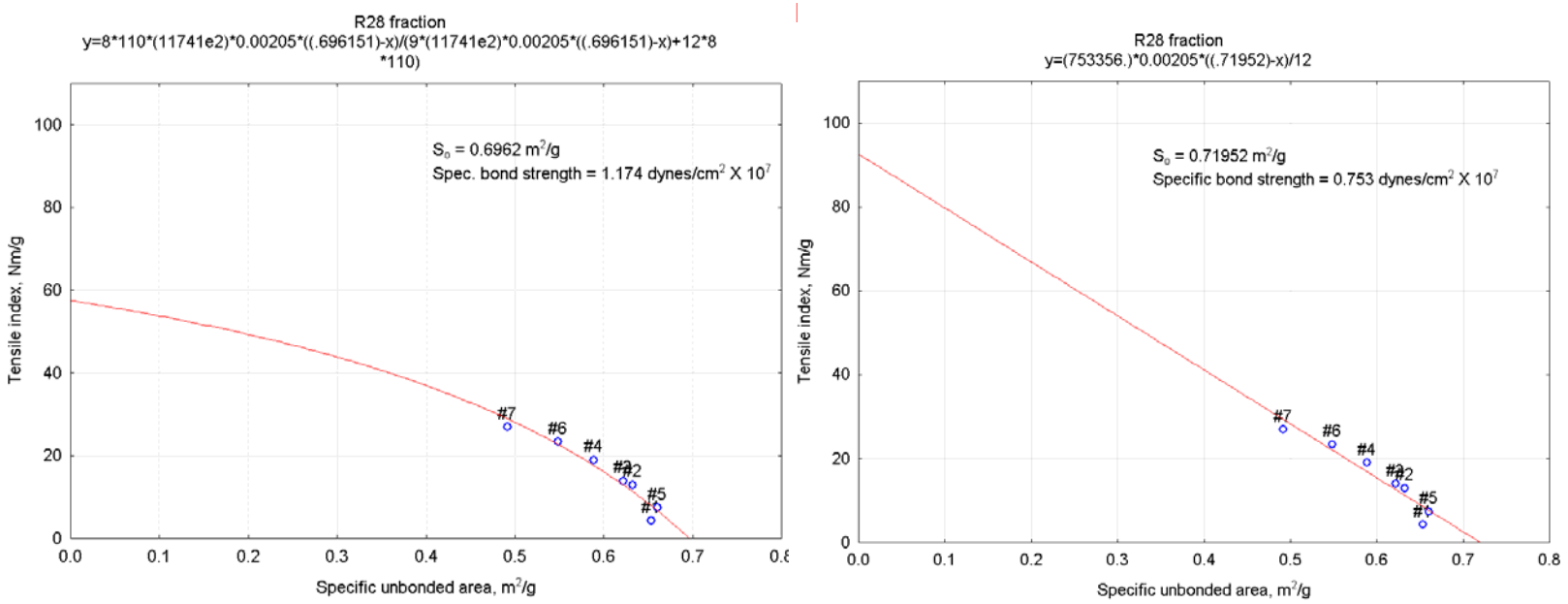

Figure 38. Page equation and linear least square fits for unbonded specific surface area vs. tensile strength of the Long fiber fraction (R28)

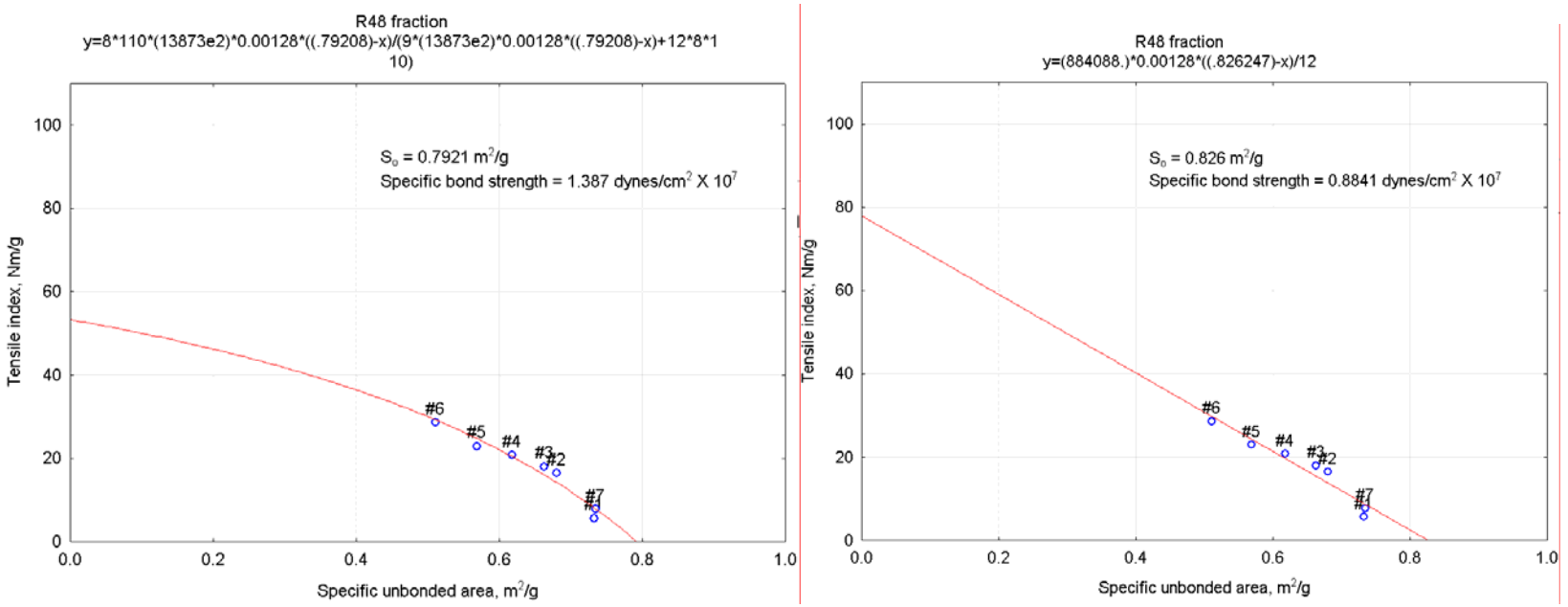

Figure 39. Page equation and linear least square fits for unbonded specific surface area vs. tensile strength of the Short fiber fraction (R48)

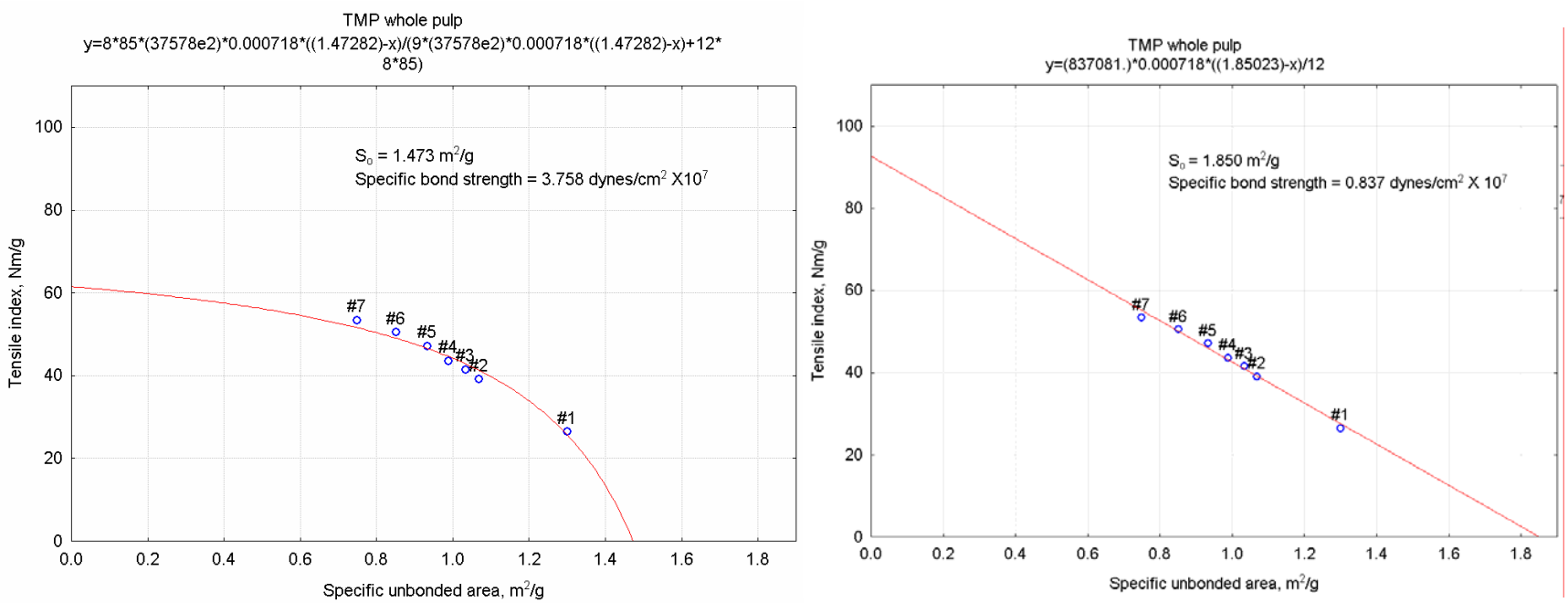

Figure 40. Page equation and linear least square fits for unbonded specific surface area vs. tensile strength of the whole pulp TMP

Discussion

In this study it was shown that press drying produced similar scattering coefficient vs. tensile strength relationship in mechanical pulps as the Ingmansson and Thode wet pressing method has been shown to produce in chemical pulps. Significant bonding increase of a mechanical pulp can be achieved by press drying the sheets until they approach their 50% relative humidity moisture content. The use of higher temperatures decreases the time to dry the sheet, and thus the time to produce the bonded sheet. Bonding can be further increased by applying higher pressing pressures, eventually to a point where no additional increase in tensile strength can be achieved.

However, there are several aspects that need to be addressed before the press drying assisted Ingmansson and Thode method can be applied to explain strength properties of heterogeneous structures. In pressing, a force is applied through the sheet in order to assist the collapse of the material under pressure. Mechanical pulps consist of extremely heterogeneous material, ranging form *nanoscopic* fine particles to *microscopic* fibers. These different components represent different morphologies and often also slightly different chemical compositions. Although it was indicated here that press drying increases bonding of individual fractions the same rate as the whole pulp, it is likely that certain fractions in the sheet will restrict the collapse of the sheet, whereas others will bond readily. This is especially likely in the case of fiber-fines mixtures, which were not studied in this paper.

It was indicated in this study that the consolidation mechanism of the mechanical pulp sheet is dependent on the temperature used to press dry the sheet. This is in agreement with earlier findings where significant bonding without altering the density of the sheet has been achieved when higher pressing temperatures were used [144, 154, 156]. There are indications that this bonding without consolidation is related to the increased bonding ability of the finer fractions in the sheet [155, 156]. It is likely that two same pulp sheets with two different densities and constant bonded areas have different tensile strengths due to the distance affected stress-transfer ability between bonded elements of the sheet, manifesting itself as a difference in specific bond strength when press dried and wet pressed sheets are compared.

Due to the limited amount of research done with mechanical pulps, it is unclear whether scattering coefficient accurately reflects the specific surface area of the material. Despite the extensive work of Rennel [115], there are indications that the “detection” ability of scattering coefficient is limited to certain pore sizes, possibly depending on the wavelength of light used to measure scattering coefficient [126]. Thus, it is unclear if the reduction in scattering coefficient in the press drying assisted Ingmansson and Thode method accurately reflects the change in bonded area.

The efficient use of Ingmansson and Thode method relies on a theoretical relationship between bonded area and tensile strength. It is generally believed that these low bonding mechanical pulp structures can be explained by two factors; fiber length and bonding. In respect to Ingmansson and Thode method this means that the equation relating bonding and tensile strength is likely linear, as was suggested by Shallhorn and Karnis. However, there are indications that a third factor is necessary in explaining the strength of mechanical pulps. So far, the evidence points into a new factor that is possibly related to the strength of fibers [3, 5, 6, 27, 48, 66]. If the fiber strength is important already at low bonding levels, it would indicate that an equation similar to the Page equation would provide the needed fit for relating bonding and tensile strength, where fibers are assumed to break even at low bonding levels. The fact that in this study a fiber-failure emphasizing model (Page equation) predicted the fiber fraction data better than a fiber-failure neglecting linear model, and a linear model predicted the whole TMP data better than the Page equation, indicates that the correct bonding-tensile strength relationship is likely a combination of these two models, where the fiber fraction undergoes fiber failure and finer fractions pure bond failure.

Indications of the above mentioned problems related to the applicability of the Ingmansson and Thode method in mechanical pulps was reflected into the specific bond strength values. The values obtained here were significantly lower than were obtained from single fiber studies with chemical and mechanical pulp fibers [82, 83, 100, 101, 165].

Conclusions

In mechanical pulps two factors are generally adequate to describe the properties of these pulps. These factors are bonding and fiber length. Bonding has been traditionally described with two separate variables: bonded area and specific bond strength. By definition, specific bond strength is the efficiency of the bonded area to produce bond strength. For practical purposes it is important to separate these two variables, because bonded area affects the optical and strength properties, whereas specific bond strength is only reflected in the strength properties of the sheet. In chemical pulps the most used method to separate these two variables is to use Ingmansson and Thode method and fit the Page equation to the tensile scattering relationship, letting specific bond strength and total unbonded specific surface area (S_o) float. In lignin rich mechanical pulps the bonding cannot be significantly increased by using wet pressing. This is likely due to the fact that lignin, and thus mechanical pulp fibers are not plasticized under normal temperatures. In this paper press-drying was used to induce bonding in lignin rich mechanical pulp. It was shown that tensile strength increased and scattering coefficient decreased significantly when a 130 °C platen temperature and variable pressing pressures were used to press mechanical pulp handsheets, indicating that bonded area was increased significantly as the handsheets were pressed at elevated temperatures. The significant bonding increase was achieved independent of pressing temperature when pressing was carried out above the glass transition temperature of lignin. Ultimately similar scattering coefficient vs. tensile strength relationships were obtained here for mechanical pulp as have been obtained for chemical pulps using the Ingmansson and Thode method. The Page equation and linear models were used to separate bonded area and specific bond strength for the press-dried mechanical pulps. Both models fitted the data extremely well. It was shown that the predictions of specific bond strength and total unbonded surface areas were different depending on the model used to relate bonded area and tensile strength. Linear models predicted that the specific bond strength of various mechanical pulp fractions and whole pulp are very similar, whereas the Page equation showed that the specific bond strength of whole pulp TMP is approximately three times larger than that of the fiber fraction. In both cases the specific bond strength values were below the earlier literature findings.

Chapter 2: Scattering coefficient as a measure of specific surface area in mechanical pulps

Abstract

Relative bonded area (RBA) is an important paper structure-defining parameter that is reflected in the strength and optical properties of the paper. The traditional determination of RBA relies on the measurement of specific surface area at various bonding states (Ingmansson-Thode method). The determination of RBA is significantly easier if the scattering coefficient can be used as a measure of specific surface area. However, in mechanical pulps, where the absorption coefficient might affect the scattering coefficient, and the pore size structure is variable, the use of scattering coefficient as a measure of specific surface area cannot be taken for granted. In this paper, the fundamental relationship between scattering coefficient and specific surface area in mechanical pulps was studied using mercury porosimetry and BET nitrogen absorption to measure specific surface area. It is shown that the scattering coefficient is a measure of specific surface area when the wavelength of light used is above that which the scattering coefficient is not limited by significant absorption. The limit depends on the composition of the sheet and the pressing level and type used to induce bonding. However, there was no significant reduction in scattering coefficient in any of the samples when the wavelength of light used to measure scattering was above 600nm. The scattering efficiency, defined as the ratio of scattering coefficient and specific surface area, was fully explained by the wavelength used to measure scattering coefficient. A plausible explanation for the wavelength dependency of the scattering efficiency was given, which relates the increase in scattering efficiency to the change in refractive index of the material when the wavelength of light to measure scattering coefficient is altered.

Introduction

Kubelka-Munk theory [166] is the only readily applicable approach for estimating optical constants in paper [167]. In Kubelka-Munk theory, light flux is treated as two separate dependent parameters, and their intensity is determined by the scattering and absorption coefficients [132]. K-M Scattering coefficient, defined using the Kubelka-Munk theory,

has a special importance in understanding paper structure property-relationship due to its physical ability to efficiently reflect the specific surface area of the material [113, 115, 116, 122, 124-126, 128, 129, 135, 167-173]. Thus, scattering coefficient is a very applicable parameter in estimating bonded area in paper and has been widely used for this purpose frequently in chemical pulps [113, 122, 168, 170]. However, there are a few important limiting factors that need to be addressed before scattering coefficient can be used as a measure of specific surface area in pulps which have a very porous structure with significant amount of small pores and yield high absorption coefficients, i.e., mechanical pulps.

High absorption coefficient effect

It has been shown that the K-M scattering coefficient is significantly reduced at high levels of absorption [131-133]. This effect is known as the NAM (Nordman, Aaltonen and Makkonen) anomaly [133] or Foote effect [131]. It is not clear whether this significant decrease in scattering coefficient at higher absorption is an intrinsic error in the Kubelka-Munk theory or an actual physical material property. In the theory where the decrease in scattering coefficient at high absorption is seen as a material property, the scattering decrease has been explained to be a combination of two phenomena: the influence of the absorption on the surface reflectivity of the cell wall and the absorption of light internal to the cell wall [132]. However, it has also been shown using a Discrete Ordinate Radiative Transfer (DORT) model that there is an intrinsic error in the K-M model at high absorption levels, explaining roughly 20% of the decrease in scattering coefficient [134]. It needs to be recognized that when scattering coefficient is to be used as a measure of bonding in paper, the wavelength of light used in the measurement should be at such a level where the scattering is not affected by the strong absorption [135].

Small pores and light scattering

Davis was the first to suggest that the K-M scattering coefficient should be proportional to the specific surface per unit mass of the material [171]. Parsons [173] was the first to obtain proof of this. They used a modified Clark [174] silvering method to measure specific surface area of pulp. Later, Haselton introduced the use of gas adsorption

(nitrogen) in determining specific surface area and related it to specific scattering coefficient of paper [170]. Haselton found a linear correlation between scattering coefficient and nitrogen adsorption specific surface area of sulphite pulps refined and wet pressed to different levels of bonding. The correlation obtained by Haselton showed a linear slope of 0.045 (or 45.0 based on m^2/kg scattering and m^2/g specific surface area units). Later, Rennel [115] showed similar linear relationships between scattering coefficient and nitrogen gas adsorption specific surface area (wavelength used in scattering measurements was not mentioned) for various pulps wet pressed and refined to different levels of bonding. In his data, all pulps produced unique scattering coefficient and gas adsorption specific surface area relationships. Also, Swanson and Steber [113] showed that each type of pulp has a unique nitrogen adsorption/scattering coefficient relationship; however, the relationship approached a similar value of 0.044 (or 44.0 based on m^2/kg scattering and m^2/g specific surface area units) for the linear slope at higher wavelengths of light (650nm). Rennel also obtained similar linear slopes using cylindrical model fibers of glass, as long as the diameters of the glass fibers remained larger that 1 micrometer, or the specific surface area approximately below 1.5 m^2/g. In 1959 Van den Akker (mentioned in [113]) made an interesting observation that 0.044 is approximately the value which would be expected by application of Fresnel's law of reflection to a diffusely reflecting body of randomly oriented fibers. This has been later demonstrated theoretically, using Stoke's approach for layered paper structures, to be an accurate approximation by Scallan and Borch [124, 164].

However, there are indications that the ability to detect surface area is limited by the wavelength of light used in the scattering coefficient determination. Swanson and Steber [113] as well as Ingmansson and Thode [168] showed that by using lower wavelengths of light the measured scattering coefficient increased, depending on the pulp used. This behavior has also been observed in mechanical pulps [175].

The effect of particle shape on the scattering efficacy of various types of fibers was studied first by Arnold [125], who showed that the light scattering coefficient was greater for dog-bone shaped fibers than circular ones. Later this was confirmed by Rennel [122], who utilized model glass fibers with variable cross-sectional shapes and showed that each shape represented unique nitrogen absorption specific surface area and light scattering relationships (at 557 nm wavelength of light and a specific surface area range

between 0.2 m^2/g to 0.37 m^2/g). The reason for this type of behavior was attributed to the possible variable pore size distribution in the sheet by stating "It should be borne in mind, however, that the determinations of the light-scattering coefficient and surface area (BET) are not concerned with the same thing. The former applies to surfaces down to a distance about 500-600 Å, whereas the nitrogen molecule, which measures 3.6 Å, record nearly all surfaces – even those not scattering light". Later, it was assumed that the specific surface area detection ability of light in a pulp sheet is approximately a half wavelength of light, based on paint and filler optical research [126-128, 176].

The microporosity approach of paper, measured with mercury intrusion, considers paper to be a continuous solid phase containing air voids that are the light scattering elements. Using this approach, Alince *et al.* [126], Fineman *et al.* [128], and Rundlöf *et al.* [129], have shown that there is a correlation between the void specific surface area and scattering coefficient in paper; however, the correlation is better when void pores smaller than 100-200nm are excluded from the data. This is believed to be due to the experimental observations that only voids with the size in the proximity of the wavelength of visible light are optically effective. Interestingly, the relationship between the cumulative specific pore area above 200nm and scattering coefficient from the data from Alince *et al.* produces a linear correlation following the approximate slope of 0.045 (up to approximately 1.5 m^2/g mercury intrusion specific surface area, after which a slight curvature appears). This indicates that the minimum optically-effective pore sizes are in the range of 200nm. However, these results are not in agreement with the BET nitrogen adsorption results, wherein similar slopes between scattering coefficient and specific surface area were detected. The detection ability of the nitrogen adsorption method is related to the size of the nitrogen molecule, and thus pores down to the size of 3.6 Å should be detected.

The main objective of this paper was to relate scattering coefficient and specific surface area in mechanical pulps at various wavelengths of light, and also to determine the limiting absorption coefficient beyond which the scattering coefficient is significantly reduced and cannot be used as a measure of specific surface area.

Experimental

Fiber middle and fines fractionation: The Bauer McNett apparatus was used to fractionate a hot disintegrated 110 CSF Norway spruce (Picea abies) unbleached TMP. R48 fraction (all above R48) R200 and P200 fraction was collected. P200 fraction was collected using the sedimentation method. The R48 fiber fraction was fractionated twice in order to achieve a near pure fiber fraction without any fines present.

Handsheet forming: Handsheets were formed using a standard Tappi handsheet mold with 150 mesh screen and recirculation of whitewater. Fines handsheets were formed on a dense glass fiber filter paper. Fines contents of the fiber- fines mixed sheets were measured from the formed handsheets using the DDJ method, T 261 cm-00. All handsheets were restrain-dried if not dry after pressing. The target handsheet basis weight was 60 g/m^2 O.D.

Wet pressing: Couched handsheets were not pressed. Wet pressing was conducted at 65, 489 and 978 psi's and 23°C using a carver press and 3 blotter papers on one side and a chrome plate on the other side of the handsheet. Wet pressed handsheets were pressed for 1 minute.

Press drying: Press drying was conducted at 6 pressing levels 0, 0.8, 8.1, 16.3, 48.9 and 163 psi's. Individual handsheets were pressed between hot plates heated to 120°C and a sandwich that consisted of a felt, wet blotter (to increase drying time and humidity above 100°C), handsheet, chrome plate, and a filter paper (to protect the chrome plate). All handsheets were pressed until completely dry.

Testing: BET was measured at Micromeritics, Norcross, Georgia, U.S.A., using the TriStar 3000 nitrogen absorption surface area equipment. The nitrogen gas partial pressure was changed by altering the helium/nitrogen mixture. The samples were degassed at 60°C. Mercury intrusion porosimetry specific surface area measurements were performed also at *Micromeritics,* using the AutoPore IV equipment. The intrusion pressure and pore size was related using the Washburn equation. Since the Washburn equation is based on cylindrical capillaries with circular openings, the specific surface area based on the voidal pore structure was calculated using a cylindrical pore model

assumption. The pressure range used in the mercury porosimetry was between 1.3 – 60,000 psi, corresponding to a pore size range from 150 µm to 4nm.

The UV/vis spectra were recorded on a Perkin-Elmer Lambda 900 UV/vis spectrometer equipped with a diffuse reflectance and transmittance accessory (PELA-1000). The accessory is essentially an optical bench that includes double-beam transfer optics and a six-inch integrating sphere. Background corrections were recorded using a Labsphere SRS-99-020 standard. Reflectance data were measured over a black and a white background with known reflectance values. For each sample and background, an average of five measurements was utilized to determine both the light scattering (*s*) and light absorption (*k*) coefficients. The absorption and scattering coefficients were calculated from the reflectance data by means of the Kubelka-Munk theory and the following equations:

$$k = \frac{s(1 - R_\infty)^2}{2R_\infty} \qquad \textbf{Equation 15}$$

$$s = \frac{1}{w(1/R_\infty - R_\infty)} \ln \frac{(1 - R_W R_\infty)(R_\infty - R_{GW})}{(1 - R_{GW} R_\infty)(R_\infty - R_W)} \qquad \textbf{Equation 16}$$

$$\frac{1}{R_\infty} + R_\infty = \frac{(R_{GW} - R_{GS})(1 + R_W R_S) - (R_W - R_S)(1 + R_{GW} R_{GS})}{R_S R_{GW} - R_W R_{GW}} \qquad \textbf{Equation 17}$$

where R_∞ is the reflectance of an optically thick sample, *k* is the absorption coefficient (m^2/kg), *s* is the scattering coefficient (m^2/kg), w is the grammage (kg/m^2), R_{GW} is the reflectance for the white background, R_{GS} is the reflectance for the black background, R_W is the reflectance for the sample over a white background, and R_S is the reflectance for the sample over a black background. Data were collected from 300 to 800 nm.

Results

Limiting absorption

The method used in the analysis was similar to that of Rundlöf *et al.* [175], where the scattering and absorption coefficients were measured at a broad range of wavelengths, as shown in Figures 41 and 42.

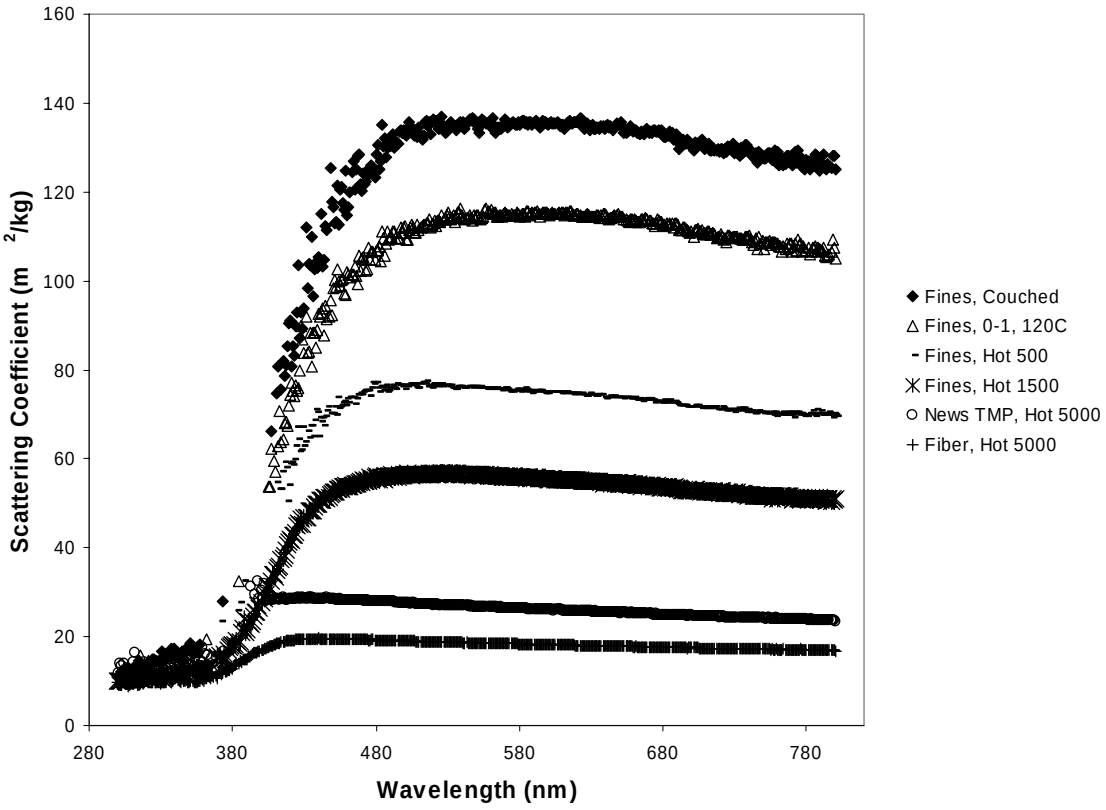

Figure 41. Scattering coefficient at various wavelengths of fines (P200), whole pulp (TMP) and fiber (R48) sheets wet pressed and press-dried to various levels of bonding.

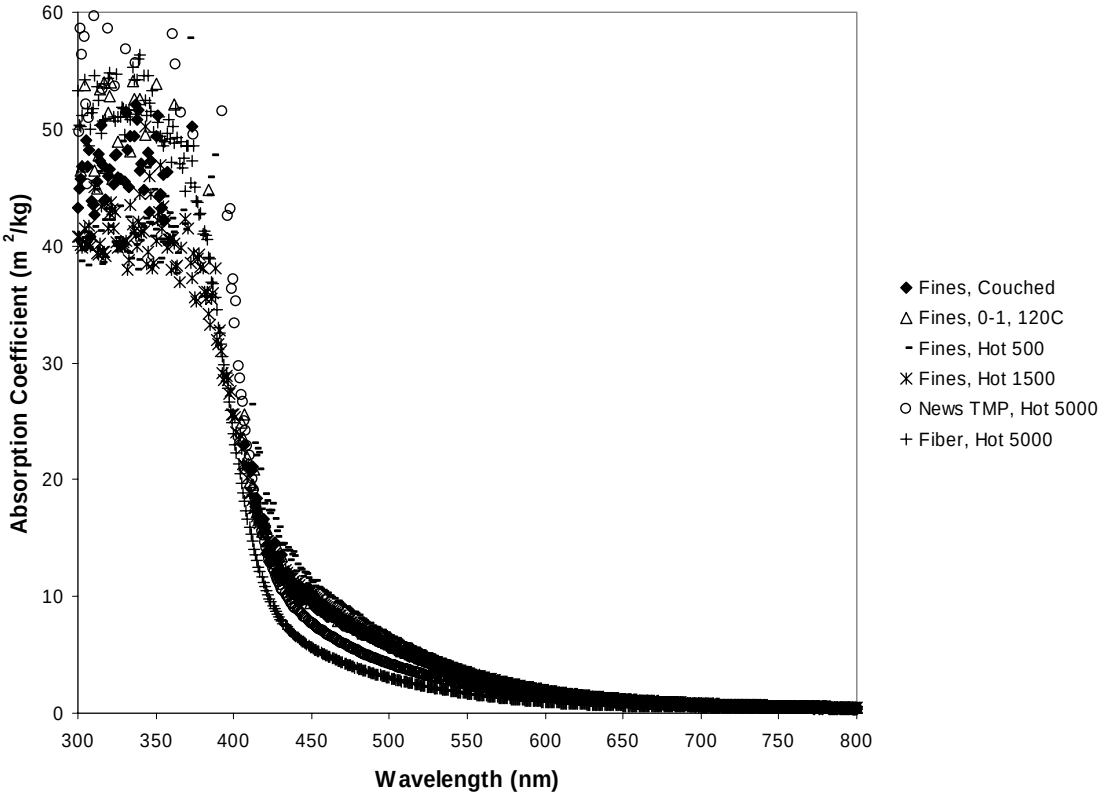

Figure 42. Absorption coefficient at various wavelengths of fines (P200), whole pulp (TMP) and fiber (R48) sheets wet pressed and press dried to various levels of bonding.

The range between the scattering coefficient at the highest wavelength 800 nm and the maximum scattering coefficient was considered as the range where scattering coefficient was not affected by the strong absorption. For this range, a linear least significant squared correlation line was calculated. This methodology is depicted in Figure 43.

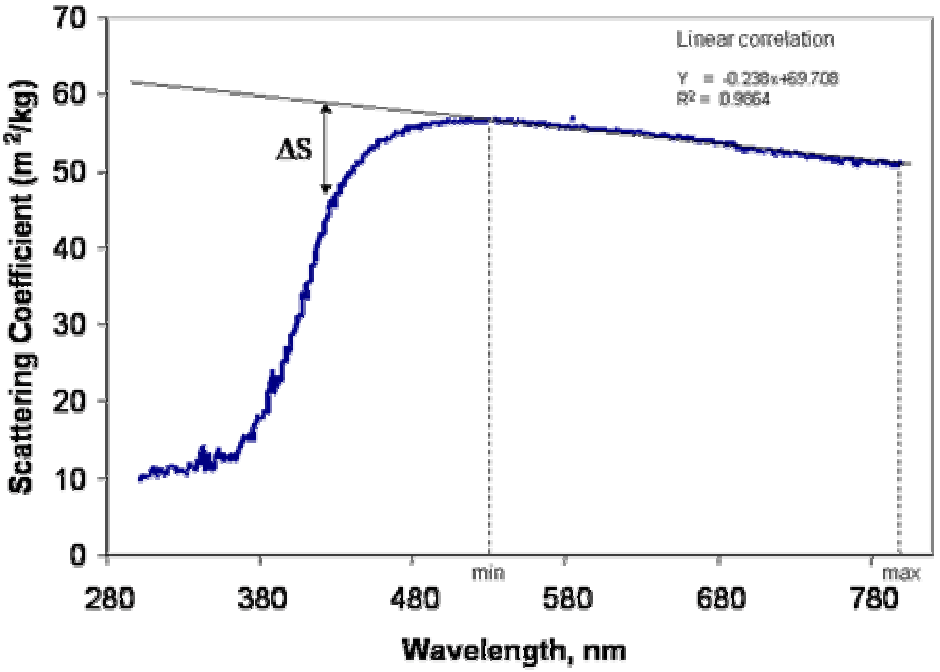

Figure 43. Scattering coefficient wavelength dependency of fines sheet press dried at 120ºC and 48.9 psi pressure.

The linear least square correlation results for all the samples included in the study are shown in Table 7. Also the range of wavelengths where the scattering coefficient was not affected by strong absorption is shown.

Table 7. Linear correlation slopes, intercepts, applicable range and R^2 values for all samples.

Sample	Pressure	Temperature	Time	s (scattering)=xλ(wavelength)+c			Applicable λ range, nm	
	psi	ºC	min	Slope	Intercept	R^2	min	max
Fines couched	0	23	0	-0.0383	157.71	0.8319	526	800
Fines wet 2000	65	23	1	-0.0438	153.57	0.9098	561	800
Fines wet 15000	489	23	1	-0.0416	134.21	0.8913	531	800
Fines wet 30000	978	23	1	-0.0381	123.96	0.933	540	800
Fines hot 0	0	120	6	-0.0409	139.76	0.908	557	800
Fines hot 30	0.8	120	6	-0.0257	102.08	0.8821	649	800
Fines hot 250	8.1	120	5	-0.0246	94.283	0.9383	608	800
Fines hot 500	16.3	120	4	-0.0269	90.866	0.9712	514	800
Fines hot 1500	48.9	120	3	-0.0238	69.708	0.9864	533	800
Fines hot 5000	163	120	3	-0.0225	57.394	0.9959	442	800
Fiber hot 5000	163	120	3	-0.0074	22.734	0.991	440	800
TMP couched	0	23	0	-0.0223	83.651	0.93	492	800
TMP wet 2000	65	23	1	-0.0304	87.25	0.9893	482	800
TMP wet 5000	163	23	1	-0.0297	84.207	0.9902	471	800
TMP wet 15000	489	23	1	-0.0289	82.036	0.9896	475	800
TMP wet 30000	978	23	1	-0.0324	80.588	0.9861	415	800
TMP wet 2000 on	65	23	1440	-0.0247	73.531	0.98	474	800
TMP hot 0	0	120	6	-0.0237	77.79	0.9754	446	800
TMP hot 30	0.8	120	6	-0.0186	61.168	0.9929	483	800
TMP hot 250	8.1	120	5	-0.0215	58.266	0.9942	440	800
TMP hot 500	16.3	120	4	-0.0199	54.502	0.9962	479	800
TMP hot 1500	48.9	120	3	-0.0177	46.718	0.9961	449	800
TMP hot 5000	163	120	3	-0.014	34.6	0.9711	398	800
TMP hot 10000	326	120	3	-0.0113	29.021	0.9978	442	800

The slope of the scattering dependency of the wavelength of light was related to the intercept of the same relationship (Figure 44), and also specific surface area obtained from the BET measurements (not shown here), clearly showing a stronger wavelength dependency of K-M scattering coefficient at higher specific surface area. This indicates that the slope of the scattering coefficient-wavelength dependency was also a factor of the sheet structure.

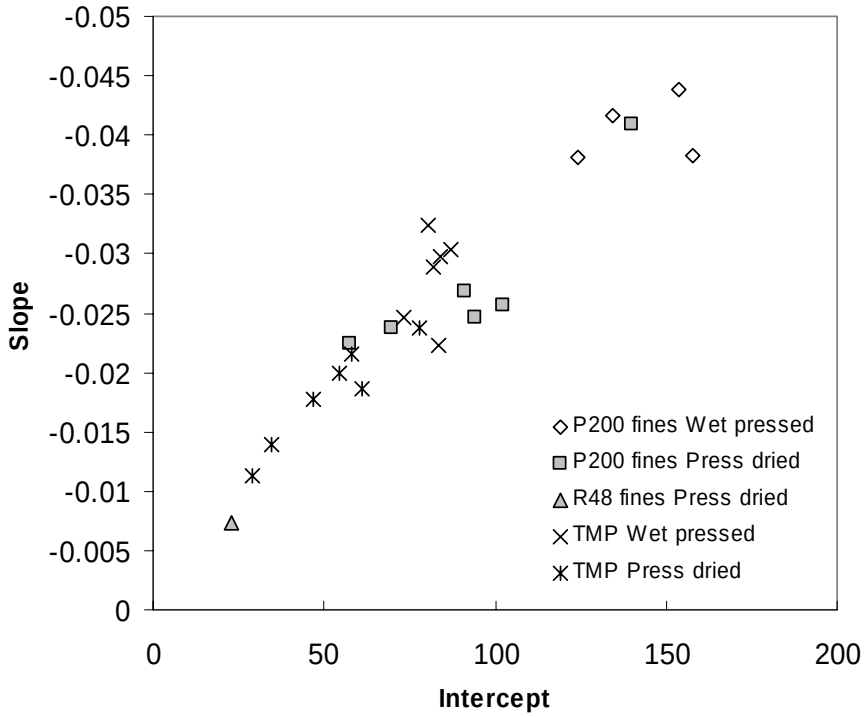

Figure 44. Scattering coefficient wavelength dependency linear slope vs. intercept.

The difference in the apparent K-M scattering coefficient and the linear model at various wavelengths of light is depicted in Figure 45, which shows that when the wavelength of light used in the scattering coefficient was beyond 600 nm, there was no significant change in the scattering coefficient regardless of pressing type, level or sheet composition. However, the limiting wavelength was different for each fraction, being mostly higher for pure fines sheets (P200) and lower for whole pulp and fiber sheets (R48).

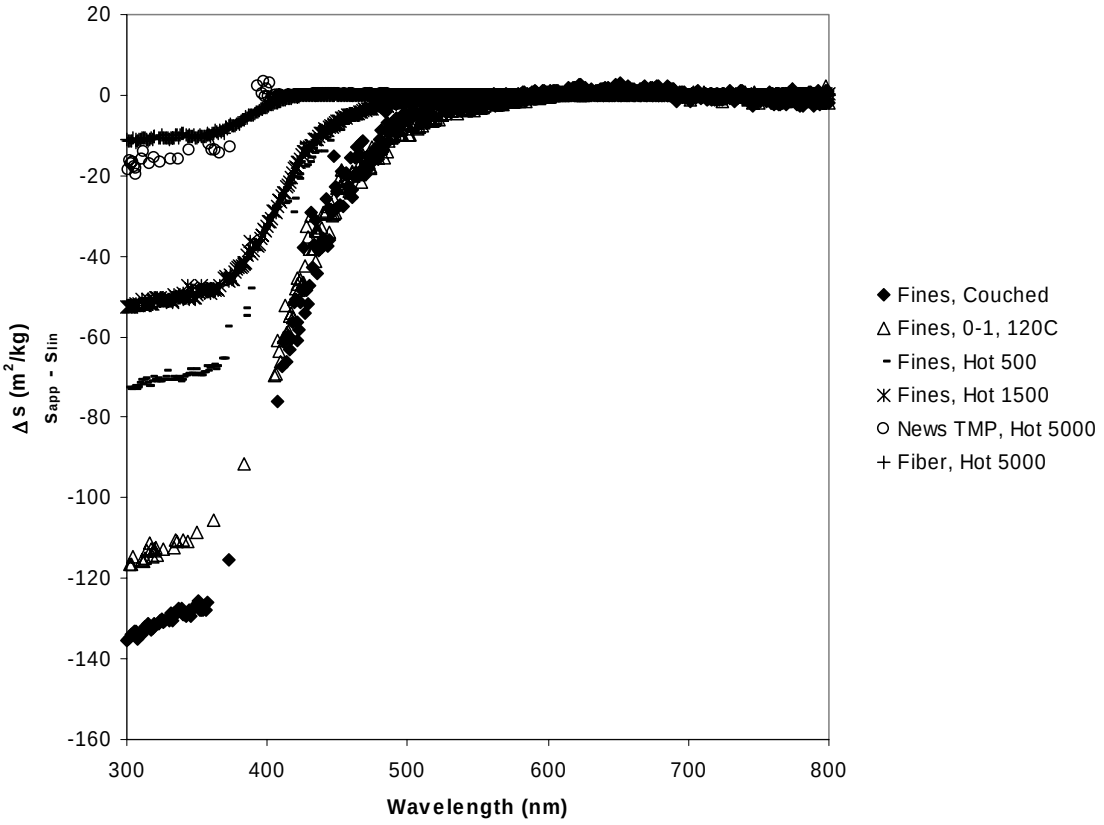

Figure 45. Reduction is scattering coefficient as a function of wavelength for various mechanical pulp whole pulp, fiber (R48) and fines (P200) sheets pressed to different levels of bonding.

This also resulted in that the level of absorption at which a significant decreased in scattering coefficient occurred was dependent on the sheet composition, as shown in Figure 46. The absolute reduction in scattering coefficient at high absorption was related to the level of scattering coefficient at negligible absorption, being higher for the fines (P200) sheets than for the whole pulp (TMP) and fiber sheets.

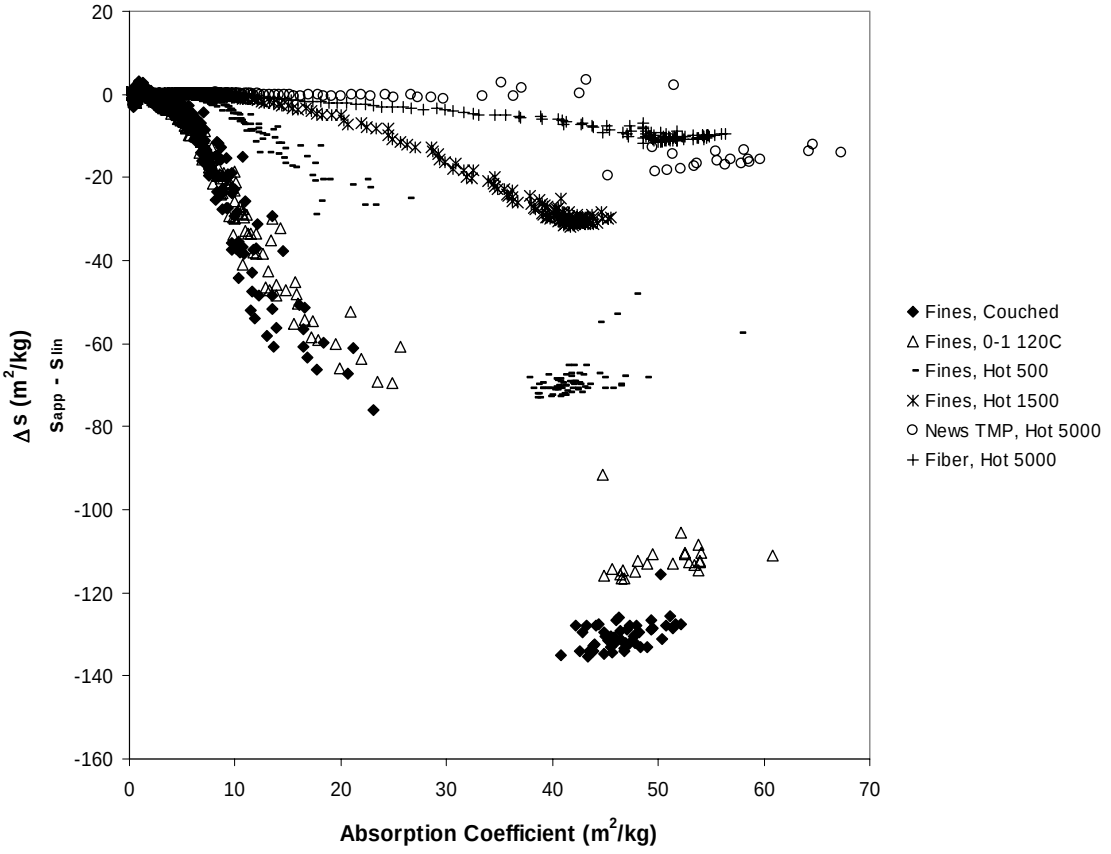

Figure 46. Reduction is scattering coefficient as a function of absorption for various mechanical pulp whole pulp, fiber (R48) and fines (P200) sheets pressed to different levels of bonding. Absorption changed by changing the wavelength.

Scattering coefficient and mercury porosimetry specific surface area

Earlier studies indicated that the scattering efficiency, defined as the scattering coefficient at constant specific surface area, of the sheet void structure is directly related to the wavelength of light, and that the optically effective pore size decreases as the wavelength of light is decreased. Thus, herein the K-M scattering coefficient was correlated with the cumulative specific surface area obtained from the mercury porosimetry pore size distribution measurements, using the hypothesis where the highest correlation with these two parameters at various wavelengths of light will be obtained when pore sizes close to the proximity of the wavelength of light will be excluded from the specific surface area calculation. In this section the linear wavelength

dependence of scattering coefficient, shown in Table 7, was used to study the effect of pore size distribution on the scattering coefficient. The absorption limit was neglected, in order to allow the use of all samples throughout this part of the study for a wide range of wavelengths. Specific surface area was calculated from the mercury porosimetry pore volume measurements excluding certain pores sizes systematically from the calculation. The calculated specific surface areas, where certain pore sizes were systematically excluded, were then correlated with scattering coefficients at various wavelengths of light.

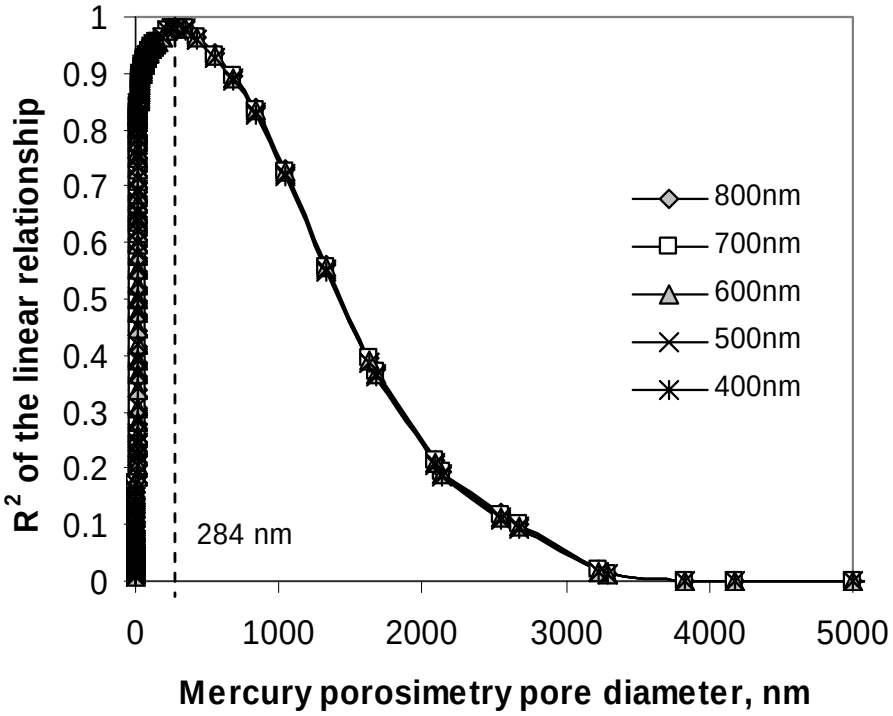

Figure 47. R^2 of the linear relationship between scattering coefficient and mercury porosimetry specific surface area as a function of the excluded pore sizes.

The initial hypothesis, in which the increase in scattering efficiency at lower wavelength of light was explained with the enhanced ability of light to detect smaller pores, was not supported. The highest correlation coefficient (shown in Figure 47 as R^2) between mercury porosimetry and scattering coefficient was obtained when pores smaller than 284 nm were excluded from the calculation, independent of the wavelength of light used. The expected shift to smaller pores sizes at lower wavelengths of light did not occur.

However, the scattering efficiency of the calculated specific surface area from mercury porosimetry when pores smaller than 284 nm were excluded was still wavelength dependent, resulting in higher scattering coefficients for lower wavelengths of light at a constant specific surface area, as seen in Figure 48. No significant differences were observed in the scattering coefficient - specific surface area relationship between various sheet compositions and pressing conditions.

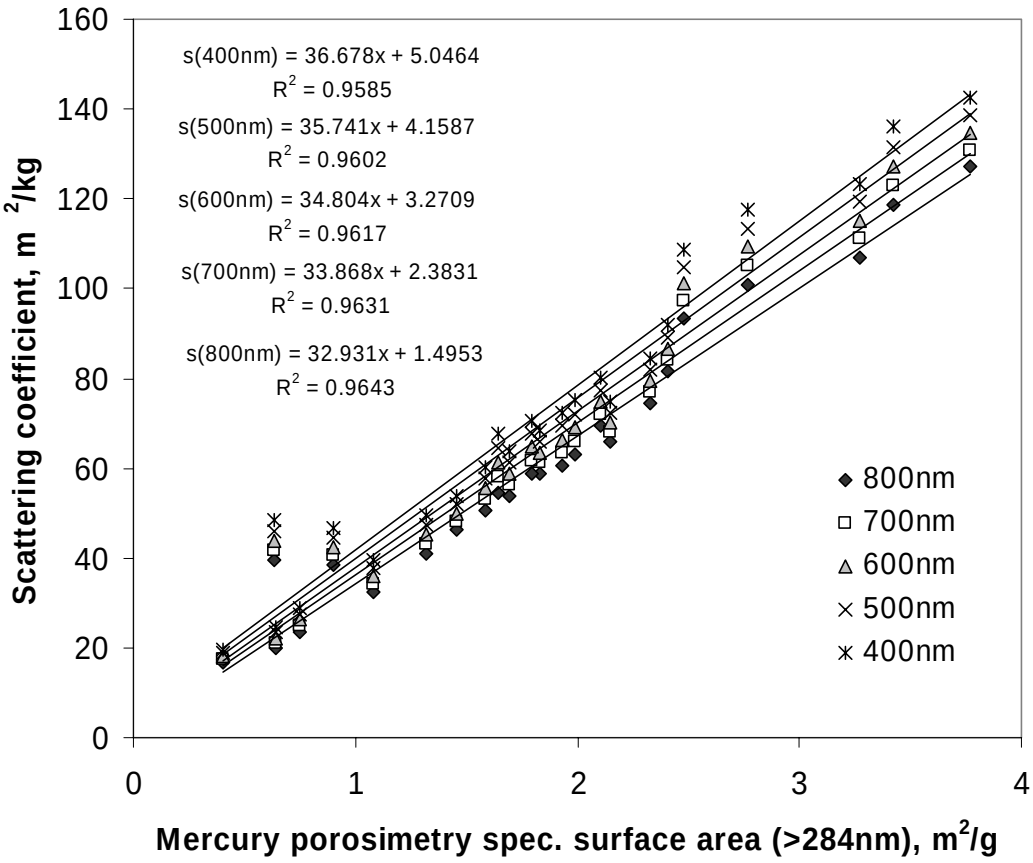

Figure 48. Mercury porosimetry specific surface area excluding surface area from pores smaller than 284 nm vs. K-M scattering coefficient at various wavelengths of light.

The slope and the intercept of the mercury porosimetry specific surface area (excluding pores smaller than 284 nm) and scattering coefficient relationship was fully explained by the wavelength of light used in measuring scattering coefficient, depicted in Figure 49. The slope at zero intercept was 32.675, and was obtained at wavelength of 968.5 nm.

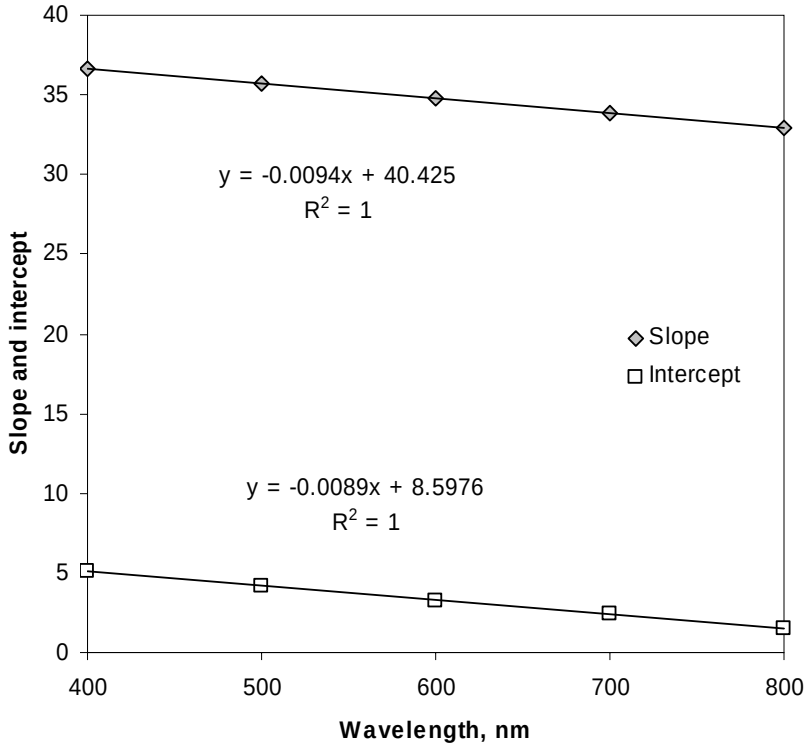

Figure 49. Wavelength dependency of the mercury porosimetry (excluding pores below 284nm) vs. scattering coefficient slope and intercept

Scattering coefficient and BET nitrogen adsorption specific surface area

The BET nitrogen adsorption and scattering coefficient relationship was dependent on the wavelength of light used, as was observed for mercury porosimetry. An increase in scattering efficiency was observed as the wavelength of light was decreased (Figure 50).

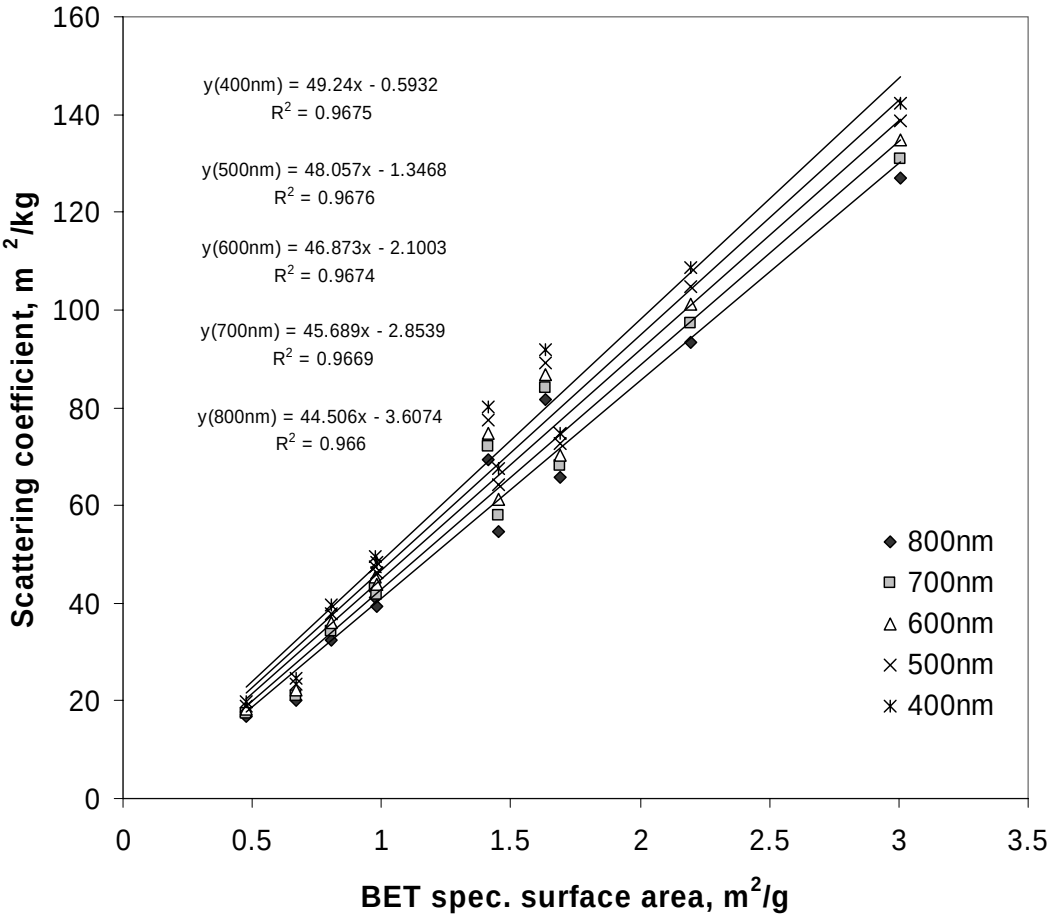

Figure 50. BET specific surface area vs. scattering coefficient at various wavelengths of light.

Also here the slope and intercept of the linear relationship was fully explained by the wavelength of light used in measuring scattering coefficient (Figure 51). The linear correlation line passed through the origin at 321 nm and the corresponding slope then was 50.2.

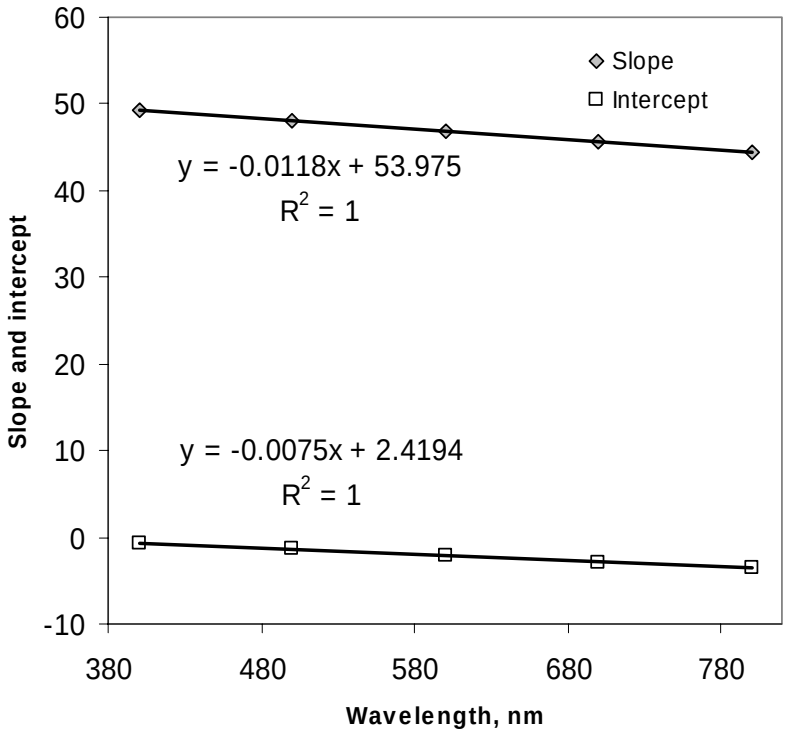

Figure 51. Wavelength dependency of the BET nitrogen adsorption – scattering coefficient relationship, slope and intercept.

Discussion

In this paper it was shown that the increase in scattering efficiency at lower wavelengths of light is not due to the increased pore detection ability of the scattered light. The pore size needed to be excluded from the surface area calculation (<284nm) to obtain the highest correlation (R^2=0.97) coefficient with scattering coefficient was constant regardless of wavelength of light used. However, the scattering efficiency was still wavelength dependent, resulting in higher scattering coefficients for lower wavelengths of light at constant specific surface area. These findings were supported by the results obtained from the BET nitrogen adsorption measurements.

Scallan and Borch [124, 164], using a multilayer Stokes approach for determining scattering coefficient in paper, have shown that for pulps of negligible absorption (bleached, or measured at high wavelength of light) the scattering coefficient and specific surface area are related according to the following equation:

$$s = \frac{r}{(1-r)} A_0 \qquad \textbf{Equation 18}$$

where s is the specific scattering coefficient, r the reflectivity of the material (fiber) and A_0 the specific surface area of the paper.

Reflectivity (r) on the other hand can be expressed using Fresnel equations for negligible absorption and normal incidence, with air being the medium, as a function of refractive index of the material:

$$r = \frac{(n-1)^2}{(n+1)^2} \qquad \textbf{Equation 19}$$

Earlier it has been shown that the refractive index of the lignocellulosic fiber material is fairly constant, varying only slight depending on the chemical composition of the cell wall

(cellulose 1.56, lignin 1.61), and this variation has very little or no significant impact on the optical properties of paper [124, 172]. It is known that refractive index of material is wavelength dependent; however the variation being small in the visible wavelength region, for water for example, ranging from 1.334 to 1.35 at wavelengths from 700nm to 400nm, respectively [132, 177]. Although the increase in the refractive index appears to be minor, the impact on the scattering coefficient – specific surface area relationship is accentuated through the relationship between reflectivity and refractive index (equation 17) as well as between reflectivity and the scattering coefficient (equation 18).

Based on these observations the increase in scattering at lower wavelengths can be fully explained by the change in the refractive index of the material as a function of the wavelength of light. As an example, if one is to use the variability in the refractive index of water in visible wavelength range, a decrease of 3% in refractive index results in a 10% increase in the slope of scattering coefficient-specific surface area relationship. This 10% increase is comparable with the increase in the slopes obtained in this study for scattering coefficient and specific surface area relationship (11%) for the visible wavelength range.

The refractive indices calculated using equations 17 and 18 are shown in Figure 52 for mercury porosimetry (excluding pores below 284 nm) and BET based on the linear relationships between scattering coefficient and specific surface area. The results obtained from the mercury porosimetry linear relationships are significantly below the values reported for pure cellulose and lignin [172]. However, the BET-based calculated refractive indices yield values in close proximity to those of the pure cell wall constitutive polymers (1.52-1.55). The wavelength explains all the variation in the calculated refractive index due to the fact that wavelength explained all the variation in scattering coefficient – specific surface area slopes. The rate of refraction index decrease is very similar to that reported by Parsons [173], where the refractive index of ramie fiber decreased from 1.6082 to 1.5969 at wavelengths 486 nm and 656 nm respectively.

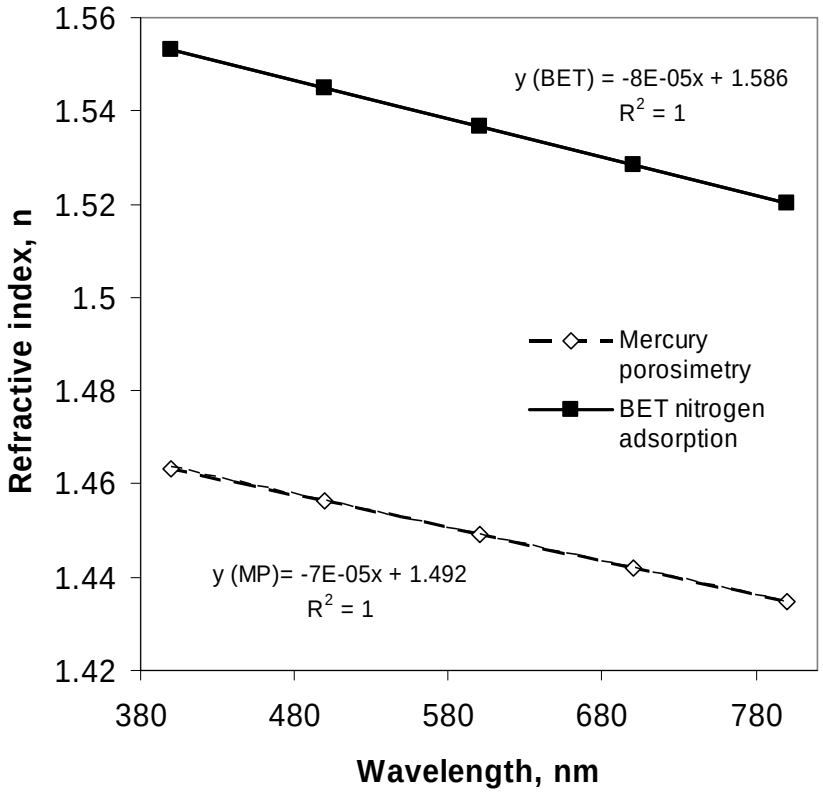

Figure 52. Wavelength dependency of refractive index for mercury porosimetry and BET nitrogen adsorption based results.

There is another plausible explanation for the discrepancy between mercury porosimetry and BET nitrogen adsorption reported here, and it implies that there is something inherently inaccurate in the mercury porosimetry specific surface area measurement. In mercury porosimetry, due to the fact that mercury doesn't wet fibers, a positive pressure is needed to penetrate the mercury into the pore structure. In order to detect nanometer-scale pores, significantly high pressures (up to 60,000 psi) are needed. It has been stated that these high pressures will possibly lead to structural changes in the material under investigation [130]. The mercury porosimetry specific surface areas when all pore sizes were included in the calculation were significantly higher than that of the BET specific surface areas. Thus, it is likely that the low correlation between specific surface area measured by mercury intrusion and light scattering coefficient below the 100-200 nm pore size is due to the destructive nature of the mercury intrusion method.

In Figure 53 the linear correlation coefficient (R^2 shown) of BET nitrogen absorption specific surface area and specific surface area calculated from the mercury porosimetry pore volume distribution was plotted against the excluded pore size in mercury porosimetry. The highest correlation coefficient was obtained exactly at the same pore size as for the scattering coefficient- mercury porosimetry relationship, 284 nm. The specific surface area detection ability of nitrogen molecule is 3.6 Å, thus it is unlikely that the pore size-based highest correlation for the BET-mercury porosimetry correlation would be obtained at a pore size of 284nm. This supports the idea that mercury intrusion destroys the sheet beyond 284nm, which corresponds to an intrusion pressure of 637 psi.

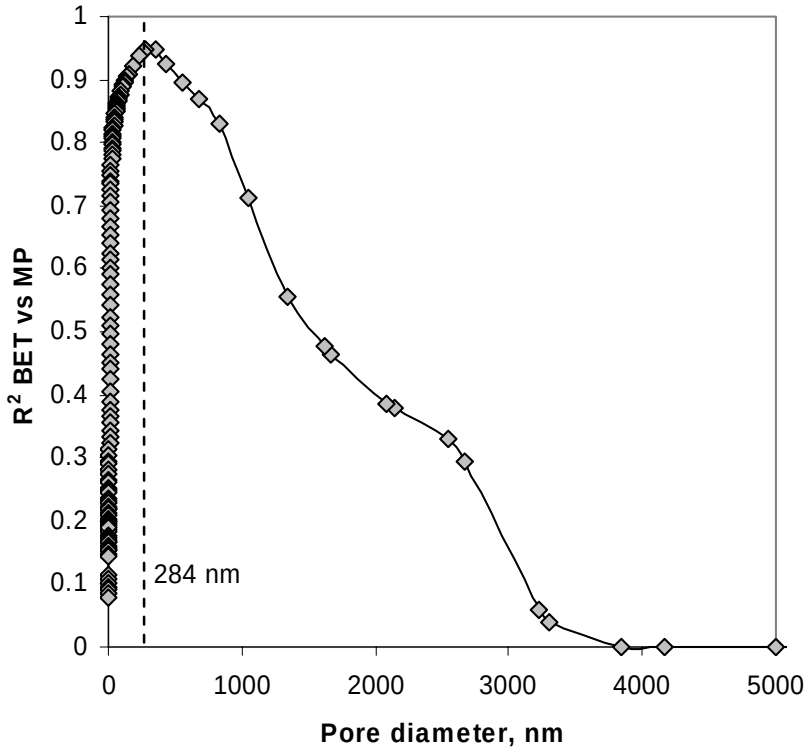

Figure 53. R^2 of the linear relationship between BET nitrogen adsorption and mercury porosimetry specific surface area as a function of the excluded pore sizes.

However, due to the comparable results obtained here for BET nitrogen adsorption and scattering coefficient with the earlier findings, and the significant similarity in the calculated refractive indices with the pure lignin and cellulose we believe that scattering coefficient is indeed a measure of specific surface area in mechanical pulps.

Conclusions

In this paper, the fundamental relationship between scattering coefficient and specific surface area in mechanical pulps was studied using mercury porosimetry and BET nitrogen absorption to measure specific surface area. The pulps included in the study were sheets of TMP fines (P200), whole pulp TMP and fiber (R48) wet pressed and press dried to various levels of specific surface area. It was shown that the scattering coefficient is a measure of specific surface area when the wavelength of light used in measuring scattering coefficient is beyond at which the scattering coefficient is not limited by significant absorption. For these samples the limit depended on the composition of the sheet and the pressing level and type used to induce bonding. However, there was no significant decrease in scattering coefficient in any of the samples when the wavelength of light used to measure scattering was beyond 600 nm[1].

The scattering efficiency, defined as the ratio of scattering coefficient and specific surface area, was a factor of wavelength used to measure scattering coefficient. It was shown using mercury porosimetry pore size distribution data that the increase in scattering efficiency was not due to the ability to detect smaller pores at lower wavelengths of light. A plausible explanation was given, which relates the increase in scattering efficiency to the change in refractive index of the material when the wavelength of light to measure scattering coefficient is altered.

[1] The bulk of the scattering coefficient data in the following chapters was measured using a wavelength of 572 nm. This had insignificant effect on the measured scattering coefficient.

Chapter 3: Distribution of load between various fractions in a heterogeneous mechanical pulp sheet in wet pressing and press drying

Abstract

The Ingmansson and Thode wet pressing method is one of the most widely accepted procedures capable of distinguishing between the changes in specific bond strength and specific bonded area. However, in heterogeneous pulps, such as mechanical pulps, it was not known if the various types of particles experience the same forces during pressing. In this paper it is shown that the middle and fines fractions bond in a lesser degree in a mixed sheet than they do as a homogeneous pure sheet at a constant pressing level. This indicates that in a heterogeneous mechanical pulp sheet the pressing force is transferred more through the fibers than the middle and fines fractions. However, the overall deviation from the linear addition model, where the mixture scattering coefficient was dictated by the individual component of the sheet, was only 4.8%. Thus, it is concluded that for practical purposes the scattering coefficient of heterogeneous mechanical pulp is the mass fraction based sum of scattering coefficients of individual fractions at all pressing levels.

Introduction

Relative bonded area (RBA) has been identified as an important property within chemical pulps, affecting the strength properties of these pulps [60]. The most widely accepted method for measuring RBA within chemical pulps involves a forced consolidation of the sheet by means of increasing wet pressing pressure, also known as the Ingmansson-Thode method [59]. This induces sheet consolidation and additional dewatering resulting in an enhanced bonded area without significantly altering any other properties of the sheet and fibers. When the change in total surface area is then plotted against tensile strength the relationship has been shown to follow an equation defined by Page [60]. By extrapolating the tensile strength to zero according to the Page equation, one is able to define the total unbonded, non swollen specific surface area of the sheet, then bonded area, and RBA of the sheet.

Mechanical pulps are very heterogeneous in nature, where the range of particle size varies from fairly sound wood fiber particles with length of 2 mm and width of approximately 50 µm to small fines particles with a size distribution from nanometer scale to several hundred microns in length [2]. Due to this heterogeneity in a mechanical pulp sheet, there can expected to be a large distribution of bonded area, i.e. the bonded area of the fine particles, bonded area of the fibers, and a range of everything in between. When the Ingmansson and Thode wet pressing method is used to determine the total unbonded specific surface area (S_o) of the heterogeneous mechanical pulp sheet, it is unclear whether the pressing procedure induces bonding of all the fractions homogenously. Thus, it is not known if the increase in tensile strength in pressing is associated with increase in bonding of all fractions or just some of the fractions.

Therefore, in this paper the heterogeneity of the specific surface area reduction as a function of sheet composition at various pressing levels was approached by fractionating pulp into three different fractions (fiber-R48), middle-R200 and fines-P200), mixing the fractions back together in known proportions, and then pressing them into different levels of bonding using press-drying at 120 °C and wet pressing at 23 °C. The linear addition of specific surface area was studied using scattering coefficient as a measure of specific surface area.

The theoretical approach followed the hypothesis described in Figure 54. When two materials with different specific surface areas are mixed and a totally unbonded sheet is formed (where no interaction between the components occur), the mixture should follow a linear addition rule. However, when a heterogeneous sheet composed of significantly variable particles is compressed in z-direction it is likely that some particles experience higher loads than others, resulting in deviation from the linear addition rule.

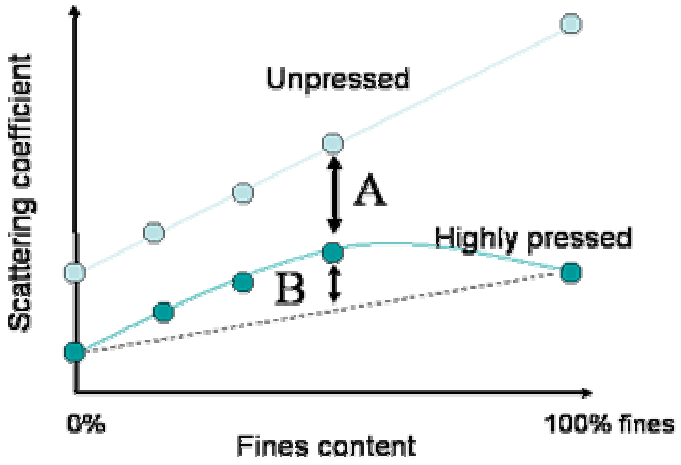

Figure 54. Theoretical approach to pressing of heterogeneous structures. The unbonded sheet is depicted as the unpressed sheet.

Figure 54 depicts an assumed case where fines experience less force and remain unbonded in a mixed sheet. The parameter B describes the amount of surface area (measured as scattering coefficient) which does not experience load during pressing. If B=0, then all fines are pressed and experience similar load, and reduce scattering coefficient accordingly. If B>0 then only part of the fines experience load in a mixed sheet. If B<0 then fines experience more load than the fiber fraction. A similar approach is applied to the other mixtures as well.

Experimental

Fiber middle and fines fractionation: The Bauer McNett apparatus was used to fractionate a hot disintegrated 110 CSF Norway spruce (Picea abies) TMP. The Bauer McNett was set up with 14, 48 and 200 mesh screens, and run for various times until no fines were observed coming with the excess water. Then the R14 and R48 fractions were mixed back together, and fractionated again using only hte R48 screen in order to achieve a near pure fiber fraction without any fines present. During the fractionation the P200 fraction was collected using the sedimentation method, as described by Luukko [30].

Handsheet forming: Handsheets were formed using a standard British handsheet mold with 150 mesh screen and recirculation of whitewater. Fines handsheets were formed on a dense glass fiber filterpaper (18.5 cm Whatman 934AH). Fines contents of the fiber-fines mixed sheets were measured from the formed handsheets using the DDJ method,

T 261 cm-00. All handsheets were restraint dried if not dry after pressing. The target handsheet basis weight was 60 g/m^2 O.D.

Wet pressing: Couched handsheets were not pressed. Wet pressing was conducted at 65, 489 and 978 psi's and 23 ℃ using a Carver press and 3 blotter papers on one side and a chrome plate on the other side of the handsheet. Wet pressed handsheets were pressed for 1 minute.

Press drying: Press drying was conducted at 6 pressing levels 0, 0.8, 8.1, 16.3, 48.9 and 163 psi's. Individual handsheet were pressed between hot plates heated to 120 ℃ and a sandwich that consisted of a felt, wet blotter (to increase drying time and humidity above 100 ℃), handsheet, chrome plate, and a filter paper (to protect the chrome plate). All handsheets were pressed until dry.

Testing: Scattering coefficient was measured using the Tappi (T 1214 sp-98) standard with 572 nm wavelength. Tensile strength was measured using the Tappi (T 494) standard, but with the exception of a reduced span length 2 inches, in order to minimize the effect of faulty strip edges due to strip cutting especially on fines handsheets. Also 0.5 inches/min strain velocity was used, in order to be able to gather enough data points (20 points/sec) to produce a sound stress-strain curve. BET specific surface area measurements were performed at Micromeritics, Norcross, GA, USA.

Results

Two-sidedness and the effect on scattering coefficient

It has been shown that surface smoothness has an effect on the scattering properties of the sheets. A visual inspection of the sheets showed extreme differences between the plate side and blotter side for the press dried sheets. Similar differences were also seen in wet pressed sheets, also the surface smoothness and gloss of the handsheets varied depending on fines content and pressing procedure. However, the surface smoothness had no impact on the scattering properties, when the scattering coefficient was measured from the rough and smooth sides of the sheet. Figure 55 shows the correlation smoothside and roughside scattering coefficients of fiber, fines and middle fractions, their mixtures, and whole pulps pressed to various levels of bonding using wet pressing and press drying. The scattering coefficients measured from the roughside of the sheet were 0.87-1.29% higher than those of smoothside, the difference being larger for press dried sheets. This shows that the observed two-sidedness had no significant

impact on the measured scattering coefficient, and is consistent with the earlier findings where scattering measured using Tappi standard opacimeter has been shown to be independent of the sheet surface gloss [178].

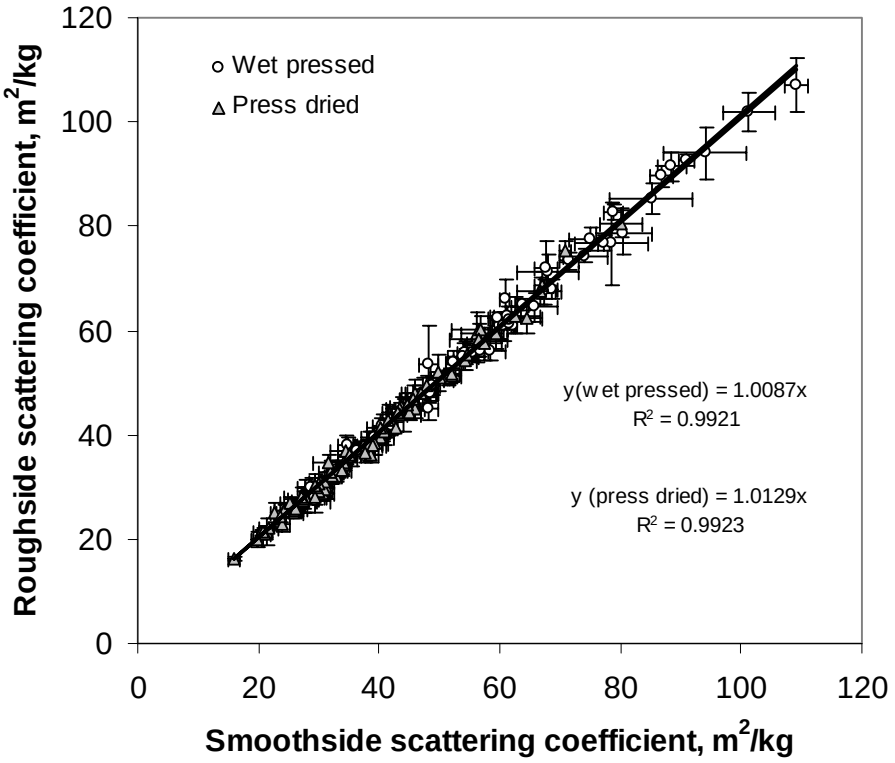

Figure 55. Roughside vs. smoothside scattering coefficients of fiber, fines, middle fractions, their mixtures, and whole pulp handsheets.

Throughout the rest of the study scattering values measured from the smooth-side were used.

Scattering coefficient and specific surface area relationship

BET specific surface area was measured from a series of fines, fiber and whole pulp sheets wet pressed and press dried to various levels of bonding (couched, wet pressed and high pressure press dried). BET specific surface area correlated well with scattering coefficient (R^2=0.948) measured at 572 nm and 15^o angle, and the relationship was independent of pressing pressure, temperature or sheet composition. The intercept of the linear line passes the origin within the limits of statistical significance, and the slope

of the linear correlation line is slightly lower but similar to that obtained by Haselton [111] for chemical pulps or Rennel [115] for mechanical pulps (Figure 56).

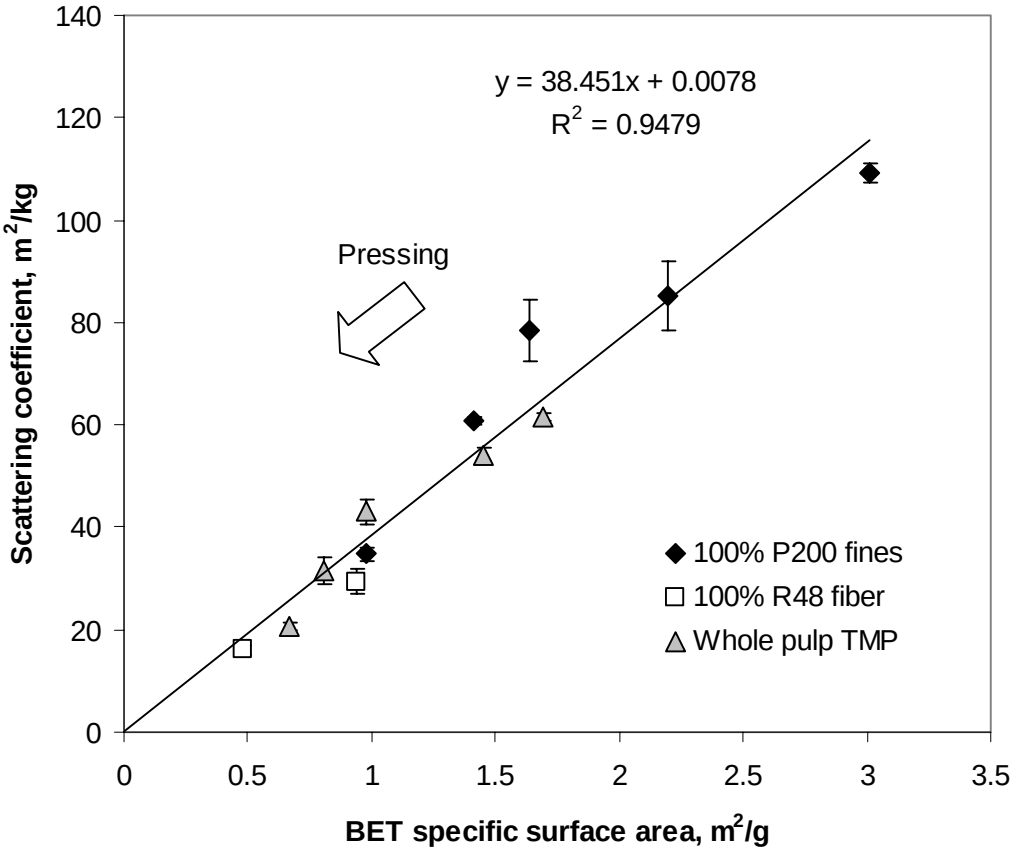

Figure 56. BET specific surface area vs. scattering coefficient (572 nm, 15°) of fines (P200), fiber (R48) and whole pulp TMP sheets pressed to various levels of bonding.

Statistical approach

Statistical analysis was done by using a multiple regression approach, where two independent factors for binary mixtures and four for ternary mixtures were used to explain the variation in scattering coefficient at one pressing level. The independent factors are:

- Fines and/or middle fraction content to the first power
- Fines and/or middle fraction content to the power of two

This approach enables a statistical analysis of the significance of the first and second order terms in explaining the variation in scattering coefficient as a function of fines or middle fraction content. Thus, it provides a whole series based analysis of the possible deviation from the linear addition rule. As an example, the approach is depicted graphically in Figure 57 for one pressing level (couched) and fiber (R48) and fines (P200) mixed sheets.

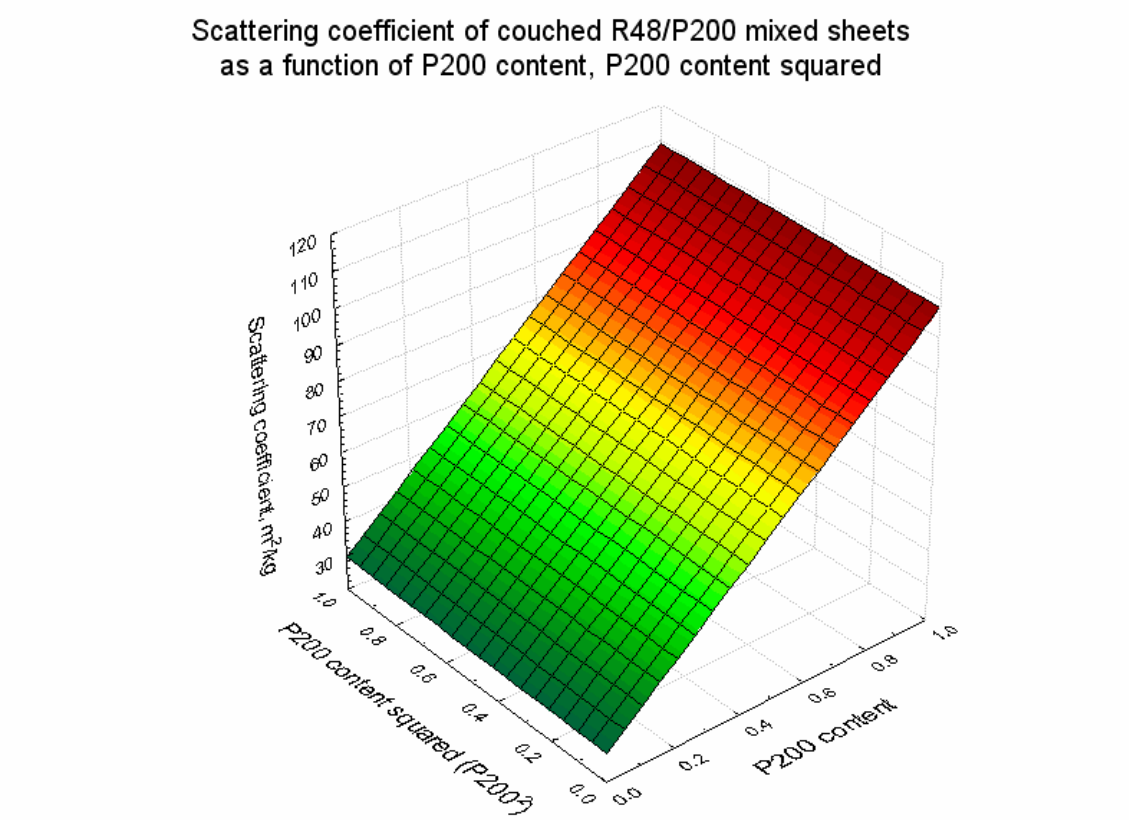

Figure 57. Scattering coefficient of couched R48 and P200 mixed sheets as function of P200 fines content and P200 fines content squared.

The statistical analysis of the couched fiber (R48) and fines (P200) mixed sheets show that the squared term was not statistically significant and did not add to the model (Table 8).

Table 8. Multiple regression analysis of couched fiber (R48) and fines (P200) mixed sheets

R squared = 0.9998	BETA	Std. error of BETA	B	Std. error of B	t(2)	p-level
Intercept			28.16584	0.610103	46.16573	0.000469
P200 content	0.981921	0.042895	79.69553	3.481497	22.89117	**0.001903**
P200 content squared	0.018577	0.042895	1.40959	3.254732	0.43309	0.707182

Ternary approach results

In the ternary approach P200 fines and R200 middle fraction were mixed into the R48 fiber at various contents so that a full range of mixtures were obtained. Then these various mixtures were pressed to 10 different levels of bonding, or sheet consolidation (4 wet pressing and 6 press drying levels). All the various mixture levels are shown in Figure 58. Only case based average data was used in the statistical analysis.

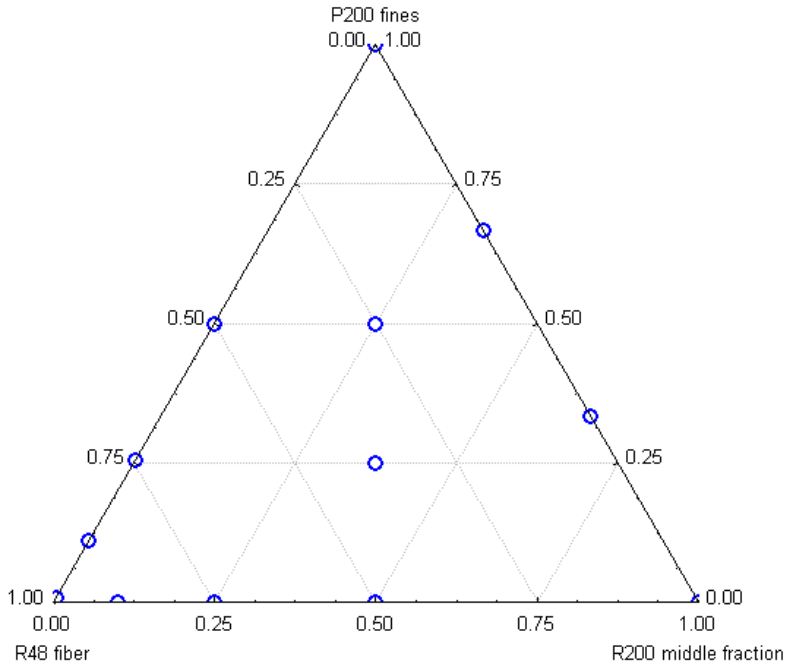

Figure 58. Mixtures used in the study

The multiple regression analysis was then done using four independent variables to explain the dependent scattering coefficient at various pressing levels. The independent variables were:

- P200 fines content
- P200 fines content squared
- R200 middle fraction content
- R200 middle fraction content squared

All sheets that were wet pressed to various levels of bonding showed only significant first order linear terms for P200 fines content and R200 middle fraction content ($p<0.05$). All press dried sheets, excluding the 0 psi pressed sheets), in addition to the linear first order terms showed significant second order terms. These were assigned to various pressing levels as follows:

- Press dried at 0.8 psi: $R200^2$ and $P200^2$
- Press dried at 8.1 psi: $R200^2$
- Press dried at 16.3 psi: $R200^2$
- Press dried at 48.9 psi: $R200^2$ and $P200^2$
- Press dried at 163 psi: $R200^2$

The statistical analysis results are shown in Table 9, and the quadratic models of scattering coefficient as a function of R48, R200 and P200 fraction contents is depicted in Figure 59. Middle fraction R200 was responsible for most of the non-linear behavior in the mixed sheets. Although the second order terms were statistically significant, they did not appear to have a major impact on the models, as seen in Figure 59.

Table 9. Ternary approach statistical results for R48 fiber, R200 middle fraction and P200 fines sheets at various pressing levels

Mixture	R48+R200+P200						Mixture	R48+R200+P200					
Pressing level	Couched						Pressing level	Hot 0.8 psi					
R squared	BETA	Std. error of BETA	B	Std. error of B	t(2)	p-level	R squared	BETA	Std. error of BETA	B	Std. error of B	t(2)	p-level
0.99543904							0.99649514						
Intercept			29.1997	1.096645	26.62637	0.000000	Intercept			28.3581	0.588402	48.19512	0.000000
R200	0.553126	0.070519	43.4787	5.543149	7.84367	0.000050	R200	0.509495	0.061817	24.5128	2.974163	8.24192	0.000035
P200	0.972675	0.071288	75.4190	5.527533	13.64424	0.000001	P200	0.823430	0.062492	39.0788	2.965784	13.17654	0.000001
$R200^2$	-0.128002	0.070757	-10.9840	6.071790	-1.80903	0.108052	$R200^2$	-0.206881	0.062027	-10.8659	3.257804	-3.33536	0.010302
$P200^2$	0.044352	0.071118	3.7958	6.086484	0.62364	0.550227	$P200^2$	0.214164	0.062343	11.2185	3.265688	3.43527	0.008886
Mixture	R48+R200+P200						Mixture	R48+R200+P200					
Pressing level	Wet 65 psi						Pressing level	Hot 8.1 psi					
R squared	BETA	Std. error of BETA	B	Std. error of B	t(2)	p-level	R squared	BETA	Std. error of BETA	B	Std. error of B	t(2)	p-level
0.99696947							0.99243351						
Intercept			33.19272	0.761423	43.59299	0.000000	Intercept			27.4965	0.743984	36.95848	0.000000
R200	0.447255	0.057482	29.94581	3.848723	7.78071	0.000053	R200	0.604427	0.090829	25.0250	3.760572	6.65458	0.000160
P200	1.004809	0.058110	66.36297	3.837881	17.29157	0.000000	P200	1.107451	0.091820	45.2289	3.749978	12.06112	0.000002
$R200^2$	-0.069005	0.057677	-5.04376	4.215770	-1.19640	0.265791	$R200^2$	-0.271055	0.091136	-12.2513	4.119212	-2.97418	0.017758
$P200^2$	0.021821	0.057971	1.59069	4.225972	0.37641	0.716400	$P200^2$	-0.101231	0.091600	-4.5633	4.129180	-1.10514	0.301225
Mixture	R48+R200+P200						Mixture	R48+R200+P200					
Pressing level	Wet 489 psi						Pressing level	Hot 16.3 psi					
R squared	BETA	Std. error of BETA	B	Std. error of B	t(2)	p-level	R squared	BETA	Std. error of BETA	B	Std. error of B	t(2)	p-level
0.99261568							0.98965137						
Intercept			31.5588	1.009580	31.25933	0.000000	Intercept			25.7117	0.750581	34.25576	0.000000
R200	0.519166	0.089729	29.5261	5.103065	5.78595	0.000412	R200	0.634124	0.106223	22.6488	3.793921	5.96976	0.000334
P200	1.043835	0.090708	58.5589	5.088689	11.50765	0.000003	P200	1.072285	0.107382	37.7783	3.783233	9.98571	0.000009
$R200^2$	-0.162804	0.090032	-10.1078	5.589736	-1.80828	0.108174	$R200^2$	-0.305607	0.106582	-11.9159	4.155741	-2.86733	0.020915
$P200^2$	-0.025716	0.090491	-1.5924	5.603263	-0.28419	0.783484	$P200^2$	-0.066596	0.107125	-2.5897	4.165798	-0.62166	0.551464
Mixture	R48+R200+P200						Mixture	R48+R200+P200					
Pressing level	Wet 978 psi						Pressing level	Hot 48.9 psi					
R squared	BETA	Std. error of BETA	B	Std. error of B	t(2)	p-level	R squared	BETA	Std. error of BETA	B	Std. error of B	t(2)	p-level
0.99211774							0.98998305						
Intercept			30.8627	0.976423	31.60791	0.000000	Intercept			22.43478	0.565269	39.68865	0.000000
R200	0.494398	0.092705	26.3211	4.935472	5.33305	0.000700	R200	0.643967	0.104507	17.60620	2.857235	6.16197	0.000270
P200	0.980435	0.093716	51.4882	4.921569	10.46174	0.000006	P200	1.231790	0.105647	33.22003	2.849186	11.65948	0.000003
$R200^2$	-0.194642	0.093018	-11.3124	5.406160	-2.09251	0.069746	$R200^2$	-0.318406	0.104860	-9.50333	3.129725	-3.03647	0.016150
$P200^2$	0.045367	0.093492	2.6297	5.419243	0.48525	0.640510	$P200^2$	-0.245375	0.105395	-7.30414	3.137299	-2.32816	0.048300
Mixture	R48+R200+P200						Mixture	R48+R200+P200					
Pressing level	Hot 0 psi						Pressing level	Hot 163 psi					
R squared	BETA	Std. error of BETA	B	Std. error of B	t(2)	p-level	R squared	BETA	Std. error of BETA	B	Std. error of B	t(2)	p-level
0.99127509							0.96991568						
Intercept			29.23888	1.242825	23.52614	0.000000	Intercept			17.16658	0.682672	25.14615	0.000000
R200	0.529880	0.097534	34.12887	6.282038	5.43277	0.000621	R200	0.791670	0.181111	15.08347	3.450665	4.37118	0.002377
P200	1.011788	0.098598	64.28278	6.264341	10.26170	0.000007	P200	1.136827	0.183088	21.36546	3.440945	6.20918	0.000257
$R200^2$	-0.139948	0.097864	-9.84022	6.881146	-1.43003	0.190580	$R200^2$	-0.420401	0.181725	-8.74407	3.779750	-2.31340	0.049426
$P200^2$	0.005148	0.098363	0.36103	6.897799	0.05234	0.959541	$P200^2$	-0.168750	0.182650	-3.50055	3.788897	-0.92390	0.382561

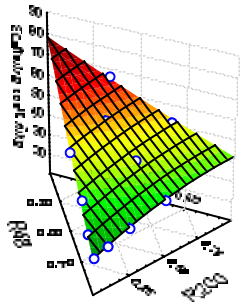

Press dried 0.8 psi

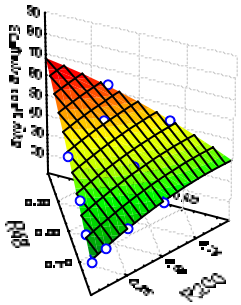

Press dried 8.1 psi

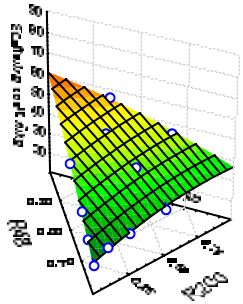

Press dried 16.3 psi

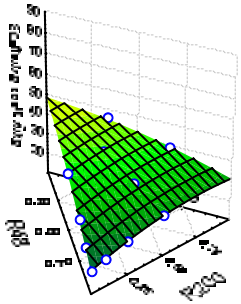

Press dried 48.9 psi

Figure 59. Quadratic models of the scattering coefficient as a function of R48 fiber, R200 middle fraction and P200 fines contents in the sheet

Binary approach results

The results from the ternary approach indicated that the R200 middle fraction was mostly responsible for the non-linear behavior of surface area reduction in the sheet. Thus, in order to quantify the extent of the various components contribution to the non-linear addition of scattering coefficient, a statistical analysis based on binary approach was done. The binary mixtures analyzed were:

- R48 fiber and P200 fines mixtures
- R48 fiber and R200 middle fraction mixtures
- R200 middle fraction and P200 fines mixtures
- 50% R48 fiber + 50% R200 middle and P200 fines fraction mixtures

Hereafter individual handsheet data was used in the statistical analysis, and thus it was expected that some of the significant terms observed here were different from the ternary approach analysis.

Addition rule in fiber and fines fraction mixtures

The fiber (R48) and fines (P200) mixtures are the two extremes in terms of particles size heterogeneity in mechanical pulps. Thus, it was expected that if there was a variations in the load bearing behavior of the heterogeneous structure, and a deviation from the linear addition rule, it should be especially visible in sheets consisting of fiber (R48) and fines (P200) fractions.

Figure 60 depicts the scattering coefficient of fiber (R48) and fines (P200) mixed sheets as a function of fines (P200) content. Most of the reduction in scattering coefficient was due to the fines, this was especially obvious in wet pressing, where the decrease in scattering coefficient of fibers (R48) was not statistically significant. In general the mixed sheets followed the linear addition rule. However, a slight deviation from linear addition rule was visible, and also more pronounced for the highly wet pressed (489 psi) sheets.

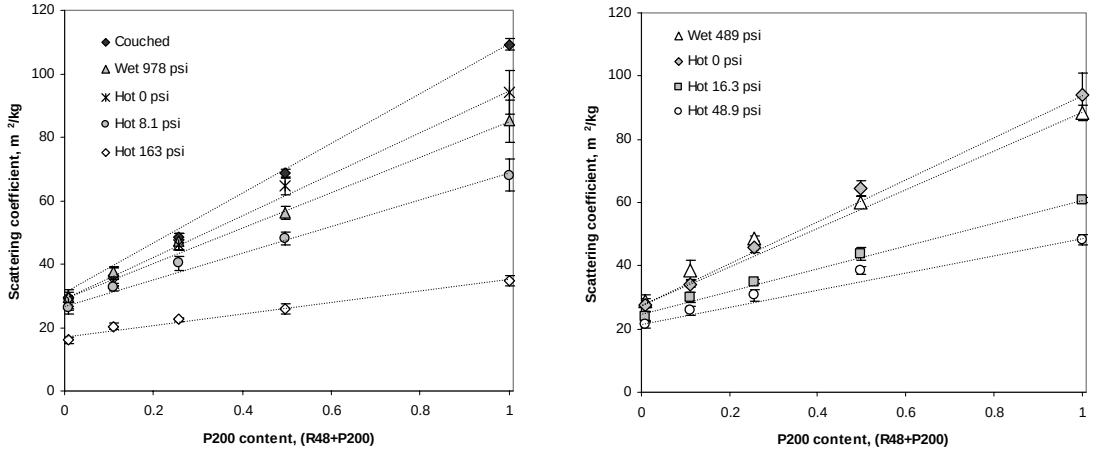

Figure 60. Scattering coefficient as a function of fines content (P200 added into R48 fraction) at various pressing levels.

Multiple regression analysis (described earlier) was performed for fiber (R48) and fines (P200) mixed sheets pressed to various levels of bonding. Individual single handsheet based data was used in the statistical analysis. The results of the statistical analysis are shown in Table 10. The linear term was statistically significant in each of the cases. Statistically significant second order terms were found in the following cases:

- Wet pressed at 489 psi
- Press dried (hot dried) at 0 psi
- Press dried at 16.3 psi
- Press dried at 48.9 psi

These results were slightly different from the ternary approach results regarding the significant second order terms, and was due to the fact that in the ternary approach only average data from 5 handsheets per data point was used, whereas here all handsheet data was included.

The absolute deviation from the linear addition model is depicted in Figure 61 for the statistically significant cases.

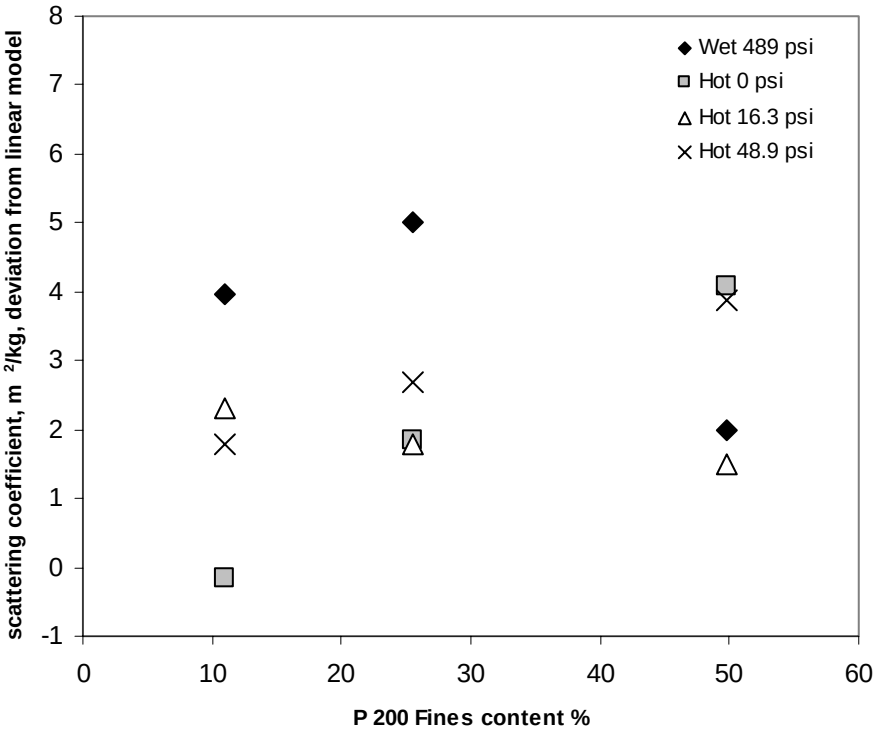

Figure 61. Absolute difference (measured – linear model) in scattering coefficient at various fines contents and pressing levels for the statistically significant cases.

The relative error of the linear model was studied by plotting the real measured data against the linear model based calculated data. Throughout the study the following equation was used for the linear model for each pressing level separately:

$$S_{mix} = x_{fibers}S_{fiber} + x_{middle}S_{middle} + x_{fines}S_{fines} \qquad \textbf{Equation 20}$$

Where the S_{mix} is the scattering coefficient of the mixed sheet based on the linear model, S_{fiber}, S_{middle} and S_{fines} are the scattering coefficients of fiber (R48), middle (R200) and fines (P200) fractions respectively at a constant pressing level, and x_{fiber}, x_{middle} and x_{fines} the mass fractions of fiber (R48) middle (R200) and fines (P200) fractions.

The relative error of the linear model was small. On average for the statistically significant non-linear cases the linear model underestimates the real data by 6.05%, as seen in Figure 62.

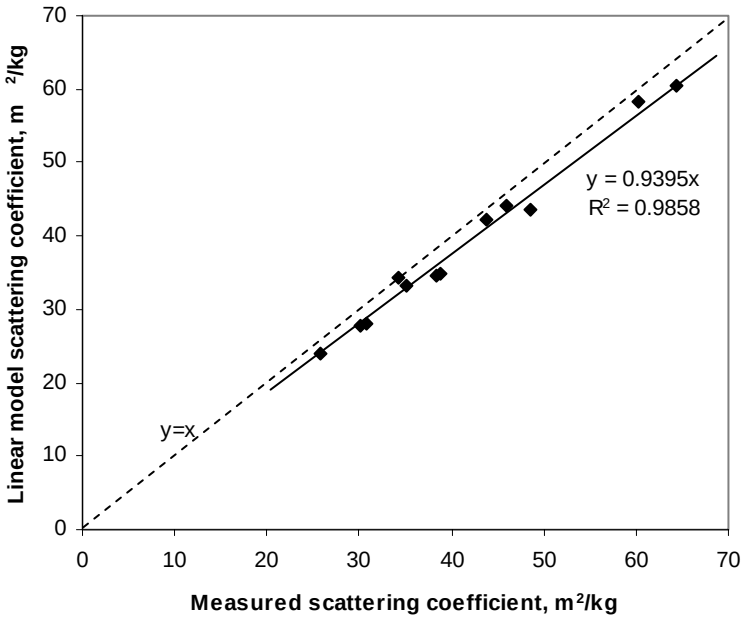

Figure 62. Measured scattering coefficient vs. scattering coefficient from the linear models for the statistically significant non-linear cases.

Table 10. Multiple regression results of fiber (R48) and fines (P200) mixed sheets at various pressing levels

Mixture	R48/P200						Mixture	R48/P200					
Pressing level	Couched						Pressing level	Hot 0.8 psi					
R squared	BETA	Std. error of BETA	B	Std. error of B	t(2)	p-level	R squared	BETA	Std. error of BETA	B	Std. error of B	t(2)	p-level
0.99542766							0.97687731						
Intercept			28.11745	0.796231	35.31318	0.000000	Intercept			28.10656	1.186599	23.68666	0.000000
P200 content	0.980562	0.056752	79.80915	4.619079	17.27815	0.000000	P200 content	0.811493	0.127168	41.64133	6.525539	6.38129	0.000002
P200 content squared	0.017670	0.056752	1.33269	4.280150	0.31137	0.758211	P200 content squared	0.181798	0.127168	8.58572	6.005724	1.42959	0.166883
Mixture	R48/P200						Mixture	R48/P200					
Pressing level	Wet 65 psi						Pressing level	Hot 8.1 psi					
R squared	BETA	Std. error of BETA	B	Std. error of B	t(2)	p-level	R squared	BETA	Std. error of BETA	B	Std. error of B	t(2)	p-level
0.99251354							0.96631431						
Intercept			31.60409	0.869210	36.35954	0.000000	Intercept			26.75797	1.126917	23.74440	0.000000
P200 content	1.112565	0.071261	77.43943	4.960072	15.61256	0.000000	P200 content	1.176413	0.155843	48.97106	6.487334	7.54872	0.000000
P200 content squared	-0.120930	0.071261	-7.86898	4.637000	-1.69700	0.103801	P200 content squared	-0.201534	0.155843	-7.87033	6.085979	-1.29319	0.209991
Mixture	R48/P200						Mixture	R48/P200					
Pressing level	Wet 489 psi						Pressing level	Hot 16.3 psi					
R squared	BETA	Std. error of BETA	B	Std. error of B	t(2)	p-level	R squared	BETA	Std. error of BETA	B	Std. error of B	t(2)	p-level
0.98719882							0.98846398						
Intercept			29.4201	0.901881	32.62083	0.000000	Intercept			24.52488	0.561783	43.65543	0.000000
P200 content	1.217793	0.089809	71.8318	5.297396	13.55984	0.000000	P200 content	1.175573	0.088459	42.60303	3.205765	13.28950	0.000000
P200 content squared	-0.234354	0.089809	-13.0637	5.006254	-2.60947	0.015674	P200 content squared	-0.189005	0.088459	-6.40345	2.996959	-2.13665	0.043997
Mixture	R48/P200						Mixture	R48/P200					
Pressing level	Wet 978 psi						Pressing level	Hot 49.8 psi					
R squared	BETA	Std. error of BETA	B	Std. error of B	t(2)	p-level	R squared	BETA	Std. error of BETA	B	Std. error of B	t(2)	p-level
0.96839638							0.98230497						
Intercept			30.43624	1.413799	21.52798	0.000000	Intercept			21.0743	0.535456	39.35766	0.000000
P200 content	1.037403	0.146414	57.16325	8.067719	7.08543	0.000000	P200 content	1.574089	0.113096	42.4169	3.047585	13.91819	0.000000
P200 content squared	-0.055322	0.146414	-2.84980	7.542232	-0.37785	0.709166	P200 content squared	-0.613179	0.113096	-15.2787	2.818031	-5.42176	0.000016
Mixture	R48/P200						Mixture	R48/P200					
Pressing level	Hot 0 psi						Pressing level	Hot 163 psi					
R squared	BETA	Std. error of BETA	B	Std. error of B	t(2)	p-level	R squared	BETA	Std. error of BETA	B	Std. error of B	t(2)	p-level
0.98287065							0.9539825						
Intercept			26.0109	1.292135	20.13021	0.000000	Intercept			16.85637	0.559401	30.13287	0.000000
P200 content	1.221856	0.107791	83.5810	7.373452	11.33539	0.000000	P200 content	1.185937	0.176675	21.42760	3.192174	6.71254	0.000001
P200 content squared	-0.240618	0.107791	-15.3874	6.893186	-2.23226	0.036098	P200 content squared	-0.218293	0.176675	-3.68724	2.984253	-1.23557	0.229652

Addition rule in fiber and middle fraction mixtures

The fraction retained on the 200 mesh screen is very heterogeneous. Pieces of fiber, fibril type fines, fairly sound juvenile fibers, as well parenchyma cells dominate [2]. The character of the middle fraction resembles more that of the fiber fraction, indicating that the linear addition rule is more likely to apply, than it is for fiber and fines mixed sheets. However, there was more consistent deviation from the linearity than was observed for fiber (R48) and fines (P200) fraction mixed sheets. Both, the linear and second order term were statistically significant at all pressing levels.

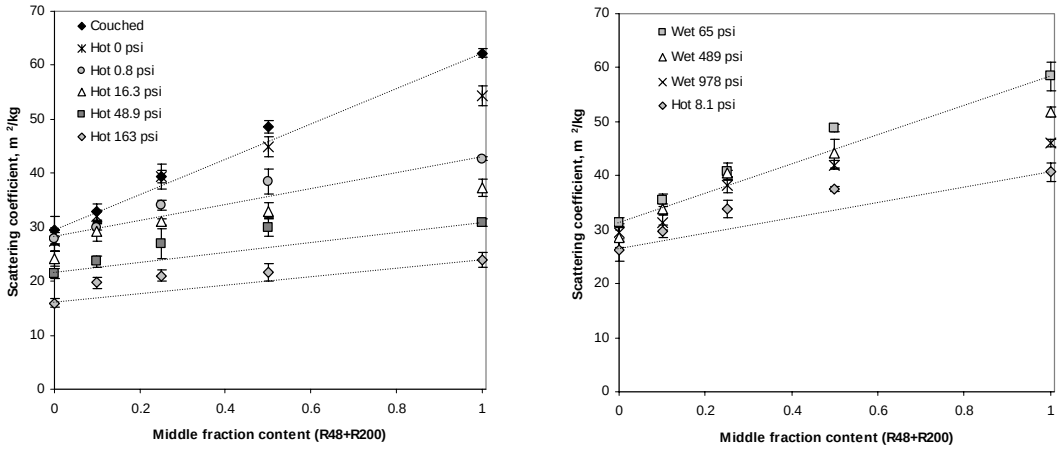

Figure 63. Scattering coefficient as a function of middle fraction content (R200 added into R48 fraction) at various pressing levels.

The absolute deviations from the linear addition model are depicted in Figure 64 for the statistically significant cases. In general the absolute deviations from the linear addition rule were small. As the pressure was increased the maximum deviation from the linear addition rule was obtained at lower middle fraction content. In general this deviation was largest at 25% middle fraction content. This is likely related to the total amount void area between fibers and the ability of middle fraction particles to fill these interstices.

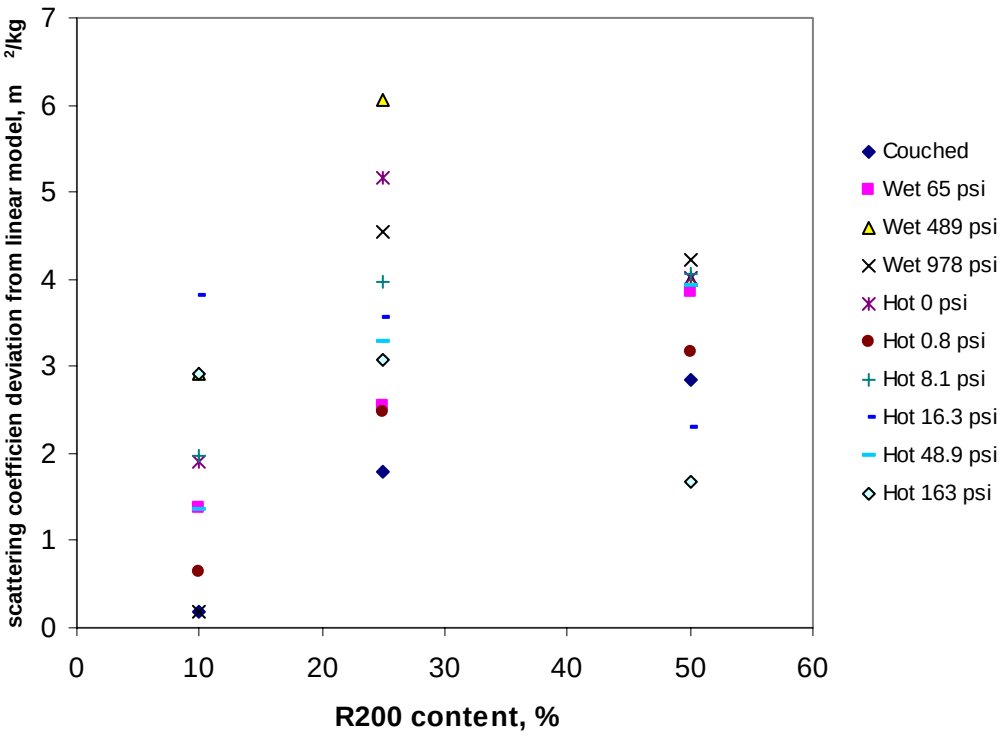

Figure 64. Absolute difference (measured – linear model) in scattering coefficient at various middle fraction contents and pressing levels for the statistically significant cases.

On average for the statistically significant non linear cases the linear model underestimated the real measured scattering coefficient by 8.45%, as shown in Figure 65.

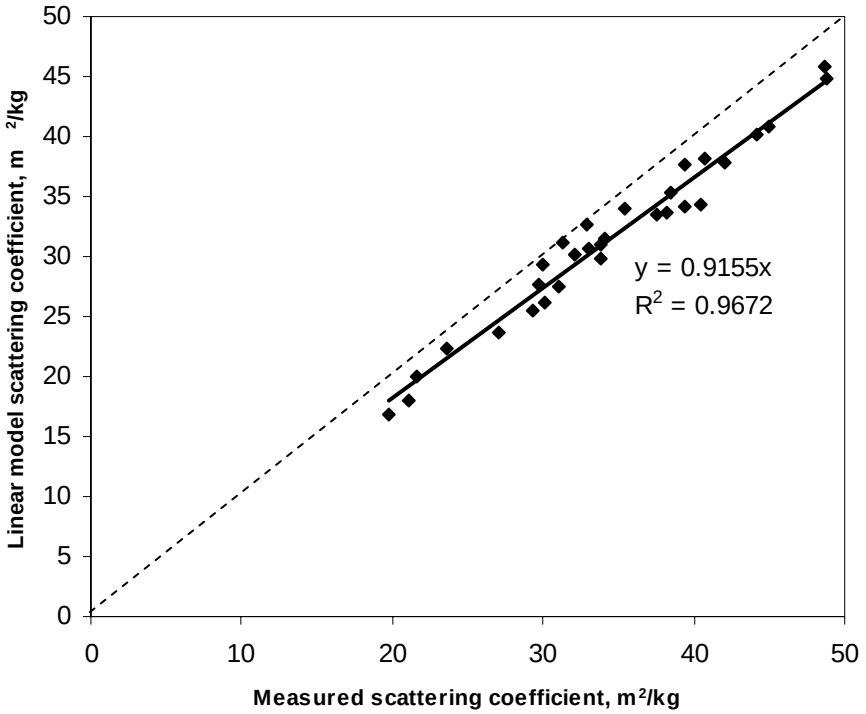

Figure 65. Measured scattering coefficient vs. scattering coefficient from the linear models for the statistically significant non-linear cases (R48 and R200 mixtures).

Table 11. Multiple regression results of fiber (R48) and middle fraction (R200) mixed sheets at various pressing levels

Mixture	R48/R200						Mixture	R48/R200					
Pressing level	Couched						Pressing level	Hot 0.8 psi					
R squared	BETA	Std. error of BETA	B	Std. error of B	t(2)	p-level	R squared	BETA	Std. error of BETA	B	Std. error of B	t(2)	p-level
0.98184479							0.95566535						
Intercept			28.99038	0.609281	47.58128	0.000000	Intercept			27.67418	0.495835	55.81330	0.000000
R200 content	1.329520	0.107429	44.50327	3.595981	12.37584	0.000000	R200 content	1.878471	0.180518	28.25531	2.715282	10.40603	0.000000
R200 content squared	-0.355376	0.107429	-11.24875	3.400447	-3.30802	0.003070	R200 content squared	-0.967507	0.180518	-13.51064	2.520816	-5.35963	0.000030
Mixture	R48/R200						Mixture	R48/R200					
Pressing level	Wet 65 psi						Pressing level	Hot 8.1 psi					
R squared	BETA	Std. error of BETA	B	Std. error of B	t(2)	p-level	R squared	BETA	Std. error of BETA	B	Std. error of B	t(2)	p-level
0.97937532							0.93415386						
Intercept			31.32951	0.549965	56.96636	0.000000	Intercept			26.51984	0.541451	48.97923	0.000000
R200 content	1.533492	0.116173	41.98332	3.180538	13.20007	0.000000	R200 content	2.097733	0.207576	31.64444	3.131298	10.10586	0.000000
R200 content squared	-0.575932	0.116173	-14.87669	3.000825	-4.95753	0.000058	R200 content squared	-1.230795	0.207576	-17.51754	2.954367	-5.92937	0.000006
Mixture	R48/R200						Mixture	R48/R200					
Pressing level	Wet 489 psi						Pressing level	Hot 16.3 psi					
R squared	BETA	Std. error of BETA	B	Std. error of B	t(2)	p-level	R squared	BETA	Std. error of BETA	B	Std. error of B	t(2)	p-level
0.95242099							0.86337176						
Intercept			29.3839	0.662818	44.33185	0.000000	Intercept			25.49763	0.655870	38.87604	0.000000
R200 content	1.838528	0.170144	42.6351	3.945615	10.80570	0.000000	R200 content	1.769747	0.299008	22.44980	3.793004	5.91874	0.000006
R200 content squared	-0.928485	0.170144	-20.5378	3.763544	-5.45705	0.000015	R200 content squared	-0.903550	0.299008	-10.81418	3.578684	-3.02183	0.006269
Mixture	R48/R200						Mixture	R48/R200					
Pressing level	Wet 978 psi						Pressing level	Hot 49.8 psi					
R squared	BETA	Std. error of BETA	B	Std. error of B	t(2)	p-level	R squared	BETA	Std. error of BETA	B	Std. error of B	t(2)	p-level
0.95567387							0.86303424						
Intercept			29.06646	0.522893	55.58779	0.000000	Intercept			21.3241	0.571478	37.31391	0.000000
R200 content	2.058882	0.170311	36.55678	3.023975	12.08898	0.000000	R200 content	2.341568	0.299377	25.8496	3.304952	7.82148	0.000000
R200 content squared	-1.172932	0.170311	-19.64941	2.853109	-6.88702	0.000001	R200 content squared	-1.564392	0.299377	-16.2942	3.118210	-5.22550	0.000031
Mixture	R48/R200						Mixture	R48/R200					
Pressing level	Hot 0 psi						Pressing level	Hot 163 psi					
R squared	BETA	Std. error of BETA	B	Std. error of B	t(2)	p-level	R squared	BETA	Std. error of BETA	B	Std. error of B	t(2)	p-level
0.97247337							0.75593418						
Intercept			27.8269	0.653972	42.55053	0.000000	Intercept			17.10030	0.548905	31.15348	0.000000
R200 content	1.660550	0.143033	44.7167	3.851710	11.60957	0.000000	R200 content	1.920450	0.399637	15.25458	3.174408	4.80549	0.000084
R200 content squared	-0.716609	0.143033	-18.3460	3.661804	-5.01010	0.000067	R200 content squared	-1.145622	0.399637	-8.58576	2.995041	-2.86666	0.008965

Addition rule in middle and fines fraction mixtures

The middle fraction (R200) and fines (P200) mixed sheet followed the linear addition rule almost in all cases. The only exceptions were the couched and high pressure press dried (48.9 psi and 163 psi) sheets.

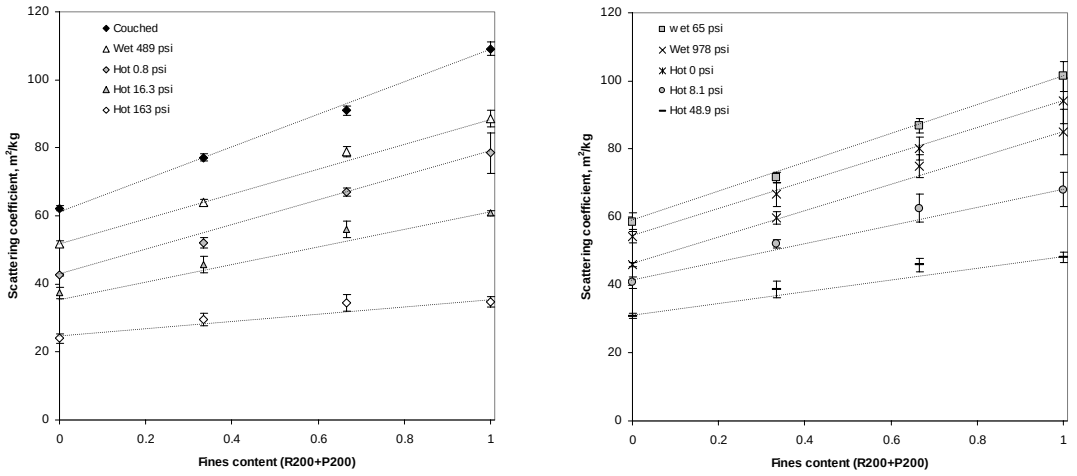

Figure 66. Scattering coefficient as a function of fines fraction (P200) content (P200 added into R200 fraction) at various pressing levels.

The absolute deviations from the linear addition model are depicted in Figure 67 for the statistically significant cases. These deviations were negative for the couched sheets, and positive for the highly press dried sheets.

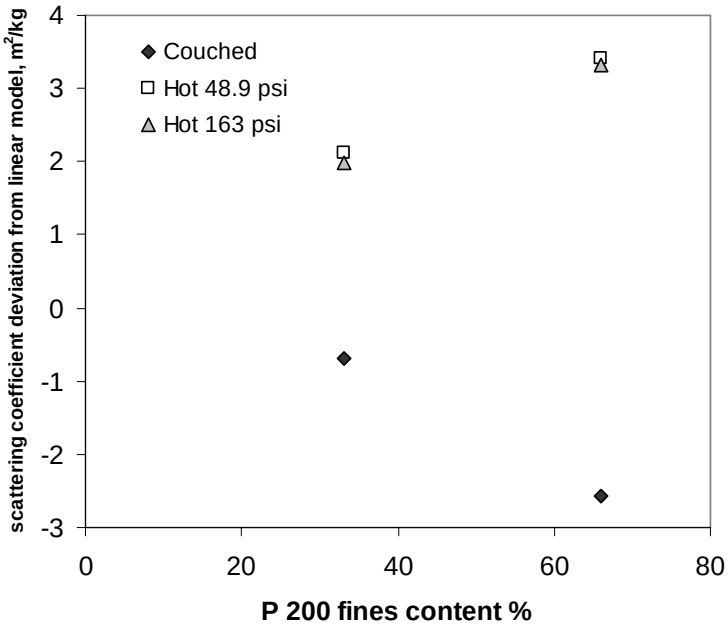

Figure 67. Absolute difference (measured – linear model) in scattering coefficient at various middle fraction contents and pressing levels for the statistically significant cases.

The average relative error of the linear model was small. On average for the statistically significant non linear cases the linear model underestimated the real data only by 0.62%, as shown in Figure 68.

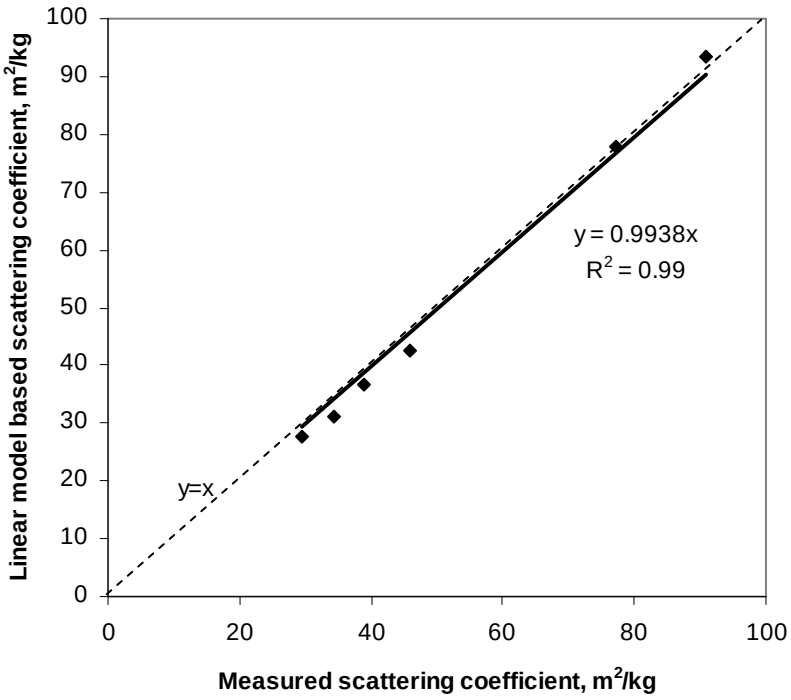

Figure 68. Measured scattering coefficient vs. scattering coefficient from the linear models for the statistically significant non-linear cases.

Table 12. Multiple regression results of middle fraction (R200) and fines (P200) mixed sheets at various pressing levels

Mixture	R200/P200						Mixture	R200/P200					
Pressing level	Couched						Pressing level	Hot 0.8 psi					
R squared	BETA	Std. error of BETA	B	Std. error of B	t(2)	p-level	R squared	BETA	Std. error of BETA	B	Std. error of B	t(2)	p-level
0.99386126							0.95489148						
Intercept			62.47943	0.654015	95.53204	0.000000	Intercept			41.96370	1.416481	29.62531	0.000000
P200 content	0.833449	0.066879	39.00106	3.129602	12.46199	0.000000	P200 content	0.863847	0.180291	32.69772	6.824228	4.79142	0.000170
P200 content squared	0.168953	0.066879	7.46774	2.956064	2.52624	0.021122	P200 content squared	0.117665	0.180291	4.26810	6.539759	0.65264	0.522717
Mixture	R200/P200						Mixture	R200/P200					
Pressing level	Wet 65 psi						Pressing level	Hot 8.1 psi					
R squared	BETA	Std. error of BETA	B	Std. error of B	t(2)	p-level	R squared	BETA	Std. error of BETA	B	Std. error of B	t(2)	p-level
0.97462361							0.91766288						
Intercept			58.26447	1.228793	47.41601	0.000000	Intercept			40.52169	1.478309	27.41084	0.000000
P200 content	0.915835	0.135226	40.09408	5.919997	6.77265	0.000003	P200 content	1.395213	0.243580	40.79498	7.122095	5.72795	0.000025
P200 content squared	0.074263	0.135226	3.11559	5.673221	0.54918	0.590026	P200 content squared	-0.465988	0.243580	-13.05716	6.825210	-1.91308	0.072734
Mixture	R200/P200						Mixture	R200/P200					
Pressing level	Wet 489 psi						Pressing level	Hot 16.3 psi					
R squared	BETA	Std. error of BETA	B	Std. error of B	t(2)	p-level	R squared	BETA	Std. error of BETA	B	Std. error of B	t(2)	p-level
0.98598302							0.95749111						
Intercept			51.3289	0.790096	64.96549	0.000000	Intercept			36.94513	0.905121	40.81789	0.000000
P200 content	1.139352	0.100501	43.1528	3.806469	11.33671	0.000000	P200 content	1.304663	0.175018	32.50604	4.360630	7.45444	0.000001
P200 content squared	-0.153767	0.100501	-5.5811	3.647796	-1.53001	0.144410	P200 content squared	-0.345546	0.175018	-8.25048	4.178857	-1.97434	0.064818
Mixture	R200/P200						Mixture	R200/P200					
Pressing level	Wet 978 psi						Pressing level	Hot 49.8 psi					
R squared	BETA	Std. error of BETA	B	Std. error of B	t(2)	p-level	R squared	BETA	Std. error of BETA	B	Std. error of B	t(2)	p-level
0.94617019							0.9414399						
Intercept			45.71239	1.671048	27.35552	0.000000	Intercept			30.7014	0.793373	38.69728	0.000000
P200 content	1.171188	0.196950	47.87438	8.050663	5.94664	0.000016	P200 content	1.642821	0.206563	30.1937	3.796457	7.95312	0.000000
P200 content squared	-0.209024	0.196950	-8.18805	7.715070	-1.06131	0.303397	P200 content squared	-0.721244	0.206563	-12.5208	3.585942	-3.49164	0.002605
Mixture	R200/P200						Mixture	R200/P200					
Pressing level	Hot 0 psi						Pressing level	Hot 163 psi					
R squared	BETA	Std. error of BETA	B	Std. error of B	t(2)	p-level	R squared	BETA	Std. error of BETA	B	Std. error of B	t(2)	p-level
0.93667368							0.87232281						
Intercept			54.2700	1.826550	29.71173	0.000000	Intercept			23.74645	0.792101	29.97906	0.000000
P200 content	0.872358	0.213617	35.9363	8.799829	4.08375	0.000773	P200 content	1.836442	0.303320	23.10469	3.816131	6.05448	0.000013
P200 content squared	0.099181	0.213617	3.9154	8.433006	0.46429	0.648329	P200 content squared	-0.987222	0.303320	-11.90271	3.657055	-3.25473	0.004664

Addition rule in fiber, middle and fines fraction mixtures

In the three component mixed sheets, analyzed here as a binary mixture, fines (P200) were added into a 50/50 mixture of fiber (R48) and middle fraction (R200). Slight deviations from linearity were observed, as shown in Figure 69, where scattering coefficient was plotted as a function of fines in a 50% fiber (R48) and 50% middle fraction (R200) sheets at various pressing levels. All linear terms were statistically significant. In addition, the highly pressed press dried sheets (16.3 psi, 48.9 psi and 163 psi) had statistically significant second order terms.

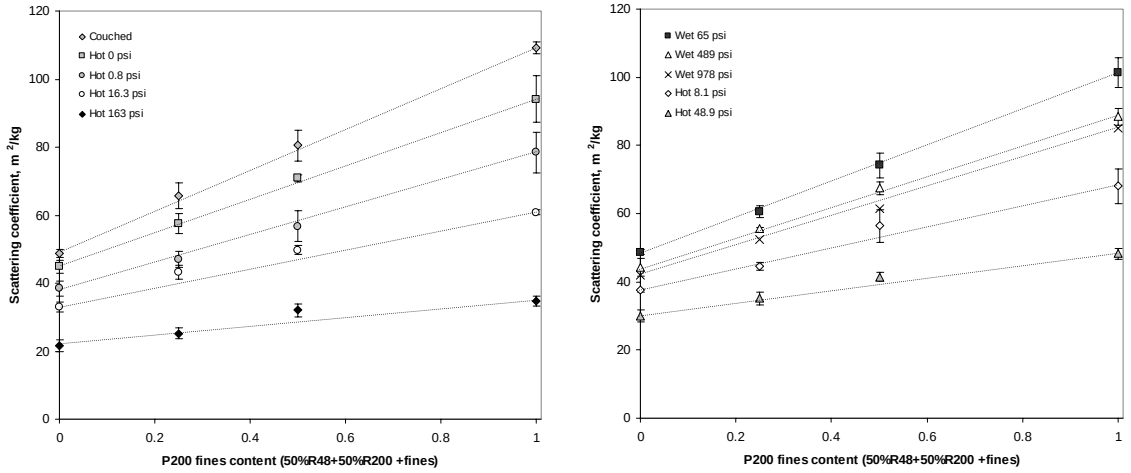

Figure 69. Scattering coefficient as a function of fines fraction (P200) content (P200 added into 50%R48+50%R200 fraction) at various pressing levels.

The absolute deviations from the linear addition model are depicted in Figure 70 for the statistically significant cases.

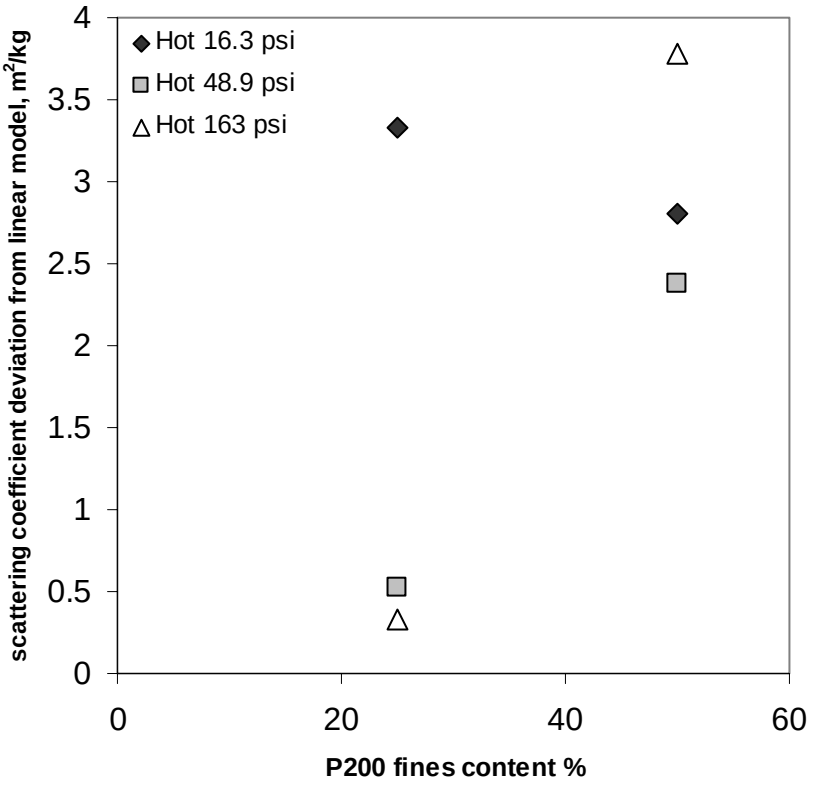

Figure 70. Absolute difference (measured – linear model) in scattering coefficient at various middle fraction contents and pressing levels for the statistically significant cases.

The average relative error of the linear model was small. On average for the statistically significant non linear cases the linear model underestimated the real data by 5.91%, as shown in Figure 71.

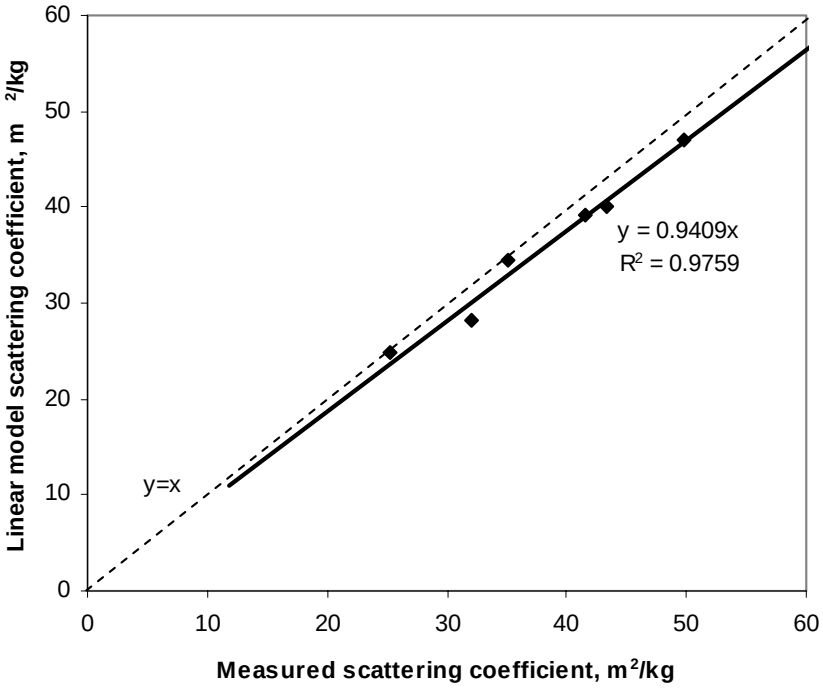

Figure 71. Measured scattering coefficient vs. scattering coefficient based on the linear addition model for the statistically significant non-linear cases.

Table 13. Multiple regression results of 50/50 fiber (R48) +middle fraction (R200) and fines (P200) mixed sheets at various pressing levels

Mixture	R48+R200/P200						Mixture	R48+R200/P200					
Pressing level	Couched						Pressing level	Hot 0.8 psi					
R squared	BETA	Std. error of BETA	B	Std. error of B	t(2)	p-level	R squared	BETA	Std. error of BETA	B	Std. error of B	t(2)	p-level
0.98486596							0.94304771						
Intercept			48.83955	1.307817	37.34434	0.000000	Intercept			38.37795	1.707240	22.47953	0.000000
P200 content	1.119325	0.109645	67.62098	6.623920	10.20861	0.000000	P200 content	0.793611	0.208257	33.03411	8.668707	3.81073	0.001398
P200 content squared	-0.132245	0.109645	-7.32765	6.075392	-1.20612	0.243386	P200 content squared	0.183382	0.208257	7.07971	8.040034	0.88056	0.390837
Mixture	R48+R200/P200						Mixture	R48+R200/P200					
Pressing level	Wet 65 psi						Pressing level	Hot 8.1 psi					
R squared	BETA	Std. error of BETA	B	Std. error of B	t(2)	p-level	R squared	BETA	Std. error of BETA	B	Std. error of B	t(2)	p-level
0.98105915							0.92063867						
Intercept			48.60855	1.264142	38.45179	0.000000	Intercept			36.84377	1.576399	23.37211	0.000000
P200 content	0.903170	0.120100	48.27049	6.418829	7.52014	0.000001	P200 content	1.264311	0.245838	41.16533	8.004348	5.14287	0.000081
P200 content squared	0.090563	0.120100	4.48917	5.953322	0.75406	0.461131	P200 content squared	-0.321658	0.245838	-9.71350	7.423855	-1.30842	0.208146
Mixture	R48+R200/P200						Mixture	R48+R200/P200					
Pressing level	Wet 489 psi						Pressing level	Hot 16.3 psi					
R squared	BETA	Std. error of BETA	B	Std. error of B	t(2)	p-level	R squared	BETA	Std. error of BETA	B	Std. error of B	t(2)	p-level
0.98751199							0.98119929						
Intercept			44.0140	0.858418	51.27333	0.000000	Intercept			33.28588	0.648369	51.33784	0.000000
P200 content	1.082352	0.097519	48.3768	4.358718	11.09886	0.000000	P200 content	1.469321	0.119655	40.42670	3.292170	12.27965	0.000000
P200 content squared	-0.092597	0.097519	-3.8386	4.042614	-0.94953	0.355656	P200 content squared	-0.508971	0.119655	-12.98818	3.053415	-4.25366	0.000536
Mixture	R48+R200/P200						Mixture	R48+R200/P200					
Pressing level	Wet 978 psi						Pressing level	Hot 49.8 psi					
R squared	BETA	Std. error of BETA	B	Std. error of B	t(2)	p-level	R squared	BETA	Std. error of BETA	B	Std. error of B	t(2)	p-level
0.95898805							0.94995065						
Intercept			42.24451	1.529849	27.61352	0.000000	Intercept			29.7671	0.737425	40.36628	0.000000
P200 content	0.817181	0.176725	35.91928	7.767984	4.62402	0.000242	P200 content	1.400263	0.199394	26.2291	3.734961	7.02260	0.000001
P200 content squared	0.167593	0.176725	6.83232	7.204632	0.94832	0.356252	P200 content squared	-0.448843	0.199394	-7.7113	3.425668	-2.25104	0.037118
Mixture	R200/P200						Mixture	R200/P200					
Pressing level	Hot 0 psi						Pressing level	Hot 163 psi					
R squared	BETA	Std. error of BETA	B	Std. error of B	t(2)	p-level	R squared	BETA	Std. error of BETA	B	Std. error of B	t(2)	p-level
0.96617333							0.89404117						
Intercept			44.8201	1.684792	26.60276	0.000000	Intercept			21.10136	0.819582	25.74649	0.000000
P200 content	1.070501	0.179167	53.5527	8.962964	5.97489	0.000025	P200 content	1.727622	0.284061	25.30979	4.161522	6.08186	0.000012
P200 content squared	-0.091115	0.179167	-4.2526	8.362225	-0.50855	0.618466	P200 content squared	-0.845006	0.284061	-11.48162	3.859719	-2.97473	0.008500

Discussion

The statistically significant deviations from linear addition rule were observed for various mixtures of fiber (R48), middle fraction (R200) and fines (P200) mixed sheets at various pressing levels, and more so for when middle fraction (R200) was present. In general the deviation from the linearity was positive, indicating that the z-directional force applied to the sheet is transferred more through the fiber fraction than the middle or fines fractions. Thus, the middle and fines fractions in the sheet do not experience same z-directional force, and thus do not bond as efficiently in a mixed sheet as they would in a pure middle or fines fraction sheet. This mechanism is illustrated in Figure 72.

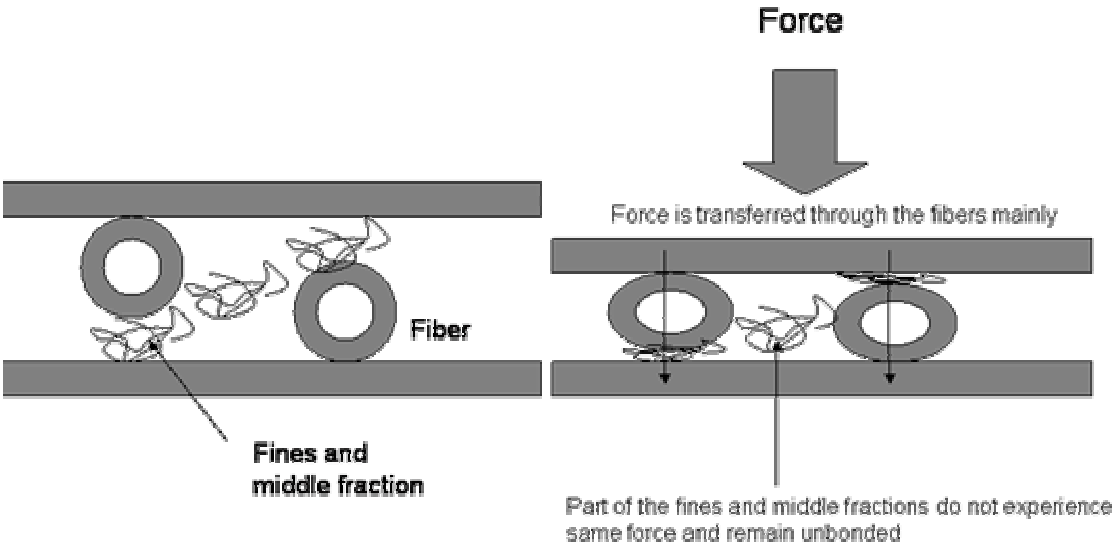

Figure 72. A suggested mechanism for pressing of mixed mechanical pulp sheets

The fact that middle fraction showed more absolute and relative deviation from linearity than the fines fractions indicate, that middle fractions are more likely to accumulate in areas where they do not experience the same average forces as the rest of the sheet.

Small differences regarding the significance of the first and second order terms between the binary and ternary approaches were observed. These differences were likely due to the fact that in the ternary approach average data was used in the analysis, whereas in binary approach individual handsheet based data was used.

Overall, the deviations from the linear addition rule were small, indicating that the fraction of fines and middle fractions that do not experience the same average force in pressing is relatively small. The range of the statistically significant absolute deviations from the linearity was between -2.57-6.06 m^2/kg, measured as scattering coefficient units. Thus, the linear addition model explained most of the variation (98.4%) in the scattering coefficient, as depicted in Figure 73, where the measured scattering coefficient of all the mixed sheets was plotted against the estimated scattering coefficient based on the linear addition rule. On average the scattering coefficient estimated based on the linear addition rule was systematically 4.8% below that of the real measured scattering coefficient.

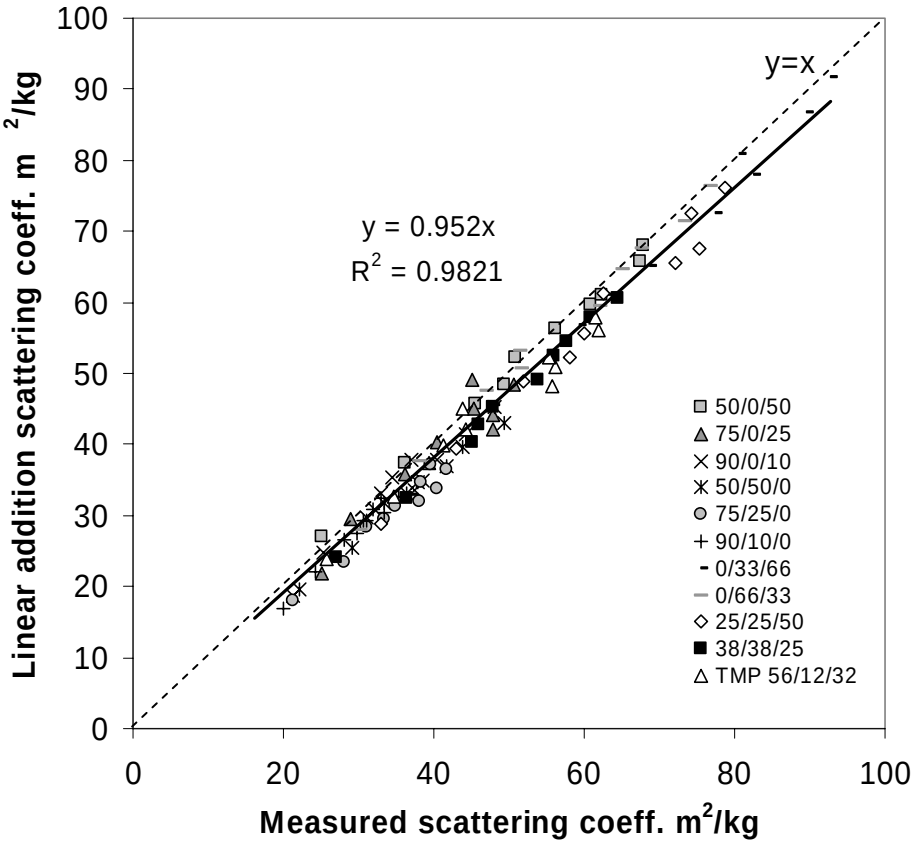

Figure 73. Measured scattering coefficient vs. estimated scattering coefficient from the linear addition rule for various mixtures of fiber, middle and fines fractions (excludes pure fraction data)

The results obtained here show that the scattering coefficient and also specific surface area of the heterogeneous mechanical pulp sheet follows a linear addition rule very accurately, and the specific surface area of a mixed sheet is the mass based fractional sum of the individual fractions in the sheet. If one then considers a totally unbonded sheet, where no interaction between different fractions occur, the total unbonded specific surface area can be then reasonably assumed to follow a similar linear addition rule as obtained for the pressed sheets. This implies that the specific bonded area in the sheet is also a sum of the mass fraction based specific bonded areas of various fractions in the sheet when compared at a constant pressing level. This view is supported by the behavior of density as a function of sheet composition. In Figure 74 the apparent density was calculated based on linear addition rule (Equation 1) and plotted against the measured density of mixed sheets. Density also followed linear addition rule

independent of sheet composition and pressing level. The systematic deviation from the linearity was similar to that of the scattering coefficient (4.9%).

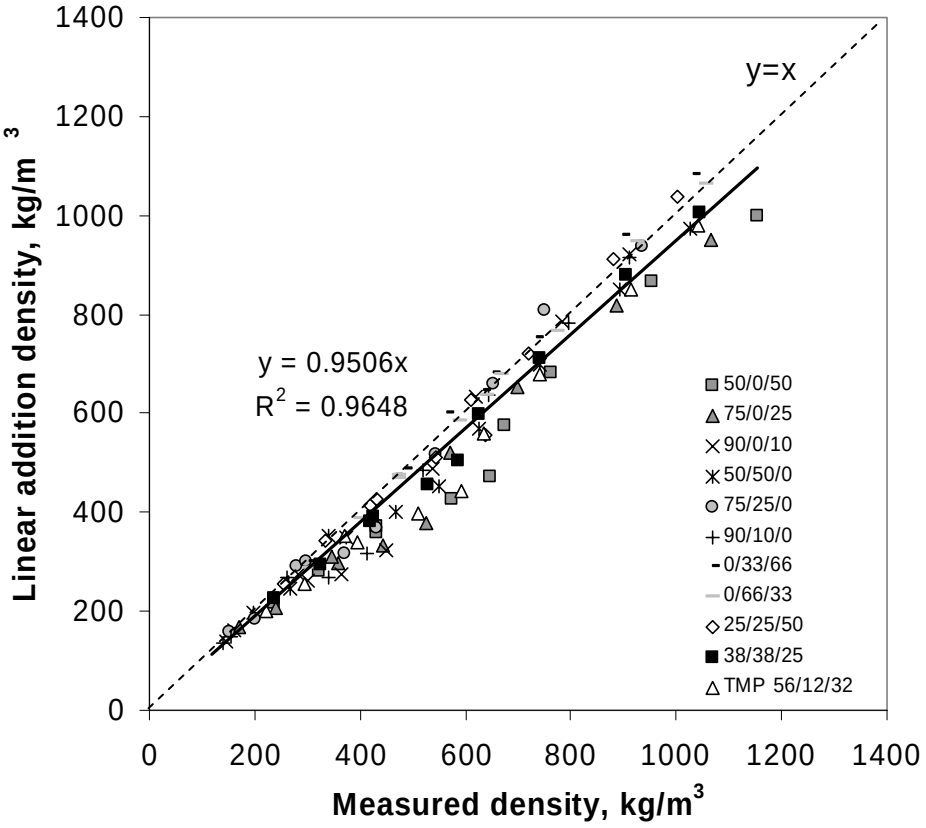

Figure 74. Measured apparent density vs. estimated apparent density from the linear addition rule for various mixtures of fiber, middle and fines fractions (excludes pure fraction data)

The fact that the observed systematic errors in scattering coefficient and density were similar (4.8% and 4.9%) indicates that this error was caused by one common phenomenon, and was likely related to the amount of fines and middle fraction particles that fill interstices between fibers. As was suggested earlier, these particles were not likely to experience the same pressing pressures as fines located between fibers (in z-direction), but remain partly unbonded adding to the measured scattering coefficient more than would have been expected from the linear addition rule. In addition, fines and middle fractions that fill the interstices between fibers only add to the mass of the sheet without significantly affecting the thickness of the sheet. Hence these fines and middle

fractions added more to the measured density than would have been expected from the linear addition rule.

Conclusions

Although considered a crude method, the Ingmansson and Thode procedure using wet pressing to induce bonding is the most accepted method for estimating Relative Bonded Area in chemical pulps. However, in extremely heterogeneous structures such as mechanical pulps, it was not known whether the bonding induced during pressing was evenly distributed between all different types of fractions in the sheet. In this paper a commercial thermo-mechanical pulp was fractionated into three different fractions (fiber (R48), middle (R200) and fines (P200)) and then mixed back at known ratios to be pressed to various levels of bonding. Wet pressing at 23 ^{o}C and press drying at 120 ^{o}C were used to induce bonding in the sheet. First, it was confirmed that scattering coefficient is an adequate estimate of the specific surface area of the heterogeneous mechanical pulp sheet. Second, it was observed that the scattering coefficient in mixed sheets deviated from the linear addition rule based on the pure fractions. This deviation was most significant when R200 middle fraction was present in the sheet. However, the overall deviation from the linear addition rule was very modest, on average, comprising only 4.8% error between measured and estimated linear addition rule based scattering coefficient. Thus, it was concluded that pressing reduces scattering and thus also induces bonding fairly homogeneously throughout the mixed sheet, regardless of pressing level, pressing procedure (wet pressing or press drying), and sheet composition.

Chapter 4: The Intrinsic Non-linearity of RBA in Heterogeneous Pulps

Abstract

Relative bonded area is a sheet structure factor, which is present in most of the in-plane strength theories of papers. However, the use of RBA in heterogeneous structures is limited by the difficulty of being able to define RBA. In a heterogeneous sheet it is expected that all fractions have their own RBA, and it is not known if the RBA follows the linear addition rule[2]. The focus of this paper is on the behavior of Relative Bonded Area as a function of sheet composition in mechanical pulps. Earlier it was shown that the scattering coefficient of the sheet in mixtures of mechanical pulp followed accurately a linear addition model based on the sheet composition. In this paper it is shown that the total unbonded specific surface area (S_o), defined using linear models for tensile strength and scattering coefficient relationship, also accurately followed the linear addition model. This results in that when the total unbonded surface areas of the individual components are not the same, RBA is intrinsically a non-linear function of the sheet composition. Thus, it is recommended that specific bonded area rather than RBA be used to differentiate between specific bond strength and bonded area when heterogeneous structures are studied.

Introduction

Relative bonded area (RBA) is a term present in most of the in-plane strength theories of papers [179]. The relative bonded area concept has been widely used with appreciable success in homogeneous sheets [59, 60, 102, 104, 108, 111, 113, 115, 173, 180]. The significance of the variable cannot be disputed, due to the fact that all stresses in the paper are transferred through the bonded areas between fibers. RBA instead of absolute bonded area is used mainly due to the difficulty of measuring the real specific bonded area in a sheet, and in theoretical equations the RBA is converted into bonded area using the average fiber dimensions.

The most used method for measuring RBA is based on the Ingmansson and Thode method. Ingmanson and Thode [59] suggested, in contrast to the erroneous solvent

[2] As was pointed out by D.H. Page in the early stages of this research

method, to circumvent the problem by plotting specific scattering coefficient against tensile strength, and extrapolating to zero tensile strength in order to obtain a fully unbonded scattering coefficient. They used refining and wet pressing to increase tensile strength of spruce sulphite pulp. In their data refining and wet pressing produced similar scattering tensile relationship, allowing them to conclude that the fibril structure of chemical pulps collapse completely on the surface of the fiber, and thus refining produces results similar to wet pressing.

However, later Swanson and Steber [113] showed that the fibrillar structure created in refining does not collapse completely upon drying and that beating develops non-collapsible surface area. This was supported by Luner *et al.* [114] finding that using high yield pulps beating produced different scattering tensile relationships at different wet pressing levels. Later Rennel also showed the same behavior using a large variety of different pulps, including mechanical pulps [115]. Ultimately, Hartler used unbonded (spray-dried) fiber sheets and nitrogen absorption technique to show that the dry-fiber specific surface area of chemical pulp fibers does not remain constant during the beating process [116]. For high yield and mechanical pulps the spray dried unbonded dry specific surface area increases with additional beating [115].

Due to the fact that finer fractions created in refining in high yield pulps do not completely collapse upon drying, the use of RBA in heterogeneous structures is questionable. In a heterogeneous sheet it is expected that all fractions have their own RBA, and it is not known whether the RBA follows the linear addition rule in heterogeneous pulps. There are indications that it might not. It has been shown that most strength properties do not follow a linear addition rule as a function of sheet composition in heterogeneous pulp sheets, both in mechanical pulps [3-6, 76], and mixtures of mechanical and chemical pulps [27]. This non-linearity is explained by different shrinkage properties of the various components in the sheet [181], or variable collapse of fibers depending on the amount of components in the sheet [182]. Lately part of this non-additivity of strength properties was assigned by using a fiber geometry based statistical model of paper network to the non-linear addition of Relative Bonded Area of heterogeneous sheets [183].

It was shown earlier that the scattering coefficient is a good approximation of the specific surface area in mechanical pulps, independent of sheet composition or pressing procedure. It was also shown that scattering coefficient accurately follows the linear addition rule at various levels of wet pressing and press drying (in Chapter 3). It is also reasonable to assume that the total unbonded specific surface area of a mixture, where no interactions occur between the fractions, also follows a linear addition rule. This automatically results in that the specific bonded area is also a linear function of the sheet composition.

In this paper the additivity of total unbonded surface area (S_o) and Relative Bonded Area (RBA) was studied using mixtures of mechanical pulp fiber (R48), middle (R200) and fines (P200) fractions. The use of the RBA term in defining specific bonded area in heterogeneous pulp is discussed.

Experimental

Fiber middle and fines fractionation: The Bauer McNett apparatus was used to fractionate a hot disintegrated 110 CSF Norway spruce (Picea abies) TMP. The Bauer McNett was set up with 14,48 and 200 mesh screens, and run for various times until no fines were observed coming with the excess water. Then the R14 and R48 fractions were mixed back together, and fractionated again using only the R48 screen in order to achieve a near pure fiber fraction without any fines present. During the fractionation the P200 fraction was collected in 55 gallon drums and isolated using the sedimentation method, as described by Luukko [30].

Handsheet forming: Handsheets were formed using a standard British handsheet mold with 150 mesh screen and recirculation of whitewater Total of 8 handsheets were made prior to making sheets for use. Fines handsheets were formed on a dense glass fiber filterpaper. Fines contents of the fiber - fines mixed sheets were measured from the formed handsheets using the DDJ method, T 261 cm-00. All handsheets were restraint dried if not dry after pressing. The target handsheet basis weight was 60 g/m^2 O.D.

Wet pressing: Couched handsheets were not pressed. Wet pressing was conducted at 65, 489 and 978 psi's and 23 ̊C using a carver press, 3 blotter papers on one side and a

chrome plate on the other side of the handsheet. Wet pressed handsheets were pressed for 1 minute.

Press drying: Press drying was conducted at 6 pressing levels 0, 0.8, 8.1, 16.3, 48.9 and 163 psi's. Individual handsheet were pressed between hot plates heated to 120 ℃ and using a "sandwich" that consisted of a felt, wet blotter (to increase drying time and humidity above 100 ℃), handsheet, chrome plate, and a filter paper (to protect the chrome plate). All press dried handsheets were pressed until completely dry.

Testing: Scattering coefficient was measured using the Tappi (T 1214 sp-98) standard with 572 nm wavelength. Tensile strength was measured using the Tappi (T 494) standard, but with the exception of a reduced span length of 2 inches and reduced strain velocity. This adjustment was done to minimize the effect of faulty strip edges due to strip cutting especially on fines handsheets. The 0.5 inches/min strain velocity was used, in order to be able to gather enough data points (20 points/sec) to produce a sound stress-strain curve.

Results

S_o (total unbonded area) in mechanical pulps as a function of sheet composition

The S_o was approximated according to the assumption that the mechanical pulps generally operate in domain where fiber breaking is negligible [7, 24]. Thus, a linear relationship between scattering coefficient and tensile strength was used to determine the S_o of the pulp. The alternative assumption, using the Page Equation to determine S_0 gave unrealistic values of S_0 and specific bond strength for the pure 100% fines sheets. The linear relationships and equations for fiber-fines, fiber-middle fraction, middle fraction – fines, and 50%fiber/50%middle-fines sheets were constructed as shown in Figure 75 for fiber (R48) and fines (P200) mixtures. The linear equations for all mixtures are presented in Table 14. The statistical significance of the linear models varied partially due to the fact that both wet pressed and press dried samples were included in the analysis. It is known that drying of mechanical pulp based paper at elevated temperatures produces bonding that can be different from bonding that is induced at

lower temperatures. This is an issue that will be dealt in a later publication. However, similar results were obtained when only press dried sheets were used in the analysis.

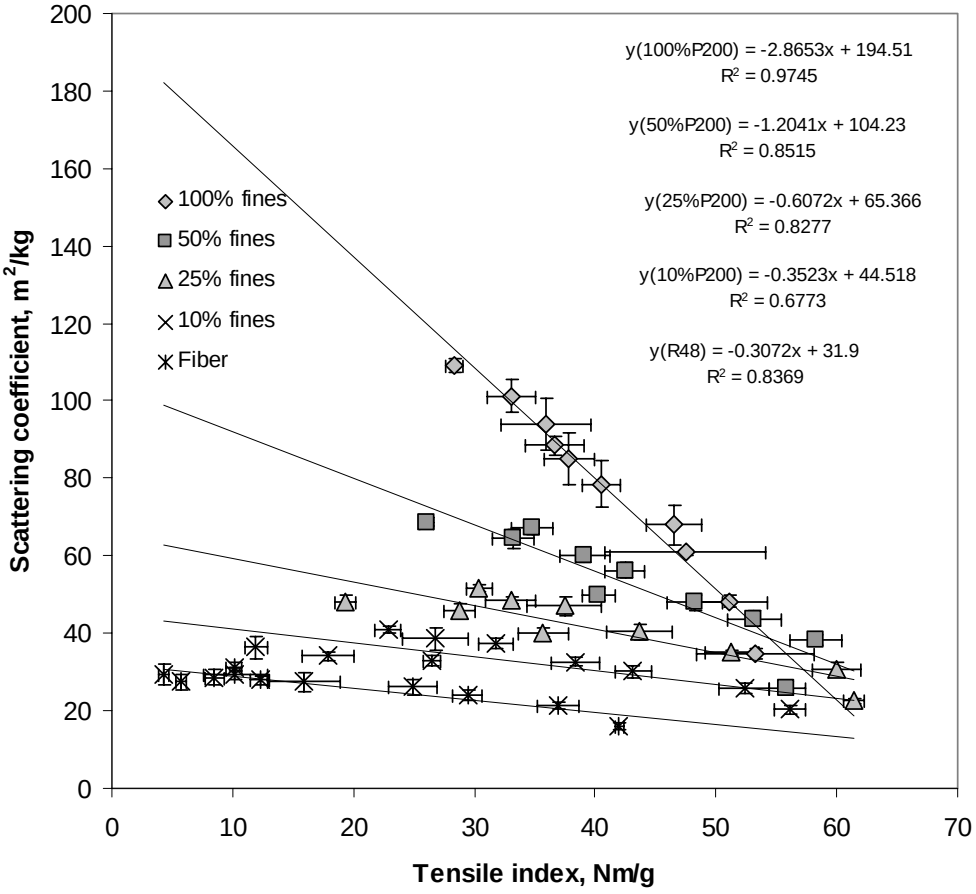

Figure 75. Scattering coefficient vs. Tensile index of R48 fiber and P200 fines mixed sheets wet pressed and press dried to various levels of bonding

Table 14. Linear equations for the scattering coefficient - tensile index relationship for various mixtures of fiber (R48), middle (R200) and fines fractions(P200)

Mixture sheet composition			s=a(Tensile Index)+s_o		
%R48	%R200	%P200	a	s_o	R^2
0	0	100	-2.8653	194.51	0.9745
50	0	50	-1.2041	104.23	0.8515
75	0	25	-0.6072	65.366	0.8277
90	0	10	-0.3523	44.518	0.6773
100	0	0	-0.3072	31.9	0.8369
0	100	0	-1.1934	103.01	0.932
50	50	0	-0.67	67.36	0.9076
75	25	0	-0.4236	49.263	0.849
90	10	0	-0.3501	38.605	0.8104
0	33	66	-2.1523	155.98	0.9541
0	66	33	-1.5211	123.42	0.9287
25	25	50	-1.5002	119.41	0.9717
37.5	37.5	25	-1.0357	92.429	0.8842

In Figure 76 the S_o obtained from the linear models in Table 14 was plotted against the P200 fines and R200 middle fraction contents for various mixtures. The total unbonded specific surface area (S_o) follows the linear addition model with significant accuracy as depicted in Figure 76.

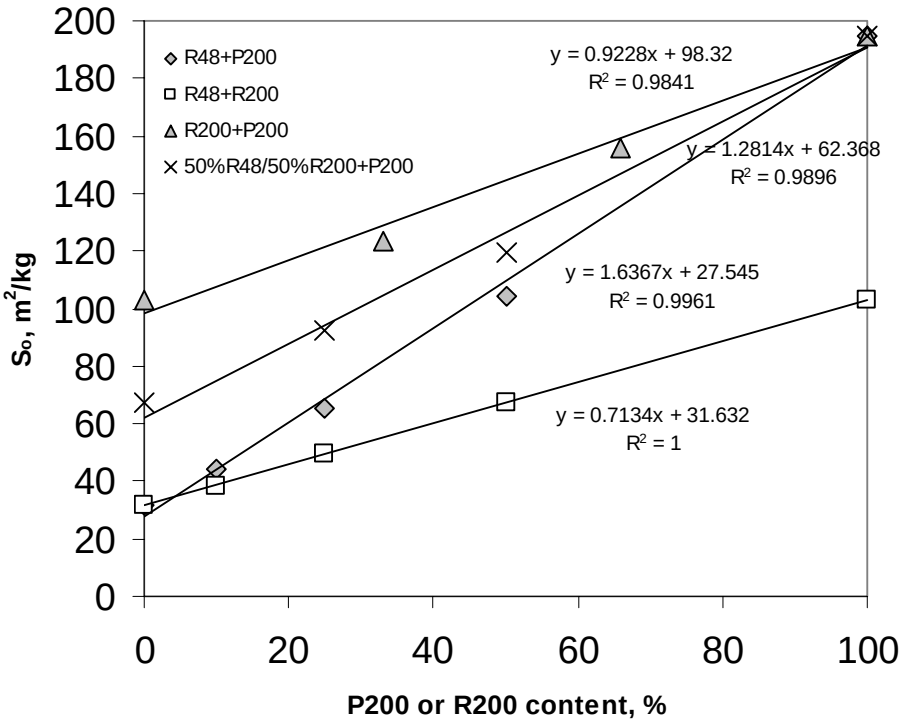

Figure 76. Total unbonded specific surface area of mixtures of fines (P200), middle fraction (R200) and fiber (R48), as a function of fines (P200) or middle fraction (R200) content in the sheet.

Statistical analysis was done by using a multiple regression approach, where two independent factors for binary mixtures and four for ternary mixtures were used to explain the variation in scattering coefficient at each pressing level. The independent factors are:

- Fines and middle fraction content to the first power
- Fines and middle fraction content squared

This approach enables a statistical analysis of the significance of the first and second order terms in explaining the variation in scattering coefficient as a function of fines or middle fraction content. Thus, it provides a whole series based analysis of the possible deviation from the linear addition rule. The results are shown in Table 15, and show that both linear, first order terms, for (P200) and (R200) were significant. In addition, the fines ($P200^2$) second order term was statistically significant. The coefficient of the second

order term (Beta) of the significant $P200^2$ term was positive, indicating that the S_o of fines obtained using the linear scattering vs. tensile strength relationship results in a value for S_o that is higher than would be obtained based on a linear addition rule. It indicates that the linear scattering coefficient-tensile strength assumption may not be valid, since the total unbonded specific surface area should be linearly additive when no interaction occurs between the components. However, overall the $P200^2$ Beta term was small, having no significant effect in the model, as seen in Figure 77.

Table 15. Statistical analysis results of the S_o as function of first and second order terms

Mixture	R48+R200+P200					
Pressing level	Hot 0.8 psi					
R squared	BETA	Std. error of BETA	B	Std. error of B	t(8)	p-level
0.99979129						
Intercept			31.9694	0.464119	68.88190	0.000000
R200	0.440479	0.015143	69.2358	2.380299	29.08703	0.000000
P200	0.798975	0.015274	123.3911	2.358876	52.30929	0.000000
$R200^2$	0.009493	0.015180	1.6238	2.604733	0.62341	0.550371
$P200^2$	0.230175	0.015254	39.3585	2.608334	15.08950	0.000000

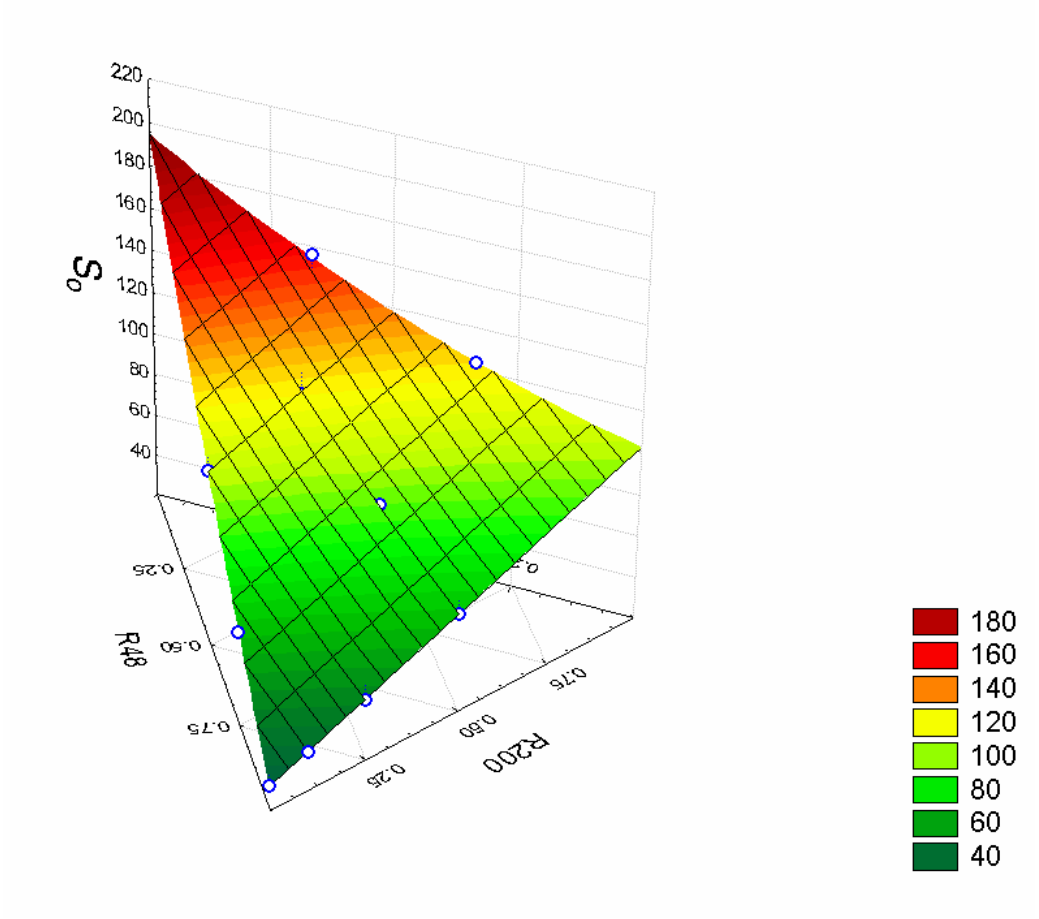

Figure 77. Total optical unbonded specific surface area of mixtures of fines (P200), middle fraction (R200) and fiber (R48), quadratic ternary fit.

In Figure 4 the measured S_o was plotted against the calculated linear addition rule based S_o, where the calculated S_o is the sum of the products of S_o obtained from the individual components and the mass fraction. The measured S_o followed the sheet composition based linear addition model very well, showing a R^2 of 0.993. The linear model systematically overestimated the S_o by 4.11% in respect to the measured S_o. This systematic error could be related to the linear scattering coefficient – tensile strength assumption made to determine the S_o of the pulp.

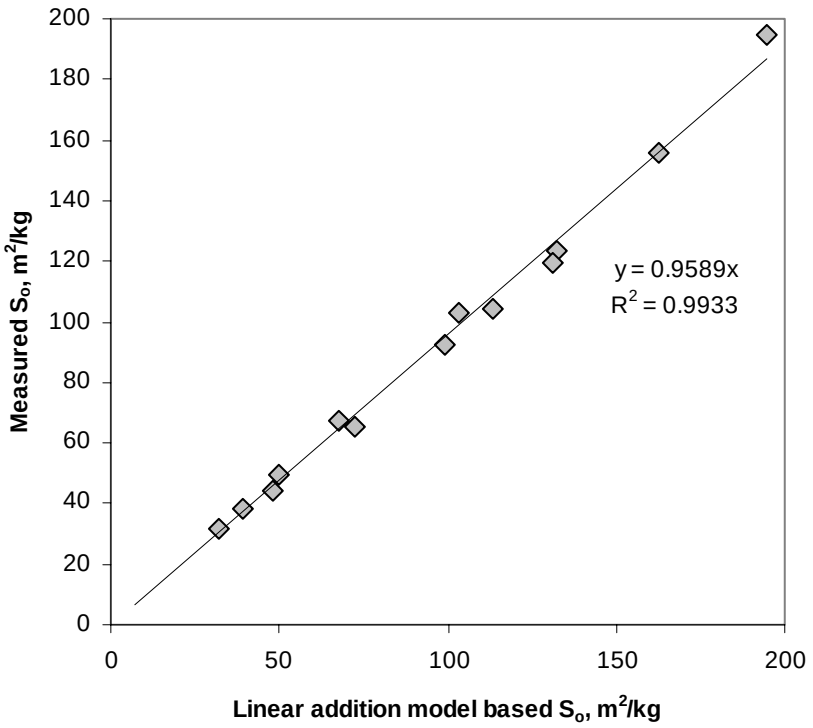

Figure 78. Linear addition rule based total unbonded (optical) specific surface vs. measured total unbonded (optical) specific surface area for all the mixtures shown in Table 14.

RBA as a function of sheet composition in heterogeneous structures

The total unbonded specific area (S_o) was not a linear function of the sheet composition, but showed statistically significant second order terms in explaining the variation in S_o. Also, it was shown earlier (Chapter 3) that the scattering coefficient (S) is not linearly additive as a function of the sheet composition at various pressing levels. However, in both cases the significant second order terms had very little impact on the model, and both variables (S and S_o) followed the linear model with very high accuracy. Thus, it is reasonable to conclude that the total unbonded area (S_o), and unbonded area (S) follow the linear addition rule as a function of the sheet composition. Bonded area is determined as the difference of S_o and S, hence it is reasonable also to assume that the bonded area follows a linear addition rule as a function of sheet composition. In fact, Mohlin has shown that bonded area is linearly additive as a function of the sheet composition in mixtures of mechanical and chemical pulp [181]. If one then considers a

binary mixture of two different pulps (or pulp fractions) with different total unbonded specific surface area and bonded area, the resulting optical specific bonded area can be defined as:

$$_{\text{mix}}BA_{optical} = ax + b \qquad \textbf{Equation 21}$$

or as specific bonded area based on BET nitrogen surface area:

$$_{\text{mix}}BA_{BET} = k(ax + b) \qquad \textbf{Equation 22}$$

where BA is the bonded area, k the correlation coefficient between scattering coefficient and specific surface area (obtained from BET), x the share of component 2 in the mixed sheet, and a and c are the linear addition coefficients.

The total unbonded specific surface area S_o is also a linear function of the sheet composition:

$$_{\text{mix}}S_{O(optical)} = cx + d \qquad \textbf{Equation 23}$$

or as specific area based on BET nitrogen surface area:

$$_{\text{mix}}S_{O(BET)} = k(cx + d) \qquad \textbf{Equation 24}$$

If RBA is then defined as a function of the sheet composition we obtain the following:

$$RBA = \frac{S_o - S}{S_o} = \frac{BA}{S_o} \qquad \textbf{Equation 25}$$

then for the binary mixture as a function of component x we obtain for both optical and BET based RBA:

$$RBA = \frac{ax + b}{cx + d} \qquad \textbf{Equation 26}$$

This results in that RBA is a function of two linear models divided by each other, and is intrinsically non-linear in nature, as the derivate depicts:

$$\frac{d}{dx}\left(\frac{ax + b}{cx + d}\right) = \frac{ad - cb}{(cx + d)^2} \qquad \textbf{Equation 27}$$

Equation 26 shows that for the RBA to be a linearly additive as a function of the sheet composition, the derivative has to be constant. This is only true if c=0, which means that RBA is intrinsically a linear function of sheet composition only as long as the total unbonded specific surface areas (S_o) for all the components are the same.

RBA of mechanical pulp as a function of sheet composition

The RBA for the mixed mechanical pulp sheets were determined using the equation 5 and the linear equations shown in Table 14. The RBA of the fiber (R48) and fines (P200) mix is plotted in Figure 79, and shows how fibers and fines have significantly different relative bonded areas at constant pressing level. The RBA did not follow the linear addition rule, but showed behavior similar to that predicted by equation 25. The non-linearity was existent at all pressing levels. These results are in agreement with the mixture pulp RBA model developed by Gates *et al.* [183].

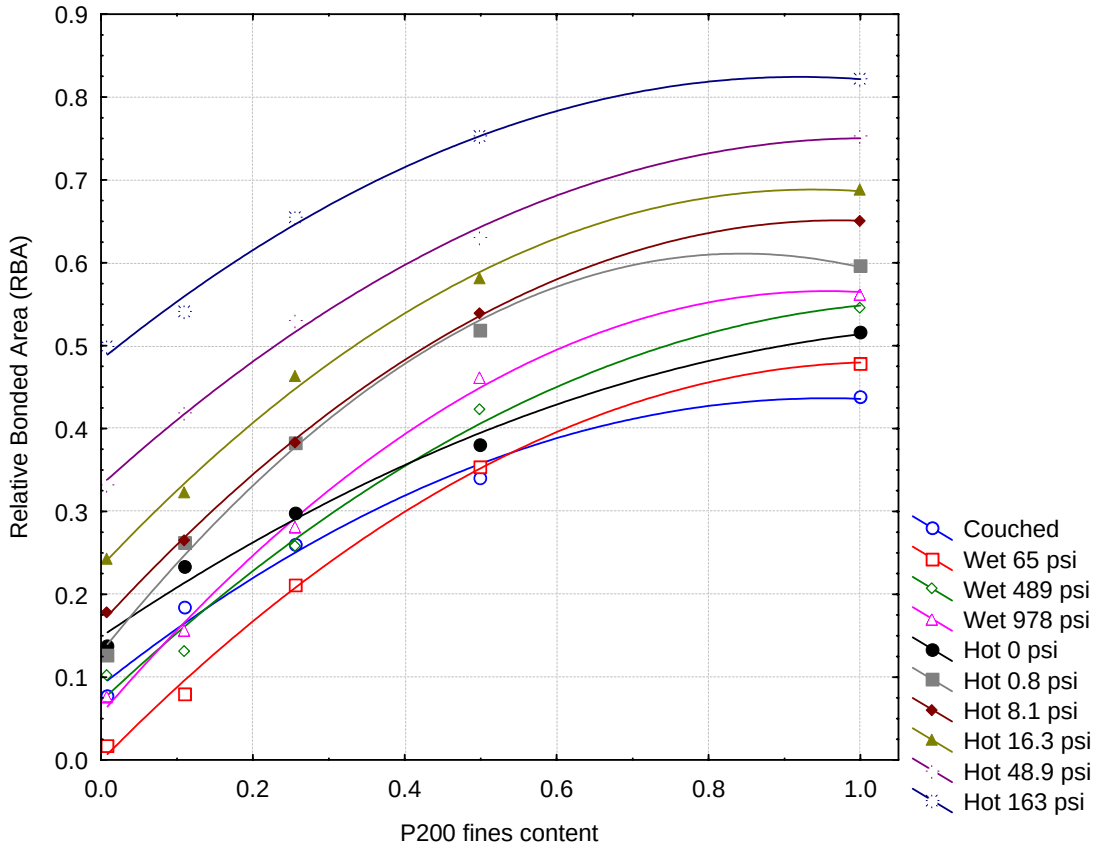

Figure 79. Relative Bonded Area (RBA) as a function of fines (P200) content mixed in with fibers (R48) at various wet pressing and press drying pressures (Quadratic fits shown).

In Figure 80 RBA of a mixed fiber (R48) and middle fraction (R200) was plotted as a function of middle fraction content. The non-linear behavior was obvious, but less pronounced than for the fiber and fines mixture sheets. This logically followed the model given in equation 25, which predicts that the non-linearity is less pronounced as the total unbonded specific surface areas of the components approach each other.

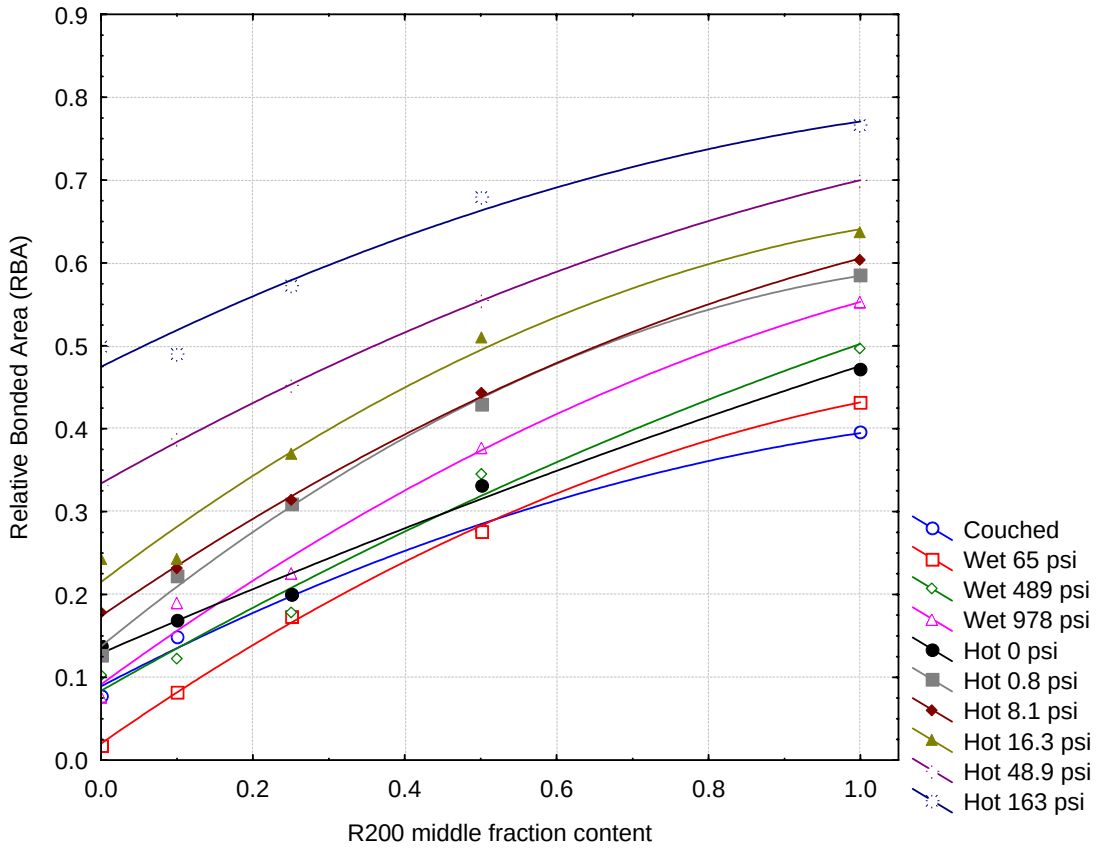

Figure 80. Relative Bonded Area (RBA) as a function of middle fraction (R200) content mixed in with fibers (R48) (Quadratic fits shown).

In Figure 81 the RBA was plotted in ternary format for all the samples estimated. The non-linearity was obvious, and more pronounced when fines were added into the sheet at all pressing (bonding) levels.

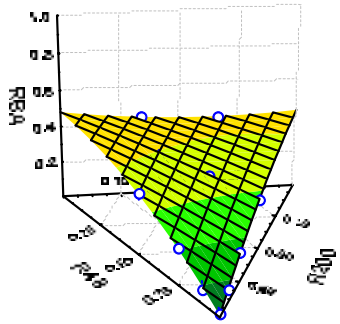

Wet pressed 65 psi

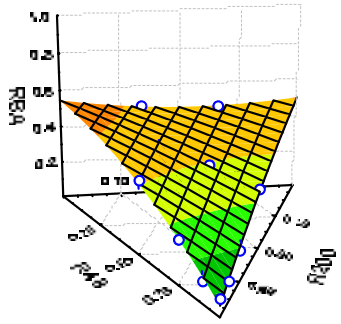

Wet pressed 489 psi

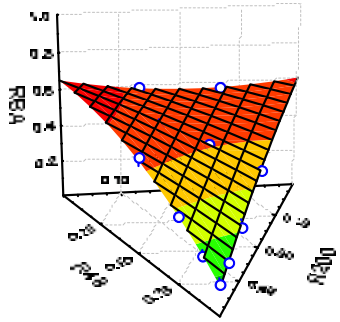

Press dried 8.1 psi

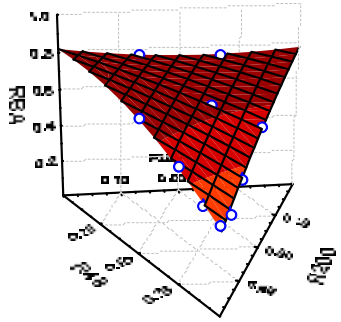

Press dried 163 psi

Figure 81. Relative Bonded Area as a function of sheet composition (R48, R200 and P200 fractions), ternary graph, quadratic fits.

Discussion

Figure 79 depicts how RBA was changed at various pressing levels, and showed how in wet pressing (even at high pressing pressures) fiber fraction could not be bonded efficiently. Higher temperatures were needed to achieve this. Fines bond readily in wet pressing, however, reach their maximum close 1000 psi of wet pressing pressure. This corresponds to a RBA close to 50%. In order to bond fines beyond the RBA of 50%, elevated press temperature is needed. This is due to the fact that approximately 50% of the mechanical pulp surfaces are lignin covered [55], and lignin surfaces do not bond readily at temperatures below their glass transition temperature [25, 149].

In wet pressing, the RBA of the fiber fraction (R48) decreased, as shown in Figure 79. Similar behavior has been observed in chemical pulps for summerwood fibers at low bonding levels [184]. This has been generally explained with creation of total specific surface area in pressing, as stated by Alexander and Marton:" In the initial stages, beating and wet pressing increase the total surface area more than bonding decreases it, and more surface becomes available to scatter light" [184]. Gregersen *et al [185]* have shown that mechanical pulp fiber walls experience cracking during calandering. It is possible that this type cracking occurs when mechanical pulp fibers are pressed at temperatures below the glass transition of lignin, which then creates additional specific surface area.

Relative bonded area concept is generally used due to the difficulty of being able accurately measure the absolute specific bonded area in the sheet. In strength theories the use of RBA is based on the assumption that all fibers are similar in dimensions, and RBA is used to calculate the bonded area in the sheet by using average fiber dimensions for conversion. In this paper it was shown that in extremely heterogeneous structures, such as mechanical pulp fiber and fines mixtures, RBA did not follow a linear addition rule. This was shown to be due to the intrinsic non-linear nature of the RBA term in heterogeneous structures, and was due to the difference in the total unbonded area (S_o) of the components in the sheet. Thus, in heterogeneous structures RBA loses its traditional meaning, and cannot be used to determine specific bonded area of the sheet. Specific bonded area, on the other hand, follows the linear addition rule as a function of sheet composition with high accuracy, and thus is believed to adequately describe the

other bonding parameter in heterogeneous structures. After all, stresses between components in the sheets are transferred through the bonded areas in the sheet.

Conclusions

In this paper the behavior of Relative Bonded Area as a function of sheet composition was studied in mechanical pulps. It was shown earlier that the scattering coefficient of the sheet in mixtures of mechanical pulp follows a linear addition model based on the sheet composition. In this paper it was shown that the total unbonded specific surface area (S_o), defined using linear models for tensile strength and scattering coefficient, also accurately followed the linear addition model. This automatically resulted in a Relative Bonded Area (RBA) that was intrinsically a non-linear function of the sheet composition in heterogeneous structures. In heterogeneous structures RBA loses its traditional meaning, and cannot be used in traditional sense for understanding the strength properties of these structures. Bonded area, on the other hand, followed the linear addition rule as a function of sheet composition, and thus is believed to adequately describe the other bonding parameter in heterogeneous structures.

Chapter 5: Mechanical pulp sheet consolidation in press drying and wet pressing

Abstract

Press drying of mechanical pulps at elevated temperatures has been shown to reduce the scattering coefficient for handsheets measured at constant density. The reduction in scattering is often accompanied with an increase in strength properties, which indicates that the observed scattering reduction is associated with increase in bonding. In this paper the problem of observed bonding increase without consolidation was approached using two different mechanisms to increase the density of mechanical pulp sheets; wet pressing and press drying using various pressing pressures. Wet pressing was conducted at 23 °C and press drying at 120 °C and 140°C. It is shown that the significant decrease in scattering at constant density in press drying is due to the mechanical pulp fines fraction (P200) pore size distribution. When wet pressed and press dried fines sheets are compared at a constant void volume or density the wet pressed sheets have significantly smaller pores and thus higher specific surface area. It is also shown that at a constant scattering coefficient the tensile strength of the press dried press dried sheets is significantly lower. This observed higher specific bond strength associated with wet pressing is assigned to the better stress transfer between fibers, and is also explained with the shift in pore size distribution of fines. In order to obtain the same level of fines bonding using wet pressing and press drying, significantly higher fines density is required when the fines are wet pressed. This is likely to affect the stress transfer efficiency between fibers in the sheet. A mechanism explaining the pore size distribution difference of press dried and wet pressed fines is proposed. This relates the shift in pore size distribution to the rebound tendency of fines when pressed at temperatures below the glass transition of lignin.

Introduction

Mechanical pulp fibers are stiff at temperatures below the glass transition temperature of lignin. Thus a limited increase in density can be obtained, when wet pressing is used to induce consolidation in mechanical pulp sheet. It has been demonstrated that even high pressing pressure can not overcome this behavior [50]. It is unknown whether this phenomenon is due to the rebound of the fibers to their original shape, or if the fibers

resist the induced pressure and remain uncollapsed under pressure. Whole mechanical pulp responds better to the wet pressing than the fiber fraction alone. This behavior has been attributed to the ability of fines to restrict fiber rebound [28].

The rigidity of mechanical pulp fibers can be overcome by press drying the fibers at elevated temperatures [50, 137-141]. The effective temperature has been shown to be in the proximity of 100 ^{o}C, indicating that the lignin matrix in the fiber restricts the collapsibility of the fiber [141]. The press-drying consolidation efficacy is dependent on the initial moisture content of the sheet, because water acts as plasticizer and prolongs the effective time needed to dry the sheet [141, 142]. The induced fiber collapse is permanent, presuming that the press drying is prolonged so that the sheet is dried under load. Back and Norberg [143] showed that in pressing an Asplund pulp there was a significant springback of the of the pulp pad depending on the pad moisture content and temperatures used in pressing. However, at high initial sheet moisture content and prolonged press drying at 90 ^{o}C the springback decreased to virtually nil.

Press drying of lignin rich pulps increases the strength properties of the sheet through higher inter-fiber bonding [144]. At low levels of pressing the most significant strength enhancements are seen in the wet strength properties of the sheet. This has been attributed to the flow of hemicelluloses and lignin at elevated temperatures, where lignin covers the hemicellulose bonds making them more hydrophobic, and thus more resistant to water [139, 145]. However, in order to induce lignin flow it is essential that the lignin glass transition temperature of 90-110 ^{o}C is exceeded by 60-70 ^{o}C. This has been shown to apply in case of spruce CTMP, where no significant changes in the fiber surface chemistry was observed, when the pulp sheets were pressed below 140 ^{o}C [146]. In addition to the flow of lignin and hemicellulose, during the heat treatment of wood there is a significant redistribution of extractives to the surfaces of the material [147]. However, Nordman and Levlin [148] showed that this temperature induced redistribution of extractives has no effect on the bonding characteristics of groundwood pulp.

Based on the studies by Gupta and Goring [25, 149] it is believed that lignin surfaces on fibers do not present any bonding ability at temperatures below their softening

temperatures. However, when the temperature is raised to the softening temperature of lignin, the lignin surfaces bond readily [25]. There are several possible bonding mechanisms that can explain lignin bonding, ranging from polymer cross-linking and mechanical interlocking to polymer diffusion [150-153]. Mechanical pulp fibers and fines have a significant portion (~50-65%) of the total specific surface area covered by lignin and extractives [30, 55]. In other words half of the specific surface area cannot be bonded at temperatures below the softening temperature of lignin, but can be bonded when temperature is raised above the glass transition temperature of lignin.

Interestingly the studies, where wet pressing and press drying are used to induce consolidation in mechanical pulps, indicate that press drying is an extension of wet pressing in respect to sheet bonding. Seth *et al.* [144, 154] showed that wet pressed and press dried (180 °C) mechanical pulp sheets represent the same scattering coefficient to tensile strength ratio when sheets are densified using variable pressures . This indicates that even though the bonding mechanisms of wet pressing and press drying are believed to be different, the bonded area to tensile strength relationship is not affected. However, this is not true if density is considered as the measure of bonding in the sheet. At constant sheet density the press dried sheet have higher strength properties and lower scattering coefficient than that of wet pressed sheets. This observed “bonding” without consolidation is pronounced for TMP pulps, and is also observed in Newsprint production [155], but is almost non-existent within kraft pulps [144, 154]. Seth *et al*. attributed this to the difference in moisture contents of the dried sheets at 50% relative humidity. They also argued that the difference in sheet surface roughness would cause error in the density measurement partly explaining the difference in wet pressing and press drying of mechanical pulp sheets. However, Rajan *et al*. [186] showed using mercury intrusion porosimetry to measure sheet density that press dried mechanical pulp sheets had significantly higher tensile strength and elastic modulus at a constant density. Later Poirier *et al.* [156] showed that when a TMP sheet is dried with superheated steam there is a significant drop in scattering coefficient with subsequent increase in tensile strength, however without significant change in bulk (or density). In addition, they observed a significant decrease in fibrillation of the steam dried sheet when observed in SEM. Thus, it seems that bonding without consolidation can be at least partially attributed to the collapsing behavior of fines and fibrils. When considering that sheet density is inversely

proportional to the void volume of the sheet, and scattering coefficient is directly proportional to the surface area of the sheet, it is likely that press drying induces a different type void volume collapse mechanism than wet pressing.

In this paper the different sheet consolidation characteristics associated with wet pressing and press drying of mechanical pulp was elucidated using whole pulp and mixtures of fiber (R48) and fines (P200). The sheet internal structure was analyzed using mercury porosimetry. Then mercury porosimetry results were related to the scattering coefficient, density and tensile strength behavior observed using these two pressing applications.

Experimental

Whole pulp: A hot disintegrated 35 CSF Norway spruce TMP pulp was used in all experiments. Handsheets were made using a standard British handsheet mold and recirculation of fines. The whole pulp sheets were then pressed at room temperature (23 °C) and press dried at 120° and 140 °C to different levels of bonding using various pressing pressures.

Fiber middle and fines fractionation: The Bauer McNett apparatus was used to fractionate the TMP. The Bauer McNett was set up with 14,48 and 200 mesh screens, and run until no fines were observed coming with the excess water. Then the R14 and R48 fractions were mixed back together, and fractionated again using only the R48 mesh screen in order to achieve a near pure fiber fraction without any fines present. During the fractionation the P200 fraction was collected in 55 gallon plastic drums and concentrated using the sedimentation method, as described by Luukko [30]. A P200 fraction of a 110 CSF Norway spruce TMP was also collected and concentrated.

Handsheet forming: Handsheets were formed using a standard British handsheet mold with 150-mesh screen and recirculation of whitewater. Fines handsheets were formed on a dense glass fiber filter paper (Whatman 934AH). Fines content was measured from the formed handsheet using the DDJ method, T 261 cm-00. All handsheets were restraint dried if not dry after pressing. The target handsheet basis weight was 60 g/m^2 O.D.

Wet pressing: Couched handsheets were not pressed. Wet pressing was conducted at 489 psi and 23°C using a standard Carver press and 3 blotter papers on one side and a chrome plate on the other side of the handsheet. Handsheets were pressed for 1 minute.

Press drying: Press drying was conducted at two pressing levels, 1 psi and 49 psi. Individual handsheet were pressed between hot plates heated to 120°C and 140 °C using a sandwich that consisted of a felt, wet blotter (to increase drying time and humidity above 100°C), handsheet, chrome plate, and a filter paper (to protect the chrome plate). The 1-psi pressed handsheets were pressed for 6 minutes, and the 49-psi handsheets for 3 minutes. The handsheet weight after pressing was constant for all the handsheets (between 1.3-1.37 g) with a target of 65 g/m^2. Whole pulp sheets were press dried for 3 minutes.

Testing: Scattering coefficient was measured using TAPPI (T 1214 sp-98) standard and 572 nm wavelength. Tensile strength was measured using TAPPI standard (T 494), but with the exception of a reduced span length (2 inches) and a strain speed of 0.5 inches/min in order to minimize the effect of faulty strip edges due to strip cutting especially on fines handsheets. Zero-span tensile strength was measured using a Pulmac zero-span tensile tester. Mercury porosimetry was analyzed at Micromeritics, Norcross, USA, using a pressure range from 0-60 000 psi's.

Results

Wet pressing vs. press-drying of whole pulp TMP

The different consolidation mechanism associated with wet pressing and press drying of mechanical pulp sheet was elucidated by wet pressing at 23 ^{o}C and press drying at 120 ^{o}C and 140 ^{o}C a whole pulp (35 CSF) Norway spruce thermo-mechanical pulp using variable pressing pressures. Wet pressing and press drying increased sheet density substantially, however in press drying significantly lower pressing pressure were needed to achieve the same density obtained with wet pressing (Figure 82). The whole pulp TMP sheets showed a significant decrease in scattering coefficient at a constant density, when the sheets were press dried (Figure 82). This reduction in scattering coefficient was fairly constant at all density levels.

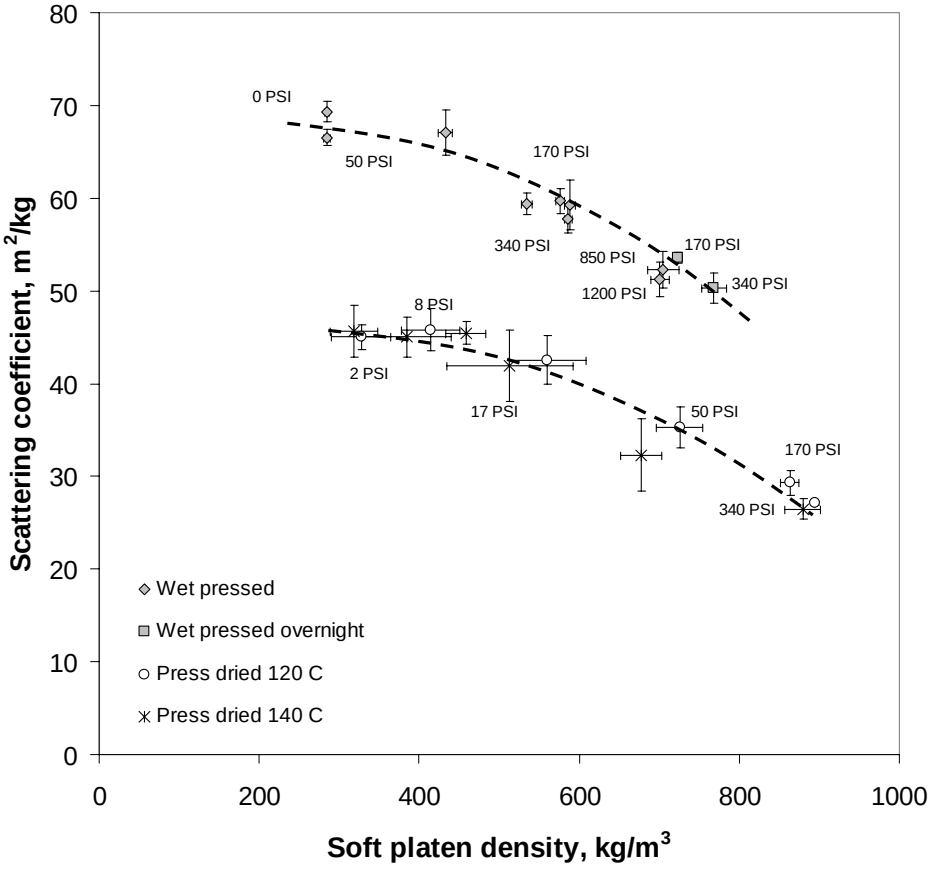

Figure 82. Scattering coefficient vs. apparent density of whole pulp TMP wet pressed and press dried at 120 °C and 140 °C at various pressing pressures.

The scattering coefficient tensile strength relationship showed a similar decrease in scattering coefficient at a constant tensile strength, where wet pressed sheets had significantly higher scattering coefficients at constant tensile strength (Figure 83). This reduction in scattering was more pronounced at low tensile strength levels, and the two curves (wet and press-dried) approached each other at higher tensile strengths. These results differ from those of Seth *et al.* [144] whose data showed that the press dried series was a perfect extension of the wet pressed series in term of scattering-tensile relationship. This could be partially explained by the significantly higher press-drying pressing pressures used in their study. Their lowest press drying was conducted at 17 psi pressure on the sheet, which is in the proximity of the range where the two (wet pressing and press drying) curves united in this study.

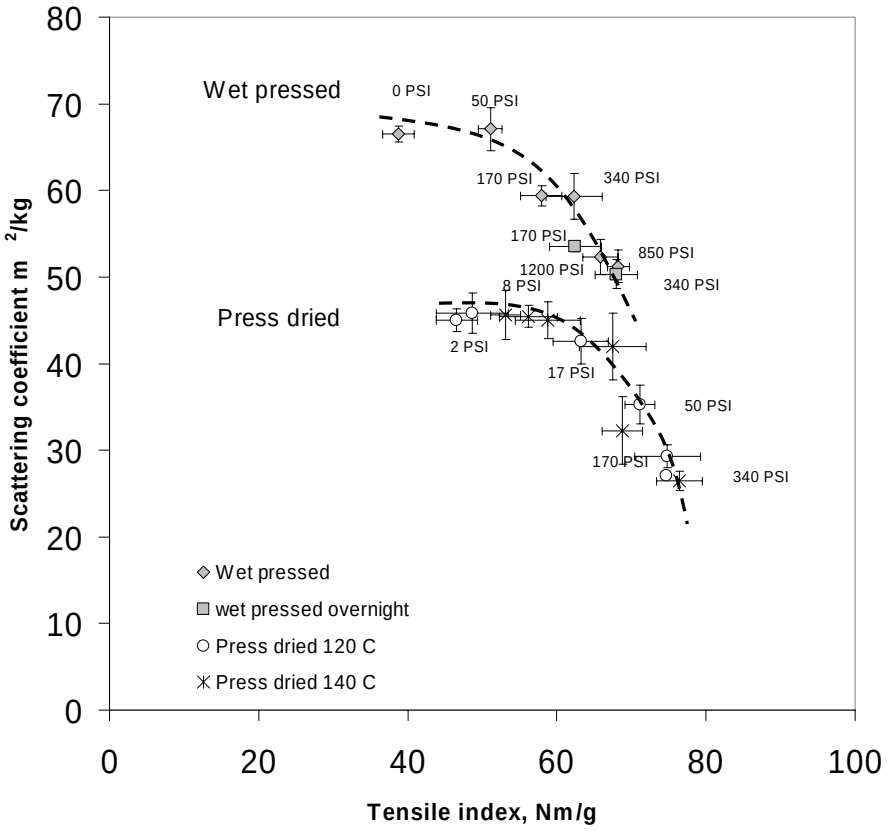

Figure 83. Scattering coefficient vs. tensile strength of whole pulp TMP wet pressed and press dried at 120 and 140 °C at various pressing pressures.

There are two plausible explanations for the observed higher tensile strength at constant scattering coefficient associated with wet pressing. First, the bonded area of wet pressed sheets could be significantly higher, which then would mean that the total unbonded specific surface area (S_o) of wet pressed sheets is significantly higher than that of the press dried. A reduction in total unbonded specific surface area of the pulp could be due to a flow of lignin and hemicellulose in press drying, which would make the surfaces of the pulp fibers and fiber fragments smoother and have less surface area for the same mass. Second, the stress transfer in wet pressed sheets could be better, which would manifest itself as an increase in bond strength at constant bonded area (specific bond strength).

Wet pressing vs. press-drying of TMP fractions

The reduction in scattering coefficient at constant density observed here (Figure 82) was larger than what was observed earlier by Seth *et al*. [144]. However, the pulp used by Seth *et al.* was a standard Newsprint grade 100 CSF pulp, whereas the pulp used here was a 35 CSF printing paper grade TMP, with very high fines content. This indicates that the extent of the difference in scattering coefficient at a constant apparent density is a factor of fines content in the sheet, as has been suggested earlier by Mackie *et al.* [155].

In order to study the effect of fines on the reduction in scattering at constant density and tensile strength, a series of mixed fiber (R48) and fines (P200) sheets were prepared using the same Norway spruce thermo-mechanical (35 CSF) pulp as earlier. The mixed sheets were then wet pressed at 23 °C and press dried at 120 °C. In Figure 84 the scattering coefficient was plotted against the density of various fiber (R48) and fines (P200) content sheets unpressed and pressed at 489 psi at 23 °C and 1 psi and 49 psi at 120 °C. The difference in scattering coefficient (wet pressed- press dried) at constant density increased as the fines content increased, and was highest for the pure fines (P200) content.

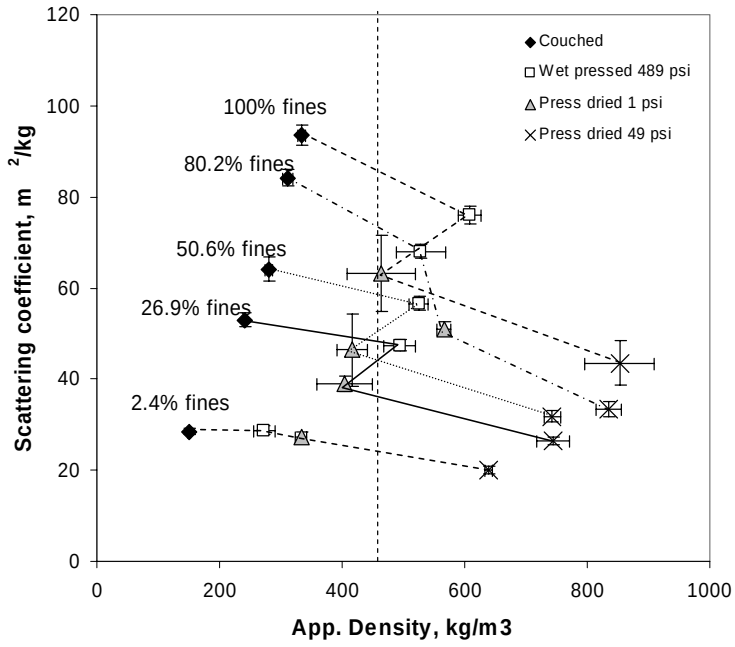

Figure 84. Scattering coefficient vs. apparent density at various wet pressing and press drying pressures for mixed fiber (R48) and fines (P200) sheets.

To obtain the data for Figure 85, the two points for wet pressed and the two for press dried were each fit to a line and the scattering coefficient at 450 kg/m^3 determined from this line, and it shows that the difference in scattering coefficient (wet pressed – press dried) increased as fines content in the sheet was increased. This indicates that fines are mostly responsible for the observed significant reduction in scattering coefficient supporting the earlier suggestion of Mackie *et al.* [155].

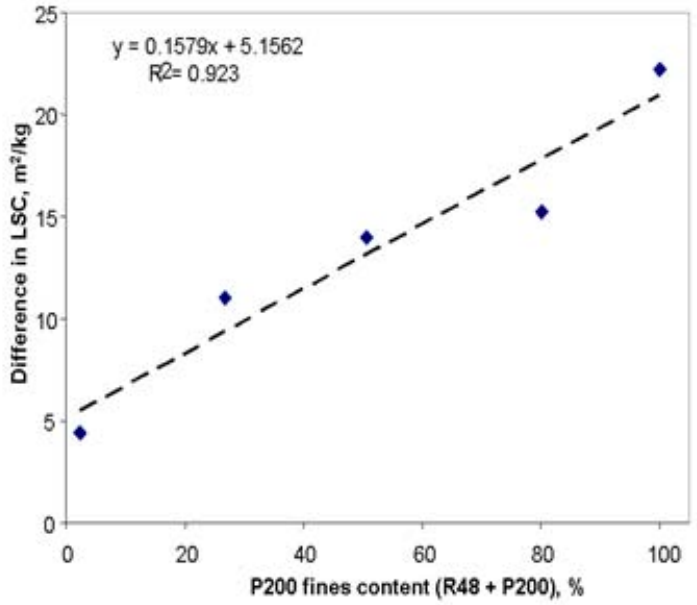

Figure 85. Difference in scattering coefficient between wet pressed and press dried sheets at a constant density (450 kg/m^3) as a function of P200 fines content in a fiber (R48) fines (P200) mixed sheet.

Although the linear fit did not pass the origin in Figure 85, it suggests that fines were responsible for the reduction in scattering coefficient when sheets were dried at higher temperatures. The fiber fraction in mechanical pulps, especially low freeness pulp, is usually fibrillated. These fibrils may act as fines, and partially explain why the linear fit in Figure 85 did not pass through the origin. The absorption coefficients for the press dried sheets were between 1.04 m^2/kg and 2.68 m^2/kg for fiber and fines respectively, and were not expected to affect the scattering coefficient.

The tensile strength - scattering coefficient relationship did not follow the same type of behavior (Figure 86) as the density – scattering coefficient relationship, where the

absolute difference in scattering coefficient at constant density was related to the fines content. The pure fractions (100% R48 fiber and 100% P200 fines) wet pressed and press dried sheets plotted on a common tensile-scattering curve, whereas mixed press dried sheets (50.6% P200 fines + 49.4% R48 fiber sheets shown) plotted on a lower scattering coefficient at a constant tensile strength than the wet pressed sheets.

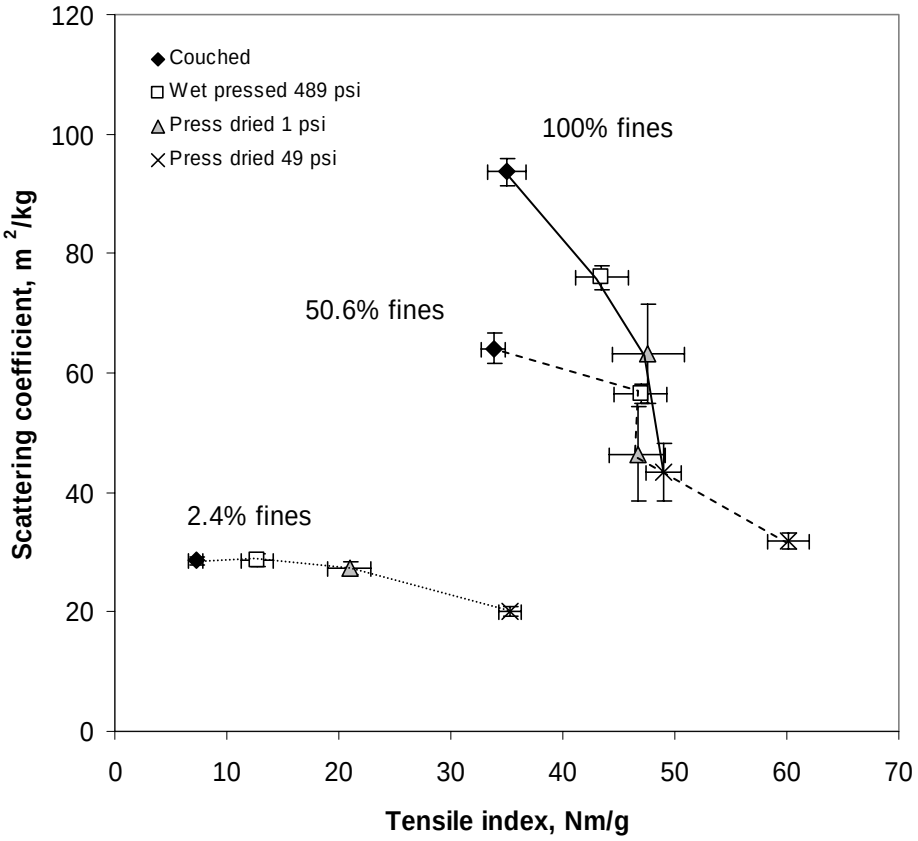

Figure 86. Scattering coefficient vs. tensile index at various wet pressing and press drying pressures for mixed fiber (R48) and fines (P200) sheets.

The reduction in scattering coefficient for mixed sheets at constant tensile strength was statistically significant, as shown in Table 16, where the scattering coefficient are compared at similar tensile strengths.

Table 16. Mixed sheets t-test of scattering coefficient and tensile strengths for wet pressed at 489 psi and press dried 1 psi sheets.

		Wet pressed 489 psi Tensile index		Press dried 1 psi Tensile index			
Fiber (R48) %	Fines (P200) %	Nm/g	St.dev.	Nm/g	St.dev.	Difference	p-values (t-test)
73.1	26.9	47.07	2.45	48.56	1.09	-1.49	0.249529
49.4	50.6	46.95	2.35	46.67	2.52	0.28	0.857274
		Wet pressed 489 psi Scattering coeff.		Press dried 1 psi Scattering coeff.			
Fiber (R48) %	Fines (P200) %	m^2/kg	St.dev.	m^2/kg	St.dev.	Difference	p-values (t-test)
73.1	26.9	47.41	1.3	39.03	1.64	8.38	0.000019
49.4	50.6	56.55	1.52	46.41	7.96	10.14	0.016962

The reduction in scattering at constant tensile strength for the press dried sheets was only observed for mixed sheets. The pure fraction (100% R48-fiber and 100% P200-fines) sheets plotted on a common curve independent of pressing procedure used. This strongly suggests that the total unbonded specific surface areas (S_o) of pure fibers (R48) and fines (P200) fractions were not altered in press drying. This result was verified using another set of P200 fines fractionated from a different pulp (News pulp grade-110 CSF Norway spruce TMP P200 fraction and wider range of wet pressing and press drying pressures, shown in Figure 87).

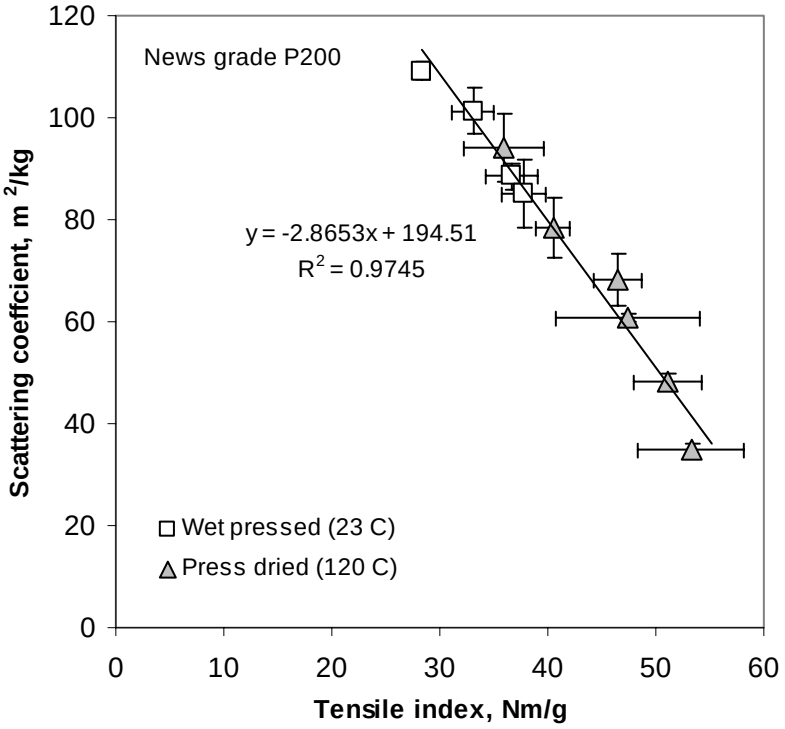

Figure 87. Scattering coefficient vs. tensile strength of News grade Norway spruce TMP P200 fines wet pressed at 23 °C and press dried at 120 °C using variable pressing pressures.

The constant S_o was further supported by SEM images of fines (P200) dried at 23 °C and 120 °C. They revealed no visible melting of fines due to the elevated temperature used in press drying (Figure 88).

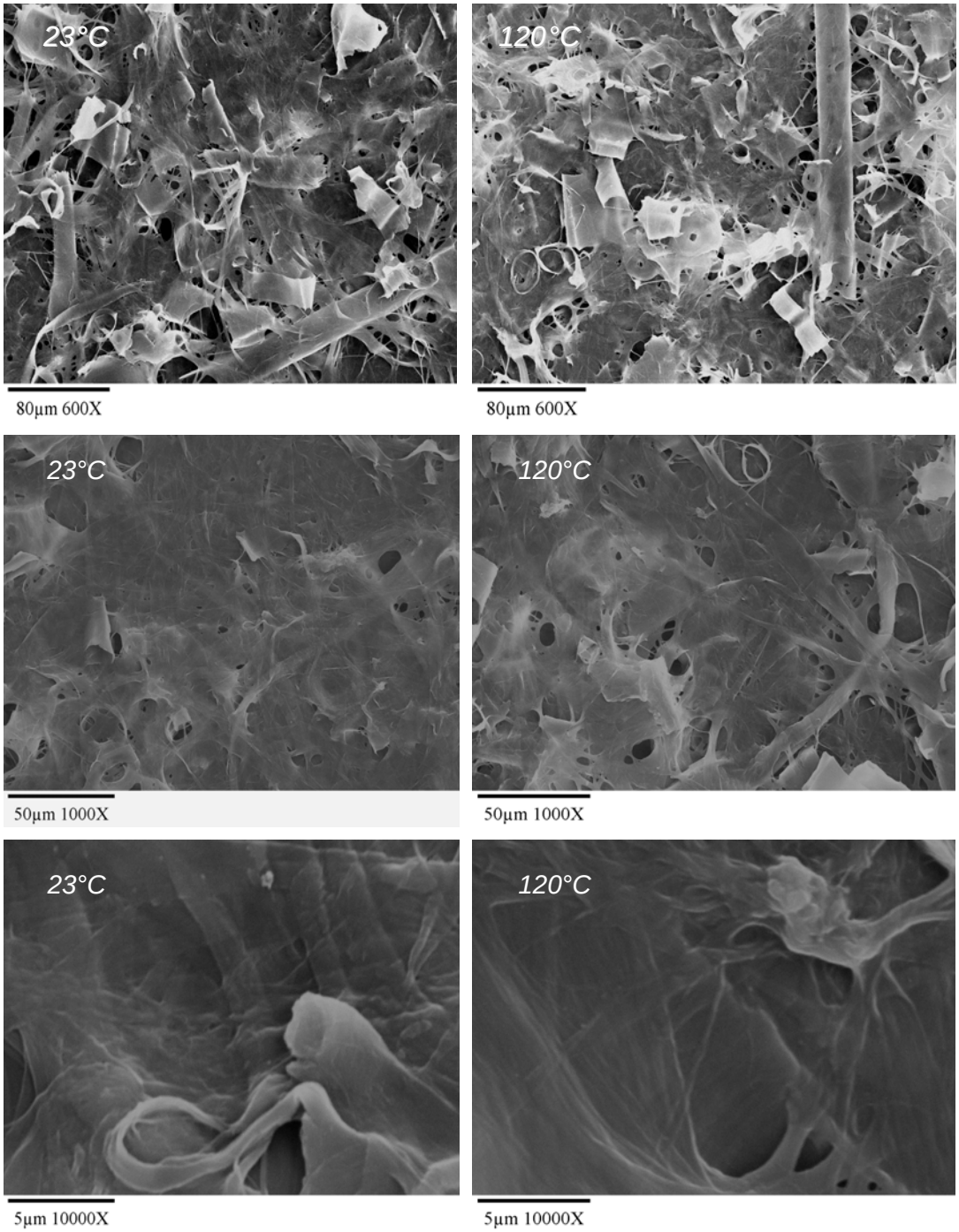

Figure 88. SEM surface images of P200 fines dried at 23 °C and 120 °C

These findings indicate that the total unbonded areas (S_o) of pure fines and fiber sheets were the same independent of pressing procedure. Based on earlier findings (Chapters 3 and 4), where it was shown that scattering coefficient and total unbonded area (S_o) followed a linear addition rule as a function of the sheet composition, indicates that the

S_o of the mixed sheets was also constant independent of pressing procedure. This suggests that the different scattering-tensile relationship of wet pressed and press dried mixed sheets can be interpreted as a difference in the specific bond strength. A possible explanation for the higher specific bond strength associated with wet pressing is related to the structure of the sheet. For wet pressed sheets to have the same bonded area (scattering coefficient) as the press dried sheets, they need to be pressed to significantly higher sheet density (using two orders of magnitude higher pressures), as shown in Figure 84. Higher density means smaller distance between bonded elements, and is likely to increase the stress transfer ability between the load bearing elements in the sheet.

The fines fraction was responsible for the difference in scattering coefficient between wet pressing and press drying (Figure 84), which indicates that the observed difference in stress transfer efficiency (specific bond strength) between wet pressed and press dried sheets was solely due to the different response of fines fraction to wet pressing and press drying.

It has been shown earlier that scattering coefficient correlates with specific surface area of paper [126, 129]. In addition at constant skeletal density (material density) the sheet apparent density is inversely related to the void volume of the sheet. This indicates that differences in scattering coefficients associated here with the two pressing methods were due to the altered pore collapse mechanism of the fines fraction in the sheet.

Sheet density and scattering coefficient in relation to mercury porosimetry

Mercury intrusion porosimetry is an efficient method to study the internal void structure of materials, and has been successfully used to study the structure of paper. It has been shown that mercury porosimetry specific surface area has high correlation with scattering coefficient when pores sizes smaller that 100-200 nm are excluded from the data [126, 129]. Also, in this study the scattering coefficient correlated well with mercury intrusion porosimetry specific surface area when pores smaller than 107nm were excluded from the data, and the correlation was independent of sheet composition or pressing procedure used (wet pressing and press drying), as shown in Figure 89.

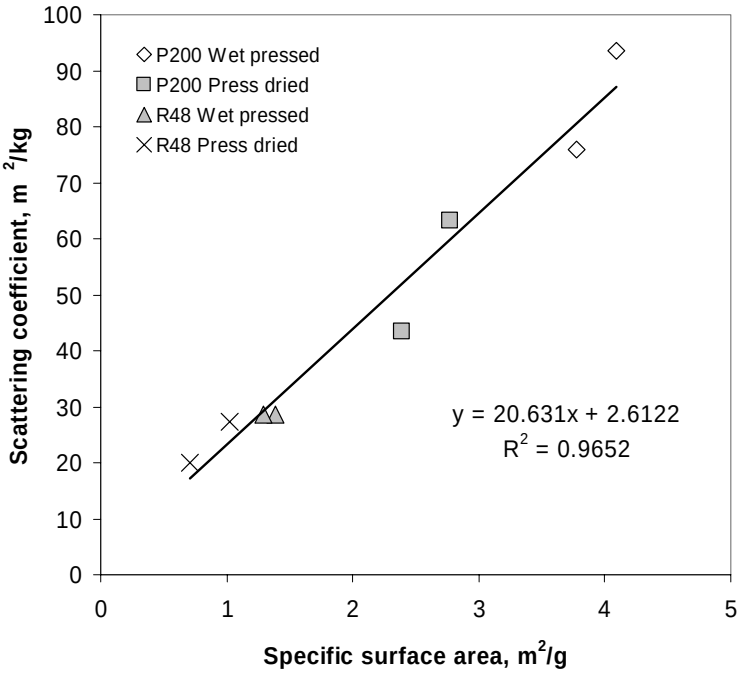

Figure 89. Mercury porosimetry specific surface area (pores larger than 107 nm) vs. scattering coefficient of fiber (R48) and fines (P200) handsheet pressed to different levels of bonding (wet pressed and press dried)

The average skeletal densities for P200 fines and R48 were 1.517 g/cm^3 and 1.508 g/cm^3 respectively, and the difference was not statistically significant (two tailed t-test, p=0.831). Thus, the void volume of the sheet inversely correlated with the density of the sheet, regardless of the sheet composition. The sheet density measured using a standard caliper and basis weight based method (apparent sheet density) is subjective to measurement error due to the compressibility characteristics and surface rougheness of the sheet. However, this error was small and the bulk density measured using mercury porosimetry and the apparent density correlated well regardless of sheet composition (R^2=0.963). This resulted in that the total mercury porosimetry pore volume explained most of the variation in apparent sheet density regardless of pressing method and sheet composition, as seen in Figure 90.

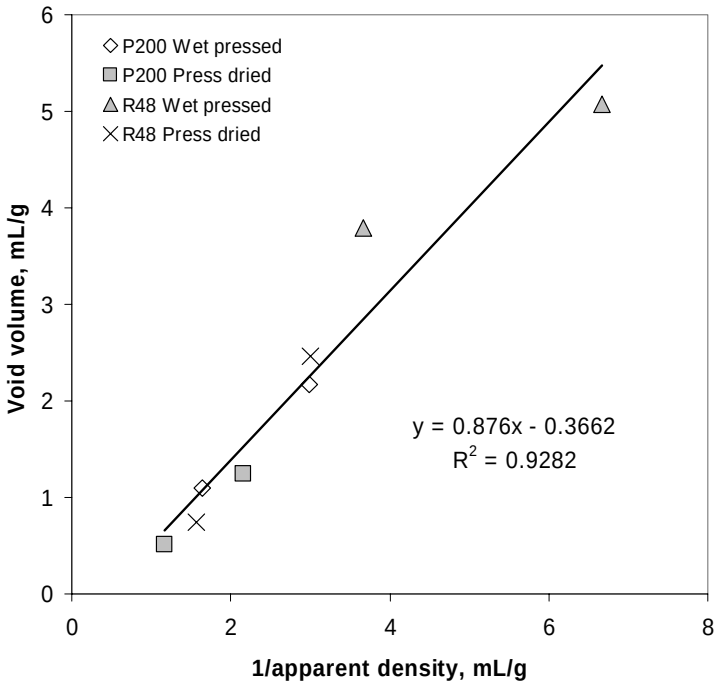

Figure 90. Mercury porosimetry vs. 1/apparent sheet density of fiber (R48) and fines (P200) sheets pressed to different levels of bonding using wet pressing and press drying.

These results show that the difference in scattering coefficient at constant density when wet pressed and press dried sheets were compared was due to the different void volume to specific surface area relationships.

The effect of pore size distribution on scattering coefficient, density and bonding

Mercury porosimetry yields mercury intrusion volume data for a specific applied intrusion pressure. The Washburn equation relates the applied intrusion pressure to pore diameter. Thus, one is able to extract pore size distributions from the mercury intrusion data. The pore size distributions were calculated for pure fiber (R48) and fines (P200) sheets pressed to various levels of bonding using the mercury intrusion data.

In Figure 91 the pore volume of the 100% fiber (R48) at various pore diameters was plotted for couched, wet pressed at 489 psi, and press dried at 1 and 49 psi sheets. Most of the pore volume in 100% fiber sheets was located in pores of 10 μm and larger in

diameter. As the sheets were pressed to higher densities they reduced all sizes of pores independent of pressing procedure, and no shift in pores size distribution was apparent.

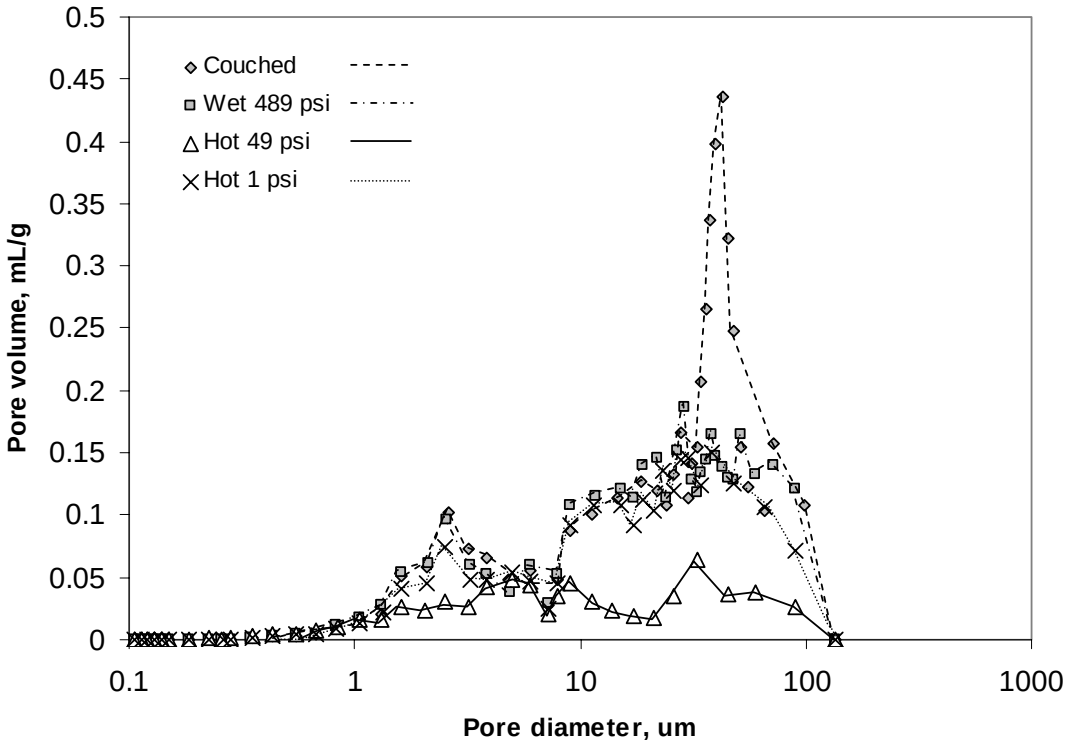

Figure 91. Mercury intrusion pore size distribution of 100% fiber (R48) sheets at various pressing levels.

In Figure 92, the pore volume of the pure fines (P200) at various pore diameters was plotted for couched, wet pressed at 489 psi, and press dried at 1 and 49 psi sheets. The bulk of the pore volume in fines sheet was in the 1µm pore size range. This explains the significant contribution of fines to scattering coefficient when fines are added in the sheet. The sheet pore size distribution is shifted to smaller pores, which in turn results in a higher total specific surface area at a constant pore volume.

However, an effect similar to fines addition in to the fiber sheet was also apparent in pure fines sheet when they were wet pressed and press dried to various levels of bonding. As the pure fines (P200) sheets were pressed using same pressing pressures and

procedures as for the fiber sheets, in addition to the reduction of total pore volume, there was also a significant shift in the pore size distribution (Figure 92).

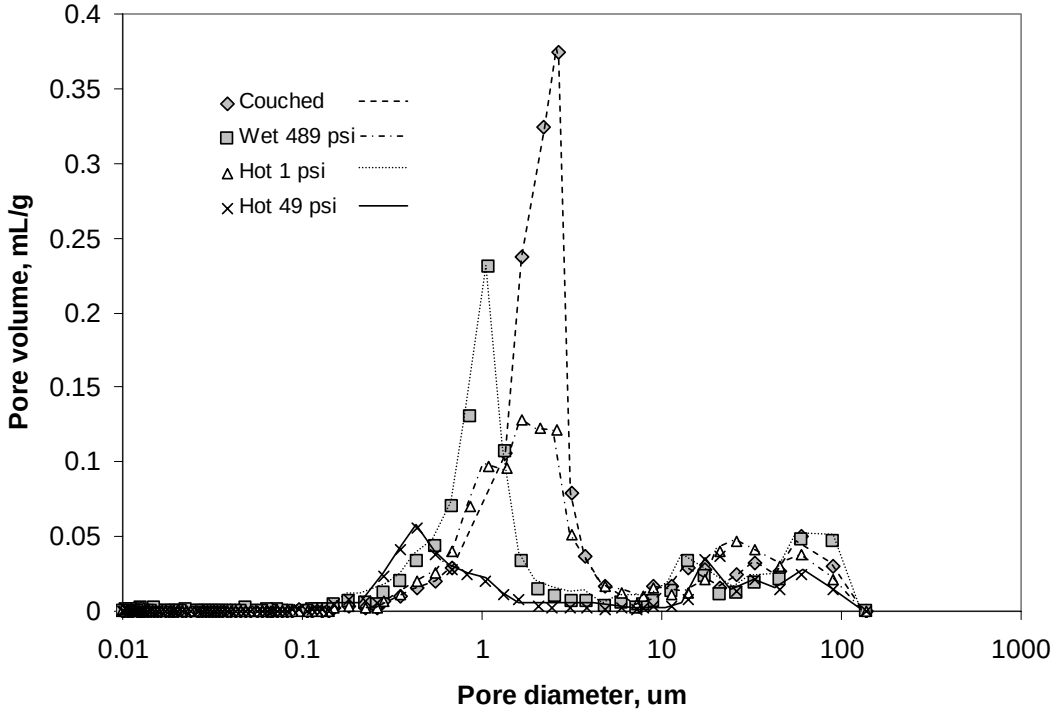

Figure 92. Mercury intrusion pore size distribution of 100% fines (P200) sheets at various pressing levels.

When the wet pressed and press dried fines sheets were compared at a similar total pore volume the press dried sheets had more pore volume associated with larger pores, and thus less total specific surface area at a constant total pore volume (Figure 93).

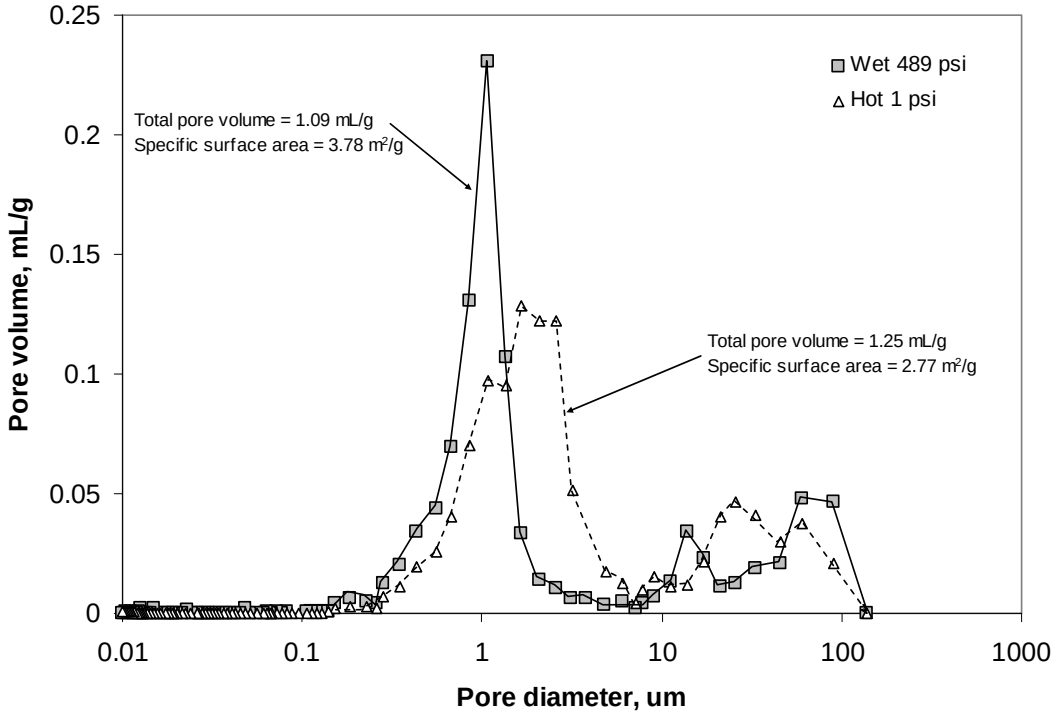

Figure 93. Mercury intrusion pore size distribution of 100% fines (P200) sheets wet pressed at 489 psi and press dried at 1 psi.

The shift of fines pore size distribution to smaller pores in wet pressing resulted in that the wet pressed fines had significantly higher specific surface area at a constant pore volume. However, the 100% fiber sheets where there was no shift in pores size distribution plotted on a common total specific surface area and pore volume line independent of pressing procedure used (Figure 94). Thus, the difference in scattering coefficient at a constant apparent sheet density of the mechanical pulp was due to the shift in pore size distribution of fines.

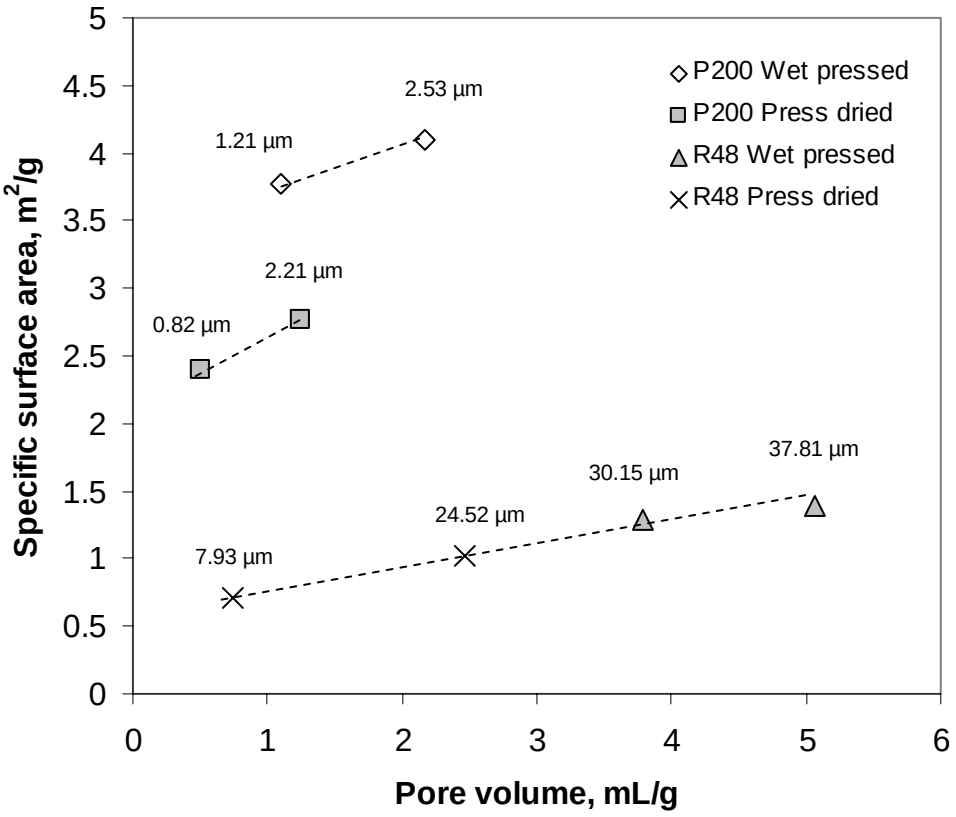

Figure 94. Mercury intrusion pore volume vs. specific surface area of fines (P200) and fiber (R48) pressed at various temperatures and pressures. Median pore diameters shown in numbers.

In 100% fines (P200) sheet the difference in pore size distribution was so drastic that it was readily observed in SEM cross-section images, as Figure 95 depicts. The sheets in the Figure 95 had similar densities, but the press dried sheet had a significantly lower scattering coefficient (76 m^2/kg vs. 63 m^2/kg) and higher tensile strength (43.5 Nm/g vs. 47.6 Nm/g).

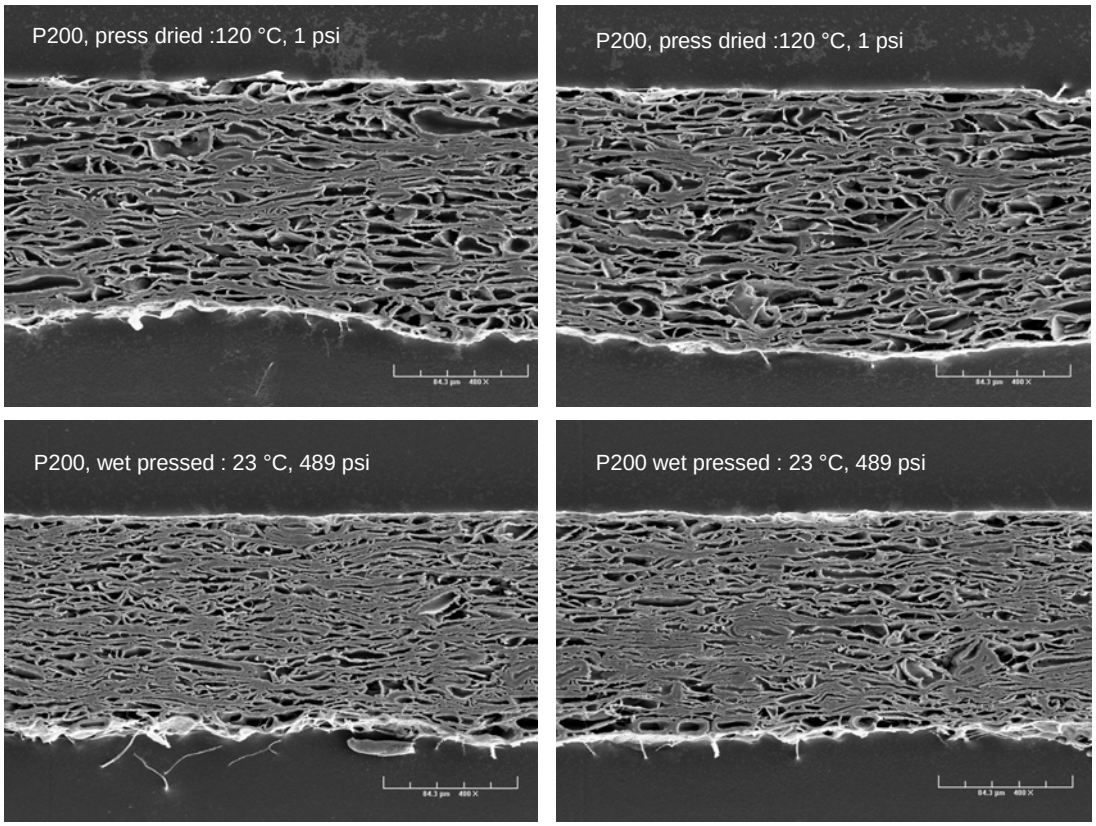

Figure 95. Cross-sectional SEM images of fines wet pressed at 489 psi (below), and press dried at 1 psi (top). Sheets have similar densities and total pore volumes.

The Figure 95 depicts a case where the densities are similar, but the press dried sheet has higher tensile strength and lower scattering and thus is better bonded. In order to compare the sheets at the same bonding (or scattering coefficient) the wet pressed sheet needs to be significantly denser than shown in Figure 95. This behavior using mixed sheets is depicted in Figure 96, where a brominated fines (45%-P200) fraction was added into a fiber fraction (55%-R48) and then wet pressed and press dried to same scattering coefficients. The bromination and SEM imaging was done according to a method described by Gorres [23], and the brominated fines appear brighter than the fibers. Figure 96 depicts how in wet pressing the fines need to be significantly more collapsed in order to achieve the same sheet scattering coefficient as in press drying. This results in that the distances between the fibers in the sheet are significantly

reduced, and is likely to enhance the stress transfer efficiency (tensile strength at constant bonded area) between the load bearing elements in the sheet.

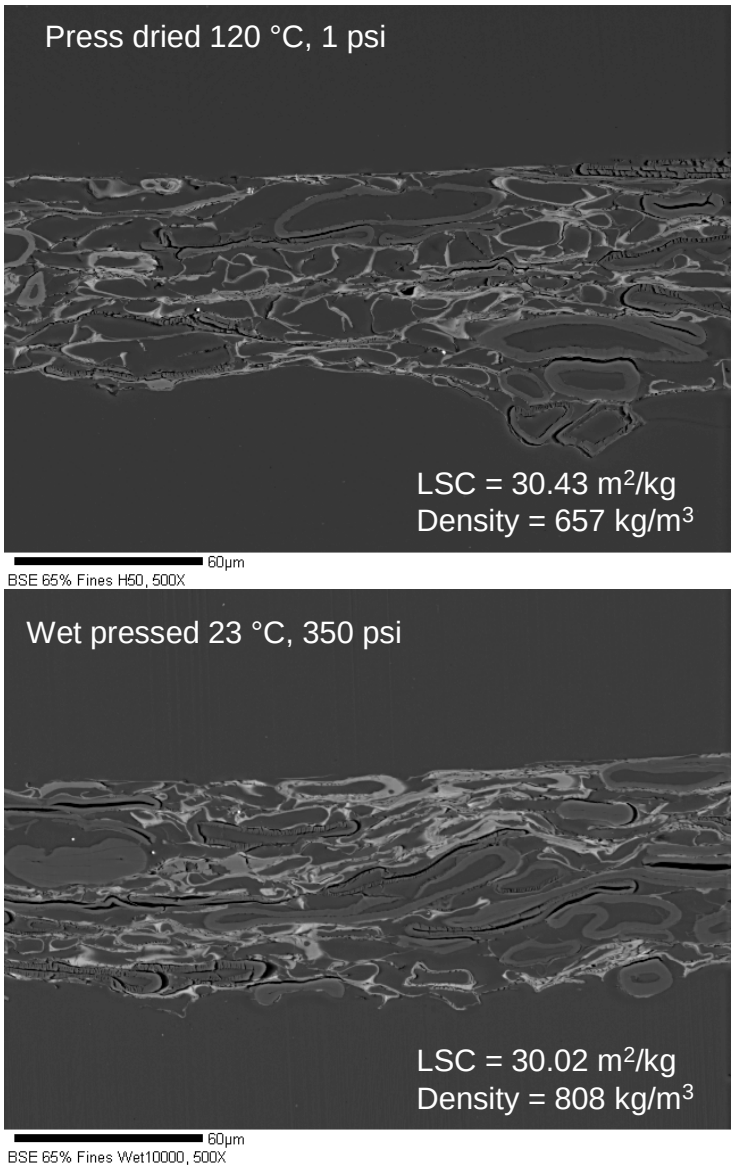

Figure 96. Cross-sectional BSE-SEM images of mechanical pulp brominated fines (45% P200) and fiber (R48) mixed sheets wet pressed and press dried to a common scattering coefficient. (LSC=scattering coefficient, density=apparent sheet density)

Thus these results support the earlier suggestion that the difference in fines density at a constant bonded area (scattering coefficient) was responsible for observed decrease in specific bond strength associated with press drying of heterogeneous mechanical pulp. The pore size distribution of fines was significantly different when the fines are wet

pressed (23 °C) or press dried (120 °C) to the same bonded area (scattering coefficient). In press dried sheets there were significantly higher proportion of larger pores and thus have significantly lower fines density at a constant specific surface area or scattering coefficient (Figure 94). This affects the distance between bonded elements in the sheet and is likely to affect the stress transfer efficiency between them.

Discussion

It has been shown that approximately 35% of the bulk material of P200 TMP fines is comprised of lignin [30]. And roughly 50% of the fines total surface area is shown to be lignin covered [30, 55]. The glass transition temperature of lignin is in the range of 60-140 °C depending on the moisture content of the lignin. In addition lignin has been shown not to provide any significant adhesive properties below its softening (glass transition) temperature [25, 149]. Thus, it is likely that when the fines sheet was wet pressed below the softening temperature of lignin, the sheet experiences rebound due to the stiff lignin rich matrix and inefficient bonding. These observations led us to examine the extent of collapse in the fines sheets under significant wet pressing load. A series of fines handsheet were prepared and pressed at 490 psi. A copper wire sheet was put on both sides of the sheet, and the caliper was measured using a sensitometer on the pressing plate by subtracting the upper wire distance from the bottom wire distance. When the fines sheet was wet pressed at 23 °C the sheet collapsed readily reaching a caliper between 107 and 110 microns at 489 psi, at basis weights 69.3 g/m^2 and 71.0 g/m^2 respectively. A pressure vs. caliper curve of one of the runs (71.0 g/m^2) is shown in Figure 97.

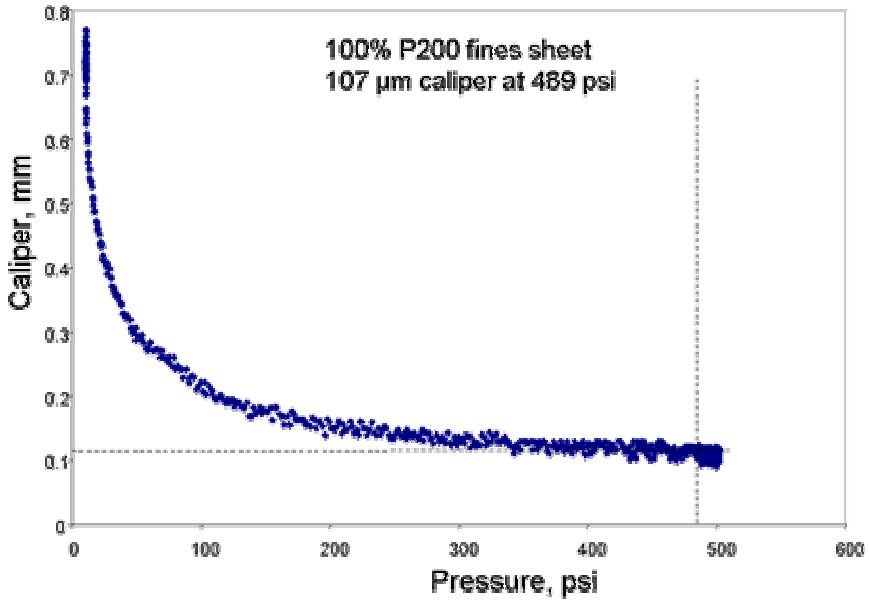

Figure 97. Pressing pressure vs. caliper of 100% fines (P200) sheet pressed at 23 °C.

A set of fines sheets of same pulp batch wet pressed to 489 psi and restrain dried at 50% relative humidity had an average soft caliper of 117 microns at a basis weight of 71.0 g/m^2. Based on the data shown here the fines sheets rebounded 6-8% in caliper. Considering that the press dried sheets were dried under load and were likely not to rebound, as was shown by Back *et al* [143], the major difference between press dried and wet pressed sheets was that the press dried sheets approached the end state density from a lower density state, whereas the wet pressed sheet achieve its final density from a higher density.

Based on the above observations and results presented in this paper a mechanism is proposed that explains the significant shift in pore size distribution of the fines sheet in wet pressing. In wet pressing at high pressing pressures a fines sheet collapses almost completely and then rebounds. In the fully collapsed state almost all of the initial free surface area of the fines particle in the sheet is in contact with another fine particle. When the pressure is released the sheet rebounds due to the stiff lignin rich structure. During the rebound only areas where bonding exceeds the rebound tendency remain bonded. Areas that cannot be bonded at temperatures below the glass transition remain unbonded, and as the pressure is released the sheet starts to rebound creating a significant amount of newly formed small pores. This proposed mechanism in relation to pore size distribution is depicted in Figure 98.

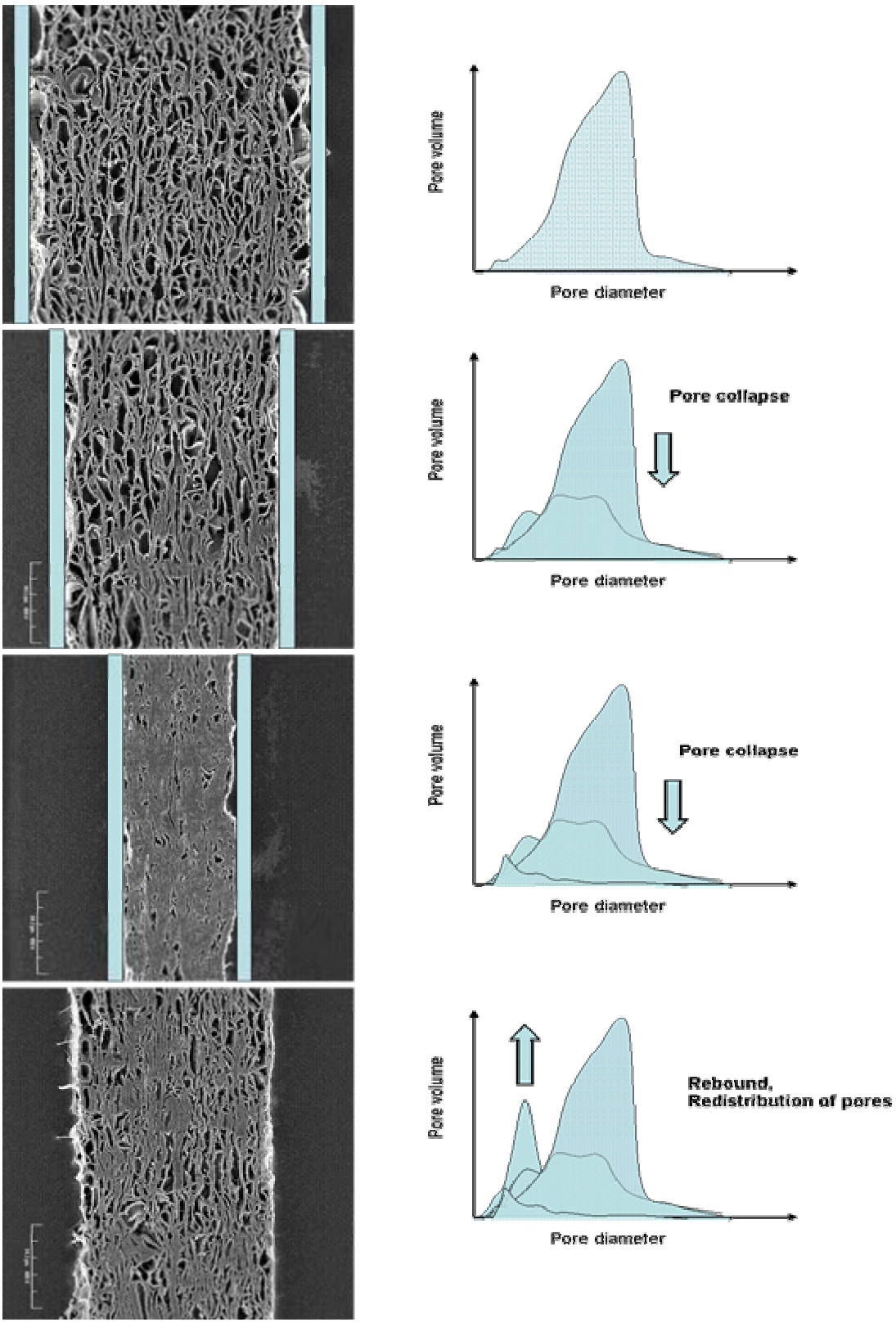

Figure 98. Illustration of the proposed mechanism of the redistribution of pores in wet pressing of mechanical pulp fines.

In press drying, where the temperature (and moisture) is above the glass transition of lignin making the fines particles soft and conformable very little pressure is needed to collapse the structure. The sheets are pressed until the moisture is removed and the structure is frozen into the form it was under load. Fines are readily bonded onto the neighboring surface creating significant amount of bonded area. When wet pressed and press dried fines sheets are then compared at constant void volume or density the wet pressed sheets have the void volume located in smaller pores. Thus the wet pressed sheets have significantly higher specific surface area and hence scattering coefficient. This proposed mechanism is depicted in Figure 99, where the press drying and wet pressing are compared at a constant density or void volume.

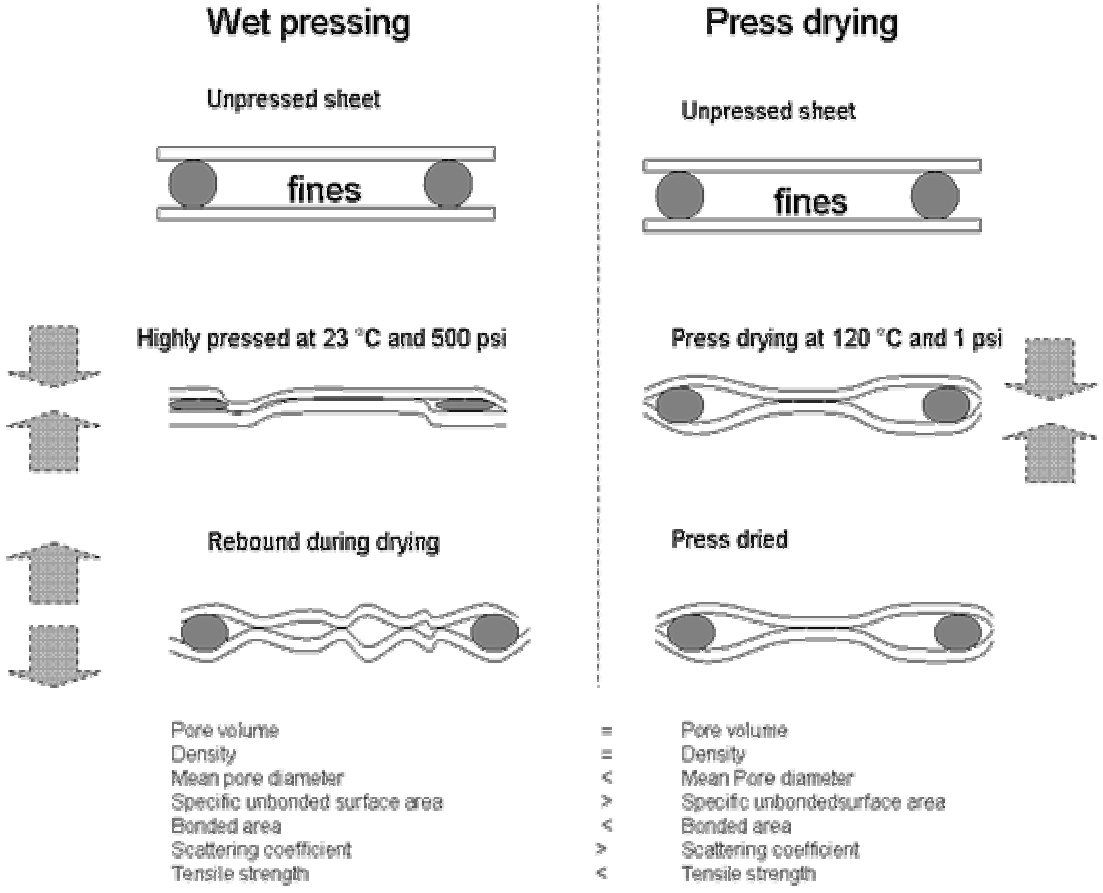

Figure 99. Proposed mechanism explaining differences in pressing fines at temperatures below the glass transition of lignin (wet pressing), and above (press drying). Compared at a constant void volume and density. All particles in the figure are fines.

Conclusions

Press drying has been shown to reduce the scattering coefficient of mechanical pulp without significantly affecting the density of the sheet. This type of significant reductions in scattering coefficients are also observed in commercial Newsprint production, when the drying temperatures exceed a certain threshold usually close to the glass transition temperature of lignin. In this paper it was shown that the reduction in scattering coefficient at constant density is caused by the fines (P200) in the sheet. Using mercury porosimetry it was shown scattering coefficient is related to the total specific surface area of the sheet, and the apparent density is a factor of the void volume of the sheet. In wet pressing of fines there was a significant shift in the pore size distribution, whereas at low press drying pressures all pores of all sizes were reduced equally and there was no significant shift in pore size distribution. This shift in pore size distribution of fines resulted in that the specific surface area - void volume relationship for wet pressed and press dried fines sheets were significantly different. Wet pressed fines sheet had higher amount of smaller pores at constant pore volume. Thus, the scattering coefficient of wet pressed fines sheet remained significantly higher when compared at a constant density.

In pure fiber and fines sheets the decrease in specific surface area (scattering coefficient) was transposed into tensile strength independent of pressing procedure, indicating that the total unbonded specific surface area was not changed. However, wet pressed mixed sheets of fibers (R48) and fines (P200) as well as whole pulp had higher strength properties than press dried sheets when pressed to the same scattering coefficient. This was explained with better stress transfer between bonded elements in mixed wet pressed sheets due to the significantly higher fines density required to obtain the same bonded area as in press drying.

Addendum to chapter 5

Moisture content difference at 50% RH and effect on strength properties

Seth *et al.* [144] have argued that the differences between press dried and normally dried samples could be partly explained by the differences in moisture content of the sheet at 50% relative humidity. In this study the moisture contents of the sheets were measured from three sets of mixed sheets: 100% fiber (R48), 50%fiber+50% fines and 100% fines (P200) sheets. The wet pressed sheets had roughly 1%-unit higher moisture content at 50% relative humidity in comparison to the press dried sheets, as shown in Table 17.

Table 17. Moisture contents of wet pressed and press dried sheets at 50% RH

	Moisture content at 50% Relative Humidity			
	Wet pressed		Press dried	
	23 °C		120 °C	
Mixture	%	ST. DEV	%	ST. DEV
100% fiber (R48)	8.21	0.31	7.30	0.46
50%fiber+50%fines	8.63	0.29	8.01	0.22
fines	9.94	0.11	8.97	0.60

The moisture content for all the sheets were then measured at various levels of relative humidity by letting the sheets to gain moisture for at least 12 hours prior to weight measurements. The moisture contents of the sheets were then plotted against the relative humidity, shown in Figure 100. All sheets showed similar extent of increase in moisture content as the relative humidity was increased.

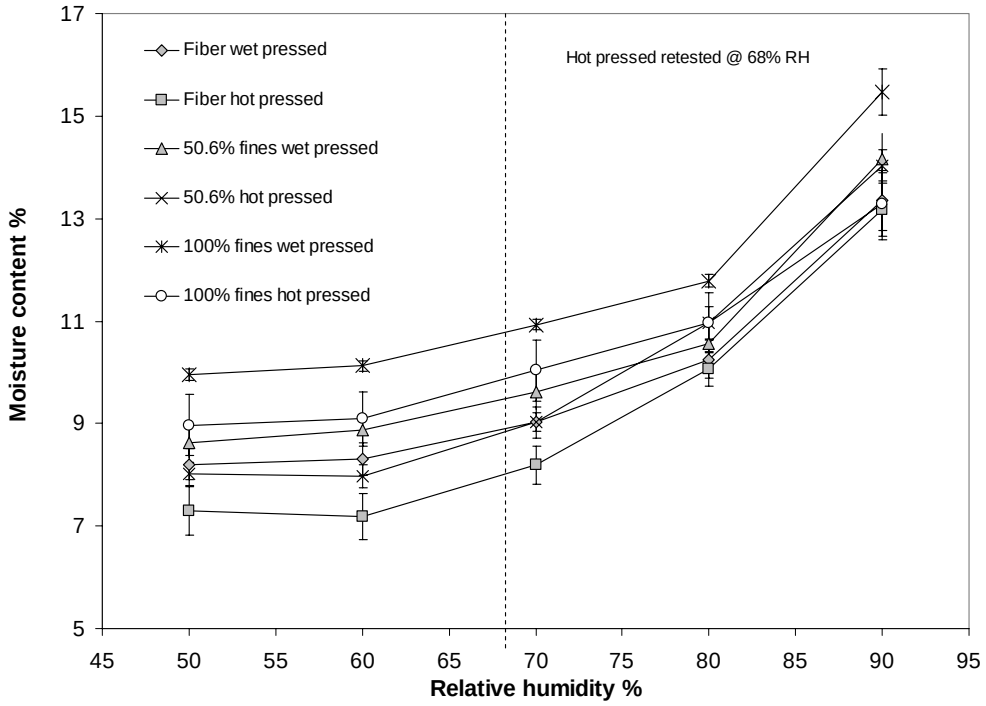

Figure 100. Moisture contents of mechanical pulp fiber (R48) and fines (P200) mixed sheets at various levels of relative humidity.

Then the press dried sheets were tested at higher relative humidity (68%), which brought the moisture content of the press dried sheets close to the wet pressed sheets. The resulting moisture contents for the press dried sheets at 68% RH are shown in Table 18.

Table 18. Sheet moisture contents of press dried sheets at 68% RH and wet pressed at 50% RH

	m.c. at 50% RH		m.c. at 68% RH
	Wet pressed 23 °C	Press dried 120 °C	Press dried 120 °C
Mixture	%	%	%
100% fiber (R48)	8.21	7.30	7.99
50%fiber+50%fines	8.63	8.01	8.82
fines	9.94	8.97	9.85

After the conditioning at higher relative humidity tensile strength testing was conducted for all fiber (R48) and fines (P200) mixed press dried sheets at 68% relative humidity. The results are shown in Table 19, where the tensile strength, specific modulus and

stretch measurements at 50% and 68% relative humidity were tested for statistical significance. Table 19 shows that in tensile only the 50% fines (P200) content sheets were statistically significantly different when tested at these two relative humidity levels. In specific modulus the 100% fines sheets were statistically different. In stretch the 50% fines (P200) and almost pure fiber (R48) sheets showed statistically significant differences. However, overall these differences were small and could not explain the large differences in the scattering coefficient-tensile strength relationship between press-dried and wet pressed sheets.

Table 19. Tensile properties of press dried sheets measured at 50% RH and 68% RH

Sheet	Tensile strength					
R48+P200	Tested at 50% RH		Tested at 68% RH			
Fines %	Average Nm/g	Variance	Average Nm/g	Variance	% Difference	p(one-tailed)
100	48.96	2.44	49.32	18.37	0.73	0.409
80.2	53.04	1.08	52.19	1.22	-1.60	0.105
50.6	60.05	3.79	57.74	2.42	-3.84	**0.009**
26.9	66.93	3.84	63.44	6.55	-5.21	0.062
2.36	35.30	1.20	36.09	2.32	2.24	0.185
Sheet	Specific modulus					
R48+P200	Tested at 50% RH		Tested at 68% RH			
Fines %	Average kNm/g	Variance	Average kNm/g	Variance	% Difference	p(one-tailed)
100	4.76	0.04	4.93	0.05	3.49	**0.006**
80.2	5.39	0.01	5.37	0.02	-0.38	0.338
50.6	5.81	0.03	5.64	0.03	-3.00	0.062
26.9	6.13	0.04	6.08	0.06	-0.84	0.389
2.36	4.94	0.04	5.14	0.05	3.94	0.089
Sheet	Stretch					
R48+P200	Tested at 50% RH		Tested at 68% RH			
Fines %	Average %	Variance	Average %	Variance	% Difference	p(one-tailed)
100	1.59	0.04	1.61	0.10	1.28	0.434
80.2	1.47	0.01	1.52	0.02	3.61	0.137
50.6	1.89	0.00	2.05	0.02	8.55	**0.005**
26.9	2.31	0.02	2.42	0.02	4.96	0.101
2.36	1.24	0.00	1.29	0.01	3.99	**0.050**

Chapter 6: The operating regime in mechanical pulps - the significance of fiber failure

Abstract

The significance of fiber failure in tear and tensile failure of mechanical pulps remains an enigma, partly due to the difficulty to increase bonding without altering the sheet composition. To circumvent this problem wet pressing and press drying were used to increase bonding. It is shown, using tear and tensile strength data that most mechanical pulps are in a domain where fiber failure can be considered a significant factor. Only sheets with very high long fiber content are in the negligible fiber failure domain. The region where the domain transitions from negligible fiber failure to significant fiber failure was 0.3-0.45 T/Z (Tensile strength/Zero Span Tensile strength), and 30-40 Nm/g tensile index with the transitions somewhat dependent on the sheet composition. Tear strength was found to be a linear function of the sheet composition in the low strength region.

Introduction

It has generally been assumed that mechanical pulps operate in a strength domain where fiber breaking has an insignificant effect on the fracture mechanism in tensile and tear test, and the main failure is believed to occur through the bonds between the structural elements in the sheet [7, 24, 33, 34, 38, 61]. There are indications, however, that modern mechanical pulps, which are mainly composed of fines and long fiber with a bimodal fiber length distribution, undergo significant fiber failure in tensile and tear testing [6, 27, 75, 77].

Several authors have investigated this problem. However, the experimental approach has been limited by the fact that bonding in mechanical pulps cannot be significantly increased without changing the sheet composition [6, 24, 77]. Refining as a means to increase bonding in mechanical pulps produces a significant amount of additional fines which alters the composition of the sheet [2, 115]. Wet pressing has limited effect on mechanical pulps, increasing bonding slightly in some cases, and having no effect at all in others [50, 136]. This is likely due to the fiber rebound after the pressure is released [50, 136]. Thus, most of the studies have relied on artificial blends, where bonding was

increased by increasing the fines content. To maintain the fiber length constant, the R28, R48 and R200 composition of the sheet is adjusted [3-6, 76, 77]. This approach has provided significant results, and has altered the perception about the operating domain, however, it has not been able to provide unambiguous proof of the significance of fiber failure on strength properties in mechanical pulps.

The currently accepted explanation for tear strength was initially formulated by Van Den Akker, who proposed that tear work is controlled by two competing mechanisms: stretching of fibers until they break and fiber pull-out out of the network [187]. Shallhorn and Karnis have proposed a theory that describes the tear and tensile behavior of mechanical pulps using the mechanisms proposed by Van Den Akker [24]. The Shallhorn-Karnis model considers two cases where either only bond failure or bond and fiber failure control the fracture mechanism. Based on their theory, the domain transitions from negligible fiber failure to significant fiber failure where the sheet tear strength reaches its maximum. Thus, the Shallhorn-Karnis theory provides a method for analyzing the domain where the pulp is likely to operate. Tear-tensile relationships based on the Shallhorn-Karnis model are depicted in Figure 101 at various fiber lengths.

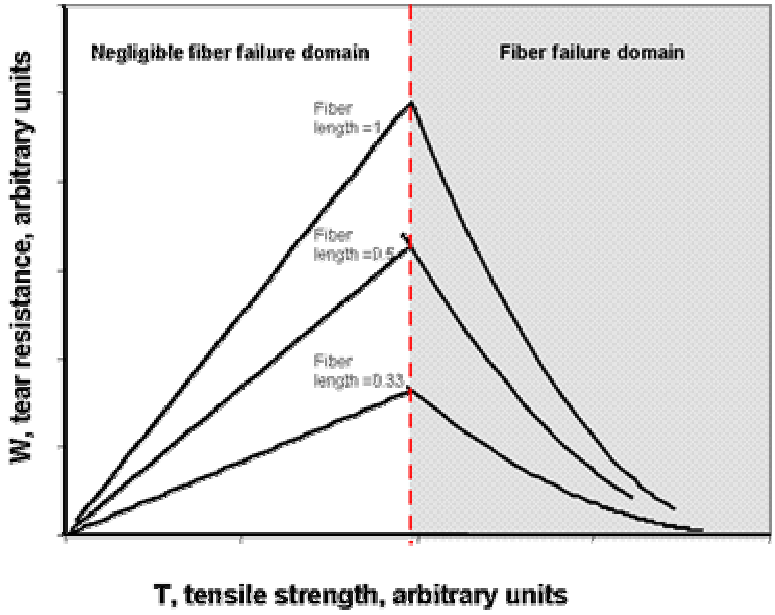

Figure 101. Shallhorn-Karnis equation based tear index at various tensile index and shear bond strength for various fiber lengths

In order to circumvent the problem of altering the sheet composition to increase bonding, in this study the bonding was increased by wet pressing and press drying sheets to high levels of bonded area. The operating regime problem was then approached by interpreting the tear relative to bonding (where bonding is measured as T/Z, i.e. Tensile index divided by Zero span tensile index [188]) in whole TMP, its fractions and mixtures of these fractions. Also, the tear-tensile relationship was investigated. In addition, the effect of fiber length on the tear strength at various bonding levels was studied using the data obtained from the mixture studies.

Experimental

Fiber middle and fines fractionation: The Bauer McNett apparatus was used to fractionate a hot disintegrated 110 CSF Norway spruce (Picea abies) TMP. The R28, R48, R200 and P200 fractions were collected. Later the R28 and R48 fractions were combined. The P200 fraction was collected using the sedimentation method [30]. The combined R28 and R48 fiber fraction was fractionated twice in order to achieve a near pure fiber fraction without any fines present. *Handsheet forming*: Handsheets were formed using a 150 mesh screen and recirculation of whitewater. Fines handsheets were formed on a dense glass fiber filterpaper. All handsheets were restraint dried if not dry after pressing. The target handsheet basis weight was 60 g/m^2 O.D.

Wet pressing: Couched handsheets were not pressed. Wet pressing was conducted at 0, 65 (448 kPa), 489 (3372 kPa) and 978 (6743 kPa) psi and 23^{o}C using a Carver press with 3 blotter papers on the one side and a chrome plate on the other side of the handsheet. Wet pressed handsheets were pressed for 1 minute. *Press drying*: Press drying was conducted at 6 pressing levels 0, 0.8 (5.5 kPa), 8.1 (55.8 kPa), 16.3 (112 kPa), 48.9 (337 kPa) and 163 (1124 kPa) psi. Individual handsheets were pressed between hot plates heated to 120^{o}C using a “sandwich” that consisted of a papermachine felt, wet blotter paper (to increase drying time and humidity above 100^{o}C), handsheet, chrome plate, and a filter paper (to protect the chrome plate). All press dried handsheets were pressed until completely dry. *Testing*: Tensile and Tear strengths were measured using the Tappi standard T-494, with exceptions of a reduced span length (2 inches), and 0.5 inches/min strain velocity in the tensile test. Zero span tensile strength

was measured using a Pulmac zero span tensile tester. The arithmetic fiber length was measured using the Fiber Quality Analyzer (FQA).

Results

Domain transition and bonding

Figure 102 depicts the decrease in tear index as the bonding (tensile index / zero span tensile index) is increased by wet pressing and press drying of whole pulp TMP sheets. The whole pulp TMP is already at maximum tear index without significant pressing, and decreases as pressure is increased independent of the pressing procedure used (wet pressing or press drying). Based on the Shallhorn-Karnis theory this distinctly shows that a modern whole pulp TMP, even at fairly high freeness (110 CSF), operates in a domain where fiber breaking can be considered a significant factor. Figure 102 indicates that the point where the domain changes from negligible fiber breaking to significant fiber breaking is equal or less than 0.3 T/Z.

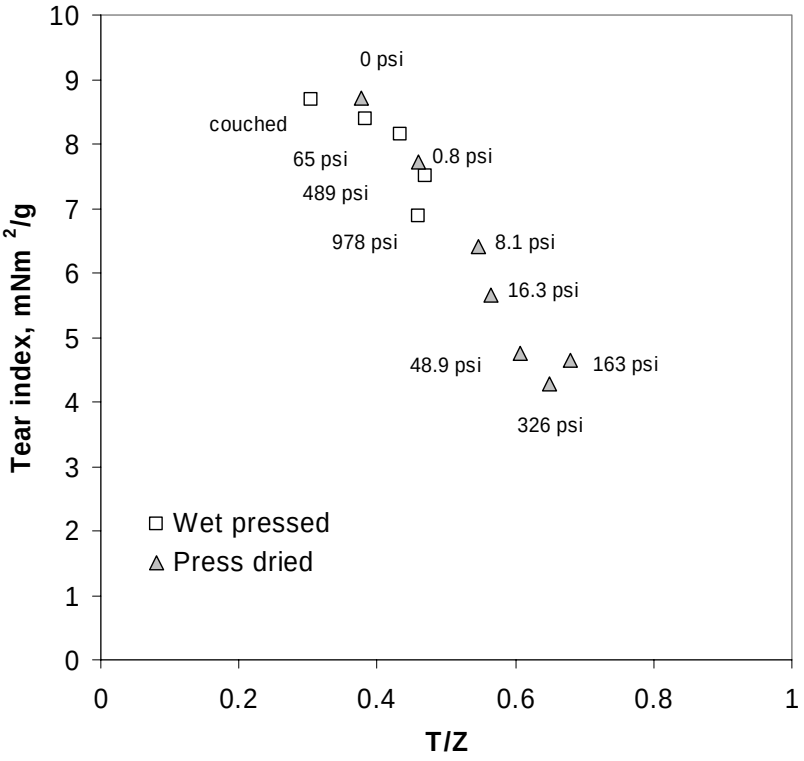

Figure 102. Tear index at various levels of bonding (Tensile index / Zero span tensile index) of TMP (110 CSF) wet pressed and press dried to various levels of bonding

The effect of various mechanical pulp fractions on the domain transition was investigated using mixtures of fiber (R48), middle (R200) and fines (P200) fractions. All sheets were then wet pressed and press dried to different levels of bonding. The tear index vs. bonding index (Tensile index divided by Zero span) for fiber (R48) and fines (P200) mixed sheets is shown in Figure 103. The shape of the relationship is similar to that of a refining series or a pressing series in chemical pulps. Second order fits, which were forced through the origin were constructed for all mixtures used in this study. The coefficients for all the mixtures are summarized in Table 20.

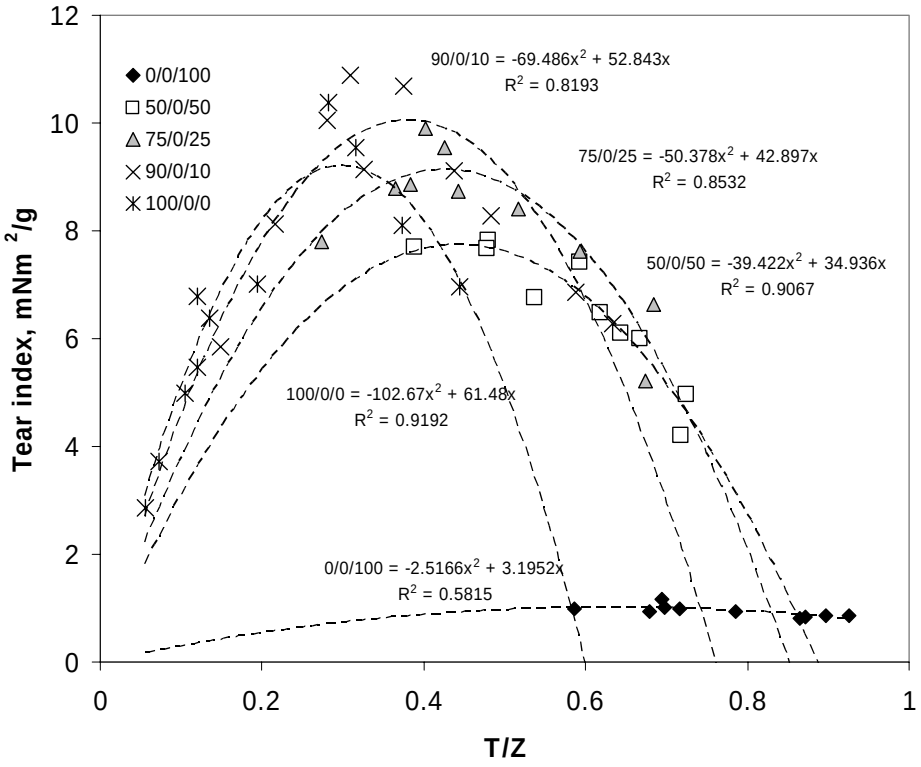

Figure 103. Tear index vs. Bonding index (T/Z) of Fiber (R48) and Fines (P200) mixed sheets.

Table 20. Coefficients for mechanical pulp mixtures.

Mixture R48/R200/P200	Tear vs. T/Z coefficients a (x^2)	b (x)	R^2	Bauer-McNett Fiber length, mm
100/0/0	-102.67	61.48	0.9192	1.884
90/10/0	-103.4	62.74	0.8153	1.738
90/0/10	-69.486	52.843	0.8193	1.700
72/25/0	-58.644	45.761	0.9232	1.496
75/0/25	-50.378	42.897	0.8532	1.435
50/50/0	-54.691	41.666	0.9265	1.092
50/0/50	-39.422	34.936	0.9067	0.994
37/37/25	-45.374	35.318	0.8859	0.839
25/25/50	-33.253	26.648	0.8038	0.586
0/100/0	-11.01	11.104	0.4769	0.283
0/33/66	-7.0009	7.0075	0.7703	0.215
0/66/33	-10.742	10.084	0.6352	0.148
0/0/100	-2.5166	3.1952	0.5816	0.080

The bonding index at the maximum tear index depicts the transition from predominantly bond failure to fiber failure, and was calculated based on the equation 28. The values for a and b were derived from the quadratic best fits in Table 20.

$$\frac{d}{dx}(ax^2 + bx) = 0$$

$$x = \frac{-b}{2a}$$

Equation 28

The maximum tear index was obtained for sheets containing R48 fiber fraction at a fairly constant bonding index between 0.3-0.45 depending on the sheet's composition. The bonding index was lowest for the pure fiber sheets, and increased as fines or middle fractions were added (Figure 104). For pure fines and middle fraction sheets the bonding index at maximum tear index was significantly higher than for sheets with a fiber fraction present. In these sheets the tear index was fairly constant and the determination of the maximum tear index using quadratic equations is questionable.

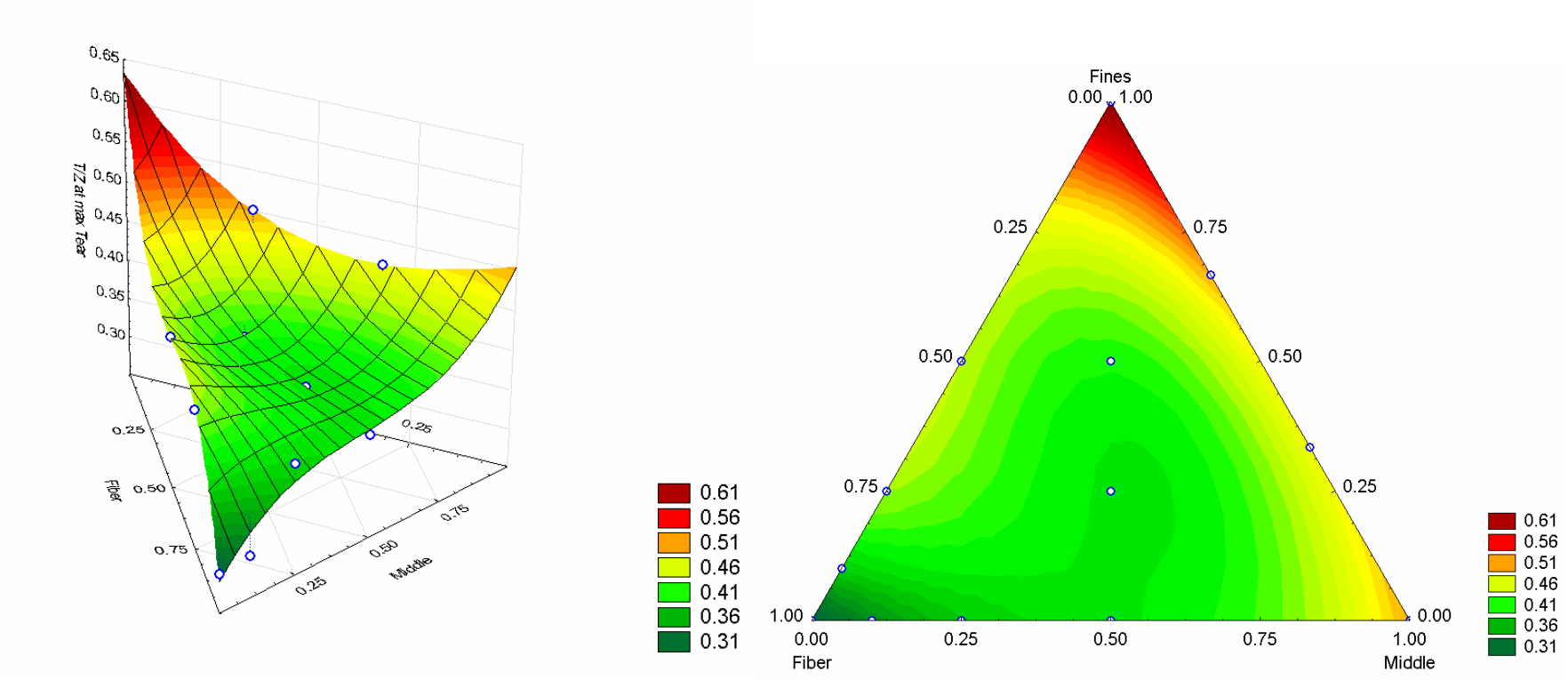

Figure 104. Bonding index (T/Z) at maximum tear index for various sheet compositions (Qubic fit)

Domain transition and tensile strength

The tensile strength to tear strength relationship provides an alternative method for analyzing the domain transition. Shallhorn-Karnis equation predicts that the maximum tear strength is obtained when the sheet tensile strength is half of the fiber strength. The tear index relative to tensile index followed similar form as the tear vs. bonding index (Figure 105) and reinforced the earlier conclusion that a modern TMP operates at a regime where fiber failure has significant effect on the fracture mechanism of the pulp. There was a slight difference between the wet pressed and press dried sheets, which was not seen in the tear index vs. bonding index plot, and was likely due to the difference in zero span tensile strength of press dried and wet pressed sheets at constant tear index. The wet pressed sheets had slightly lower zero span tensile strengths. The tensile and tear index saturated at 163 psi and no additional strength improvement was obtained at higher pressing level.

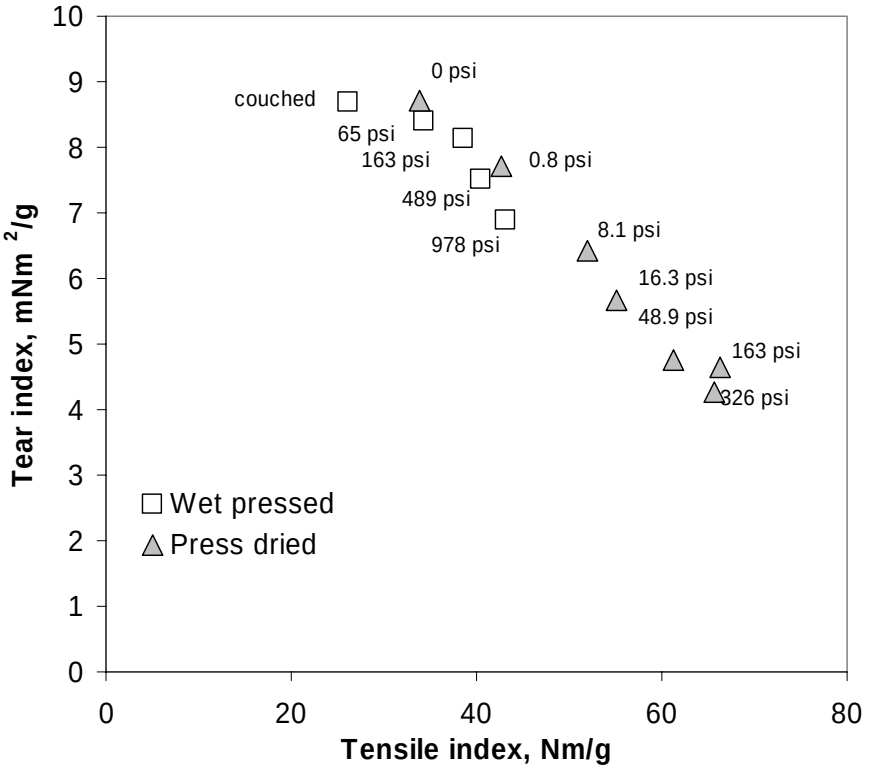

Figure 105. Tear index at various levels of tensile strength of TMP (110 CSF) wet pressed and press dried to various levels of bonding

The tear index vs. tensile index plots for fiber (R48) and fines (P200) mixed sheets are shown in Figure 106. Clear maximum tear strength was obtained for mixtures with high R48 fiber content. In Figure 106 the second order fits were plotted for each fiber (R48) – fines (P200) mixture. These were constructed for all mixtures used in this study. The coefficients for the mixtures are summarized in Table 21. No significant differences between wet pressed and press dried samples were observed.

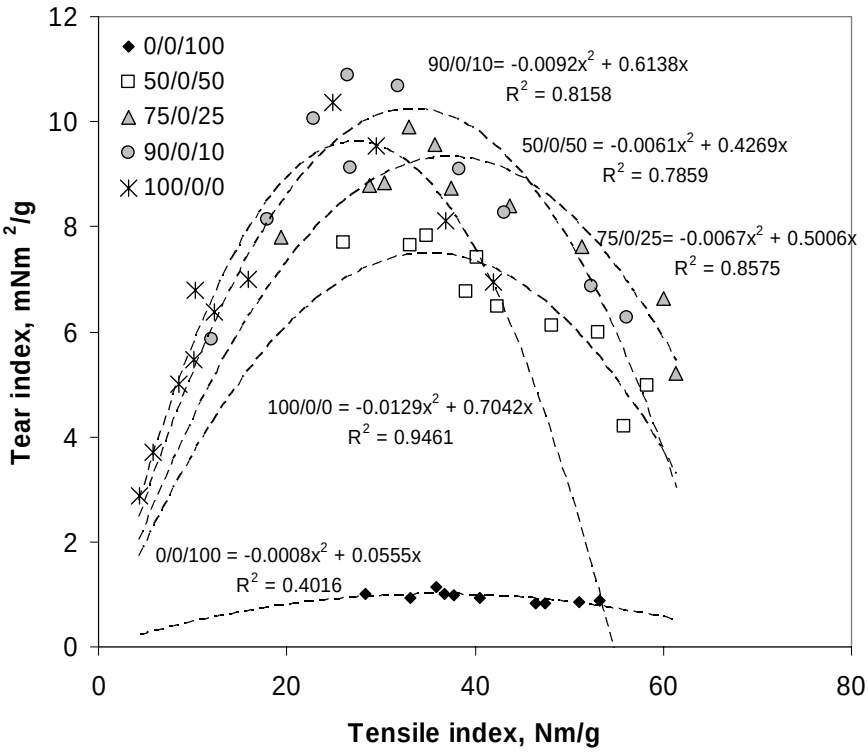

Figure 106. Tear index vs. tensile index of Fiber (R48) and Fines (P200) mixed sheets.

Table 21. Second order coefficients for mechanical pulp mixtures.

Mixture	Tear vs. Tensile index coefficients			Bauer-McNett Fiber length,
R48/R200/P200	a (x^2)	b (x)	R^2	mm
100/0/0	-0.0129	0.7042	0.9461	1.884
90/10/0	-0.0119	0.6862	0.9333	1.738
90/0/10	-0.0092	0.6138	0.8158	1.700
75/25/0	-0.0072	0.5149	0.9268	1.496
75/0/25	-0.0067	0.5006	0.8575	1.435
50/50/0	-0.0059	0.4332	0.9044	1.092
50/0/50	-0.0061	0.4269	0.7859	0.994
37/37/25	-0.0052	0.3788	0.7663	0.839
25/25/50	-0.0046	0.312	0.7688	0.586
0/100/0	-0.0014	0.1234	0.4085	0.500
0/66/33	-0.0014	0.1149	0.7325	0.215
0/33/66	-0.0013	0.097	0.5051	0.148
0/0/100	-0.0008	0.0555	0.4016	0.100

The tensile index at the maximum tear index depicts the transition from predominant bond failure to fiber failure, and was calculated based on the equation 1. The values for a and b were derived from the quadratic best fits in Table 21.

The maximum tear index was obtained for sheets containing R48 fiber fraction at a fairly constant tensile index between 28-36 Nm/g depending on the sheets composition, lowest for the pure fiber sheets (Figure 107). For pure fines and middle fraction sheets the tensile strength at maximum tear index was significantly higher than for sheet with fiber fraction present. This is likely an artifact of the quadratic fits. In pure fines and middle fraction sheets the tear index did not vary significantly making the determination of maximum tear index using quadratic fits questionable.

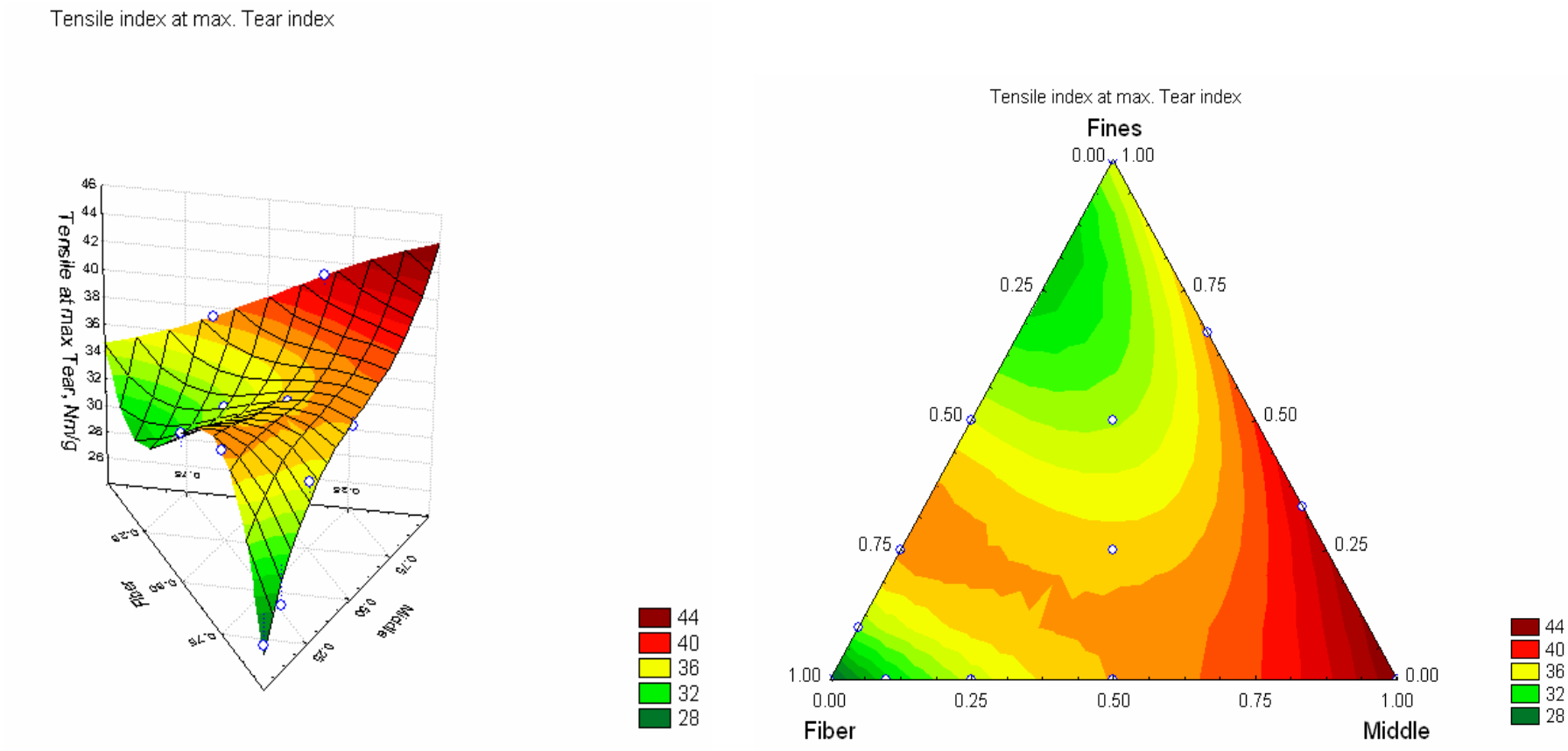

Figure 107. Tensile index at maximum tear index for various sheet compositions (Qubic fit)

Discussion

In a beating series or wet pressing series with chemical pulps, tear often decreases while bonding index increase. With coarse fibered pulps like Douglas fir or the southern pines, there is often an increase in tear at the very lowest bonding levels, with the curve going through a maximum and then a continuous decline in tear index with increased bonding [189]. The change is usually considered to be due to fibers breaking in the tear test, the maximum is near the bond strength where fiber failure begins to dominate the fracture mechanism. In mechanical pulps, tear index often increases with increased refining and this has long been considered evidence that mechanical pulps operate in the bond failure domain where tear index increases with increased bonding. In this study the maximum tear strength was obtained approximately at a Tensile strength of 30 Nm/g. This is consistent with earlier findings in mechanical pulps. Mohlin [77] has shown using the data of Lindholm [3-6, 76], where fines were added into fiber fraction, that the maximum tear strength is also obtained at approximately 30 Nm/g independent of the fiber fraction used. Most commercial mechanical pulps are well above the 30 Nm/g Tensile strength limit, and thus can be assumed to generally operate in a domain where fiber failure is a significant mechanism in the paper failure.

In this study, only sheets with very high fiber content provided data in the negligible fiber failure domain. For these, high fiber content sheets, the domain transition at higher levels of bonding resulted in a very visible break in the scattering coefficient vs. T/Z (bonding index) relationship. In Figure 108 the scattering coefficient was plotted against the bonding index (T/Z). Wet pressed sheets were not included. Figure 108 shows a clear change in slope from a linear relationship at low bonding region to a second relationship beyond the domain change. This indicates that the relationship between bonding and Tensile strength in the low bonding domain is linear, as was suggested by Kallmes [190], and predicted in the Shallhorn-Karnis equation.

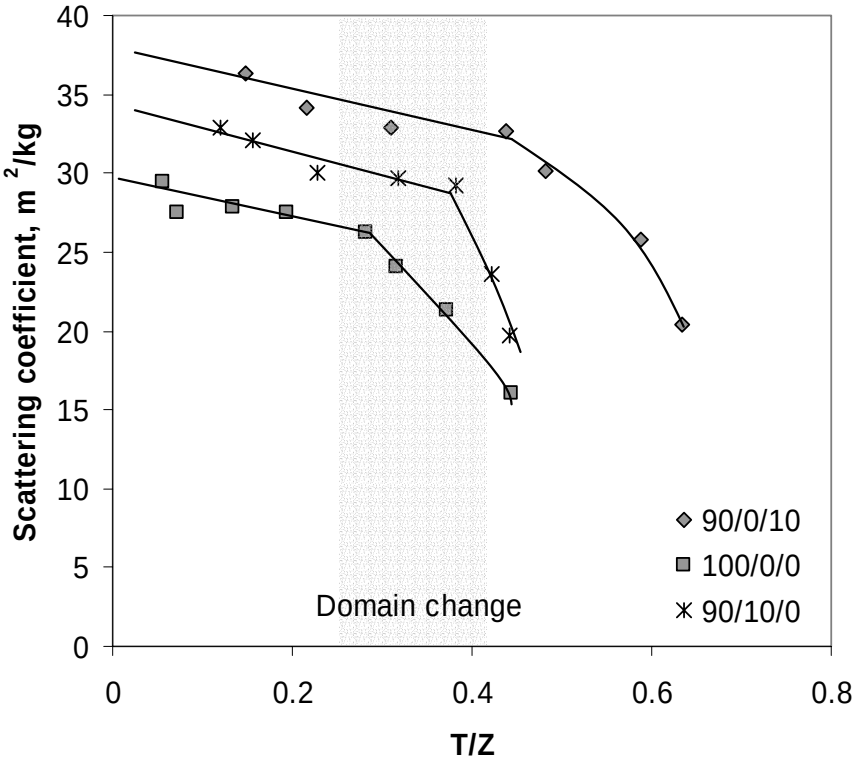

Figure 108 . Scattering coefficient vs. bonding index (T/Z) for press dried 100%R48+10%P200, 100%R48 and 90%R48+10%R200 mixed sheets

The presence of the linear region means, that when a non-linear relationship between bonded area and tensile strength is used to estimate the total unbonded specific surface area (S_o) of the pulp, the S_o obtained will underestimate of the real total unbonded dry specific surface area of the sheet. However, the non-linear behavior was only obvious for sheets with high fiber content in the high bonding regime. As fibers were replaced with fines or middle fractions the scattering-tensile relationship approached a linear model (Figure 109), suggesting that the fiber fraction undergoes fiber failure and fines fraction due to their short finer length predominantly bond failure. This is consistent with the findings in Chapter 1, where it was shown that whole pulp scattering-tensile relationship was better predicted with a linear fiber failure neglecting model than a non-linear, significant fiber failure model (Page equation). Thus, it is likely that the correct model for bonding-tensile relationship is a combination of the fiber failure model for fiber fraction and pure bond failure model for finer fractions.

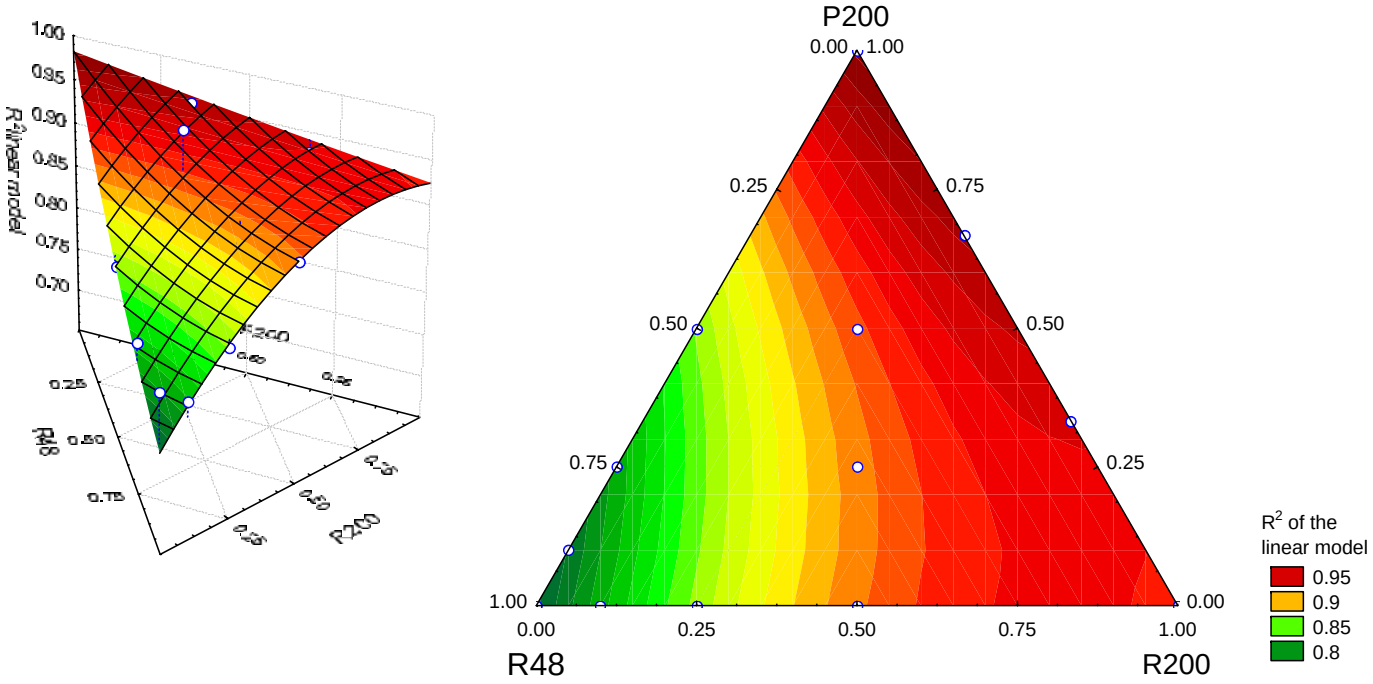

Figure 109. R^2 of the linear (s=aT+b) scattering coefficient to tensile strength relationship as a function of the sheet composition.

Tear strength in mechanical pulps is generally believed to be a factor of fiber length. Mohlin has shown that tear strength increased as the fiber length was increased at constant fines content (bonding) [77]. Similar results were also obtained here for the low bonding regime. In Figure 110 tear index estimated using the quadratic equations in Table 20 were plotted as a function of fiber length for three different bonding levels below the maximum tear index. In the low bonding regime the tear index was dependent on the fiber length of the pulp. This dependency became more pronounced as the bonding was increased until the maximum tear strength was reached. Same linear dependency on fiber length was obtained when compared at a constant Tensile strength in the low bonding regime. This relationship is depicted in Figure 115 in the addendum.

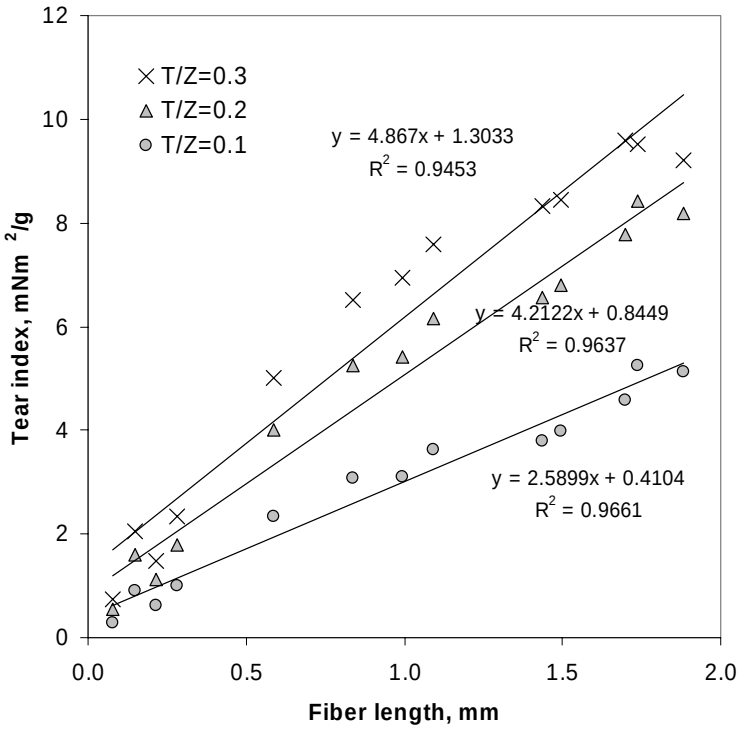

Figure 110. Fiber length dependency in the low bond strength region

The results in Figure 110 are consistent with the Shallhorn-Karnis model, which predicts that in the low bonding domain the tear strength is directly proportional to fiber length and Tensile strength. This is shown in Figure 111, where the tear index was plotted against the product of Tensile strength and fiber length for all sheets that were below their tear maximum (Table 22 in the addendum). The linear fit in Figure 111 was forced

through the origin. Considering the significant variation in the structures of the sheets the R^2 of the linear fit was high (0.75).

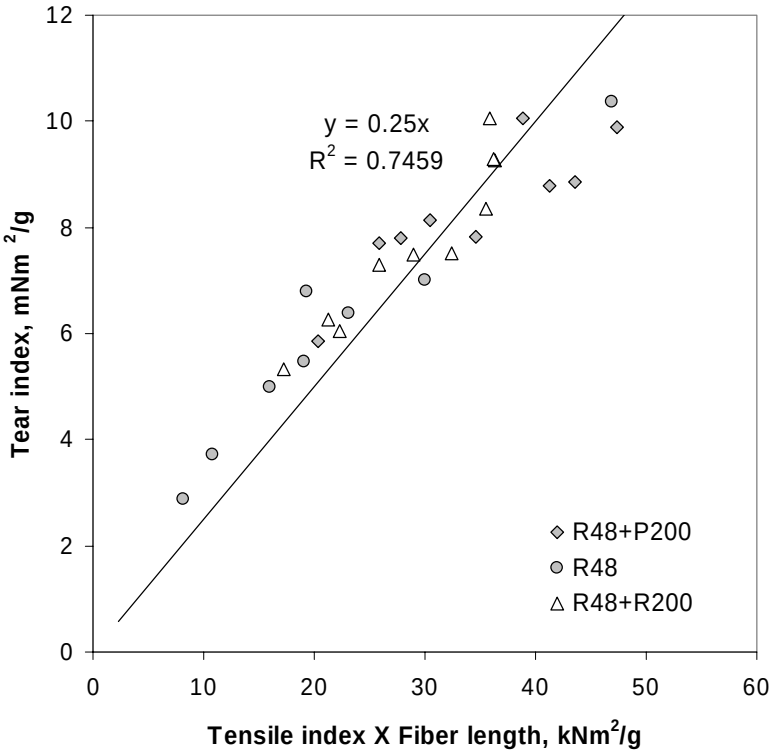

Figure 111. Tear index as a function of the product of tensile index and fiber length

In addition, the plot in Figure 110 produced the same relationship as Figure 111 when it was plotted the same way against the product of tensile strength fiber length. All the different bonding levels collapsed on to a common line with a similar slope of 0.23 (R^2 of 0.84). This implies that the quadratic fits used in the analysis describe the tear strength behavior in the low bonding regime fairly accurately.

Conclusions

Traditionally it has been assumed that mechanical pulps operate in a negligible fiber failure domain, where bond failure dominates the fracture in tear and tensile testing. In this paper it was shown, using tear and tensile strength data, that most mechanical pulps are in a domain where fiber failure can be considered a significant factor. Only sheets with very high long fiber (R48) content provide any data in the negligible fiber failure

domain. The region where the domain alters from negligible fiber failure to significant fiber failure was in the range of 0.3-0.45 T/Z (tensile strength/zero span tensile strength), and corresponded to a tensile strength range of approximately 30-40 Nm/g. The transition depends on the sheet composition, lowest for pure fiber (R48) sheets, and higher as fines or middle fractions are added. It was also shown that tear strength in the low bonding domain is a linear function of the sheet composition.

Addendum to Chapter 6

In the high bonding regime the tear index could not be explained with the commonly believed mechanisms. In chemical pulps it has been shown that the tear strength dependency on fiber length decreases and fiber strength increases as bonding is increased [191, 192]. The Shallhorn-Karnis equation also predicts this behavior, and relates tear strength to fiber strength, tensile strength and fiber length, according to the following relationship:

$$W = LT_o\left(1-\frac{T}{T_o}\right)^2 \qquad \textbf{Equation 29}$$

Where

W = Tear strength

L = Fiber length

T_o= Fiber strength

T = Tensile strength

In this study the tear strength in the high bonding regime did not correlate well with fiber length or fiber strength, nor did tear strength follow the Shallhorn-Karnis equation. As the bonding was increased beyond the tear maximum the fiber length-tear index correlation became non-existent. This was mainly due to the significant decrease in tear strength at high fiber lengths, as shown in Figure 112, where the tear index was plotted as a function fiber length for various bonding levels (T/Z) above the tear maximum.

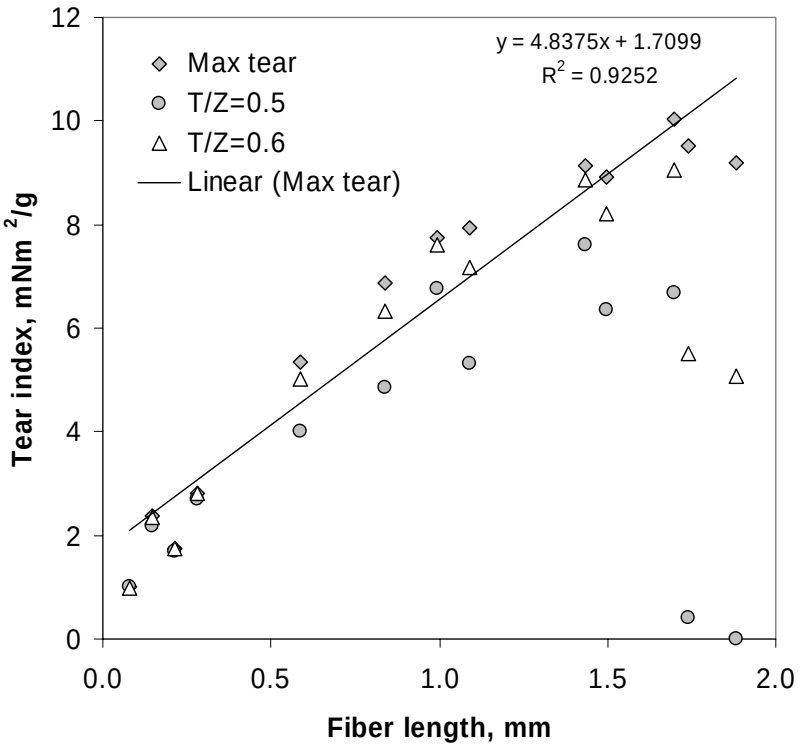

Figure 112. Tear index as a function of fiber length (weight-weighted) at maximum tear index and high bonding domain

The plot in Figure 112 is based on the quadratic equations in Table 20. However, the observed significant drop in tear index at long fiber lengths in the high bonding domain was not an artifact of the quadratic fits. The real measured data also showed this behavior as shown in Figure 106, where the 100% R48 fiber sheets showed significantly lower tear strengths at constant tensile strength in the high bonding domain in comparison with the sheets where fines were added into the fiber fraction. This behavior was also apparent when the right hand side of the equation 28 was plotted against the tear index using real measured data, assuming that T_o can be estimated using the zero span tensile strength. Each pulp produced unique relationships with the right side of the equation and the tear index, at the high bonding domain. This plot is shown in Figure 113, where the tear index was plotted as function of the fiber length, tensile strength and zero span tensile strength for pure fiber and fines and their mixture pulps. In Figure 113 only fiber (R48) and fines (P200) pure and mixed sheets that were pressed beyond the tear maximum were included.

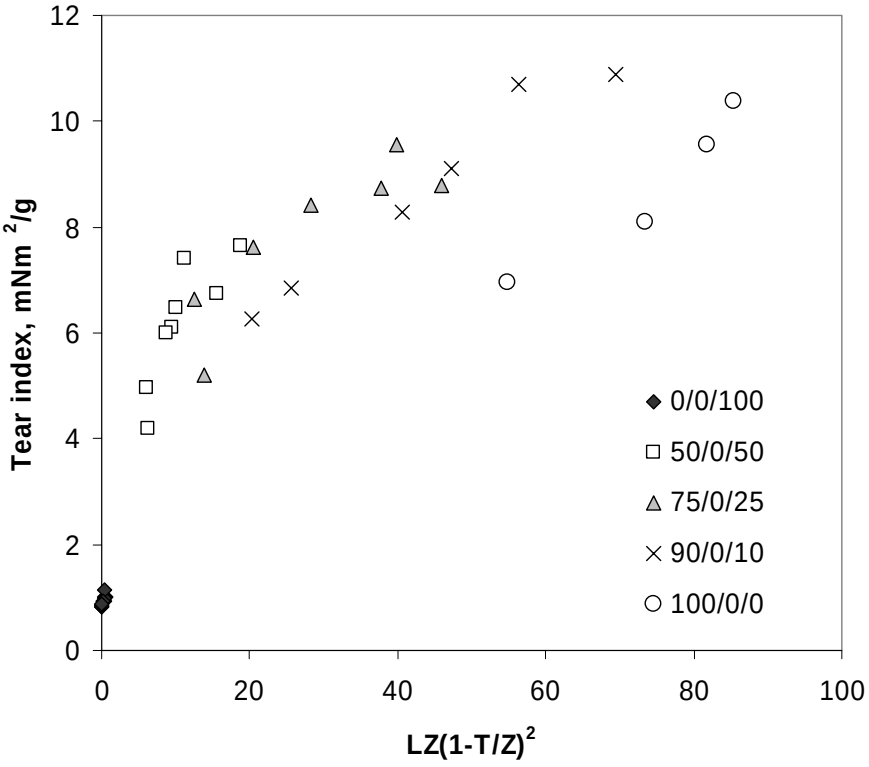

Figure 113. Tear index as a function of fiber length, tensile strength and zero span tensile strength, according to equation 2.

The tear index dependency on fiber length in the low bonding domain and the unexplained decrease in tear index at high fiber length in the high bonding domain could be better shown as a function of the sheet composition. These ternary plots are plotted in Figures 114 and 115, and they show that in the low bonding domain (measured either as tensile strength or T/Z) the tear index is a linear function of the sheet composition, whereas in the high bonding domain (beyond the tear maximum) sheets with high long fiber (R48) content show significant deviation from the linear addition rule. This is not in agreement with the earlier observations using chemical pulps or with the Shallhorn-Karnis model.

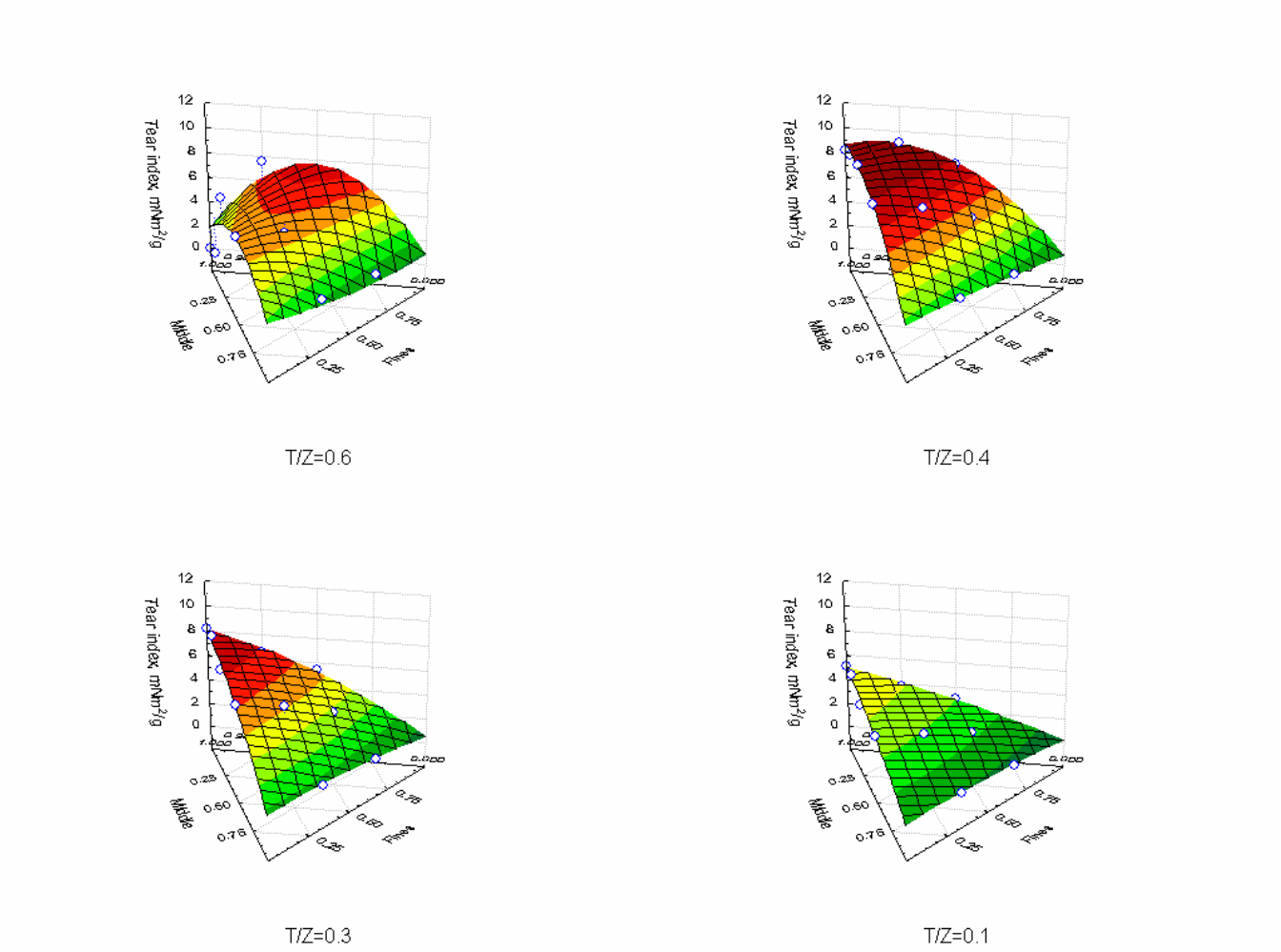

Figure 114. Tear index at various levels of bonding as a function of sheets compositions R48, R200 and P200 fractions) Qubic fits. Data based on the quadratic equations in Table 20.

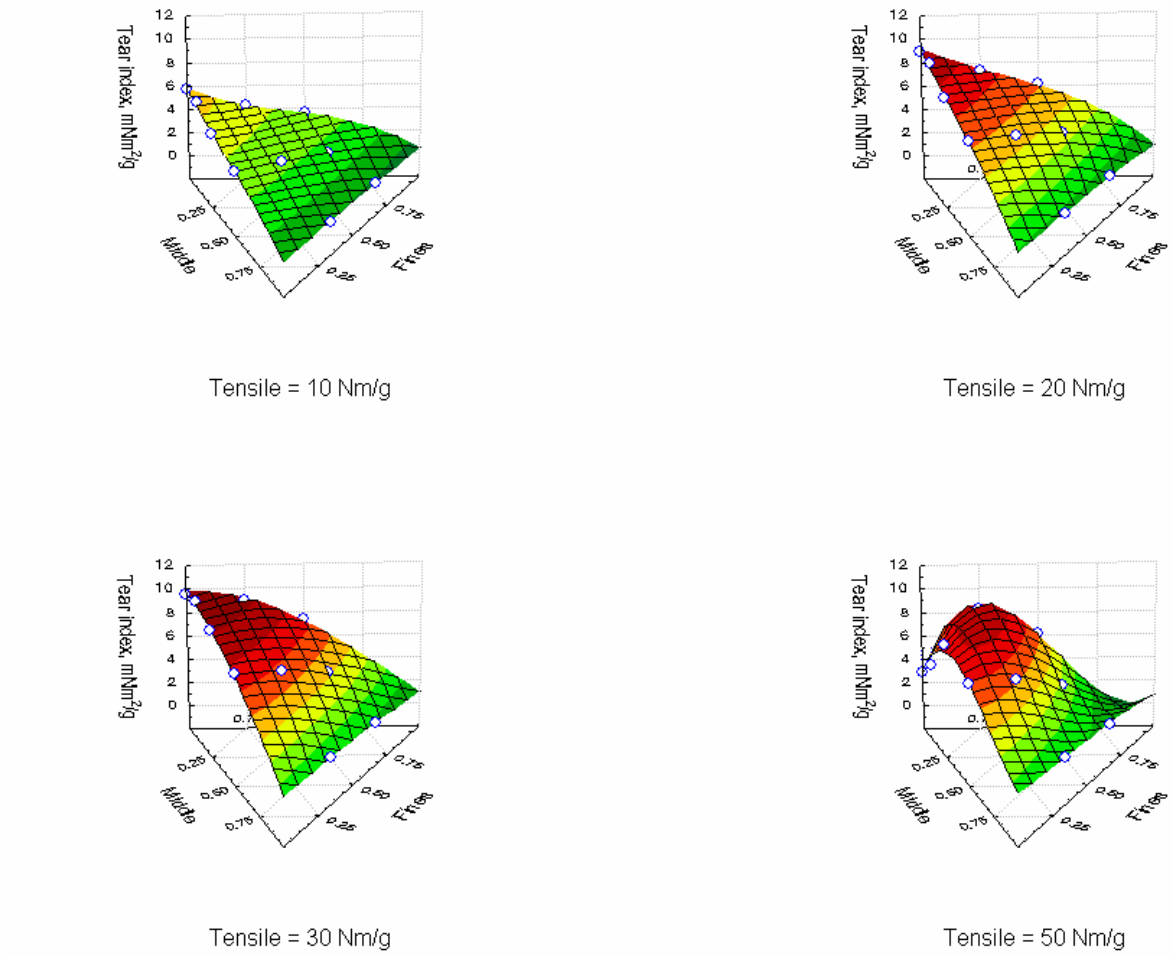

Figure 115. Tear index at various tensile strengths as a function of sheet composition, ternary graph, qubic fits. Data based on the quadratic equations in Table 21.

Table 22. Sheets below their tear index maximum

Pressing		Sheet composition			Density	Tensile index,	Tear index
load, psi	temp, °C	Fiber	Middle	Fines	kg/m^3	Nm/g	mNm^2/g
0.00	23.00	0.50	0.00	0.50	238.07	26.06	7.70
65.19	23.00	0.50	0.00	0.50	431.61	34.80	7.82
0.00	23.00	0.74	0.00	0.26	169.72	19.36	7.80
65.19	23.00	0.74	0.00	0.26	357.96	30.37	8.85
488.94	23.00	0.74	0.00	0.26	444.65	33.00	9.89
0.00	120.00	0.74	0.00	0.26	238.90	28.77	8.79
0.00	23.00	0.89	0.00	0.11	144.45	11.95	5.84
65.19	23.00	0.89	0.00	0.11	301.59	22.87	10.06
488.94	23.00	0.89	0.00	0.11	365.85	26.82	9.13
0.00	120.00	0.89	0.00	0.11	161.58	17.90	8.13
0.00	23.00	0.99	0.00	0.01	119.08	4.32	2.87
65.19	23.00	0.99	0.00	0.01	235.21	10.10	5.47
488.94	23.00	0.99	0.00	0.01	233.77	8.48	5.00
977.88	23.00	0.99	0.00	0.01	283.26	10.23	6.79
0.00	120.00	0.99	0.00	0.01	125.95	5.74	3.71
0.80	120.00	0.99	0.00	0.01	246.90	12.27	6.38
3.26	120.00	0.99	0.00	0.01	358.23	15.91	7.01
8.15	120.00	0.99	0.00	0.01	464.99	24.91	10.37
0.00	23.00	0.50	0.50	0.00	196.27	23.65	7.30
0.00	23.00	0.75	0.25	0.00	151.76	14.92	6.06
65.19	23.00	0.75	0.25	0.00	278.94	23.78	8.36
0.00	120.00	0.75	0.25	0.00	200.27	21.68	7.52
0.00	23.00	0.90	0.10	0.00	139.31	9.91	5.32
65.19	23.00	0.90	0.10	0.00	264.67	16.65	7.49
488.94	23.00	0.90	0.10	0.00	340.19	20.92	9.26
977.88	23.00	0.90	0.10	0.00	412.68	20.66	10.06
0.00	120.00	0.90	0.10	0.00	153.42	12.23	6.26
0.80	120.00	0.90	0.10	0.00	259.70	20.85	9.28

Thesis conclusions

The present investigation has dealt with the nature and significance of specific bonded area in mechanical pulps. A modified Ingmansson and Thode pressing method was selected as the most applicable means to measure bonded area in mechanical pulps. In order to overcome the rigid, non-collapsible, nature of mechanical pulp press drying was used to densify the sheets. However, due to the heterogeneous nature of the pulp several problems were identified that needed to be researched before the use of the modified Ingmansson and Thode method could be justified. These problems were approached using a multitude of methods.

Preliminary work established the reproducibility and optimum pressing technique for inducing bonding in mechanical pulps. It was shown that an efficient bonding increase of mechanical pulp can be achieved by press drying the sheets until they approach their 50% relative humidity moisture content. The use of higher temperatures decreases the time to dry the sheet, and thus the time to produce the bonded sheet. The use of elevated pressing pressures in press drying significantly induces bonding in all mechanical pulp fractions, and ultimately produces extended tensile strength to scattering coefficient relationships, similar to those in the Ingmansson and Thode method for chemical pulps.

The applicability of the Ingmansson and Thode method relies on the use of scattering coefficient as a measure of specific surface area. In this study it was shown that scattering coefficient is an accurate estimate of mechanical pulp specific surface area at a constant wavelength of light, provided that the wavelength used to measure scattering coefficient is above the significant absorption limit. In this study it was shown that 600 nm was adequate to overcome the significant absorption effect independent of sheet composition or pressing procedure. In addition it was shown that the scattering efficiency (scattering coefficient at constant specific surface area) was a function of the wavelength of light. This was explained with the wavelength dependency of refractive index of the material.

In the Ingmansson and Thode method the sheet is pressed to higher levels of bonding using progressively higher levels of pressures. In heterogeneous pulps, such as

mechanical pulps, it was not known if the various types of particles (fractions) experience the same forces during pressing, thus making the interpretation of scattering and tensile strength changes difficult. It was shown that the middle and fines fraction bond to a lesser degree in a mixed sheet than they do as a homogeneous pure sheet at a constant pressing level, indicating that the pressing force is predominantly transferred through the fiber fraction. However, the overall deviation from the linear addition model, where the mixture scattering coefficient is dictated by the individual components of the sheet was small (4.8%). If one then considers a totally unbonded sheet, where no interaction between different fractions occur, the total unbonded specific surface area (S_o) can be then reasonably be assumed to follow a similar linear addition rule as obtained for the pressed sheets. This was shown to be an accurate assumption using linear models to explain scattering coefficient as a function of tensile strength. The S_o followed the linear addition rule (R^2=0.9933) with a 4.11% systematic error between the estimated and measured S_o. Thus the relative bonded area (RBA) by definition was intrinsically non-linear as a function of the sheet composition. Thus, it is suggested that in heterogeneous structures specific bonded area rather than RBA should be used to explain the other bonding term.

It was shown that the consolidation mechanisms associated with the press drying at elevated temperatures and wet pressing were significantly different. It was shown that the higher scattering coefficient at a constant density associated with wet pressing was due to the shift in pore size distribution of the fines fraction, where the wet pressed fines had significantly smaller pores and thus higher specific surface area at a constant void volume. The higher scattering coefficient of wet pressed sheets at constant tensile strength was assigned to the better stress transfer between bonded elements in the wet pressed sheet. This was also explained with the shift in pore size distribution of fines. In order to wet press fines to the same bonded area as in press drying significantly higher fines density is required. Thus the distances between the bonded elements are smaller, which is likely to affect the stress transfer ability between them.

In order to be able to distinguish between bonded area and specific bond strength using the Ingmansson and Thode method it is necessary that the fundamental relationship between bonded area and tensile strength is established. Traditionally mechanical pulps have been assumed to operate in a domain where fiber failure can be considered

insignificant, and the bonded area to tensile strength relationship is linear. In this study it was shown indirectly, using tear resistance data at various bonding levels, that the domain transitions from the fiber failure negligible domain to significant fiber failure at 0.3-0.45 bonding index (tensile strength over zero span tensile strength), and 30-40 Nm/g tensile strength depending on the sheet composition. This indicates that most commercial pulps operate in a significant fiber failure domain. It was also shown that the bonded area – tensile strength relationship in the low bonding domain likely follows a linear form.

Acknowledgements

This thesis research was made possible by the financial support from the member companies of Institute of Paper Science and Technology, Walter Ahlström Foundation and Finnish Cultural Foundation.

Dr. Seppo Karrila lured me into taking up this challenge, and Dr. Barry Crouse significantly helped to make the decision easier. The initial idea for the thesis was borne out from the thinking of Dr. Alan Rudie.

Several people have contributed directly or in a supportive role to make this thesis better. The initial committee (Dr. Alan Rudie, Dr. Derek Page, Dr. Douglas Coffin, Dr. Timothy Patterson, Dr. Kari Ebeling, Lic. Tech. Esa Viljakainen and Dr. Gary Baum) is responsible for helping me to grasp the conceptual understanding of the problem. The committee members (Dr. Rudie, Dr. Page and Dr. Coffin) have contributed significantly in designing experiments to approach the problem. Dr. Alan Rudie has spent significant amount of his spare time reading manuscripts, correcting them and suggesting alternative interpretations of the data. Also several students (Thomas Dyer, Cameron Thomson, Andy DeMaio and Lorraine Vander Wielen) have helped to bring this thesis into a completion by listening to my ideas and arguing against them. This has significantly impacted my thinking about the topic. The technical support staff at IPST has made this thesis work easier, by helping to design and construct experimental tools, teaching experimental methods and conducting experiments for me.

Thank you.

List of References

1. Retulainen, E., K. Niskanen, and N. Nilsen, *Fibers and bonds.* Papermaking Science and Technology, 1998. **16**: p. 54-87.
2. Heikkurinen, A. and L. Leskela, *The character and properties of mechanical pulps.* Papermaking Science and Technology, 1999. **5**: p. 394-413.
3. Lindholm, C.A., *Comparison of some papermaking properties of groundwood, pressure groundwood, and thermomechanical pulp by means of artificial blends of pulp fractions. 2. The fines fractions.* Paperi ja Puu, 1980. **62**(12): p. 803-8.
4. Lindholm, C.A., *Comparison of some papermaking properties of groundwood, pressure groundwood, and thermomechanical pulp by means of artificial blends of pulp fractions. Part 1. Primary results.* Paperi ja Puu, 1980. **62**(10): p. 593-600, 603-6.
5. Lindholm, C.A., *Comparison of some papermaking properties of groundwood, pressure groundwood and thermomechanical pulp by means of artificial blends of pulp fractions. Part 3. The fiber fractions.* Paperi ja Puu, 1981. **63**(8): p. 487-92, 495-7.
6. Lindholm, C.A., *Determining optimum combinations of mechanical pulp fractions. Part 2. Optimization of the composition of SGW, PGW and TMP pulps.* Paperi ja Puu, 1983. **65**(6-7): p. 404-9.
7. Forgacs, O., *The Characterization of Mechanical Pulps.* Pulp & Paper Canada, 1963. **64**(C): p. T89-118.
8. Corson, S.R., *Wood characteristics influence pine TMP quality.* Tappi Journal, 1991. **74**(11): p. 135-46.
9. Corson, S.R., *Process impacts on mechanical pulp fiber and sheet dimensions.* TAPPI International Mechanical Pulping Conference, Proceedings, Houston, May 24-26, 1999, 1999: p. 139-154.
10. Heikkurinen, A., et al., *Effect of spruce wood and fiber properties on pulp quality under varying defibration conditions.* TAPPI International Mechanical Pulping Conference, Proceedings, Houston, May 24-26, 1999, 1999: p. 11-34.
11. Karnis, A., *The mechanism of fiber development in mechanical pulping.* JPPS, 1994. **20**(10): p. J280-8.
12. Kure, K.-A., G. Dahlqvist, and T. Helle, *Morphological characteristics of TMP fibres as affected by the rotational speed of the refiner.* Nordic Pulp & Paper Research Journal, 1999. **14**(2): p. 105-110.
13. Miles, K.B. and A. Karnis, *Wood characteristics and energy consumption in refiner pulps.* Journal of Pulp and Paper Science, 1995. **21**(11): p. J383-J389.
14. Morseburg, K. and B. Lonnberg, *The effect of wood fiber dimensions on energy consumption and pulp properties in pressurized grinding of Norway spruce.* Pulping Conference, Montreal, Oct. 25-29, 1998, 1998. **1**: p. 467-475.
15. Murton, K.D. and S.R. Corson, *Thinnings and toplogs differ for TMP manufacture.* Appita Journal, 1992. **45**(5): p. 327-31.
16. Rudie, A. and M. Sabourin, *Wood influence on thermomechanical pulp quality: fibre separation and fibre breakage.* Journal of Pulp and Paper Science, 2002. **28**(11): p. 359-363.
17. Strand, B.C., et al., *On-line prediction of mechanical pulp strength and optical properties.* Journal of Pulp and Paper Science, 1992. **18**(5): p. 176-81.
18. Hoekstra, P., P. Koivuniemi, and D. Temple. *Mechanical Pulps - Crossing Grade Barriers in the Nineties*. in *Int. Mech. Pulping Conf.* 1991. Minneapolis.

19. Wood, J.R. and A. Karnis, *Determination of specific surface area of mechanical pulp fines from turbidity measurements.* Paperi ja Puu, 1996. **78**(4): p. 181-186.
20. Retulainen, E., et al., *Papermaking quality of fines from different pulps -- the effect of size, shape and chemical composition.* Appita Journal, 2002. **55**(6): p. 457-460, 467.
21. Gullichsen, J. and H. Paulapuro, *Papermaking Science and Technology, Book 5: Mechanical Pulping*. 1999. 427 pp.
22. Yamauchi, T. and R.P. Kibblewhite, *Pore structural organization and behavior during the consolidation of thermomechanical pulp (TMP) paper webs.* Appita Journal, 1988. **41**(5): p. 383-8.
23. Gorres, J., et al., *Mechanical pulp fines and sheet structure.* Journal of Pulp and Paper Science, 1996. **22**(12): p. J491-J496.
24. Karnis, A. and P.M. Shallhorn. *Tear and Tensile Strength of Mechnical Pulps*. in *International Mechanical Pulping Conference*. 1979. Toronto: CPPA.
25. Gupta, P.R., A. Rezanowich, and D.A.I. Goring, *The adhesive properties of lignin.* Pulp & Paper Magazine of Canada, 1962. **63**: p. T21-T30.
26. Mohlin, U.B., *Fiber development during mechanical pulp refining.* Journal of Pulp and Paper Science, 1997. **23**(1): p. J28-J33.
27. Retulainen, E., *Strength properties of mechanical and chemical pulp blends.* Paperi ja Puu, 1992. **74**(5): p. 419-26.
28. Moss, P.A. and E. Retulainen, *The effect of fines on fiber bonding: cross-sectional dimensions of TMP fibers at potential bonding sites.* Journal of Pulp and Paper Science, 1997. **23**(8): p. J382-J388.
29. Morseburg, K. and B. Lonnberg, *The physiochemical properties of PGW (pressure groundwood) fibers as determined by the process intensity and wood fiber morphology.* TAPPI International Mechanical Pulping Conference, Proceedings, Houston, May 24-26, 1999, 1999: p. 35-46.
30. Luukko, K., *Characterization and properties of mechanical pulp fines.* Acta Polytechnica Scandinavica, Chemical Technology Series, 1999. **267**: p. 1-60.
31. Koran, Z., *Surface structure of thermomechanical pulp fibers studied by electron microscopy.* Wood and Fiber, 1970. **2**(3): p. 247-58.
32. Lammi, T. and A. Heikkurinen, *Changes in fiber wall structure during defibration.* Fundamentals of Papermaking Materials, Transactions of the Fundamental Research Symposium, 11th, Cambridge, UK, Sept. 1997, 1997. **1**: p. 641-662.
33. Mannstrom, B., *Characterization and quality control of mechanical pulp.* Paperi ja Puu, 1967. **49**(4a): p. 137-43, 145-6.
34. Mannstrom, B., *Characterization of refiner groundwood pulp.* Papier (Bingen, Germany), 1972. **26**(10A): p. 657-63.
35. Mannstrom, B., *Influence of groundwood quality on runnability and printability.* Tappi, 1972. **55**(4): p. 551-5.
36. Miles, K.B., W.D. May, and A. Karnis, *Refining intensity, energy consumption, and pulp quality in two-stage chip refining.* Tappi Journal, 1991. **74**(3): p. 221-30.
37. Andersson, M., *Aspects of z-strength in pulp characterization.* Svensk Papperstidning, 1981. **84**(6): p. R34-R42.
38. Andersson, M. and U.B. Mohlin, *Z-strength of mechanical pulps.* Paperi ja Puu, 1980. **62**(10): p. 583-6.
39. Murton, K.D., *Refining intensity impact on slabwood and thinnings TMP.* Appita Journal, 1998. **51**(6): p. 433-440.
40. Rudie, A.W. and M. Sabourin, *Wood Influence on Thermomechanical Pulp Quality: Fibre Spearation and Fibre Breakage.* JPPS, 2002. **28**(11): p. 359-363.
41. Yan, J.F., *Kinetic theory of mechanical pulping.* Tappi, 1975. **58**(7): p. 156-158.

42. Kano, T., T. Iwamida, and Y. Sumi, *Energy consumption in mechanical pulping.* Pulp & Paper Canada, 1982. **83**(6): p. T157-T161.
43. Koljonen, T. and A. Heikkurinen. *Delamination of Stiff Fibers*. in *International mechanical pulping conference*. 1995. Montreal.
44. Karnis, A., J. Mathieu, and M.I. Stationwala. *On the Interaction of Wood and Mechanical Pulping Equipment; Fiber Development and Generation of Fines*. in *International mechanical pulping conference*. 1995. Ottawa: CPPA.
45. Pohler, T. and A. Heikkurinen, *Amount and character of splits in fiber wall caused by disk refining.* International Mechanical Pulping Conference, Quebec City, QC, Canada, June 2-5, 2003, 2003: p. 417-423.
46. Pohler, T. and A. Heikkurinen. *Amount and character of splits in fiber wall caused by disk refining*. in *Internationa mechanical pulping conference*. 2003. Quebec: PAPTAC.
47. Seth, R.S., *The measurement and significance of fines. Their addition to pulp improves sheet consolidation.* Pulp & Paper Canada, 2003. **104**(2): p. 41-44.
48. Mohlin, U.B., *Properties of TMP fractions and their importance for the quality of printing papers. 2. The influence of particle properties and particle size distribution on pulp properties.* Svensk Papperstidning, 1980. **83**(18): p. 513-19.
49. Bichard, W. and P. Scudamore, *An evaluation of the comparative performance of the Kajaani FS-100 and FS-200 fiber length analyzers.* Tappi Journal, 1988. **42**(12): p. 149-155.
50. Chagaev, O., M.I. Stationwala, and R. Allem, *The role of fiber collapse in mechanical pulping.* TAPPI International Mechanical Pulping Conference, Proceedings, Houston, May 24-26, 1999, 1999: p. 155-169.
51. Yang, C.F., et al., *Measurements of geometrical parameters of fiber networks. Part 1. Bonded surfaces, aspect ratios, fiber moments of inertia, bonding state probabilities.* Svensk Papperstidning, 1978. **81**(13): p. 426-33.
52. Kibblewhite, R.P., *The fibers of radiata pine mechanical pulps.* Appita, 1983. **36**(4): p. 272-81.
53. Braaten, K.R., *The identification of fiber and fibril properties giving good pulp properties with low energy requirements.* TAPPI International Mechanical Pulping Conference, Proceedings, Houston, May 24-26, 1999, 1999: p. 417-426.
54. Tchepel, M., et al., *The response of the long fibre fraction to different refining intensities.* Pulp & Paper Canada, 2004. **105**(4): p. T87-T94.
55. Kleen, M., H. Kangas, and J. Kristola. *Surface and Bulk Chemical Properties of Groundwood Pulp Fibres and Fines*. in *Seventh European Workshop on Lignicellulosic and Pulp*. 2002.
56. Brecht, W. and K. Klemm, *The structural mixture in a groundwood pulp as the key to the knowledge of its technological properties.* Wochenblatt fuer Papierfabrikation, 1952. **80**: p. 364-70,451-4.
57. Sundberg, A., K. Sundberg, and B. Holmbom. *Chemical Characterization of Different Types of Fines in Mechanical Pulp*. in *11th International Symposium on Wood and Pulping Chemistry, Poster presentation*. 2001. Nice, France.
58. Wood, J.R. and A. Karnis. *The determination of the specific surface of mechanical pulp fines from turbidity measurements*. in *International Paper Physics Conference*. 1991: TAPPI.
59. Ingmanson, W.L. and E.F. Thode, *Factors contributing to the strength of a sheet of paper. II. Relative bonded area.* Tappi, 1959. **42**: p. 83-93.
60. Page, D.H., *Theory for the tensile strength of paper.* Tappi, 1969. **52**(4): p. 674-81.

61. Strand, B.C., M. Jackson, and A. Mokvist. *Improving the Reliability of Pulp Quality Data Through Factor Analysis and Data Reconciliation*. in *International mechanical pulping conference*. 1989. Helsinki.
62. Strand, B.C. *Analyzing the Effects of Raw Material Variation on Mechanical Pulp Properties Using Integrated Factor Networks*. in *CPPA 79th Annual Meeting, Technical Section*. 1993. Montreal.
63. Howard, R.C., R. Poole, and D.H. Page, *Factor Analysis Applied to the Results of a Laboratory Beating Investigation.* JPPS, 1994. **20**(5): p. J137-J141.
64. Karrila, S. and S. Rezak, *Review, developments and pulp & paper research applications of data reduction with neural networks.* TAPPI Technology Summit, Atlanta, GA, United States, Mar. 3-7, 2002, 2002: p. 171-186.
65. Garceau, J.J., et al., *Beyond 'L' and 'S'.* Pulp & Paper Canada, 1975. **76**(3): p. T67-T73.
66. Mohlin, U.B., *Distinguishing Character of TMP.* Pulp & Paper Canada, 1977. **78**(2): p. T291-T296.
67. Yan, N. and M.T. Kortschot, *Modelling of Out-of-Plane Tear Energy Absorption of Paper.* Appita, 1996. **49**(2): p. 176-180.
68. Kane, M.W., *Beating. Fibre Length Distribution and Tear.* Pulp & Paper Canada, 1960. **61**(3): p. T236-240.
69. Retulainen, E., *Fiber properties as control variables in papermaking? Part 1. Fiber properties of key importance in the network.* Paperi ja Puu, 1996. **78**(4): p. 187-194.
70. Karenlampi, P., E. Retulainen, and H. Kolehmainen, *Properties of Kraft Pulps from Different Forest Stands - Theory and Experiment.* Nordic Pulp & Paper Research Journal, 1994. **9**(4): p. 214-218,231.
71. Van den Akker, J.A., et al., *Importance of fiber strength to sheet strength.* Tappi, 1958. **41**: p. 416-25.
72. Helle, T., *Fiber strength and fiber bonding in sulfate and sulfite paper.* Svensk Papperstidning, 1963. **66**(24): p. 1015-30.
73. Page, D.H., P.A. Tydeman, and M. Hunt. *The Behaviour of Fibre-to-Fibre Bonds in Sheet under Dynamic Conditions*. in *The Formation and Structure of Paper*. 1961. Oxford: Tech. Sect. Brit. Pap Board Maker's Assoc.
74. Kallmes, O.J. and M. Perez, *New theory for the load-elongation properties of paper.* Consol. Pap. Web, Trans. Symp., 1966. **2**: p. 779-800, discussion 801-13.
75. Mohlin, U.B. *Properties of TMP Fractions and Their Importance for the Quality of Printing Papers*. in *TAPPI/CPPA Intern. Mech. Pulping Conf.* 1979. Toronto: TAPPI.
76. Lindholm, C.A., *Comparison of some papermaking properties of groundwood, pressure groundwood, and thermomechanical pulp by means of artificial blends of pulp fractions. Part 4. Results of the Series of Investigations.* Paperi ja Puu, 1981. **63**(9): p. 551-554, 557-558.
77. Mohlin, U.B. *Fiber-Bonding Ability - Key Pulp Quality Parameter for Mechnical Pulps to Be Used in Printing Papers*. in *International Mechanical Pulping Conference*. 1989. Helsinki.
78. Buchanan, J.G. and O.V. Washburn, *The Surface and Tensile Fractures of Groundwood Handsheets as Observed with the Scanning Electron Microscope.* Pulp & Paper Mag. Can., 1964: p. T52-T60.
79. Page, D.H. and F. El-Hosseiny. *Strength of Wood Pulp Fibers*. in *Can. Wood Chem. Symp.* 1976. Mont Gabriel, Que.
80. Page, D.H., et al., *Mechanical Properties of Single Wood-Pulp Fibers. (1). A New Approach.* Pulp & Paper Mag. Can., 1972. **73**(8): p. 72-77.

81. Page, D.H., R.S. Seth, and F. El-Hosseiny. *Strength and Chemical Composition of Wood Pulp Fibers*. in *Papermaking Raw Materials*. 1985: Punton, ed.
82. McIntosh, D.C., *Tensile and bonding strengths of loblolly pine kraft fibers cooked to different yields.* Tappi, 1963. **46**: p. 273-7.
83. McIntosh, D.C., *Tensile strength and bond strength of individual fibers.* Tappi, 1962. **45**(No. 2): p. 156A-157A.
84. Leopold, B. and D.C. McIntosh, *Chemical composition and physical properties of wood fibers. III. Tensile strength of individual fibers from alkali-extracted loblolly pine holocellulose.* Tappi, 1961. **44**: p. 235-40.
85. McDonough, T.J., S. Aziz, and K.L. Rankin, *The Strength of Mechanical Pulp Fibers*, in *IPC Technical Paper Series*. 1987, Insitute of Paper Chemistry: Appleton, Wisconsin. p. 7.
86. Hoffman-Jacobsen, P.M., *New method of determining the strength of chemical pulp.* Paper Trade Journal, 1925. **53**(1): p. 216-217.
87. Clark, J.d.A., *The ultimate strength of pulp fibers and the zero-span tensile test.* Paper Trade Journal, 1944. **118**(1): p. 29-34.
88. Clark, J.d.A., *Effect of fiber coarseness and length II, Improved means of measuring intrinsic strength and cohesiveness (Zero-Span).* Tappi Journal, 1958. **48**(3): p. 180-184.
89. Boucai, E., *Zero-span tensile test and fiber strength.* Pulp & Paper Mag. Can., 1971. **72**(10): p. 73-80.
90. Kellogg, R.M. and F.F. Wangaard, *Influence of fiber strength on sheet properties of hardwood pulps.* Tappi, 1964. **47**(6): p. 361-367.
91. Mohlin, U.B., U. Molin, and M. Waubert de Puiseau. *Some aspects of using zero-span tensile index as a measure of fiber strength*. in *International paper physics conference*. 2003. Victoria, BC: PAPTAC.
92. Wink, W.A. and R.H. Van Esperen, *The Development of An Improved Zero-Span Tensile Test.* Tappi, 1962. **45**(1): p. 10-24.
93. Batchelor, W.J., et al. *Effect of test conditions on measured loads and displacements in zero and short span testing*. in *International paper physics conference*. 2003. Victoria, BC: PAPTAC.
94. Seth, R.S. and B.K. Chan, *Measuring fiber strength of papermaking pulps.* Tappi Journal, 1999. **82**(11): p. 115-120.
95. Mark, R., et al., *Handbook of Physical Testing of Paper*. 2002, Marcus Dekker Inc.: New York, NY. p. 812-817.
96. Karnis, A., *The role of latent and delatent mechanical pulp fines in sheet structure and pulp properties.* Paperi ja Puu, 1995. **77**(8): p. 491-7.
97. Levlin, J.-E., *Aim of pulp and paper testing.* Papermaking Science and Technology, 1999. **17**: p. 11-17.
98. Campbell, W.B., *The Mechanism of Bonding.* Tappi, 1959. **42**(12): p. 999-1001.
99. Page, D.H. and P.A. Tydeman. *A New Theory of the Shrinkage, Structure and Properties of Paper*. in *The Formation and Structure of Paper*. 1966. Oxford.
100. Mohlin, U.B., *Cellulose fiber bonding. Determination of interfiber bond strength.* Svensk Papperstidning, 1974. **77**(4): p. 131-7.
101. Mohlin, U.B., *Cellulose fiber bonding. 3. Effect of beating and drying on interfiber bonding.* Svensk Papperstidning, 1975. **78**(9): p. 338-41.
102. Skowronski, J., *Fiber-to-Fiber Bonds in Paper. (2). Measurement of the Breaking Energy of Fiber-to-Fiber Bonds.* JPPS, 1991. **17**(no. 6): p. J217-222.
103. Retulainen, E. and K. Ebeling, *Fiber-fiber bonding and ways of characterizing bond strength.* Appita Journal, 1993. **46**(4): p. 282-8.

104. Gurnagul, N., S. Ju, and D.H. Page, *Fibre-fibre bond strength of once-dried pulps.* Journal of Pulp and Paper Science, 2001. **27**(3): p. 88-91.
105. Goerres, J., et al., *The shear bond strength of mechanical pulp fibers.* Journal of Pulp and Paper Science, 1995. **21**(5): p. J161-J164.
106. Eusufzai, A.R.K., *Sheet structure in relation to internal network geometry and fiber orientation distribution*, in *College of Environmental Science and Forestry*. 1982, SUNY: Syracuse, NY.
107. Parsons, S.R., *Optical characteristics of paper as a function of fiber classification.* Paper Trade Journal, 1942. **115**(No. 25): p. 34-42.
108. Ratliff, F.T., *The Possible Correlation Between Hemicelluloses and the Physical Properties of Bleached Kraft Pulps.* Tappi. **1949**(32): p. 357-367.
109. Keeney, F.C., *Physical Properties of Slash Pine Semichemical Kraft and of Its Fully Chlorite Component.* Tappi. **1952**(35): p. 555-563.
110. Leech, H.J., *An Investigation of the Reasons for Increase in Paper Strength when Locust Bean Gum Is Used as a Beater Adhesive.* Tappi. **1954**(37): p. 343-349.
111. Haselton, W.R., *Gas adsorption by wood, pulp, and paper. II. The application of gas-adsorption techniques to the study of the area and structure of pulps and the unbonded and bonded area of paper.* Tappi, 1955. **38**: p. 716-23.
112. Rennel, J., *Opacity in Relation to Strength Properties of Pulps.* Svensk Papperstidning, 1969. **72**(1): p. 1-8.
113. Swanson, J.W., Steber, A.J., *Fiber Surface Area and Bonded Area.* Tappi Journal, 1959. **42**(12): p. 986-994.
114. Luner, P., A.E.U. Karna, and C.P. Donofrio, *Interfiber bonding of paper. The use of optically bonded areas with high yield pulps.* Tappi, 1961. **44**: p. 409-14.
115. Rennel, J., *Opacity in Relation to Strength Properties of Pulp; Part 4 - The Effect of Beating and Wet Pressing.* Pulp and Paper Mag. Can., 1969. **70**(10): p. T151-T158.
116. Hartler, N., Rennel, J., *Opacity in Relation to Strength Properties of Pulps II. Light Scattering Coefficient and Surface Area of Unbonded Pulp Fibers.* Svensk Papperstidning, 1969. **72**(1): p. 9-13.
117. Van den Akker, J.A., *Structural aspects of bonding.* Tappi, 1959. **42**: p. 940-7.
118. Stratton, R.A., *Characterization of fiber-fiber bond strength from out-of-plane paper mechanical properties.* Journal of Pulp and Paper Science, 1993. **19**(1): p. 6-12.
119. Davis, M.N., *Use of Color Measuring Instruments in the Manufacture of Uncoated Paper.* Paper Trade Journal, 1940. **111**(14): p. 40-44.
120. Clark, J.d.A., *A New Method for Measuring Specific Surface.* Paper Trade Journal, 1942. **115**(1): p. 32-39.
121. Haselton, W.R., *Gas adsorption by wood, pulp, and paper. I. The low-temperature adsorption of nitrogen, butane, and carbon dioxide by sprucewood and its components.* Tappi, 1954. **37**: p. 404-12.
122. Rennel, J., *Opacity in Relation to Strength Properties of Pulps III, Light Scattering of Sheets of Model Fibers.* Tappi Journal, 1969. **52**(10): p. 1943-1947.
123. Page, D.H. 2002: Atlanta, GA.
124. Scallan, A.M., Borsch J., *An Interpretation of Paper Reflectance Based Upon Morphology, I. Initial Considerations.* Tappi Journal, 1972. **55**(4): p. 583-588.
125. Arnold, E.A., *Light Scattering in Fibrous Sheets.* Tappi Journal, 1963. **46**(4): p. 250-256.
126. Alince, B., Pobuska J., Van Den Ven, T.G.M., *Light Scattering and Microporosity in Paper.* JPPS, 2002. **28**(3): p. 93-98.

127. Alince, B., Lepoutre, P. *Plastic pigments in paper coatings: The effect of polystyrene particle size on porosity and optical properties*. in *1980 TAPPI Coating Conference*. 1980. Atlanta: TAPPI Press.
128. Fineman, I., Bergenblad, H., Pauler, N., *Beeinflussung der Porenstruktur von Papier durch Fullstoffe.* Das Papier, 1990. **44**(10A): p. V56-V62.
129. Rundlof, M., Hoglund, H., Htun, M., Wagberg, L. *Effect of Fines Quality on Paper Properties*. in *Intl. Mech. Pulping Conf.* 1995. Ottawa.
130. Hill, C.A.S., Papadopoulos, A.N., *A Review of methods used to determine the size of the cell wall microvoids of wood,.* Journal of the Inst. Of Wood Sci., 2001. **15**(6 (Issue 90)): p. 337-344.
131. Foote, W.J., *An Investigation of the Fundamental Scattering and Absorption Coefficients in Dyed Handsheets.* Tech. Assoc. Papers (TAPPI), 1939. **22**(1): p. 397.
132. Koukoulas, A.A., Jordan, B.D., *Effect of Strong Absorption on the Kubelka-Munk Scattering Coefficient.* JPPS, 1997. **23**(5): p. J224-J232.
133. Nordman, L., Aaltonen, P., Makkonen, T. *Relationship between Mechanical and Optical Properties of Paper Affected by Web Consolidation*. in *Symposium on Consolidation of the Paper Web*. 1966: Tech. Section Brit. Paper and Board Makers' Assoc.
134. Granberg, H., Edstrom, P., *Quantification of the Intrinsic Error of the Kubelka-Munk Model Caused by Strong Light Absorption.* JPPS, 2003. **29**(11): p. J386-J390.
135. Page, D., Appita, 1981. **35**(2): p. 173.
136. Lehtonen, L.K., et al., *On the meaning of relative bonded area in mechanical pulps.* Preprints - International Paper Physics Conference, Victoria, BC, Canada, Sept. 7-11, 2003, 2003: p. 343-346.
137. Ceragioli, G., G. Capretti, and G. Bianco, *Paper drying under Z-direction restraint to improve the strength properties of medium- and low-quality pulps and furnishes.* Industria della Carta, 1987. **25**(2): p. 69-87.
138. Byrd, V.L., *Press-drying saves energy and enhances properties.* Paper Technology (Bury, United Kingdom), 1989. **30**(5): p. V24-V28.
139. Horn, R.A., *Bonding in press-dried sheets from high-yield pulps. The role of lignin and hemicellulose.* Tappi, 1979. **62**(7): p. 77-80.
140. Pynnonen, T., et al., *Good bonding for low-energy HT-CTMP by press drying.* Preprints of Papers, Annual Meeting - Pulp and Paper Technical Association of Canada, 89th, Montreal, QC, Canada, Jan. 27-30, 2003, 2003: p. 469-475.
141. Pynnonen, T., et al., *Effect of press drying on sheet properties of high-temperature thermomechanical pulp (HTMP).* Appita Journal, 2002. **55**(3): p. 220-223.
142. Back, E.L., *Press drying compared to other means of densifying paper.* Tappi Journal, 1985. **68**(3): p. 92-6.
143. Back, E.L. and K.G. Norberg, *Influence of temperature on dewatering and compressibility of mechanical pulp during pressing in a plane press. I. Plane press studies.* Svensk Papperstidning, 1966. **69**(23): p. 824-30.
144. Seth, R.S., A.J. Michell, and D.H. Page, *The effect of press-drying on paper strength.* Tappi, 1985. **68**(10): p. 102-107.
145. Byrd, V.L., *Flow and adhesion of hemicellulose and lignin during press drying.* Annual Meeting Proceedings - Technical Association of the Pulp and Paper Industry, 1979: p. 15-21.

146. Koubaa, A., B. Riedl, and Z. Koran, *Surface analysis of press dried-CTMP paper samples by electron spectroscopy for chemical analysis.* Journal of Applied Polymer Science, 1996. **61**(3): p. 545-552.
147. Sernek, M., F.A. Kamke, and W.G. Glasser, *Comparative analysis of inactivated wood surface.* Holzforschung, 2004. **58**(1): p. 22-31.
148. Nordman, L. and J.E. Levlin, *Effect of drying on the optical properties of mechanical pulp.* Papier (Bingen, Germany), 1975. **29**(7): p. 274-80.
149. Goring, D.A.I., *Thermal softening of lignin, hemicellulose, and cellulose.* Pulp & Paper Magazine of Canada, 1963. **64**(12): p. T517-T527.
150. Garbassi, F., M. Morra, and E. Occhiello, *Polymer Surfaces*. From Physics to Technology, ed. J.W.S. Ltd. 1998. 486.
151. McKenzie, A.W., *The structure and properties of paper Part XXI: The diffusion thoery of adhesion applied to interfibre bonding.* Appita, 1983. **37**(7): p. 580-583.
152. Voyutskii, S.S., *Polymer Reviews. Vol. 4. Autohesion and Adhesion of High Polymers*. 1963. 272 pp.
153. Voyutskii, S.S., *Diffusion mechanism in the self-adhesion properties of high polymers.* Rev. Gen. Caoutchouc Plastiques, 1964. **41**(6): p. 989-92.
154. Michell, A.J., R.S. Seth, and D.H. Page, *The effect of press-drying on paper structure.* Paperi ja Puu, 1983(9): p. 536-541.
155. Mackie, D.M. *Effect of Paper Machine Drying Conditions on the Optical Properties of Paper Containing Mechanical Pulp*. in *PAPTAC 86th Annual Meeting*. 1989.
156. Poirier, N.A., et al., *The effect of superheated steam drying on the properties of TMP paper.* Journal of Pulp and Paper Science, 1994. **20**(4): p. 97-102.
157. Mann, R.W., G.A. Baum, and C. Habeger, *Determination of all nine orthotropic elastic constants of machine-made paper.* Tappi Journal, 1980. **63**(2): p. 163-166.
158. Habeger, C. and W.A. Wink, *Ultrasonic velocity measurements in the thickness direction of paper.* Journal of Applied Polymer Science, 1986. **32**: p. 4503-4540.
159. de Silveira, G., et al., *Location of fines in mechanical pulp handsheets using scanning electron microscopy.* Journal of Pulp and Paper Science, 1996. **22**(9): p. J315-J320.
160. Mohlin, U.B. *Fibre development during mechanical pulp refining*. in *International mechanical pulping conference*. 1995. Ottawa.
161. Braaten, K.R., *Fiber and fibril properties versus light scattering and surface smoothness for mechanical pulps.* Pulp & Paper Canada, 2000. **101**(5): p. 27-31.
162. Corson, S.R., et al., *Manipulation of paper structure and printability by control of the fibrous elements.* International Mechanical Pulping Conference, Quebec City, QC, Canada, June 2-5, 2003, 2003: p. 33-42.
163. Sinkey, J.D. *Development of High-Yield Pulp Properties*. in *CPPA Ann. Mtg.* 1984. Montreal.
164. Borch, J., Scallan, A.M., *An Interpretation of Paper Reflectance Based Upon MorphologyL II. The Effect of Mass Distribution.* Tappi Journal, 1976. **59**(10): p. 102.
165. Thorpe, J.L., et al., *Mechanical properties of fiber bonds.* Tappi, 1976. **59**(5): p. 96-100.
166. Kubelka, P., *New Contributions to the Optical Properties of Intensely Light Scattering Materials. Part I.* J. Opt. Soc. Am., 1948. **44**(4): p. 488.
167. Leskela, M., *Optical properties*, in *Paper Physics*, N. K., Editor. 1998, Fapet Oy: Jyvaskyla. p. 117-137.

168. Ingmanson, W.L., Thode, E.F., *Factors Contributing to the Strength of a Sheet of Paper.* Tappi Journal, 1959. **42**(1): p. 83.
169. Borch, J., *Optical and Appearance Properties*, in *Handbook of Physical Testing of Paper*, L. Borch, Mark and Habeger, Editor. 2001. p. 127-138.
170. Haselton, W.R., *Gas Adsorption by Wood, Pulp and Paper II. The Application of Gas Adsorption Techniques to the Study of the Area and Structure of pulps and the Unbonded and Bonded Area od Paper.* Tappi Journal, 1955. **38**(12): p. 712-723.
171. Davis, M.N., Paper Trade Journal, 1940. **111**(14): p. 40-44.
172. Giertz, H.W., *Opaciteten hos pappersmassor.* Svensk Papperstidning, 1951. **54**(8): p. 267-274.
173. Parsons, S.R., *Optical characteristics of paper as a function of fiber classification.* Tech. Assoc. Pap., 1942. **1942**(25): p. 360-368.
174. Clark, J.d.A., Paper Trade Journal, 1942. **115**(1): p. 32-39.
175. Rundlof, M., Bristow, J.A., *A Note Concerning the Interaction Between Light Scattering and Light Absorption in the Application of Kubelka-Munk Equations.* JPPS, 1997. **23**(5): p. J200-J223.
176. Lepoutre, P., Pauler, N., Alince, B., Rigdahl, M., *The Light-Scattering Efficiency of Microvoids in Paper Coatings and Filled Papers.* JPPS, 1989. **15**(5): p. J183-J185.
177. Lynch, D.K., Livingston, W., *Color and Light in Nature*. 2nd ed. 2001: Cambridge University Press.
178. Jordan, B., *The properties of bleached pulp. Brightness: Basic principles and measurement.* Pulp Bleaching, 1996: p. 695-716.
179. Jayaraman, K. and M.T. Kortschot, *Closed-form network models for the tensile strength of paper - a critical discussion.* Nordic Pulp & Paper Research Journal, 1998. **13**(3): p. 233-242.
180. Nordman, L. and C. Gustafsson, *Relation between tensile strength and bonded fiber area of paper.* Paper and Timber (Finland), 1951. **33B**: p. 36-41.
181. Mohlin, U.B. and K. Wennberg, *Some aspects of the interaction between mechanical and chemical pulps.* Tappi, 1984. **67**(1): p. 90-93.
182. Fernandez, E.O. and R.A. Young, *An explanation for the deviation from linearity in properties of blend of mechanical and chemical pulps.* Tappi, 1994. **77**(3): p. 221-224.
183. Gates, D.J. and M. Westcott, *Formulae for the relative bonded area of paper made from blended pulps.* Appita Journal, 2002. **55**(6): p. 468-470.
184. Alexander, S.D. and R. Marton, *Effect of Beating and Wet Pressing on Fiber and Sheet Properties, II Sheet Properties.* Tappi, 1968. **51**(6): p. 283-288.
185. Gregersen, O. and R. Holmstad. *Fibre damage during mechanical pulping and calandering*. in *The 2004 Progress in Paper Physics Seminar*. 2004. Trondheim, Norway: Tappi Paper Physics Committee.
186. Rajan, K.G., R.E. Mark, and R.W. Perkins. *Press Drying of Thermo-Mechanical Pulps*. in *Press Drying Conference 1983*. 1983. Forest Products Laboratory, Madison, Wisconsin.
187. Van den Akker, J.A., *Instrumentation Studies XLVI -Tearing strength of paper.* Paper Trade Journal, 1944. **118**(5): p. 13.
188. Law, K.N., Z. Koran, and J.J. Garceau. *Shot-span tensile analysis of mechanical pulps*. in *CPPA Ann. Mtg.* 1979. Montreal.
189. MacLeod, J.M., *Kraft Pulps from Canadian Wood Species.* Pulp & Paper Canada, 1986. **87**(1): p. 76-81.

190. Kallmes, O., *The Influence of Nonrandom Fiber Orientation and Other Fiber and Web Parameters on the Tensile Strength of Nonwoves Fibrous Webs*, in *Theory and Design of Wood and Fiber Composite Materials*, B.A. Jayne, Editor. 1972, Suracuse university press: Syracuse.
191. Page, D.H. and J.M. MacLeod, *Fiber strength and its impact on tear strength.* Tappi Journal, 1992. **75**(1): p. 172-4.
192. Seth, R.S. and D.H. Page, *Fiber properties and tearing resistance.* Tappi Journal, 1988. **71**(2): p. 103-7.

Appendix 1: Norway spruce TMP (110 CSF) data

AVERAGES Whole pulp TMP (Norway spruce 110 CSF)

Mixture			Load	Temperature	FQA	BW	Density	Smoothside		Roughside		In-plane ultrasonic			Out-plane z- direction ultrasonic			Tensile	% strain	TEA	Spec Modulus	Zero Span	ZDT	Tear index
R48	R200	P200	psi	°C	FL, mm	g/m2	g/cc	LAC, m2/kg	LSC, m2/kg	LAC, m2/kg	LSC, m2/kg	Poisson	E (Gpa)	G(Gpa)	Caliper, um	v, m/sec	stiffness km^2/s^2	index, Nm/g	at max load	J/m2	kNm/g	Nm/g	kN/g	mNm2/g
0.56	0.12	0.32	0.00	23.00	1.127	67.28	222.77	1.91	61.53	1.86	61.40	0.30	0.91	0.35	290.24	1.09	0.07	26.12	1.57	16.62	2.61	86.05	2.49	8.70
0.56	0.12	0.32	65.19	23.00	1.127	68.98	395.69	1.87	61.53	1.90	61.99	0.33	2.09	0.79	174.75	0.61	0.08	34.34	1.43	21.09	3.53	89.62	4.01	8.39
0.56	0.12	0.32	488.94	23.00	1.127	67.49	510.83	1.88	56.81	1.84	56.24	0.30	3.05	1.17	135.24	0.45	0.09	40.45	1.85	34.46	3.94	85.92	5.70	7.51
0.56	0.12	0.32	977.88	23.00	1.127	69.53	590.73	1.93	54.19	1.96	55.74	0.28	3.56	1.41	123.23	0.38	0.10	43.10	1.77	33.94	4.22	93.86	5.26	6.89
0.56	0.12	0.32	0.00	120.00	1.127	64.46	293.72	2.21	54.62	2.11	55.24	0.31	1.69	0.65	215.05	0.71	0.09	33.89	1.39	18.34	3.33	90.10	3.22	8.72
0.56	0.12	0.32	0.80	120.00	1.127	65.86	370.61	2.15	43.49	2.09	43.83	0.32	2.37	0.90	182.71	0.55	0.11	42.73	1.50	27.15	4.22	92.90	4.59	7.71
0.56	0.12	0.32	8.15	120.00	1.127	66.05	633.54	2.15	43.13	2.10	44.31	0.29	4.67	1.81	115.14	0.25	0.22	51.94	1.73	39.05	5.16	95.04	8.09	6.42
0.56	0.12	0.32	16.30	120.00	1.127	68.87	742.30	2.06	40.36	2.06	41.31	0.31	5.96	2.28	105.03	0.20	0.27	55.10	1.52	35.34	5.60	97.71	11.34	5.66
0.56	0.12	0.32	48.89	120.00	1.127	67.95	913.19	1.96	31.57	2.03	34.61	0.30	8.14	3.12	84.64	0.14	0.38	61.28	1.50	41.16	6.24	101.09	14.58	4.75
0.56	0.12	0.32	162.98	120.00	1.127	66.78	1040.43	2.04	26.26	1.94	25.71	0.28	9.72	3.82	73.66	0.11	0.46	66.36	1.53	41.94	7.09	97.71	15.89	4.64
0.56	0.12	0.32	162.98	23.00	1.127	68.67	439.45	1.85	59.28	1.79	59.39	0.30	2.49	0.96	157.47	0.54	0.09	38.56	1.73	28.24	3.84	89.04	4.58	8.14
0.56	0.12	0.32	325.96	120.00	1.127	65.98	1112.34	1.88	20.75	1.91	21.49	0.27	10.61	4.18	69.86	0.10	0.48	65.60	1.40	36.80	7.08	101.00	15.43	4.27
0.56	0.12	0.32	65.19	23.00	1.127	68.92	631.88	2.27	53.94	2.29	55.04	0.29	3.92	1.52	116.33	0.29	0.16	43.48	1.88	36.70	4.24	90.77	9.33	6.98

AVERAGES R48 fiber and P200 fines mixed sheets (Norway spruce 110 CSF)

Mixture			Load	Temperature	FQA	BW	Density	Smoothside		Roughside		In-plane ultrasonic			Out-plane z- direction ultrasonic			Tensile	% strain	TEA	Spec Modulus	Zero Span	ZDT	Tear index
R48	R200	P200	psi	°C	FL, mm	g/m2	g/cc	LAC, m2/kg	LSC, m2/kg	LAC, m2/kg	LSC, m2/kg	Poisson	E (Gpa)	G(Gpa)	Caliper, um	v, m/sec	stiffness km^2/s^2	index, Nm/g	at max load	J/m2	kNm/g	Nm/g	kN/g	mNm2/g
0.00	0.00	1.00	0.00	23.00	0.080	70.14	314.44	2.77	109.18	2.63	107.05	0.24	1.09	0.44	227.41	0.59	0.15	28.33	1.80	21.99	2.41	48.27	8.43	1.00
0.00	0.00	1.00	65.19	23.00	0.080	70.33	483.09	2.77	101.32	2.64	101.88	0.26	2.17	0.86	153.82	0.38	0.17	33.06	1.66	24.34	3.08	48.65	11.29	0.92
0.00	0.00	1.00	488.94	23.00	0.080	70.78	620.98	2.79	88.50	2.64	91.46	0.26	3.17	1.26	119.81	0.30	0.16	36.69	1.60	26.50	3.58	52.61	12.43	1.01
0.00	0.00	1.00	977.88	23.00	0.080	71.33	659.38	2.79	85.09	2.62	85.47	0.26	3.56	1.41	114.12	0.28	0.17	37.82	1.49	25.54	3.83	52.86	13.19	1.00
0.00	0.00	1.00	0.00	120.00	0.080	71.59	438.07	2.95	94.08	2.78	94.00	0.24	2.08	0.84	174.72	0.40	0.19	35.92	1.51	24.13	3.34	51.69	12.41	1.15
0.00	0.00	1.00	0.80	120.00	0.080	73.32	500.31	3.12	78.48	2.94	76.75	0.26	2.85	1.13	154.27	0.38	0.16	40.51	1.22	21.17	4.31	51.58	7.58	0.93
0.00	0.00	1.00	8.15	120.00	0.080	75.13	684.15	2.98	68.06	2.93	71.17	0.27	4.23	1.67	129.55	0.28	0.22	46.48	1.36	28.29	4.55	53.29	13.01	0.83
0.00	0.00	1.00	16.30	120.00	0.080	74.16	744.06	3.13	60.81	3.13	66.23	0.27	4.83	1.91	112.82	0.20	0.31	47.47	1.34	21.90	4.88	54.93	12.38	0.82
0.00	0.00	1.00	48.89	120.00	0.080	75.07	971.28	2.92	48.21	2.99	53.40		5.82	2.08	92.18	0.15	0.39	51.09	1.53	37.70	5.11	56.95	11.47	0.85
0.00	0.00	1.00	162.98	120.00	0.080	70.12	1099.38	2.90	34.75	2.84	37.88		5.94	1.98	73.54	0.12	0.39	53.27	1.28	26.39	5.34	57.58	15.81	0.87
0.50	0.00	0.50	0.00	23.00	0.994	71.71	238.07	2.09	68.64	1.97	67.96	0.29	0.89	0.35	290.16	0.94	0.09	26.06	1.81	22.02	2.32	67.11	2.82	7.70
0.50	0.00	0.50	65.19	23.00	0.994	72.65	431.61	2.17	67.38	2.07	67.44	0.28	2.09	0.81	173.55	0.52	0.11	34.80	1.93	32.09	3.38	72.60	4.10	7.82
0.50	0.00	0.50	488.94	23.00	0.994	71.80	575.42	2.14	60.15	2.08	60.80	0.29	3.30	1.28	135.05	0.40	0.11	39.12	1.97	34.77	3.81	72.78	5.92	6.75
0.50	0.00	0.50	977.88	23.00	0.994	72.31	647.56	2.16	56.20	2.08	56.08	0.29	3.92	1.52	116.07	0.32	0.13	42.45	2.01	43.59	4.21	68.75	4.56	6.47
0.50	0.00	0.50	0.00	120.00	0.994	64.92	322.45	2.37	64.44	2.21	62.31	0.29	1.54	0.60	202.15	0.57	0.13	33.17	1.74	24.52	3.17	69.48	5.47	7.66
0.50	0.00	0.50	0.80	120.00	0.994	66.24	432.27	2.32	50.06	2.31	50.90	0.28	2.38	0.93	160.10	0.42	0.15	40.24	1.94	33.78	3.77	67.83	7.16	7.41
0.50	0.00	0.50	8.15	120.00	0.994	68.77	674.13	2.51	48.00	2.46	49.34	0.29	4.81	1.87	117.33	0.25	0.22	48.21	1.77	38.95	4.78	74.87	10.34	6.11
0.50	0.00	0.50	16.30	120.00	0.994	67.70	761.26	2.35	43.72	2.37	45.57	0.29	5.54	2.16	102.46	0.20	0.27	53.16	1.66	39.05	5.34	79.69	11.51	6.00
0.50	0.00	0.50	48.89	120.00	0.994	67.46	954.45	2.43	38.46	2.31	36.16	0.28	7.68	3.01	83.70	0.14	0.35	58.29	1.72	44.15	5.98	80.43	14.42	4.97
0.50	0.00	0.50	162.98	120.00	0.994	69.17	1153.91	2.31	25.82	2.17	25.04	0.28	9.77	3.82	73.22	0.12	0.38	55.87	1.67	42.67	5.87	77.89	15.31	4.21
0.74	0.00	0.26	0.00	23.00	1.435	72.86	169.72	1.65	48.30	1.65	45.16	0.30	0.57	0.22	407.48	1.77	0.05	19.36	1.47	14.17	2.01	70.80	1.20	7.80
0.74	0.00	0.26	65.19	23.00	1.435	73.78	357.96	1.71	51.49	1.71	50.62	0.30	1.66	0.64	208.55	0.80	0.07	30.37	1.81	26.28	3.12	79.15	1.87	8.85
0.74	0.00	0.26	488.94	23.00	1.435	71.19	444.65	1.93	48.53	1.89	47.89	0.29	2.35	0.91	155.75	0.56	0.08	33.00	1.88	30.49	3.32	82.07	2.75	9.89
0.74	0.00	0.26	977.88	23.00	1.435	69.69	524.25	1.93	47.08	1.94	47.82	0.28	3.01	1.18	134.64	0.45	0.09	37.47	1.77	31.12	3.83	84.59	1.96	8.74
0.74	0.00	0.26	0.00	120.00	1.435	70.10	238.90	1.97	45.92	1.96	45.23	0.29	1.01	0.39	280.32	1.01	0.08	28.77	1.60	20.76	2.90	79.02	1.54	8.79
0.74	0.00	0.26	0.80	120.00	1.435	69.70	346.65	2.06	40.28	2.02	40.43	0.29	1.72	0.67	207.87	0.64	0.10	35.67	1.76	27.96	3.46	83.88	3.37	9.56
0.74	0.00	0.26	8.15	120.00	1.435	72.55	570.97	2.03	40.31	2.00	39.36	0.28	3.52	1.38	136.30	0.34	0.16	43.66	1.95	41.65	4.06	84.44	6.87	8.41
0.74	0.00	0.26	16.30	120.00	1.435	70.50	698.56	1.94	35.04	2.01	36.26	0.28	4.83	1.90	112.06	0.24	0.22	51.30	1.85	43.83	4.95	86.45	6.99	7.63
0.74	0.00	0.26	48.89	120.00	1.435	71.50	885.68	2.02	30.69	1.95	28.84	0.29	7.42	2.88	92.88	0.16	0.34	60.00	2.04	61.78	5.99	87.65	11.03	6.64
0.74	0.00	0.26	162.98	120.00	1.435	68.32	1065.58	1.96	22.54	2.07	25.17	0.27	9.57	3.76	76.64	0.12	0.42	61.38	1.86	51.54	6.26	91.09	13.41	5.21
0.89	0.00	0.11	0.00	23.00	1.700	63.82	144.45	1.47	36.32	1.56	37.00	0.27	0.45	0.18	371.00	1.92	0.04	11.95	1.33	8.26	1.35	80.27	0.82	5.84
0.89	0.00	0.11	65.19	23.00	1.700	67.79	301.59	1.50	40.97	1.56	40.45	0.26	1.28	0.51	202.70	0.96	0.05	22.87	1.50	15.70	2.50	81.59	1.16	10.06
0.89	0.00	0.11	488.94	23.00	1.700	65.73	365.85	1.56	38.71	1.57	38.44	0.27	1.74	0.68	159.69	0.72	0.05	26.82	1.60	18.39	2.85	82.39	1.37	9.13
0.89	0.00	0.11	977.88	23.00	1.700	66.42	447.98	1.58	37.54	1.65	37.50	0.25	2.31	0.93	181.01	0.54	0.07	31.80	1.76	24.54	3.30	84.83	1.54	10.69
0.89	0.00	0.11	0.00	120.00	1.700	66.87	161.58	1.55	34.14	1.60	34.43	0.32	0.66	0.25	363.55	1.71	0.05	17.90	1.22	9.88	2.13	82.59	0.87	8.13
0.89	0.00	0.11	0.80	120.00	1.700	66.53	282.09	1.74	32.85	1.74	32.98	0.28	1.26	0.49	223.96	0.91	0.08	26.53	1.33	14.25	2.86	85.67	1.41	10.90
0.89	0.00	0.11	8.15	120.00	1.700	64.10	539.04	1.99	32.72	1.96	32.15	0.28	3.23	1.26	124.41	0.34	0.15	38.41	1.43	21.56	4.22	87.82	3.10	9.11
0.89	0.00	0.11	16.30	120.00	1.700	63.54	621.00	1.87	30.18	1.91	30.98	0.28	4.22	1.65	105.96	0.26	0.17	43.13	1.70	31.86	4.71	89.39	3.35	8.28
0.89	0.00	0.11	48.89	120.00	1.700	64.01	784.61	1.83	25.84	1.83	25.37	0.29	6.33	2.46	84.58	0.16	0.28	52.34	1.76	40.88	5.76	89.02	7.17	6.86
0.89	0.00	0.11	162.98	120.00	1.700	66.75	911.87	1.75	20.39	1.80	21.25	0.29	7.96	3.10	77.16	0.13	0.35	56.11	1.97	51.22	6.06	88.62	11.72	6.28
0.99	0.00	0.01	0.00	23.00	1.884	63.07	119.08	1.37	29.41	1.30	27.48	0.29	0.23	0.09	443.67	1.59	0.08	4.32	1.10	3.29	0.49	77.98	0.23	2.87
0.99	0.00	0.01	65.19	23.00	1.884	70.25	235.21	1.35	31.36	1.29	29.28	0.22	0.71	0.29	274.94	1.47	0.03	10.10	0.93	4.32	1.41	84.23	0.38	5.47
0.99	0.00	0.01	488.94	23.00	1.884	65.43	233.77	1.27	28.61	1.34	30.04	0.23	0.66	0.27	243.29	1.29	0.04	8.48	0.86	3.81	1.20	81.45	0.40	5.00
0.99	0.00	0.01	977.88	23.00	1.884	67.55	283.26	1.37	29.49	1.31	28.00	0.24	1.00	0.41	223.23	1.17	0.04	10.23	0.82	3.90	1.88	85.25	0.50	6.79
0.99	0.00	0.01	0.00	120.00	1.884	63.78	125.95	1.35	27.51	1.37	27.25	0.28	0.31	0.12	429.98	1.57	0.07	5.74	0.84	3.02	0.80	78.83	0.31	3.71
0.99	0.00	0.01	0.80	120.00	1.884	64.28	246.90	1.58	27.87	1.58	28.23	0.24	0.92	0.37	272.40	1.11	0.06	12.27	0.74	3.42	1.96	91.21	0.58	6.38
0.99	0.00	0.01	3.26	120.00	1.884	63.63	358.23	1.59	27.45	1.55	27.85	0.22	1.64	0.67	173.95	0.61	0.08	15.91	0.87	6.09	2.24	81.95	0.71	7.01
0.99	0.00	0.01	8.15	120.00	1.884	64.87	464.99	1.57	26.23	1.53	25.93	0.25	2.67	1.07	139.18	0.40	0.12	24.91	0.93	9.11	3.68	88.14	1.13	10.37
0.99	0.00	0.01	16.30	120.00	1.884	67.64	621.86	1.56	24.12	1.60	25.31	0.25	4.10	1.64	119.20	0.29	0.17	29.45	1.00	11.68	4.27	92.99	1.26	9.55
0.99	0.00	0.01	48.89	120.00	1.884	61.23	764.43	1.56	21.32	1.51	21.33	0.23	5.94	2.42	86.50	0.16	0.30	36.94	1.04	14.58	5.36	99.07	5.66	8.10
0.99	0.00	0.01	162.98	120.00	1.884	63.31	899.34	1.39	16.00	1.40	16.23	0.20	7.60	3.16	75.37	0.12	0.40	41.96	1.29	21.97	5.66	94.42	7.92	6.95

AVERAGES R48 fiber and R200 middle fraction mixed sheets (Norway spruce 110 CSF)

Mixture			Load	Temperature	FQA	BW	Density	Smoothside		Roughside		In-plane ultrasonic			Out-plane z- direction ultrasonic			Tensile	% strain	TEA	Spec Modulus	Zero Span	ZDT	Tear index
R48	R200	P200	psi	°C	FL, mm	g/m2	g/cc	LAC, m2/kg	LSC, m2/kg	LAC, m2/kg	LSC, m2/kg	Poisson	E (Gpa)	G(Gpa)	Caliper, um	v, m/sec	stiffness km^2/s^2	index, Nm/g	at max load	J/m2	kNm/g	Nm/g	kN/g	mNm2/g
0.00	1.00	0.00	0.00	23.00	0.283	66.75	275.23	2.15	62.20	2.16	61.05	0.25	1.14	0.46	236.65	0.92	0.07	34.00	2.06	24.48	2.98	82.11	3.44	2.80
0.00	1.00	0.00	65.19	23.00	0.283	66.16	460.23	2.10	58.41	2.06	56.16	0.28	2.62	1.03	146.95	0.48	0.09	42.03	1.97	37.41	3.94	84.94	5.87	2.95
0.00	1.00	0.00	488.94	23.00	0.283	65.60	566.24	2.25	51.72	2.27	51.15	0.27	3.49	1.38	118.95	0.37	0.10	45.79	1.94	37.45	4.30	84.44	6.97	2.85
0.00	1.00	0.00	977.88	23.00	0.283	65.34	624.09	2.13	46.03	2.18	46.57	0.29	4.16	1.62	105.42	0.30	0.12	46.87	1.90	38.94	4.55	83.54	8.07	2.95
0.00	1.00	0.00	0.00	120.00	0.283	62.30	364.85	2.35	54.31	2.38	54.44	0.27	2.17	0.86	172.06	0.55	0.10	41.94	1.59	26.22	4.11	84.63	6.17	2.70
0.00	1.00	0.00	0.80	120.00	0.283	69.74	460.66	2.44	42.65	2.34	41.51	0.28	3.27	1.28	156.61	0.45	0.12	47.64	1.38	28.79	4.97	91.35	6.46	2.59
0.00	1.00	0.00	8.15	120.00	0.283	62.45	675.82	2.40	40.72	2.45	40.50	0.29	5.41	2.11	103.52	0.22	0.22	53.28	1.40	29.21	5.41	88.31	10.66	2.49
0.00	1.00	0.00	16.30	120.00	0.283	62.72	776.19	2.35	37.33	2.38	38.02	0.27	6.42	2.53	91.87	0.17	0.28	53.17	1.56	34.23	5.45	91.53	12.60	2.68
0.00	1.00	0.00	48.89	120.00	0.283	63.20	934.90	2.34	30.90	2.27	29.63	0.29	8.67	3.36	78.40	0.13	0.37	64.95	1.61	42.23	6.58	91.70	14.14	2.55
0.00	1.00	0.00	162.98	120.00	0.283	63.12	1047.65	2.26	23.95	2.26	23.00	0.28	10.41	4.06	68.87	0.10	0.47	64.61	1.53	39.73	6.76	92.50	15.02	2.26
0.50	0.50	0.00	0.00	23.00	1.092	67.57	196.27	1.79	48.65	1.79	48.07	0.28	0.66	0.26	329.82	1.49	0.05	23.65	1.94	20.43	2.04	82.32	1.83	7.30
0.50	0.50	0.00	65.19	23.00	1.092	68.03	372.58	1.79	48.74	1.87	49.42	0.28	1.79	0.70	183.63	0.71	0.07	33.20	1.99	29.70	3.10	84.30	3.33	7.85
0.50	0.50	0.00	488.94	23.00	1.092	67.66	466.37	1.75	44.16	1.79	43.84	0.27	2.61	1.03	143.67	0.52	0.08	38.24	1.96	32.92	3.67	82.56	4.00	7.71
0.50	0.50	0.00	977.88	23.00	1.092	67.65	549.29	1.82	41.98	1.85	41.74	0.27	3.31	1.30	123.40	0.40	0.09	39.71	2.10	38.80	3.76	88.92	4.50	7.21
0.50	0.50	0.00	0.00	120.00	1.092	67.41	266.92	1.94	44.93	1.95	44.29	0.29	1.30	0.50	252.54	0.98	0.07	30.89	1.59	20.04	3.10	86.46	2.64	8.07
0.50	0.50	0.00	0.80	120.00	1.092	67.52	340.64	2.14	38.42	2.23	37.93	0.28	1.73	0.74	204.48	0.68	0.09	38.64	1.83	30.67	3.55	87.41	4.65	8.47
0.50	0.50	0.00	8.15	120.00	1.092	67.77	626.41	2.05	37.54	2.11	36.42	0.28	4.62	1.80	123.60	0.29	0.18	47.17	1.65	33.96	4.80	94.43	6.60	6.92
0.50	0.50	0.00	16.30	120.00	1.092	66.86	740.65	2.01	33.02	2.10	33.32	0.29	5.96	2.31	101.60	0.21	0.24	53.68	1.65	37.65	5.51	95.77	8.81	6.19
0.50	0.50	0.00	48.89	120.00	1.092	65.70	893.22	2.12	30.04	2.08	29.06	0.28	8.03	3.14	85.12	0.14	0.35	56.96	1.62	40.61	6.07	96.85	12.81	5.25
0.50	0.50	0.00	162.98	120.00	1.092	66.30	1027.83	1.96	21.65	2.01	22.13	0.28	9.86	3.85	74.62	0.11	0.45	62.46	1.64		6.62	97.21	13.57	4.44
0.75	0.25	0.00	0.00	23.00	1.496	63.23	151.76	1.77	39.38	1.73	39.54	0.30	0.45	0.18	377.40	1.92	0.04	14.92	1.40	9.61	1.60	79.00	1.36	6.06
0.75	0.25	0.00	65.19	23.00	1.496	64.74	278.94	1.68	40.68	1.70	41.80	0.28	1.07	0.41	219.79	1.05	0.04	23.78	1.51	13.92	2.50	83.96	1.83	8.36
0.75	0.25	0.00	488.94	23.00	1.496	65.69	371.91	1.75	40.45	1.69	40.37	0.29	1.87	0.73	165.78	0.73	0.05	28.87	1.36	15.87	3.18	90.35	2.17	8.43
0.75	0.25	0.00	977.88	23.00	1.496	64.72	430.98	1.75	38.16	1.71	38.16	0.32	2.35	0.94	132.54	0.53	0.06	29.88	1.38	16.12	3.29	88.13	2.98	9.24
0.75	0.25	0.00	0.00	120.00	1.496	63.46	200.27	2.09	39.37	2.03	38.27	0.30	0.79	0.30	299.78	1.34	0.05	21.68	1.29	10.93	2.44	87.17	1.87	7.52
0.75	0.25	0.00	0.80	120.00	1.496	63.98	296.62	1.96	34.04	1.94	34.86	0.30	1.34	0.56	199.98	0.70	0.08	30.11	1.49	18.41	3.18	88.93	2.93	9.31
0.75	0.25	0.00	8.15	120.00	1.496	63.43	544.76	2.06	33.82	1.97	33.40	0.29	3.72	1.44	113.80	0.29	0.15	42.45	1.59	26.88	4.40	86.59	5.77	8.48
0.75	0.25	0.00	16.30	120.00	1.496	64.22	652.31	2.03	30.99	1.93	31.04	0.31	4.67	1.79	96.60	0.21	0.19	48.14	1.78	36.79	5.05	91.09	6.41	7.58
0.75	0.25	0.00	48.89	120.00	1.496	63.60	749.01	1.88	27.00	1.91	28.17	0.30	6.02	2.32	84.31	0.16	0.26	49.73	1.89	40.15	5.28	90.54	6.06	6.99
0.75	0.25	0.00	162.98	120.00	1.496	60.96	934.06	1.92	21.06	1.86	21.21	0.27	8.66	3.40	66.82	0.10	0.41	59.07	1.82	43.79	6.13	91.46	7.50	5.33
0.90	0.10	0.00	0.00	23.00	1.738	65.75	139.31	1.50	32.86	1.54	33.05	0.30	0.35	0.14	434.19	2.00	0.05	9.91	1.28	6.89	1.10	83.00	0.61	5.32
0.90	0.10	0.00	65.19	23.00	1.738	66.83	264.67	1.69	35.45	1.70	35.31	0.28	0.96	0.38	244.92	1.21	0.04	16.65	1.25	10.05	1.95	85.87	0.80	7.49
0.90	0.10	0.00	488.94	23.00	1.738	66.66	340.19	1.64	33.85	1.64	33.30	0.28	1.48	0.58	179.63	0.80	0.05	20.92	1.24	11.52	2.38	88.94	0.88	9.26
0.90	0.10	0.00	977.88	23.00	1.738	69.16	412.68	1.62	31.33	1.60	31.06	0.28	1.94	0.76	158.65	0.64	0.06	20.66	1.34	12.73	2.52	90.63	1.12	10.06
0.90	0.10	0.00	0.00	120.00	1.738	66.16	153.42	1.60	32.09	1.61	32.01	0.31	0.50	0.19	414.05	1.92	0.05	12.23	1.04	6.35	1.56	78.15	0.77	6.26
0.90	0.10	0.00	0.80	120.00	1.738	68.78	259.70	1.93	30.00	1.85	30.68	0.29	1.07	0.41	247.36	0.94	0.07	20.85	1.28	11.26	2.39	91.14	0.99	9.28
0.90	0.10	0.00	8.15	120.00	1.738	66.72	518.34	1.84	29.65	1.79	29.83	0.29	2.99	1.16	141.23	0.39	0.13	29.50	1.15	14.34	3.73	92.76	1.99	9.94
0.90	0.10	0.00	16.30	120.00	1.738	66.50	644.30	1.87	29.26	1.79	28.06	0.29	4.26	1.65	113.38	0.26	0.18	34.76	1.28	18.91	4.26	91.15	2.21	9.33
0.90	0.10	0.00	48.89	120.00	1.738	67.22	794.41	1.77	23.64	1.78	24.34	0.28	6.25	2.45	96.58	0.19	0.26	41.59	1.24	20.70	5.45	98.61	2.97	8.03
0.90	0.10	0.00	162.98	120.00	1.738	64.33	909.58	1.72	19.71	1.73	19.93	0.26	7.73	3.07	81.99	0.14	0.33	44.80	1.43	27.67	5.58	101.22	8.77	6.72
0.90	0.10	0.00	65.19	120.00	1.738	65.25	818.72	1.78	23.40	1.76	22.95	0.29	6.70	2.61	90.32	0.16	0.30	43.55	1.39	25.84	5.38	97.59	4.65	7.55

AVERAGES R48 fiber, R200 middle and P200 fines fraction mixed sheets (Norway spruce 110 CSF)

Mixture			Load	Temperature	FQA	BW	Density	Smoothside		Roughside		In-plane ultrasonic			Out-plane z- direction ultrasonic			Tensile	% strain	TEA	Spec Modulus	Zero Span	ZDT	Tear index
R48	R200	P200	psi	°C	FL, mm	g/m2	g/cc	LAC, m2/kg	LSC, m2/kg	LAC, m2/kg	LSC, m2/kg	Poisson	E (Gpa)	G(Gpa)	Caliper, um	v, m/sec	stiffness km^2/s^2	index, Nm/g	at max load	J/m2	kNm/g	Nm/g	kN/g	mNm2/g
0.00	0.33	0.67	0.00	23.00	0.148	66.82	303.26	2.98	90.95	2.85	92.75	0.26	1.14	0.45	223.22	0.62	0.13	28.48	1.90	18.89	2.83	64.09	7.03	1.71
0.00	0.33	0.67	65.19	23.00	0.148	66.77	467.40	3.03	86.83	2.92	89.61	0.27	2.28	0.90	150.35	0.39	0.15	33.85	1.68	26.30	3.58	65.71	10.69	1.99
0.00	0.33	0.67	488.94	23.00	0.148	66.82	564.07	2.94	78.80	2.87	82.65	0.26	3.03	1.21	125.42	0.33	0.15	35.82	1.47	23.94	3.89	67.75	11.14	1.74
0.00	0.33	0.67	977.88	23.00	0.148	67.38	633.97	2.93	74.93	2.82	77.46	0.26	3.53	1.40	114.09	0.29	0.15	37.70	1.38	22.24	4.12	70.40	9.95	1.78
0.00	0.33	0.67	0.00	120.00	0.148	65.66	411.06	3.18	80.08	3.12	80.68	0.26	2.12	0.85	163.21	0.39	0.17	34.85	1.27	18.13	3.92	65.93	9.95	1.60
0.00	0.33	0.67	0.80	120.00	0.148	61.63	487.10	3.31	67.01	3.38	68.78	0.27	2.98	1.21	131.55	0.31	0.18	44.52	1.30	22.14	4.80	70.66	14.34	1.67
0.00	0.33	0.67	8.15	120.00	0.148	66.59	653.98	3.20	62.51	3.16	62.84	0.27	4.19	1.65	113.03	0.23	0.25	43.21	2.75	20.52	4.61	67.96	14.05	1.53
0.00	0.33	0.67	16.30	120.00	0.148	65.50	736.37	3.14	56.11	3.30	59.27	0.27	5.08	2.00	96.71	0.18	0.30	45.24	1.14	19.68	5.00	71.03	13.81	1.53
0.00	0.33	0.67	48.89	120.00	0.148	66.02	898.80	3.18	45.86	3.03	47.95	0.27	6.98	2.76	83.19	0.14	0.37	52.83	1.30	27.39	5.71	72.16	16.99	1.54
0.00	0.33	0.67	162.98	120.00	0.148	65.31	1032.49	3.09	34.46	3.16	37.10	0.29	8.65	3.42	71.92	0.11	0.40	53.44	1.19	25.37	6.22	73.56	17.50	1.30
0.00	0.67	0.33	0.00	23.00	0.215	65.48	303.18	2.88	77.16	2.78	76.78	0.29	1.28	0.49	216.33	0.69	0.10	29.31	1.70	19.81	2.83	80.69	5.13	2.27
0.00	0.67	0.33	65.19	23.00	0.215	65.15	472.76	2.63	71.53	2.58	73.39	0.30	2.56	0.98	143.15	0.41	0.12	36.28	1.56	22.98	3.62	79.54	8.18	2.39
0.00	0.67	0.33	488.94	23.00	0.215	65.38	587.64	2.58	63.91	2.50	65.06	0.30	3.54	1.36	116.36	0.33	0.12	39.57	1.50	23.97	3.95	82.59	9.67	2.35
0.00	0.67	0.33	977.88	23.00	0.215	65.59	641.19	2.57	59.82	2.53	62.23	0.29	4.05	1.57	109.56	0.30	0.14	42.40	1.63	29.52	4.18	85.52	8.72	2.34
0.00	0.67	0.33	0.00	120.00	0.215	62.93	401.53	2.88	66.57	2.84	67.61	0.30	2.43	0.93	159.44	0.44	0.13	39.13	1.39	20.92	4.10	86.54	8.49	2.39
0.00	0.67	0.33	0.80	120.00	0.215	71.90	474.79	2.58	51.99	2.54	51.50	0.29	3.16	1.23	151.11	0.40	0.14	41.81	1.14	19.63	4.52	82.87	7.48	2.28
0.00	0.67	0.33	8.15	120.00	0.215	65.16	669.62	2.74	52.08	2.71	51.80	0.30	4.88	1.88	109.26	0.23	0.22	48.68	1.40	26.74	4.92	84.66	12.77	2.34
0.00	0.67	0.33	16.30	120.00	0.215	64.92	774.81	2.62	45.70	2.63	46.92	0.28	6.01	2.36	93.18	0.17	0.29	51.54	1.34	27.13	5.44	85.32	14.60	2.21
0.00	0.67	0.33	48.89	120.00	0.215	64.58	924.89	2.72	38.78	2.56	38.00	0.30	7.92	3.06	79.39	0.13	0.35	58.51	1.42	33.63	6.22	89.74	16.12	2.12
0.00	0.67	0.33	162.98	120.00	0.215	64.34	1057.27	2.61	29.52	2.60	30.28	0.31	9.59	3.69	70.48	0.11	0.41	57.95	0.95	21.18	6.39	93.15	16.57	1.91
0.25	0.25	0.50	0.00	23.00	0.586	67.52	256.52	2.74	80.45	2.71	78.72	0.30	0.93	0.36	270.64	0.85	0.10	23.92	1.66	16.60	2.36	65.33	5.98	5.49
0.25	0.25	0.50	65.19	23.00	0.586	68.38	419.86	2.55	74.13	2.48	74.29	0.28	2.01	0.79	167.56	0.47	0.13	32.55	1.79	26.34	3.31	70.29	8.95	5.42
0.25	0.25	0.50	488.94	23.00	0.586	68.04	542.37	2.59	67.53	2.69	72.15	0.28	2.90	1.14	127.76	0.35	0.13	35.12	1.78	28.58	3.76	73.02	9.82	5.01
0.25	0.25	0.50	977.88	23.00	0.586	68.84	636.70	2.66	61.38	2.62	62.62	0.28	3.73	1.46	114.29	0.29	0.15	36.35	1.62	26.70	3.71	72.62	9.34	4.58
0.25	0.25	0.50	0.00	120.00	0.586	67.47	335.15	2.86	70.81	2.86	75.22	0.30	1.74	0.67	199.57	0.54	0.14	33.61	1.43	21.21	3.74	75.04	8.26	5.36
0.25	0.25	0.50	0.80	120.00	0.586	66.71	432.48	2.94	56.74	2.98	60.10	0.29	2.71	1.05	159.55	0.39	0.16	40.84	1.36	23.37	4.33	75.04	9.55	5.25
0.25	0.25	0.50	8.15	120.00	0.586	67.00	611.35	2.94	56.40	3.03	58.18	0.30	4.39	1.69	121.52	0.22	0.29	44.38	1.30	24.06	5.00	80.06	12.17	4.60
0.25	0.25	0.50	16.30	120.00	0.586	67.59	719.61	2.85	49.72	2.82	51.99	0.29	5.39	2.09	104.87	0.18	0.35	46.97	1.26	24.57	5.24	82.98	12.22	3.99
0.25	0.25	0.50	48.89	120.00	0.586	67.19	880.51	2.80	41.50	2.78	42.92	0.29	7.13	2.76	85.47	0.12	0.48	51.53	1.23	25.94	5.79	86.96	15.96	3.64
0.25	0.25	0.50	162.98	120.00	0.586	66.54	1001.27	2.98	31.98	3.01	32.95	0.30	8.96	3.46	73.95	0.10	0.59	56.98	1.34	31.58	6.39	84.29	14.99	3.16
0.38	0.38	0.25	0.00	23.00	0.839	67.96	237.08	2.35	65.78	2.33	64.54	0.28	0.87	0.34	278.26	1.00	0.08	24.77	1.73	19.09	2.56	83.50	2.94	6.78
0.38	0.38	0.25	65.19	23.00	0.839	68.73	417.62	2.21	60.60	2.19	60.85	0.28	2.12	0.82	166.25	0.52	0.10	33.08	1.71	24.83	3.44	84.93	5.16	6.85
0.38	0.38	0.25	488.94	23.00	0.839	67.85	527.15	2.24	55.49	2.21	55.92	0.28	2.98	1.17	130.25	0.39	0.11	39.26	1.86	33.75	4.03	82.83	5.57	6.93
0.38	0.38	0.25	977.88	23.00	0.839	67.86	587.43	2.22	52.37	2.24	53.78	0.30	3.52	1.36	118.53	0.33	0.13	39.62	1.72	31.11	4.39	89.64	6.24	6.07
0.38	0.38	0.25	0.00	120.00	0.839	66.20	324.97	2.38	57.57	2.32	57.59	0.31	1.79	0.68	202.70	0.61	0.11	33.75	1.64	23.02	3.45	87.70	5.59	7.27
0.38	0.38	0.25	0.80	120.00	0.839	68.17	426.66	2.27	46.98	2.33	47.82	0.28	2.54	0.99	171.09	0.47	0.13	38.33	1.45	23.34	3.95	86.35	6.34	6.67
0.38	0.38	0.25	8.15	120.00	0.839	67.45	624.49	2.25	44.66	2.29	45.93	0.28	4.27	1.67	116.33	0.24	0.23	44.63	1.61	31.08	4.59	85.58	10.24	5.85
0.38	0.38	0.25	16.30	120.00	0.839	66.50	741.06	2.38	43.29	2.43	45.00	0.29	5.72	2.22	100.41	0.18	0.30	51.77	1.43	31.55	5.69	97.31	11.81	5.58
0.38	0.38	0.25	48.89	120.00	0.839	66.54	905.78	2.34	35.11	2.30	36.28	0.27	7.93	3.12	81.80	0.12	0.49	59.55	1.50	37.58	6.26	95.66	12.57	4.74
0.38	0.38	0.25	162.98	120.00	0.839	66.00	1045.93	2.13	25.25	2.20	26.92	0.29	9.75	3.81	70.38	0.09	0.65	57.35	1.40	33.93	6.36	89.03	13.44	3.96

STANDARD DEVIATIONS R48 fiber and P200 fines mixed sheets (Norway spruce 110 CSF)

Mixture			Load	Temperature	BW	Density	Smoothside		Roughside		In-plane ultrasonic		Out-plane z- direction ultrasonic			Tensile	% strain	TEA	Spec Modulus	Zero Span	ZDT
R48	R200	P200	psi	°C	g/m2	g/cc	LAC, m2/kg	LSC, m2/kg	LAC, m2/kg	LSC, m2/kg	E (Gpa)	G(Gpa)	Caliper, um	v, m/sec	tiffness km2/s	index, Nm/g	at max load	J/m2	Nm/g	Nm/g	kN/g
0.00	0.00	1.00	0.00	23.00	0.824	5.95	0.13	1.88	0.08	5.14	0.01	0.00	2.77	0.01	0.00	0.77	0.30	4.65	0.06	2.98	2.24
0.00	0.00	1.00	65.19	23.00	0.553	12.39	0.12	4.42	0.11	3.83	0.08	0.03	3.41	0.01	0.00	2.01	0.25	5.92	0.04	0.93	1.51
0.00	0.00	1.00	488.94	23.00	0.433	16.62	0.10	2.44	0.05	2.68	0.06	0.03	3.52	0.01	0.00	2.43	0.24	6.28	0.19	1.00	0.62
0.00	0.00	1.00	977.88	23.00	0.798	26.91	0.06	6.74	0.06	2.95	0.20	0.06	3.38	0.01	0.01	2.06	0.20	6.34	0.09	1.00	0.71
0.00	0.00	1.00	0.00	120.00	1.566	14.75	0.18	6.80	0.15	4.89	0.15	0.05	5.39	0.01	0.00	3.68	0.30	8.57	0.36	1.33	0.62
0.00	0.00	1.00	0.80	120.00	0.342	11.44	0.44	5.98	0.22	7.90	0.20	0.08	4.78	0.01	0.01	1.61	0.07	2.23	0.09	2.31	1.20
0.00	0.00	1.00	8.15	120.00	0.637	20.52	0.20	5.11	0.10	3.33	0.14	0.04	3.79	0.02	0.02	2.31	0.12	4.22	0.14	1.95	0.58
0.00	0.00	1.00	16.30	120.00	0.575	23.52	0.08	0.80	0.18	3.41	0.25	0.09	2.90	0.01	0.01	6.66	0.31	4.15	0.27	2.92	0.94
0.00	0.00	1.00	48.89	120.00	0.839	11.98	0.11	1.58	0.30	7.36	1.20	0.94	0.40	0.00	0.01	3.16	0.21	8.71	0.14	2.37	2.66
0.00	0.00	1.00	162.98	120.00	0.731	19.42	0.05	1.42	0.13	1.67	1.95	1.05	1.61	0.00	0.02	4.90	0.11	4.31	0.31	1.24	0.66
0.50	0.00	0.50	0.00	23.00	1.587	2.92	0.03	1.08	0.08	1.92	0.03	0.01	8.42	0.02	0.00	0.64	0.12	3.56	0.13	4.81	0.76
0.50	0.00	0.50	65.19	23.00	3.017	5.33	0.08	1.75	0.05	2.33	0.03	0.01	6.40	0.01	0.00	1.73	0.24	6.57	0.13	2.32	2.04
0.50	0.00	0.50	488.94	23.00	3.828	16.80	0.07	1.70	0.07	2.32	0.09	0.04	6.00	0.02	0.00	2.11	0.25	5.33	0.24	4.06	2.36
0.50	0.00	0.50	977.88	23.00	2.652	10.24	0.06	1.96	0.06	2.13	0.20	0.06	6.13	0.02	0.00	1.65	0.10	5.26	0.18	2.69	1.52
0.50	0.00	0.50	0.00	120.00	1.111	15.27	0.12	2.50	0.07	2.98	0.17	0.07	11.99	0.04	0.01	1.71	0.25	5.25	0.14	3.82	2.23
0.50	0.00	0.50	0.80	120.00	1.337	8.01	0.07	1.64	0.05	0.85	0.06	0.03	5.00	0.02	0.01	1.36	0.21	5.31	0.14	1.73	1.68
0.50	0.00	0.50	8.15	120.00	1.692	14.26	0.11	2.10	0.08	2.15	0.22	0.08	1.73	0.01	0.01	2.27	0.16	7.48	0.24	2.20	2.86
0.50	0.00	0.50	16.30	120.00	2.676	7.93	0.08	1.98	0.08	1.84	0.16	0.05	6.51	0.02	0.02	2.21	0.14	5.06	0.24	3.61	0.71
0.50	0.00	0.50	48.89	120.00	1.507	26.83	0.03	1.32	0.11	1.53	0.18	0.07	1.95	0.01	0.01	2.12	0.16	6.41	0.16	2.89	0.87
0.50	0.00	0.50	162.98	120.00	1.400	22.62	0.11	1.77	0.03	0.37	0.24	0.09	1.51	0.00	0.01	1.49	0.11	4.00	0.17	3.42	0.60
0.74	0.00	0.26	0.00	23.00	1.347	2.43	0.05	1.42	0.08	2.42	0.01	0.00	10.57	0.06	0.00	0.83	0.06	1.27	0.11	4.00	0.25
0.74	0.00	0.26	65.19	23.00	0.387	13.38	0.05	0.90	0.03	1.07	0.12	0.05	6.75	0.04	0.00	1.09	0.12	3.17	0.13	3.52	0.18
0.74	0.00	0.26	488.94	23.00	1.234	12.87	0.06	0.79	0.04	0.70	0.12	0.06	4.60	0.02	0.00	2.04	0.05	5.36	0.27	4.36	1.12
0.74	0.00	0.26	977.88	23.00	1.311	17.49	0.06	2.56	0.09	3.01	0.28	0.11	4.78	0.02	0.00	3.05	0.12	5.71	0.38	4.44	0.20
0.74	0.00	0.26	0.00	120.00	0.968	4.75	0.05	1.59	0.08	2.09	0.04	0.01	7.33	0.04	0.00	1.35	0.06	2.71	0.15	3.49	0.14
0.74	0.00	0.26	0.80	120.00	1.887	10.24	0.08	1.17	0.04	0.82	0.16	0.05	3.77	0.03	0.01	2.09	0.13	2.91	0.30	2.50	0.84
0.74	0.00	0.26	8.15	120.00	0.646	27.61	0.09	2.21	0.07	1.32	0.25	0.09	9.45	0.05	0.03	2.76	0.32	6.00	0.46	4.23	1.45
0.74	0.00	0.26	16.30	120.00	1.528	37.78	0.04	0.61	0.03	1.01	0.30	0.11	4.98	0.02	0.02	2.20	0.21	8.33	0.30	2.12	3.01
0.74	0.00	0.26	48.89	120.00	2.124	31.40	0.06	1.90	0.04	0.89	0.28	0.09	2.65	0.01	0.02	2.06	0.29	15.11	0.17	4.03	3.42
0.74	0.00	0.26	162.98	120.00	2.154	25.26	0.07	0.55	0.10	1.87	0.39	0.14	1.66	0.01	0.03	0.84	0.28	10.79	0.21	3.80	2.23
0.89	0.00	0.11	0.00	23.00	3.476	8.58	0.10	3.05	0.07	1.36	0.03	0.01	85.40	0.25	0.00	0.96	0.26	2.80	0.13	6.02	0.16
0.89	0.00	0.11	65.19	23.00	1.716	10.67	0.03	0.75	0.03	1.10	0.07	0.02	19.79	0.04	0.00	1.09	0.11	3.12	0.17	3.50	0.12
0.89	0.00	0.11	488.94	23.00	1.443	10.17	0.08	2.88	0.05	2.13	0.11	0.04	14.20	0.03	0.00	2.73	0.28	4.75	0.25	3.53	0.12
0.89	0.00	0.11	977.88	23.00	1.350	22.58	0.05	1.26	0.04	0.90	0.16	0.07	93.58	0.07	0.01	1.42	0.08	0.37	0.28	3.13	0.23
0.89	0.00	0.11	0.00	120.00	2.249	5.34	0.05	0.99	0.06	0.82	0.04	0.01	63.97	0.12	0.00	2.13	0.12	1.10	0.17	5.16	0.12
0.89	0.00	0.11	0.80	120.00	3.316	6.62	0.03	1.36	0.03	0.79	0.05	0.02	57.88	0.07	0.00	0.70	0.13	3.28	0.16	3.76	0.23
0.89	0.00	0.11	8.15	120.00	1.676	16.26	0.06	1.11	0.07	1.01	0.17	0.07	12.73	0.01	0.01	1.99	0.20	3.80	0.30	2.31	0.17
0.89	0.00	0.11	16.30	120.00	0.568	18.82	0.05	1.64	0.07	0.79	0.27	0.11	10.08	0.02	0.01	1.48	0.10	2.34	0.18	3.95	0.54
0.89	0.00	0.11	48.89	120.00	2.310	15.35	0.10	1.31	0.09	1.22	0.20	0.09	5.76	0.01	0.00	2.06	0.14	3.70	0.26	4.37	3.29
0.89	0.00	0.11	162.98	120.00	1.616	7.10	0.07	1.11	0.04	0.61	0.13	0.07	1.63	0.00	0.02	1.35	0.22	7.45	0.21	3.98	1.41
0.99	0.00	0.01	0.00	23.00	2.510	2.08	0.12	2.55	0.10	2.46	0.01	0.00	4.07	0.01	0.00	0.41	0.12	0.24	0.09	1.60	0.04
0.99	0.00	0.01	65.19	23.00	7.029	7.45	0.05	0.94	0.07	1.70	0.06	0.03	27.83	0.15	0.00	0.70	0.08	1.03	0.14	5.41	0.04
0.99	0.00	0.01	488.94	23.00	4.329	16.96	0.09	2.00	0.08	1.65	0.09	0.03	23.49	0.14	0.00	0.76	0.08	0.86	0.13	4.95	0.07
0.99	0.00	0.01	977.88	23.00	3.922	15.21	0.11	1.63	0.06	1.41	0.07	0.03	8.72	0.08	0.00	2.66	0.11	0.74	0.69	11.59	0.18
0.99	0.00	0.01	0.00	120.00	3.954	3.27	0.11	2.01	0.09	2.05	0.01	0.01	19.33	0.09	0.00	0.45	0.05	0.52	0.08	3.98	0.08
0.99	0.00	0.01	0.80	120.00	1.814	10.40	0.06	1.08	0.16	3.03	0.07	0.03	7.75	0.04	0.00	0.82	0.12	0.30	0.12	7.32	0.08
0.99	0.00	0.01	3.26	120.00	2.860	49.63	0.11	2.41	0.09	2.09	0.36	0.15	19.95	0.12	0.01	2.96	0.08	1.07	0.48	1.68	0.29
0.99	0.00	0.01	8.15	120.00	2.861	24.51	0.12	2.01	0.06	1.50	0.26	0.09	5.28	0.01	0.01	2.00	0.07	1.26	0.24	4.07	0.22
0.99	0.00	0.01	16.30	120.00	1.566	18.07	0.07	1.35	0.09	1.10	0.20	0.08	3.49	0.01	0.01	1.19	0.04	0.97	0.18	3.84	0.26
0.99	0.00	0.01	48.89	120.00	3.004	13.54	0.09	0.91	0.14	2.63	0.17	0.04	3.83	0.01	0.02	1.66	0.08	2.14	0.15	3.78	1.91
0.99	0.00	0.01	162.98	120.00	3.378	3.68	0.08	0.89	0.02	0.37	0.07	0.07	3.63	0.00	0.02	0.36	0.14	3.15	0.18	6.35	0.78

STANDARD DEVIATIONS R48 fiber and R200 middle fraction mixed sheets (Norway spruce 110 CSF)

Mixture			Load	Temperature	BW	Density	Smoothside		Roughside		In-plane ultrasonic		Out-plane z- direction ultrasonic			Tensile	% strain	TEA	Spec Modulus	Zero Span	ZDT
R48	R200	P200	psi	°C	g/m2	g/cc	LAC, m2/kg	LSC, m2/kg	LAC, m2/kg	LSC, m2/kg	E (Gpa)	G(Gpa)	Caliper, um	v, m/sec	tiffness km2/s	index, Nm/g	at max load	J/m2	Nm/g	Nm/g	kN/g
0.00	1.00	0.00	0.00	23.00	0.334	3.58	0.03	0.79	0.05	1.43	0.07	0.03	3.32	0.01	0.00	1.37	0.19	12.48	0.17	2.06	0.52
0.00	1.00	0.00	65.19	23.00	0.321	4.73	0.12	2.66	0.10	1.86	0.05	0.01	4.04	0.02	0.00	2.06	0.28	6.34	0.21	8.06	0.38
0.00	1.00	0.00	488.94	23.00	0.408	12.12	0.04	0.93	0.04	1.20	0.21	0.06	4.09	0.02	0.01	2.00	0.19	4.32	0.19	2.77	1.36
0.00	1.00	0.00	977.88	23.00	0.416	22.45	0.02	0.66	0.05	1.50	0.23	0.07	2.22	0.01	0.01	1.82	0.11	1.56	0.14	3.93	1.26
0.00	1.00	0.00	0.00	120.00	1.203	21.29	0.03	1.89	0.04	1.98	0.20	0.08	7.25	0.04	0.00	1.20	0.17	4.64	0.06	1.88	0.75
0.00	1.00	0.00	0.80	120.00	0.956	2.70	0.03	0.39	0.10	0.91	0.06	0.03	4.21	0.02	0.00	2.56	0.18	6.20	0.25	5.12	0.54
0.00	1.00	0.00	8.15	120.00	1.554	9.20	0.09	1.74	0.14	2.29	0.17	0.06	2.45	0.01	0.01	2.19	0.12	2.72	0.19	3.59	1.55
0.00	1.00	0.00	16.30	120.00	1.077	13.89	0.08	1.66	0.04	0.59	0.18	0.09	1.52	0.00	0.01	2.28	0.36	11.81	0.17	4.96	0.32
0.00	1.00	0.00	48.89	120.00	0.791	17.55	0.03	0.73	0.18	2.09	0.13	0.08	1.98	0.00	0.01	2.36	0.14	6.24	0.10	2.20	0.91
0.00	1.00	0.00	162.98	120.00	0.374	14.32	0.08	1.28	0.10	1.44	0.12	0.07	0.47	0.00	0.01	2.23	0.22	8.29	0.26	5.45	0.74
0.50	0.50	0.00	0.00	23.00	0.480	1.72	0.04	1.18	0.04	1.50	0.02	0.01	8.14	0.04	0.00	0.87	0.12	1.19	0.07	3.27	0.21
0.50	0.50	0.00	65.19	23.00	0.315	7.53	0.04	0.66	0.07	1.66	0.04	0.02	2.61	0.01	0.00	1.40	0.18	5.41	0.15	2.33	0.56
0.50	0.50	0.00	488.94	23.00	0.892	13.87	0.10	2.60	0.10	3.10	0.16	0.07	4.73	0.03	0.00	2.07	0.21	5.91	0.20	1.99	0.60
0.50	0.50	0.00	977.88	23.00	1.447	42.75	0.05	0.85	0.08	1.56	0.15	0.05	7.00	0.04	0.01	2.12	0.25	8.16	0.12	4.60	1.28
0.50	0.50	0.00	0.00	120.00	1.035	9.62	0.07	1.92	0.05	1.53	0.12	0.04	10.54	0.07	0.00	0.61	0.21	4.04	0.18	6.54	0.35
0.50	0.50	0.00	0.80	120.00	2.310	21.73	0.10	2.25	0.18	2.73	0.42	0.11	9.71	0.05	0.01	2.71	0.18	4.17	0.37	3.67	0.76
0.50	0.50	0.00	8.15	120.00	0.929	14.71	0.04	0.46	0.08	1.60	0.25	0.10	3.86	0.01	0.01	2.00	0.13	4.27	0.13	2.84	0.55
0.50	0.50	0.00	16.30	120.00	0.526	7.31	0.07	1.43	0.07	1.68	0.15	0.04	3.98	0.02	0.02	2.25	0.15	6.24	0.19	7.92	1.18
0.50	0.50	0.00	48.89	120.00	0.201	9.34	0.09	1.81	0.05	1.42	0.12	0.06	1.39	0.00	0.01	2.92	0.27	10.44	0.14	5.86	0.89
0.50	0.50	0.00	162.98	120.00	0.675	19.95	0.12	1.69	0.05	0.51	0.33	0.12	1.54	0.00	0.02	2.91	0.23		0.12	7	1.34
0.75	0.25	0.00	0.00	23.00	1.335	4.29	0.10	2.21	0.06	0.84	0.03	0.01	12.58	0.07	0.00	0.89	0.14	1.96	0.10	6.25	0.10
0.75	0.25	0.00	65.19	23.00	1.822	5.03	0.07	1.63	0.09	2.05	0.06	0.05	8.21	0.05	0.00	0.63	0.13	1.69	0.06	2.63	0.18
0.75	0.25	0.00	488.94	23.00	1.197	16.18	0.03	0.64	0.07	1.52	0.09	0.03	8.54	0.05	0.00	1.97	0.11	1.91	0.23	6.28	0.21
0.75	0.25	0.00	977.88	23.00	1.021	14.33	0.04	1.21	0.06	1.05	0.31	0.08	9.13	0.05	0.00	1.06	0.23	3.76	0.25	5.18	0.50
0.75	0.25	0.00	0.00	120.00	0.440	0.83	0.07	1.11	0.04	2.18	0.01	0.01	6.84	0.04	0.00	1.03	0.24	2.70	0.14	0.97	0.11
0.75	0.25	0.00	0.80	120.00	1.691	7.65	0.07	0.91	0.06	1.10	0.24	0.03	42.28	0.21	0.00	0.96	0.07	0.74	0.11	4.75	0.37
0.75	0.25	0.00	8.15	120.00	0.964	16.30	0.12	1.64	0.05	0.81	0.11	0.04	9.54	0.03	0.00	2.12	0.12	3.64	0.23	3.50	1.27
0.75	0.25	0.00	16.30	120.00	1.394	9.21	0.02	0.62	0.06	0.74	0.14	0.06	7.01	0.03	0.01	1.56	0.07	3.46	0.13	4.33	1.68
0.75	0.25	0.00	48.89	120.00	1.428	10.91	0.21	2.73	0.16	1.92	0.32	0.15	9.94	0.03	0.03	1.68	0.30	7.07	0.38	5.11	1.88
0.75	0.25	0.00	162.98	120.00	1.090	23.56	0.07	1.07	0.10	1.36	0.17	0.09	1.48	0.00	0.02	3.82	0.13	7.27	0.35	3.18	3.16
0.90	0.10	0.00	0.00	23.00	1.496	2.70	0.06	1.43	0.05	0.72	0.01	0.01	14.42	0.38	0.01	0.40	0.16	1.73	0.07	5.36	0.12
0.90	0.10	0.00	65.19	23.00	1.160	4.15	0.04	1.08	0.05	1.27	0.02	0.01	5.44	0.03	0.00	0.70	0.07	1.39	0.15	2.67	0.03
0.90	0.10	0.00	488.94	23.00	1.122	7.68	0.02	0.98	0.05	1.16	0.08	0.03	11.93	0.07	0.00	1.07	0.18	1.61	0.20	5.19	0.12
0.90	0.10	0.00	977.88	23.00	2.455	20.99	0.06	1.36	0.06	1.13	0.15	0.06	10.21	0.07	0.01	1.36	0.06	1.47	0.24	4.74	0.11
0.90	0.10	0.00	0.00	120.00	0.813	3.91	0.05	1.18	0.05	1.39	0.07	0.02	5.99	0.05	0.00	1.06	0.08	0.87	0.08	3.49	0.07
0.90	0.10	0.00	0.80	120.00	0.968	5.76	0.03	0.58	0.04	0.42	0.02	0.01	57.55	0.30	0.00	1.37	0.15	1.77	0.23	2.20	0.10
0.90	0.10	0.00	8.15	120.00	2.383	15.72	0.07	1.15	0.05	0.80	0.14	0.05	14.42	0.07	0.01	1.67	0.19	4.47	0.12	2.10	0.27
0.90	0.10	0.00	16.30	120.00	1.005	13.15	0.06	1.78	0.05	0.83	0.25	0.09	7.06	0.03	0.00	1.77	0.14	3.66	0.10	7.17	0.16
0.90	0.10	0.00	48.89	120.00	1.031	9.63	0.07	1.06	0.08	1.05	0.15	0.04	3.12	0.01	0.01	2.09	0.07	3.54	0.38	3.12	0.49
0.90	0.10	0.00	162.98	120.00	1.150	16.20	0.04	0.95	0.09	1.37	0.26	0.09	1.38	0.00	0.01	2.71	0.20	6.86	0.32	1.11	2.88
0.90	0.10	0.00	65.19	120.00	0.887	15.20	0.06	0.86	0.07	0.76	0.16	0.05	2.83	0.01	0.01	2.06	0.10	0.20	0.06	0.17	1.25

STANDARD DEVIATIONS R48 fiber, R200 middle and P200 fines fraction mixed sheets (Norway spruce 110 CSF)

Mixture			Load	Temperature	BW	Density	Smoothside		Roughside		In-plane ultrasonic		Out-plane z- direction ultrasonic			Tensile	% strain	TEA	Spec Modulus	Zero Span	ZDT
R48	R200	P200	psi	°C	g/m2	g/cc	LAC, m2/kg	LSC, m2/kg	LAC, m2/kg	LSC, m2/kg	E (Gpa)	G(Gpa)	Caliper, um	v, m/sec	tiffness km2/s	index, Nm/g	at max load	J/m2	Nm/g	Nm/g	kN/g
0.00	0.33	0.67	0.00	23.00	0.254	1.97	0.09	1.42	0.05	1.01	0.01	0.01	1.20	0.01	0.00	1.85	0.13	4.56	0.18	1.60	0.41
0.00	0.33	0.67	65.19	23.00	0.244	16.25	0.10	2.02	0.07	2.03	0.18	0.07	8.28	0.02	0.00	2.11	0.28	6.46	0.11	1.01	1.54
0.00	0.33	0.67	488.94	23.00	0.541	7.20	0.06	1.52	0.07	1.45	0.04	0.01	1.21	0.01	0.00	1.98	0.24	6.19	0.17	1.45	1.02
0.00	0.33	0.67	977.88	23.00	0.340	8.84	0.12	3.29	0.08	2.24	0.11	0.04	2.81	0.01	0.00	1.89	0.12	4.12	0.20	1.87	1.20
0.00	0.33	0.67	0.00	120.00	0.441	6.94	0.12	3.47	0.11	2.65	0.09	0.03	1.04	0.01	0.01	1.57	0.12	3.26	0.18	2.83	2.68
0.00	0.33	0.67	0.80	120.00	1.989	13.94	0.08	1.25	0.13	2.56	0.23	0.06	2.52	0.01	0.01	3.31	0.04	1.55	0.37	2.62	1.34
0.00	0.33	0.67	8.15	120.00	1.269	20.78	0.11	4.14	0.19	3.49	0.28	0.11	4.72	0.01	0.01	2.98	0.12	2.45	0.23	2.04	0.63
0.00	0.33	0.67	16.30	120.00	0.518	25.32	0.11	2.40	0.29	4.29	0.36	0.15	2.51	0.01	0.01	2.87	0.08	2.68	0.24	2.08	0.56
0.00	0.33	0.67	48.89	120.00	0.210	16.92	0.15	2.03	0.24	2.57	0.09	0.05	1.48	0.00	0.00	2.86	0.10	3.68	0.26	2.50	0.81
0.00	0.33	0.67	162.98	120.00	0.365	15.51	0.14	2.51	0.29	2.88	0.09	0.07	0.98	0.00	0.01	2.65	0.17	6.16	0.08	2.10	1.36
0.00	0.67	0.33	0.00	23.00	0.378	2.52	0.04	1.04	0.10	1.53	0.02	0.01	2.40	0.01	0.00	0.82	0.14	2.09	0.25	2.08	0.82
0.00	0.67	0.33	65.19	23.00	0.407	12.06	0.05	1.59	0.08	1.59	0.09	0.04	3.22	0.02	0.00	2.25	0.28	5.94	0.29	3.35	0.84
0.00	0.67	0.33	488.94	23.00	0.189	12.89	0.06	0.94	0.04	1.02	0.10	0.03	2.49	0.01	0.00	2.38	0.13	3.55	0.20	1.46	0.55
0.00	0.67	0.33	977.88	23.00	0.395	12.66	0.06	1.82	0.05	1.40	0.13	0.06	2.50	0.01	0.01	0.88	0.32	7.43	0.25	1.09	1.60
0.00	0.67	0.33	0.00	120.00	0.174	7.37	0.32	3.57	0.21	2.50	0.10	0.03	2.65	0.01	0.00	1.34	0.11	2.65	0.13	4.21	0.96
0.00	0.67	0.33	0.80	120.00	1.486	14.04	0.06	1.53	0.11	1.35	0.12	0.04	7.26	0.03	0.01	4.37	0.14	3.31	0.31	1.08	1.51
0.00	0.67	0.33	8.15	120.00	0.296	22.86	0.16	1.29	0.09	1.59	0.33	0.11	2.79	0.01	0.01	1.27	0.05	1.11	0.15	3.60	0.32
0.00	0.67	0.33	16.30	120.00	0.355	9.58	0.07	2.33	0.12	2.50	0.22	0.06	1.51	0.00	0.00	0.90	0.17	4.63	0.19	1.59	1.55
0.00	0.67	0.33	48.89	120.00	0.400	16.26	0.19	2.48	0.14	1.78	0.12	0.06	1.12	0.00	0.02	1.86	0.09	3.52	0.24	1.99	0.74
0.00	0.67	0.33	162.98	120.00	0.428	16.34	0.24	1.76	0.07	2.08	0.30	0.05	0.73	0.00	0.01	1.85	0.42	9.29	0.26	2.96	1.02
0.25	0.25	0.50	0.00	23.00	1.035	6.46	0.16	4.63	0.22	4.22	0.04	0.02	18.55	0.08	0.01	0.80	0.20	3.01	0.19	5.20	0.44
0.25	0.25	0.50	65.19	23.00	0.304	10.24	0.13	3.65	0.07	1.32	0.06	0.02	7.92	0.03	0.00	1.51	0.05	1.22	0.28	3.34	0.34
0.25	0.25	0.50	488.94	23.00	0.467	16.56	0.07	1.93	0.23	4.91	0.16	0.07	2.69	0.01	0.00	1.34	0.37	7.98	0.23	4.46	0.84
0.25	0.25	0.50	977.88	23.00	0.762	22.96	0.10	2.29	0.12	1.91	0.18	0.07	3.38	0.01	0.01	1.42	0.27	6.57	0.15	3.21	1.15
0.25	0.25	0.50	0.00	120.00	0.910	4.71	0.12	0.90	0.06	2.02	0.07	0.02	15.09	0.05	0.01	2.83	0.12	2.96	0.17	1.64	0.43
0.25	0.25	0.50	0.80	120.00	0.679	13.69	0.24	4.58	0.11	2.62	0.05	0.03	3.58	0.01	0.01	1.15	0.18	5.84	0.19	1.69	1.39
0.25	0.25	0.50	8.15	120.00	0.521	28.39	0.32	4.72	0.18	3.25	0.13	0.04	4.70	0.01	0.02	1.26	0.15	5.02	0.17	2.84	1.79
0.25	0.25	0.50	16.30	120.00	0.334	10.27	0.09	1.24	0.15	3.56	0.22	0.08	4.10	0.01	0.01	2.08	0.18	6.10	0.15	3.45	0.56
0.25	0.25	0.50	48.89	120.00	0.462	22.14	0.10	1.40	0.21	2.92	0.25	0.06	1.04	0.00	0.02	1.19	0.16	4.60	0.28	2.39	1.04
0.25	0.25	0.50	162.98	120.00	0.918	23.72	0.17	1.85	0.18	2.12	0.31	0.16	2.20	0.00	0.02	2.76	0.09	4.32	0.07	2.47	1.15
0.38	0.38	0.25	0.00	23.00	0.635	4.47	0.10	3.76	0.10	2.77	0.07	0.02	7.43	0.04	0.00	1.47	0.31	4.92	0.19	6.98	0.40
0.38	0.38	0.25	65.19	23.00	0.804	4.99	0.07	1.84	0.11	2.76	0.05	0.01	4.15	0.02	0.00	1.76	0.22	5.03	0.28	7.12	0.53
0.38	0.38	0.25	488.94	23.00	0.417	11.87	0.03	0.53	0.09	1.47	0.12	0.06	5.61	0.03	0.01	2.84	0.27	8.72	0.46	3.15	1.54
0.38	0.38	0.25	977.88	23.00	0.477	18.49	0.07	1.30	0.07	2.21	0.04	0.02	7.42	0.03	0.01	2.19	0.30	7.92	0.37	6.44	0.20
0.38	0.38	0.25	0.00	120.00	0.556	5.59	0.12	2.88	0.14	3.14	0.04	0.01	6.06	0.02	0.00	0.74	0.19	2.08	0.16	8.59	0.54
0.38	0.38	0.25	0.80	120.00	1.465	12.30	0.13	2.39	0.06	0.90	0.11	0.03	6.18	0.02	0.00	2.28	0.06	1.58	0.39	1.56	1.18
0.38	0.38	0.25	8.15	120.00	0.879	10.98	0.07	1.21	0.10	2.18	0.11	0.05	3.85	0.01	0.01	0.74	0.16	3.86	0.12	2.52	1.05
0.38	0.38	0.25	16.30	120.00	0.200	22.49	0.15	2.10	0.06	1.11	0.26	0.08	1.72	0.01	0.01	2.11	0.17	7.20	0.23	3.40	1.38
0.38	0.38	0.25	48.89	120.00	0.677	16.20	0.10	1.95	0.10	1.51	0.14	0.05	2.55	0.01	0.05	2.19	0.15	6.55	0.34	2.12	1.94
0.38	0.38	0.25	162.98	120.00	0.678	19.46	0.11	1.63	0.09	0.69	0.34	0.12	1.79	0.00	0.02	3.87	0.20	8.97	0.39	3.26	2.56

STANDARD DEVIATIONS Whole pulp TMP (Norway spruce 110 CSF)

Mixture			Load	Temperature	BW	Density	Smoothside		Roughside		In-plane ultrasonic		Out-plane z- direction ultrasonic			Tensile	% strain	TEA	Spec Modulus	Zero Span	ZDT
R48	R200	P200	psi	°C	g/m2	g/cc	LAC, m2/kg	LSC, m2/kg	LAC, m2/kg	LSC, m2/kg	E (Gpa)	G(Gpa)	Caliper, um	v, m/sec	stiffness km2/s2	index, Nm/g	at max load	J/m2	Nm/g	Nm/g	kN/g
0.56	0.12	0.32	0.00	23.00	1.436	1.50	0.04	0.91	0.03	1.22	0.01	0.00	6.37	0.02	0.00	1.13	0.23	4.56	0.28	4.99	0.46
0.56	0.12	0.32	65.19	23.00	1.261	3.42	0.05	1.20	0.06	1.51	0.13	0.06	5.45	0.02	0.00	3.00	0.23	6.05	0.36	4.42	1.64
0.56	0.12	0.32	488.94	23.00	1.396	11.77	0.03	0.56	0.03	0.64	0.11	0.03	5.13	0.02	0.00	2.34	0.19	5.06	0.24	4.65	2.36
0.56	0.12	0.32	977.88	23.00	0.644	9.73	0.04	1.30	0.07	2.08	0.16	0.04	2.59	0.01	0.00	1.68	0.15	3.53	0.32	5.52	1.46
0.56	0.12	0.32	0.00	120.00	0.816	2.82	0.04	0.22	0.07	0.74	0.02	0.01	4.08	0.02	0.00	0.40	0.14	2.20	0.09	5.81	0.28
0.56	0.12	0.32	0.80	120.00	0.838	8.94	0.09	1.33	0.07	1.18	0.11	0.04	6.66	0.03	0.01	2.09	0.16	4.89	0.19	2.00	0.74
0.56	0.12	0.32	8.15	120.00	0.717	12.51	0.13	2.47	0.04	1.08	0.14	0.04	3.44	0.01	0.01	2.81	0.20	8.12	0.26	2.59	2.03
0.56	0.12	0.32	16.30	120.00	0.662	17.26	0.10	2.53	0.07	1.85	0.21	0.06	3.80	0.01	0.02	1.46	0.09	4.19	0.32	2.90	2.76
0.56	0.12	0.32	48.89	120.00	0.557	8.47	0.16	2.54	0.09	1.72	0.11	0.05	2.23	0.00	0.02	4.57	0.25	13.15	0.57	7.01	1.04
0.56	0.12	0.32	162.98	120.00	0.951	16.55	0.09	1.05	0.09	1.05	0.24	0.10	0.97	0.00	0.02	3.41	0.18	6.01	0.59	6.17	0.42
0.56	0.12	0.32	162.98	23.00	1.208	12.30	0.04	1.04	0.07	2.73	0.11	0.04	5.01	0.02	0.00	1.62	0.12	4.13	0.23	5.94	1.08
0.56	0.12	0.32	325.96	120.00	0.587	8.33	0.08	0.74	0.03	0.58	0.14	0.05	1.20	0.00	0.01	3.07	0.19	8.92	0.49	5.38	0.92
0.56	0.12	0.32	65.19	23.00	0.636	20.00	0.09	2.67	0.08	2.73	0.10	0.05	3.55	0.01	0.01	1.28	0.22	7.72	0.25	3.88	0.94

Appendix 2: Norway spruce TMP (35 CSF) data

	Pressing				@ 50% Relative Humidity												@ 68% Relative Humidity			
Mixture	Load	Temperature	Britt jar fines	FQA	BW	Density	LAC	LSC	In-plane ultrasonic		Tensile	% Strain at	TEA	Aut Young	Spec Modulus	Zero Span	Tensile	% Strain at	TEA	Spec Modulus
R48/P200	psi	°C	%	FL, mm	g/m^2	g/cc	m^2/kg	m^2/kg	E(Gpa)	G(Gpa)	index, Nm/g	max. Load	J/m2	N/mm	kNm/g	Nm/g	index, Nm/g	Max. Load	J/m2	kNm/g
0/100	0.00	23	100.00	0.10	70.43	334.57	1.92	93.62	1.35	0.54	34.98	2.32	38.05	201.99	2.87	51.97				
0/100	488.94	23	100.00	0.10	71.00	608.56	1.89	75.96	3.30	1.32	43.47	2.25	46.87	269.64	3.80	55.62				
0/100	651.92	23	100.00	0.10	70.69	635.64	2.05	78.19	3.51	1.40										
0/100	0.98	120	100.00	0.10	69.56	464.21	2.44	63.21	2.62	1.01	47.58	1.63	33.30	306.89	4.42	56.45				
0/100	48.89	120	100.00	0.10	69.74	852.78	2.52	43.50	6.43	2.39	48.96	1.59	33.92	332.52	4.76	57.55	49.76	1.65	36.63	4.92
50/50	0.00	23	50.55	0.79	70.00	280.61	1.74	64.11	1.23	0.48	33.81	2.27	35.76	206.42	2.94	72.77				
50/50	488.94	23	50.55	0.79	69.95	525.05	1.70	56.55	3.09	1.20	46.95	2.33	53.46	306.13	4.37	76.69				
50/50	0.98	120	50.55	0.79	67.94	416.42	1.98	46.41	2.48	0.96	46.67	1.80	36.70	295.93	4.36	75.25				
50/50	48.89	120	50.55	0.79	69.10	742.44	2.08	31.83	6.08	2.38	60.14	1.87	51.44	403.15	5.83	80.97	57.74	2.05	55.37	5.64
100/0	0.00	23	2.36	1.46	70.51	149.93	1.09	28.53	0.36	0.14	7.22	1.06	4.13	65.54	0.93	91.53				
100/0	488.94	23	2.36	1.46	67.72	273.04	1.04	28.70	0.96	0.40	12.70	1.03	5.79	115.45	1.71	88.84				
100/0	651.92	23	2.36	1.46	69.93	322.73	1.06	28.13	1.33	0.53										
100/0	0.98	120	2.36	1.46	65.24	333.80	1.52	27.25	1.61	0.62	20.94	0.92	7.56	209.27	3.22	94.78				
100/0	48.89	120	2.36	1.46	67.13	639.37	1.42	20.06	4.87	1.94	35.33	1.24	19.13	332.45	4.95	103.74	36.09	1.29	20.63	5.14
75/25	0.00	23	26.92	1.12	69.36	241.43	1.66	52.97	1.03	0.40	29.33	2.10	28.16	181.31	2.61	77.78				
75/25	488.94	23	26.92	1.12	70.92	494.10	1.61	47.41	3.15	1.22	47.07	2.62	62.26	300.71	4.24	83.01				
75/25	0.98	120	26.92	1.12	71.09	404.06	1.84	39.03			48.56	2.19	51.02	306.37	4.31	81.02				
75/25	48.89	120	26.92	1.12	70.15	743.91	1.86	26.49	6.67	2.59	66.93	2.31	74.67	429.99	6.13	93.97	63.44	2.42	75.45	6.08
25/75	0.00	23	80.16	0.38	69.03	310.51	2.32	84.21	1.35	0.53	30.96	2.03	28.37	193.40	2.80	56.25				
25/75	488.94	23	80.16	0.38	68.51	528.84	2.30	68.06	2.81	1.13	40.70	2.47	47.35	251.57	3.67	61.51				
25/75	0.98	120	80.16	0.38	69.64	566.32	2.73	51.01	3.84	1.46	49.83	1.47	31.48	341.62	4.90	64.36				
25/75	48.89	120	80.16	0.38	69.62	834.90	2.68	33.41	6.65	2.59	52.78	1.46	33.17	374.25	5.37	64.92	52.29	1.52	35.03	5.39

Appendix 3: – Brominated fines study images

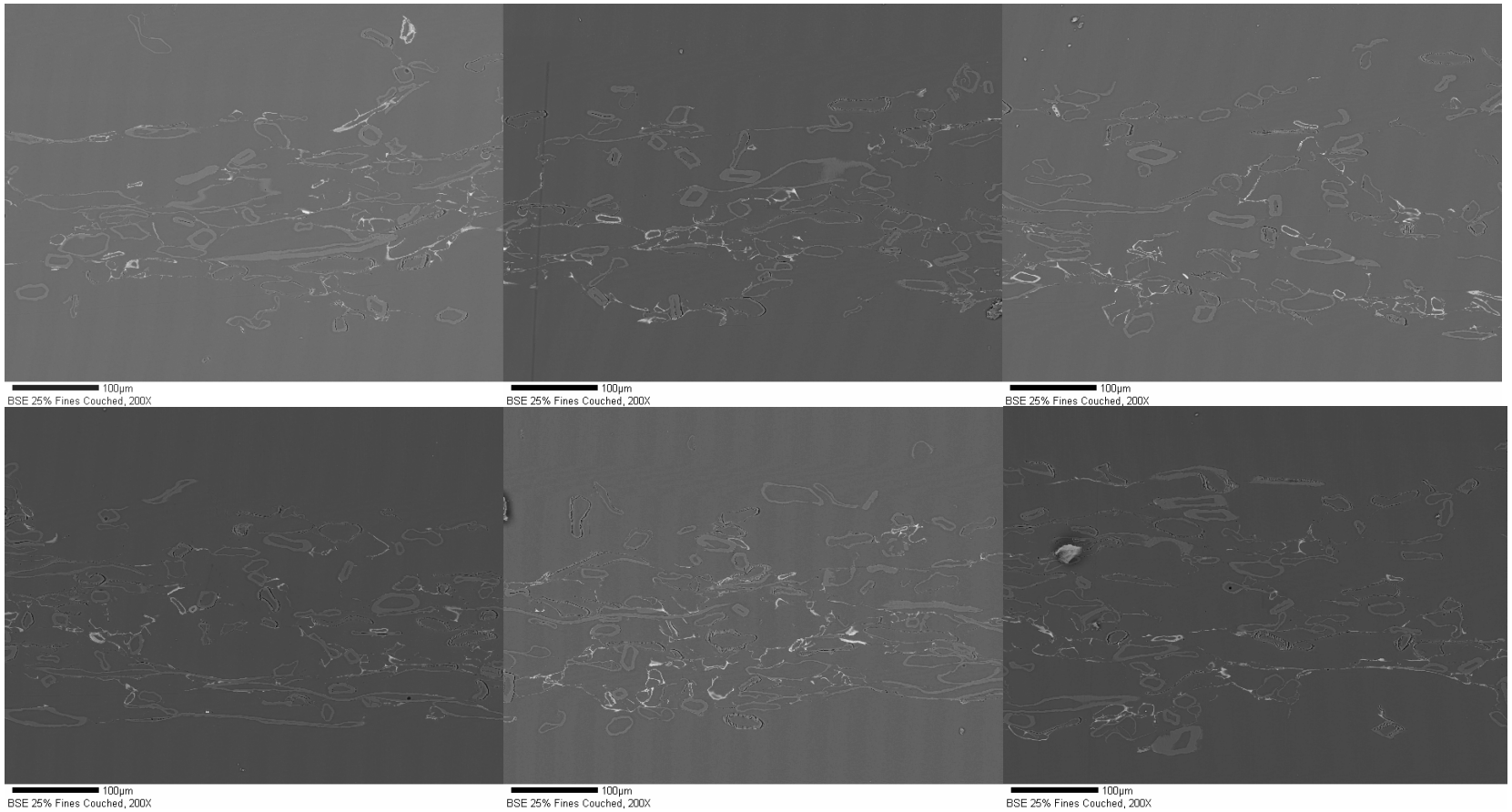

12.1% P200 fines in R48 sheet, couched (200X)

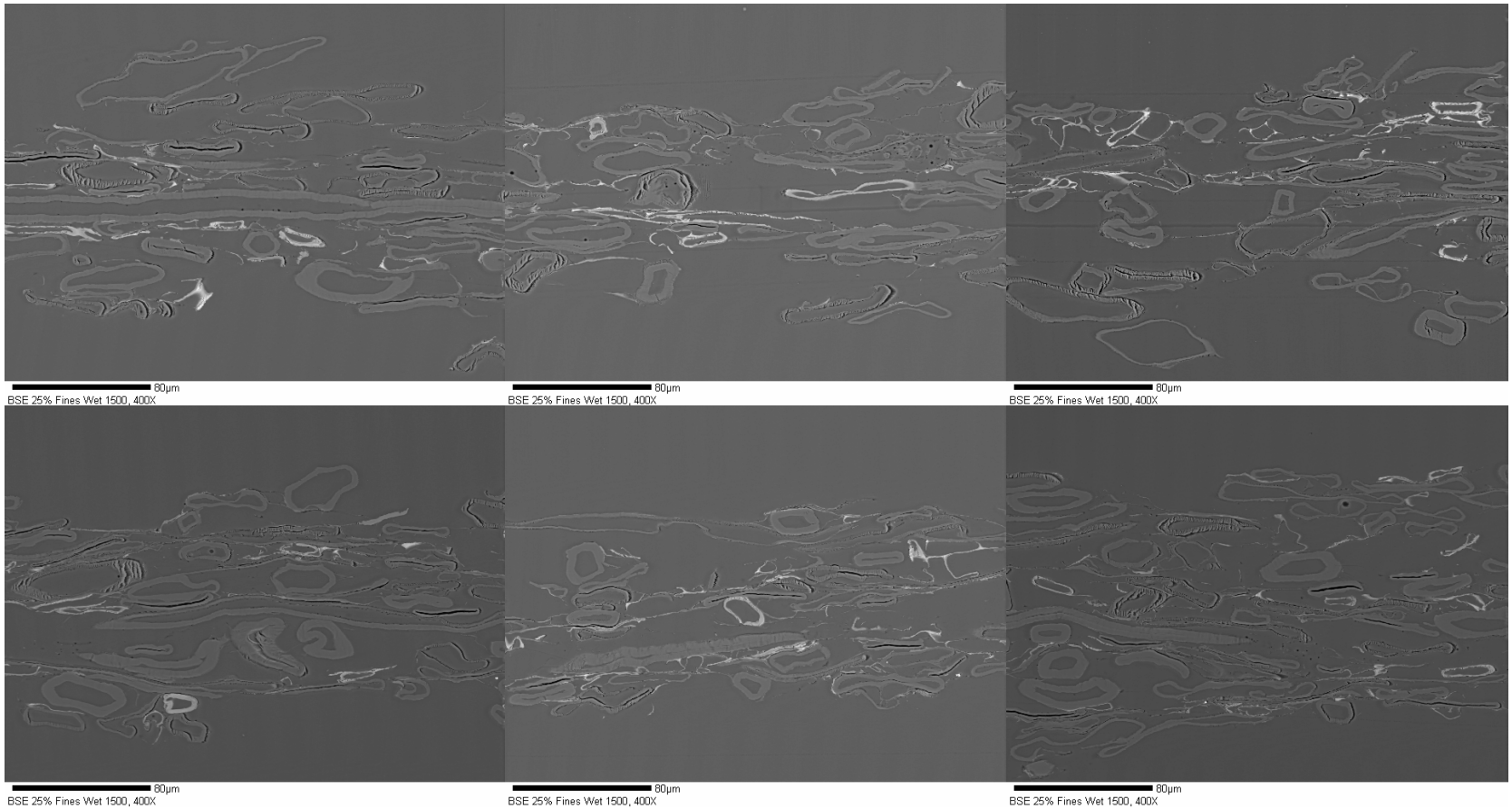

12.1% P200 fines in R48 sheet, wet pressed at 65 psi (400X)

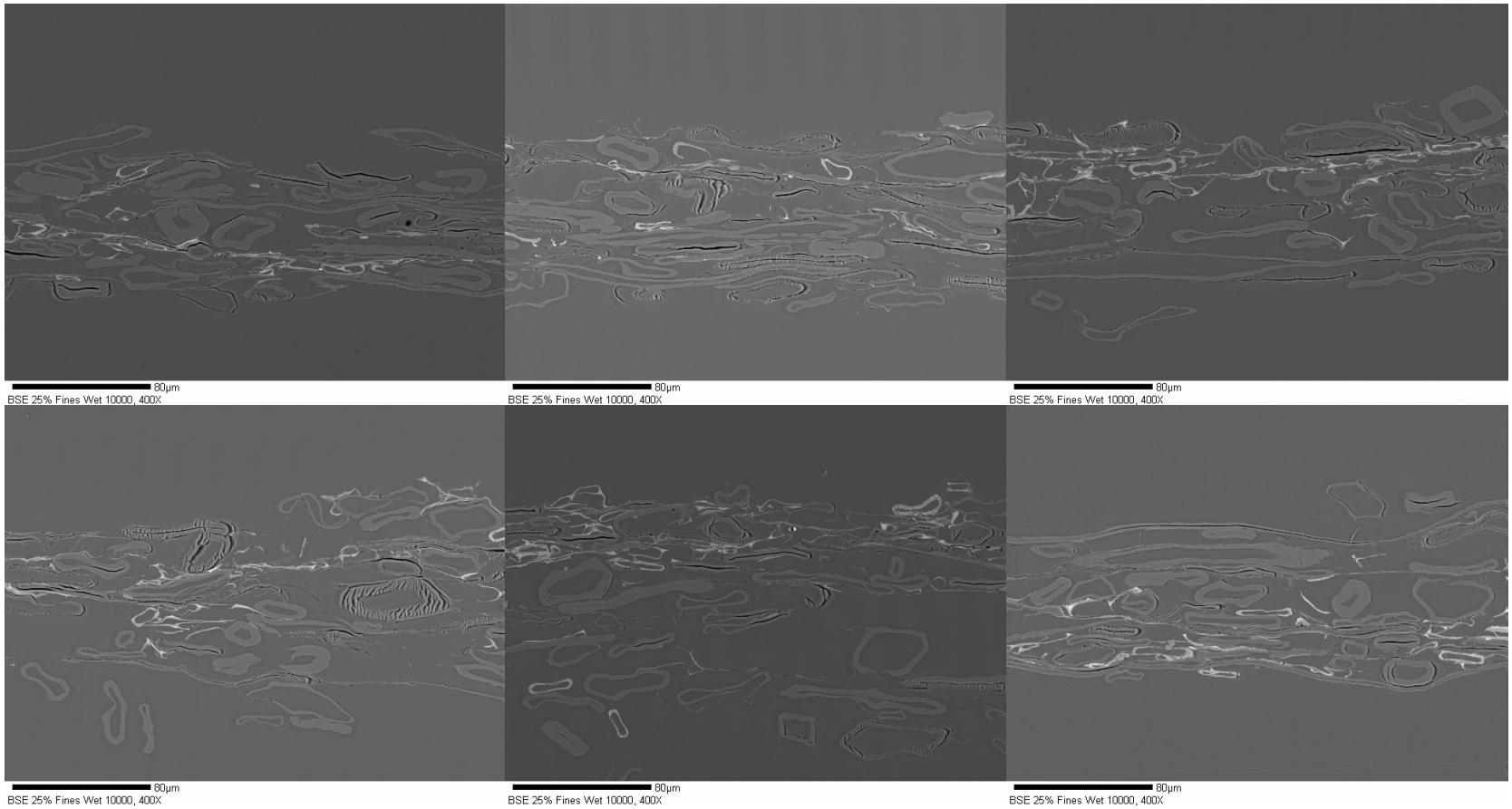

12.1% P200 fines in R48 sheet, wet pressed at 340 psi (400X)

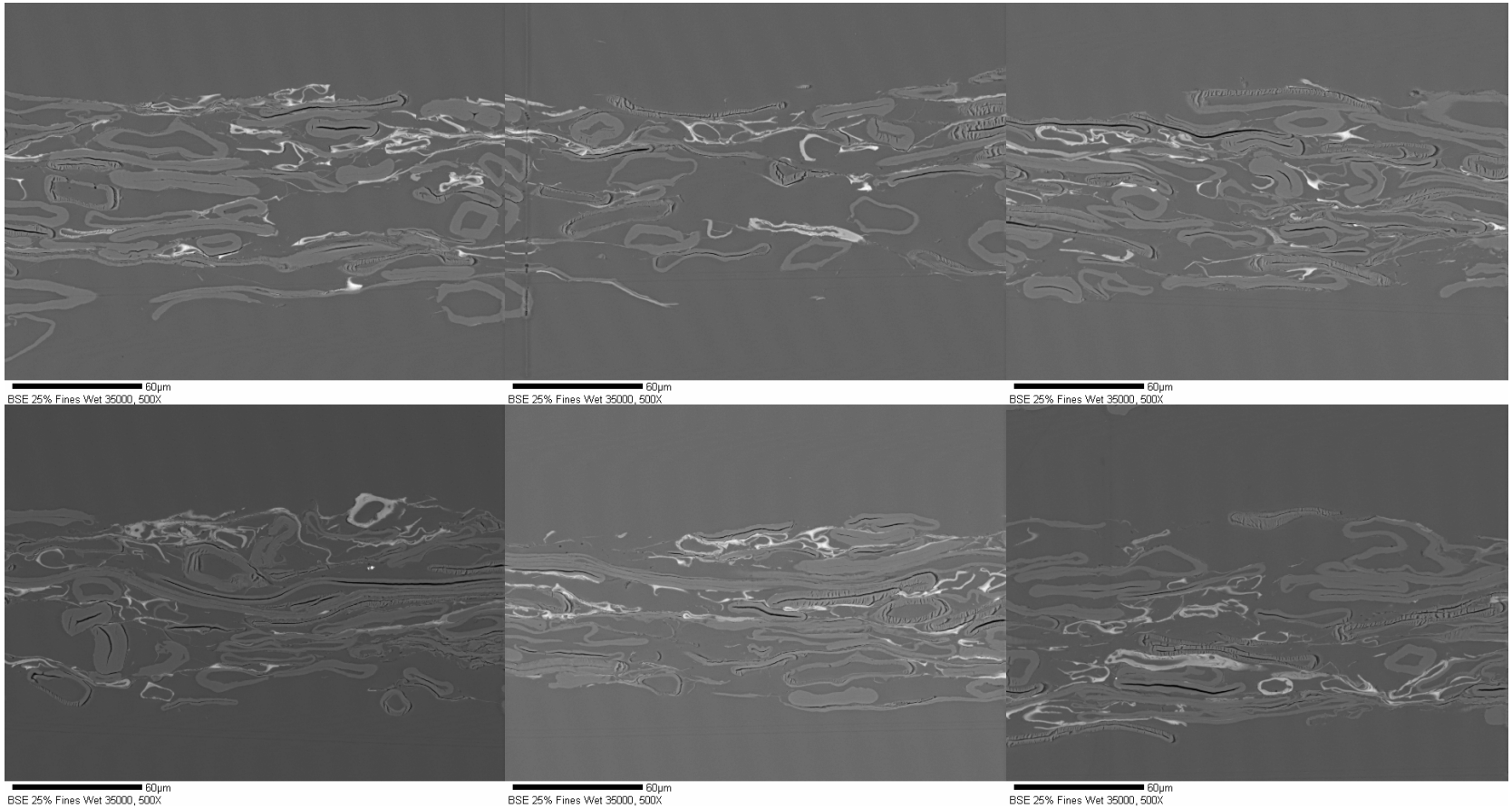

12.1% P200 fines in R48 sheet, wet pressed at 1190 psi (500X)

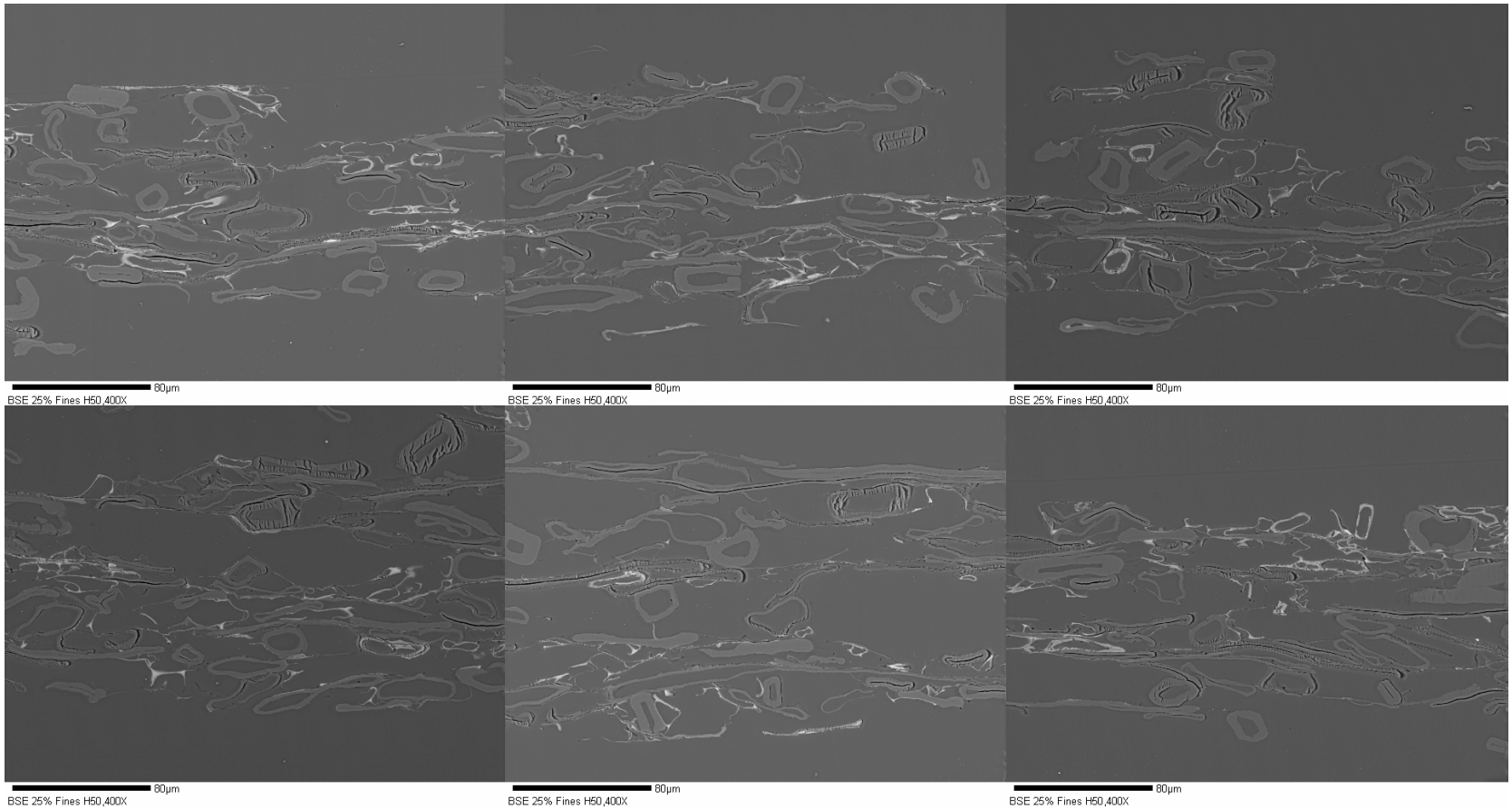

12.1% P200 fines in R48 sheet, Press dried at 120 °C and 1.7 psi (400X)

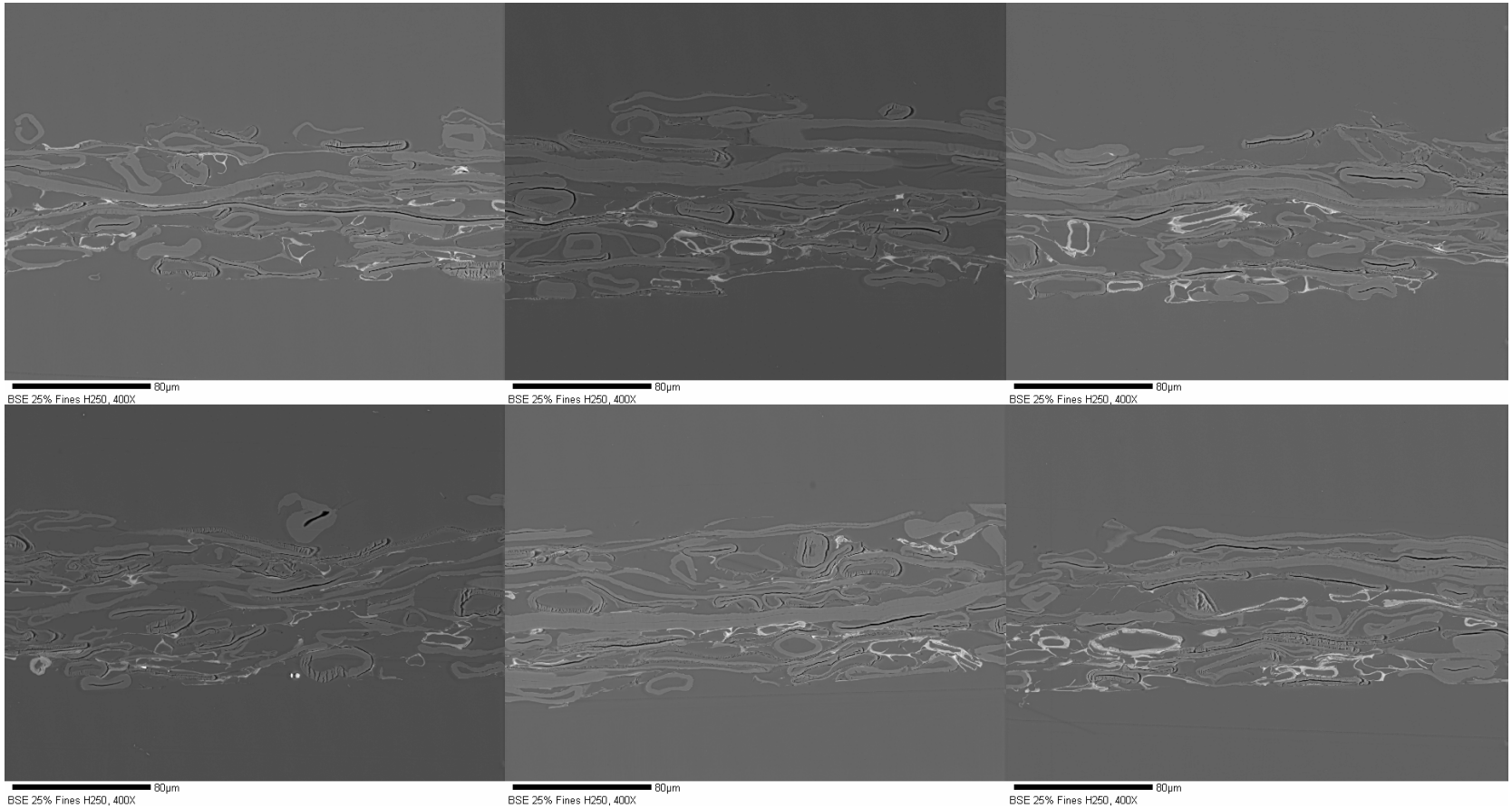

12.1% P200 fines in R48 sheet, Press dried at 120 °C and 8.6 psi (400X)

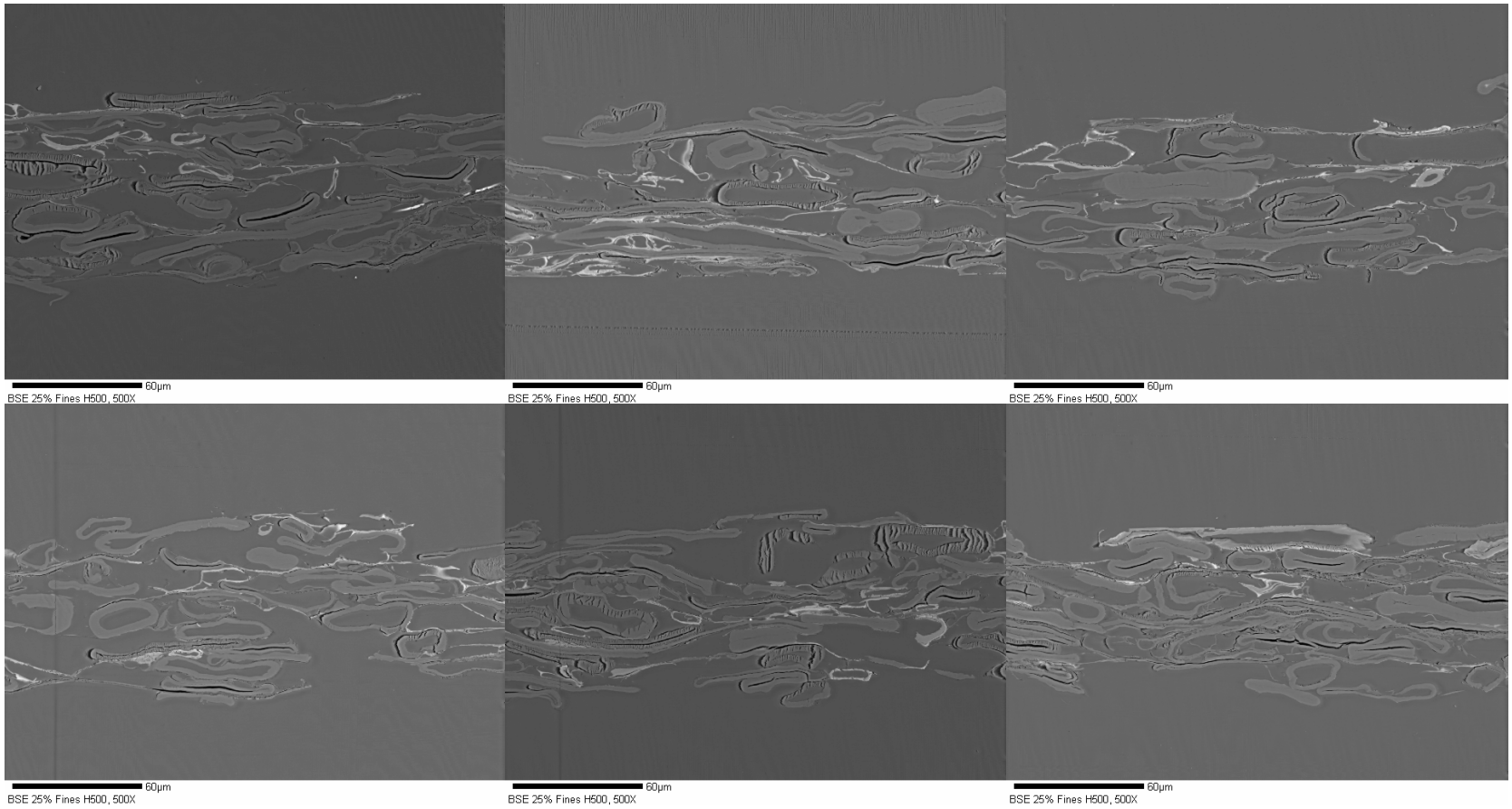

12.1% P200 fines in R48 sheet, Press dried at 120 °C and 16.9 psi (500X)

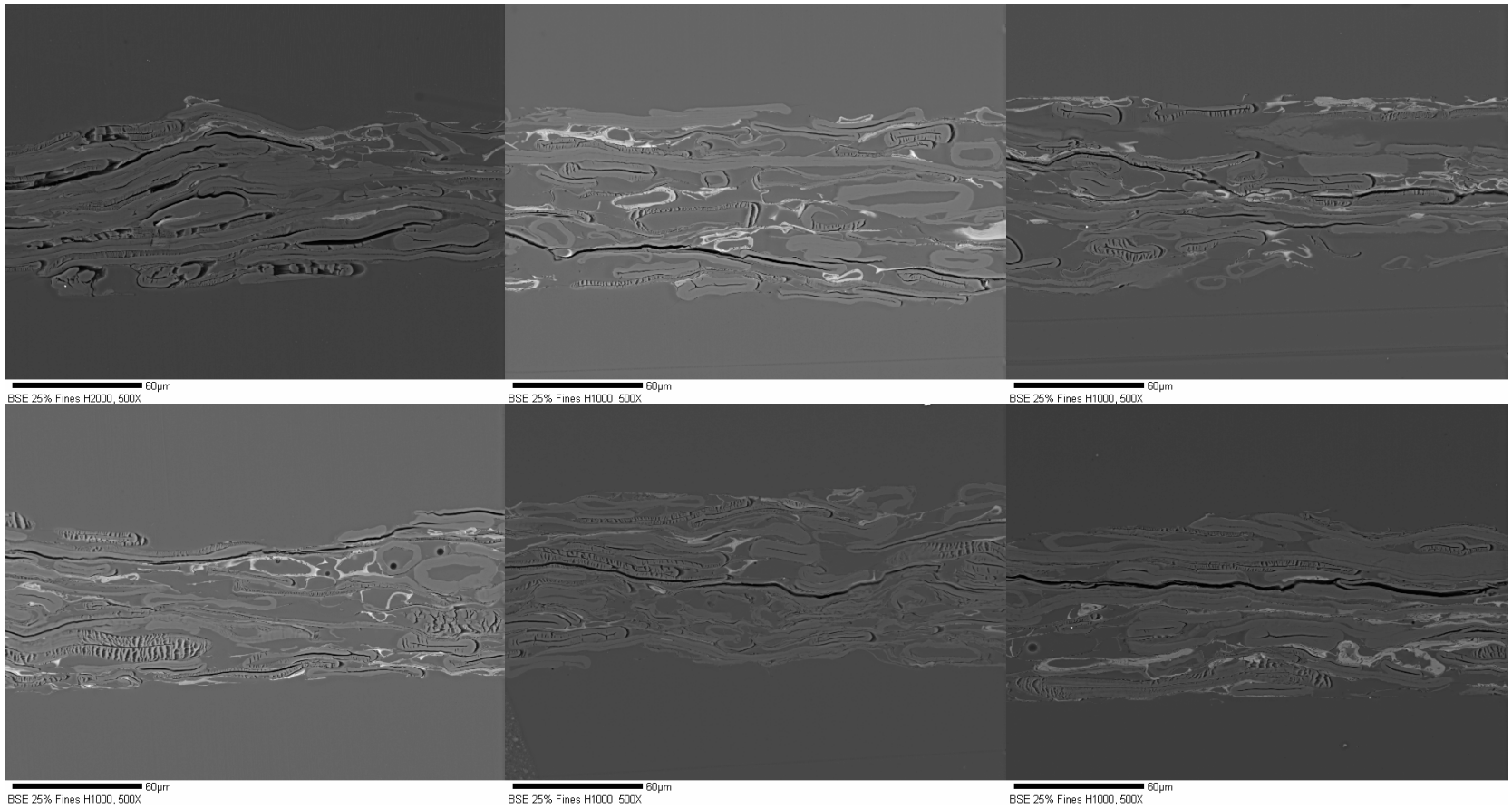

12.1% P200 fines in R48 sheet, Press dried at 120 °C and 34 psi (500X)

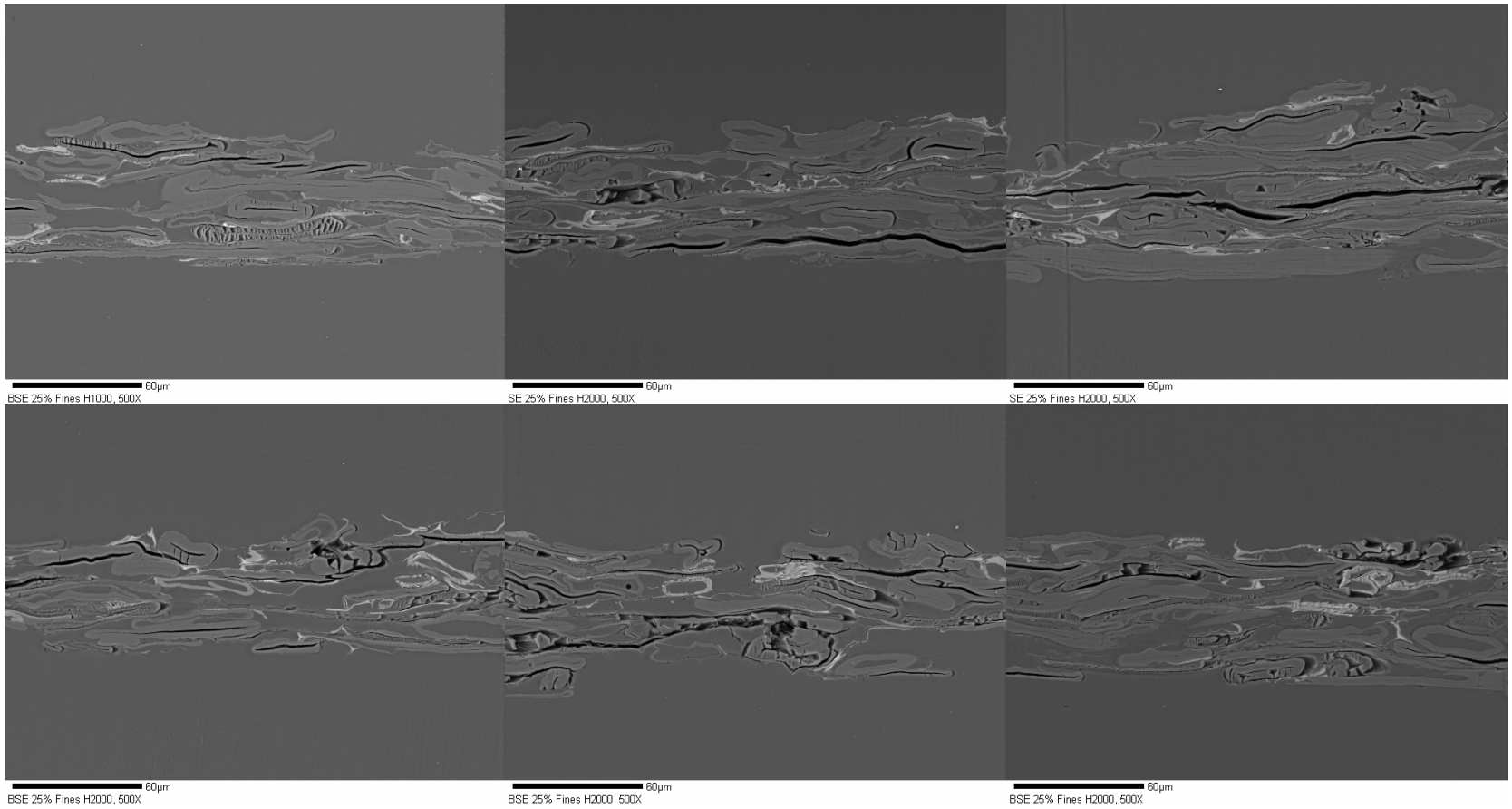

12.1% P200 fines in R48 sheet, Press dried at 120 °C and 68 psi (500X)

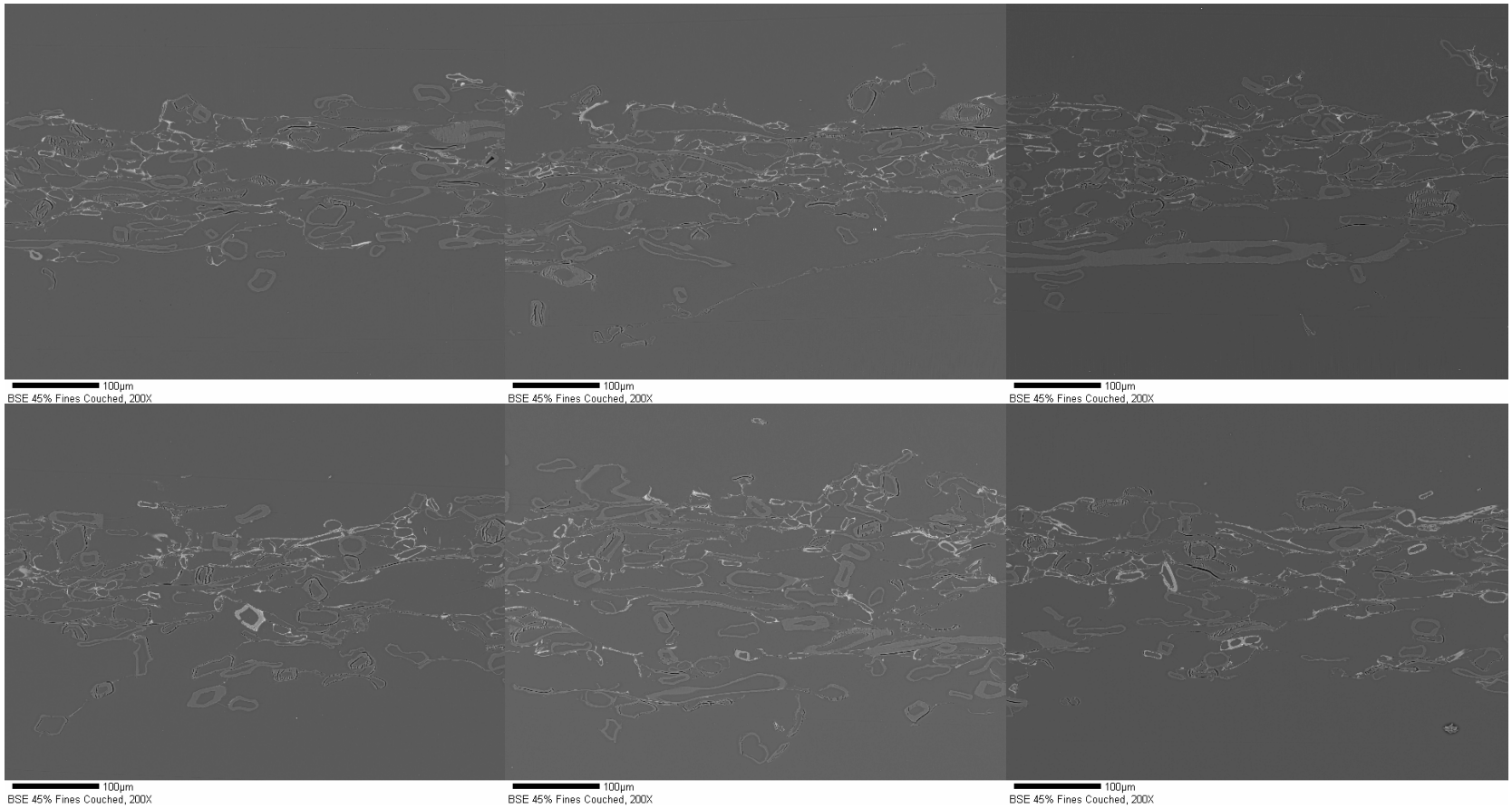

28.6% P200 fines in R48 sheet, couched (200X)

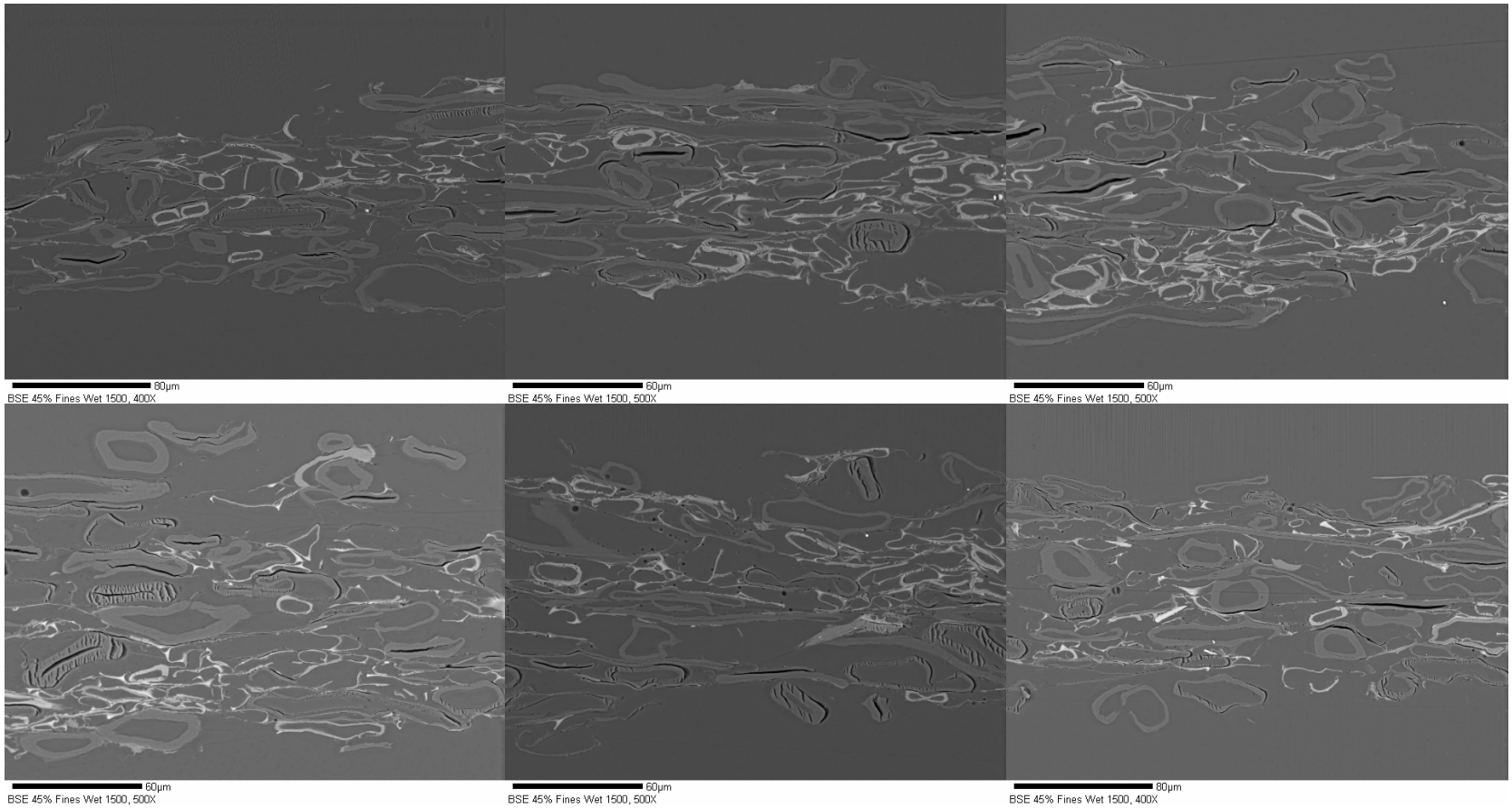

28.6% P200 fines in R48 sheet, wet pressed 65 psi (400X)

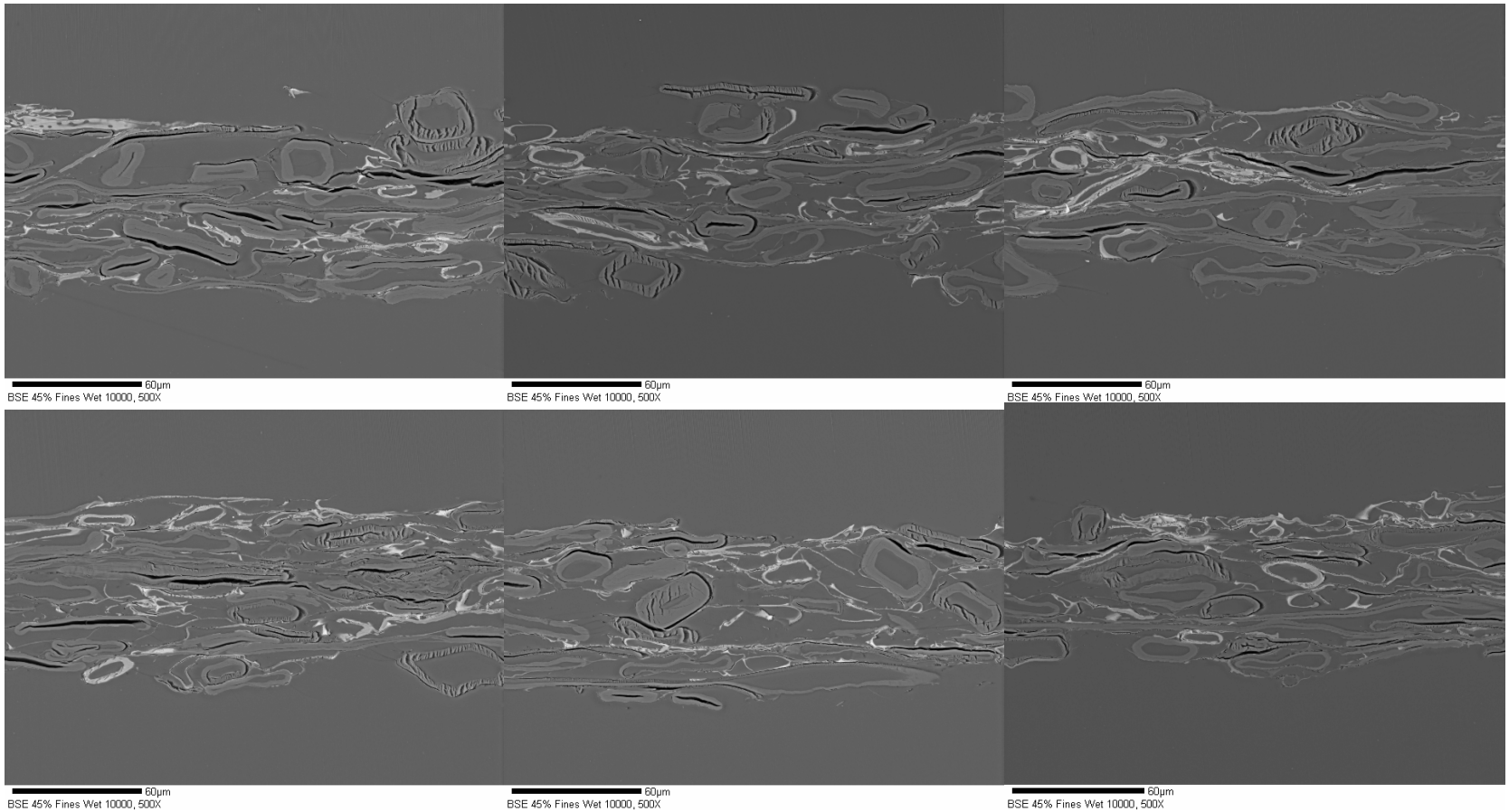

28.6% P200 fines in R48 sheet, wet pressed 340 psi (500X)

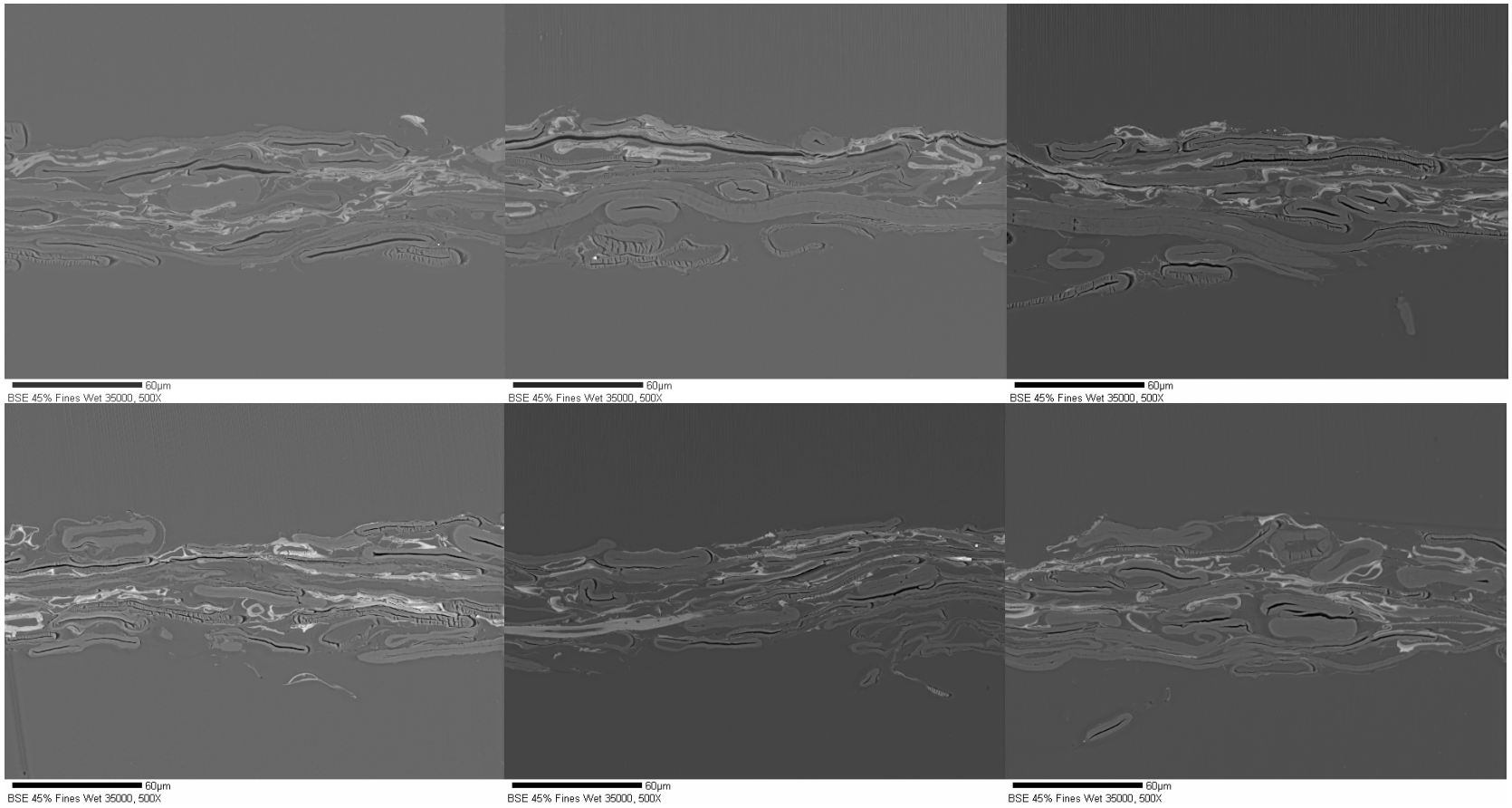

28.6% P200 fines in R48 sheet, wet pressed 1180 psi (400X)

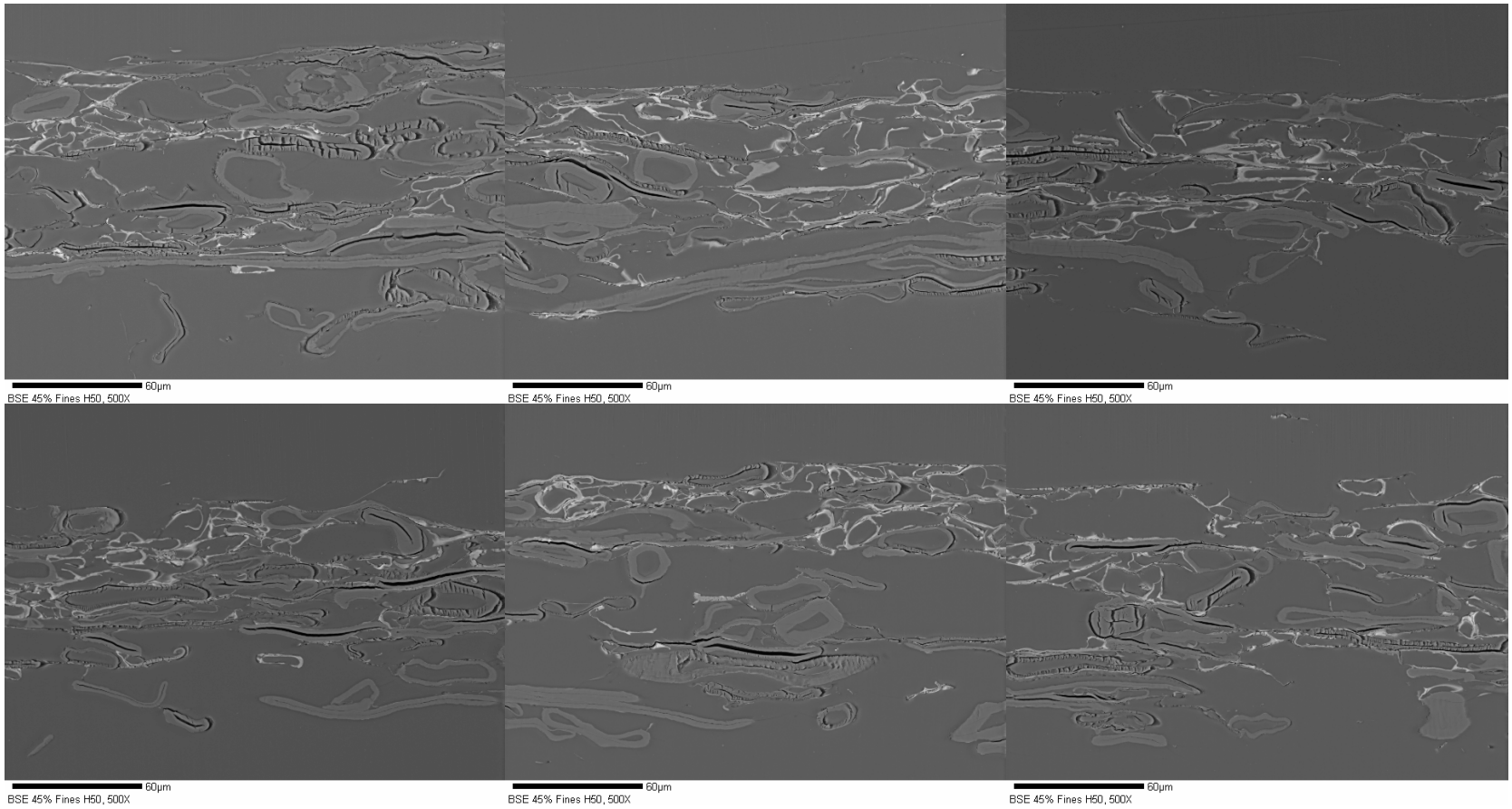

28.6% P200 fines in R48 sheet, press dried 1.7 psi (500X)

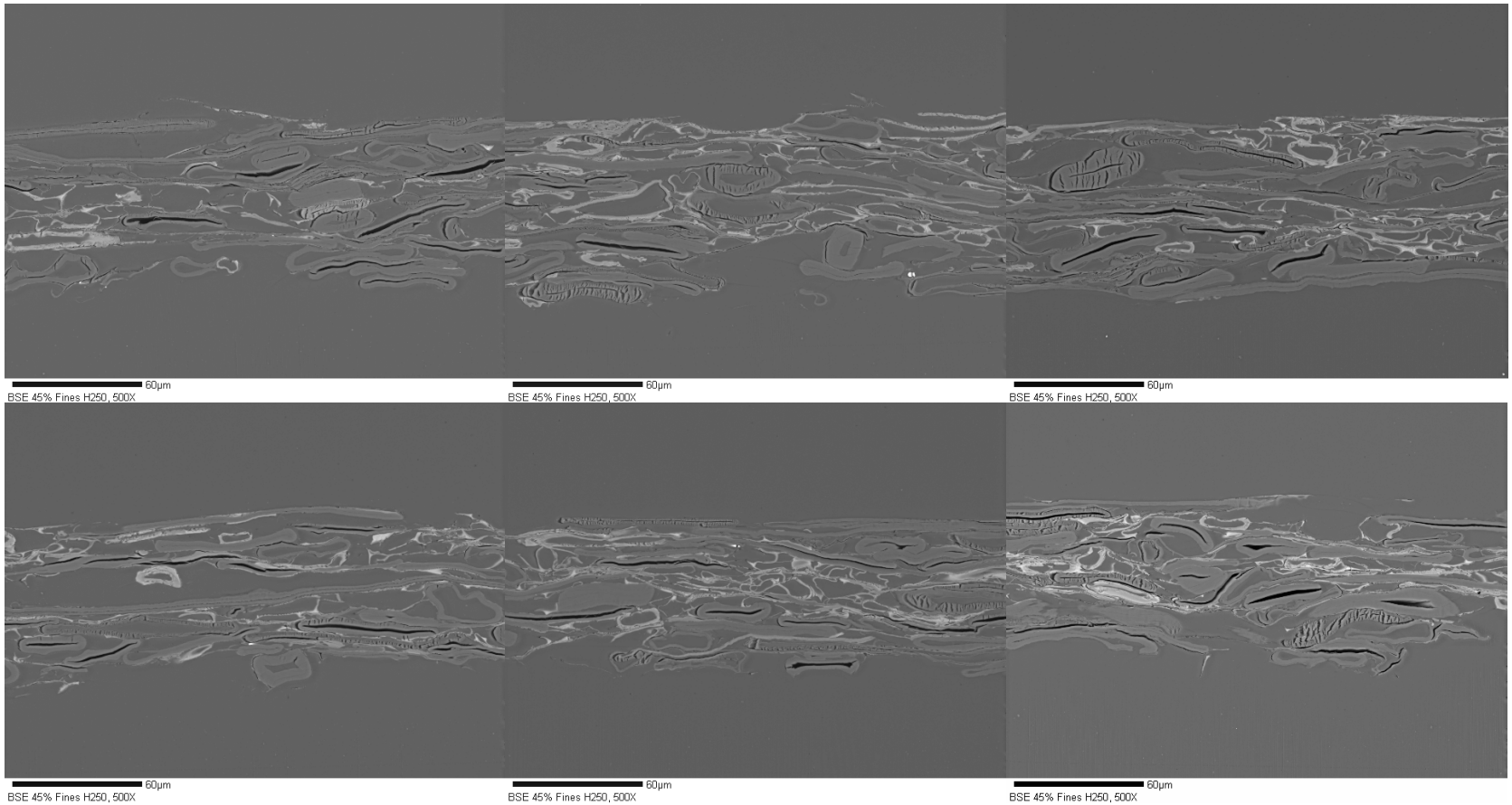

28.6% P200 fines in R48 sheet, press dried 8.5 psi (500X)

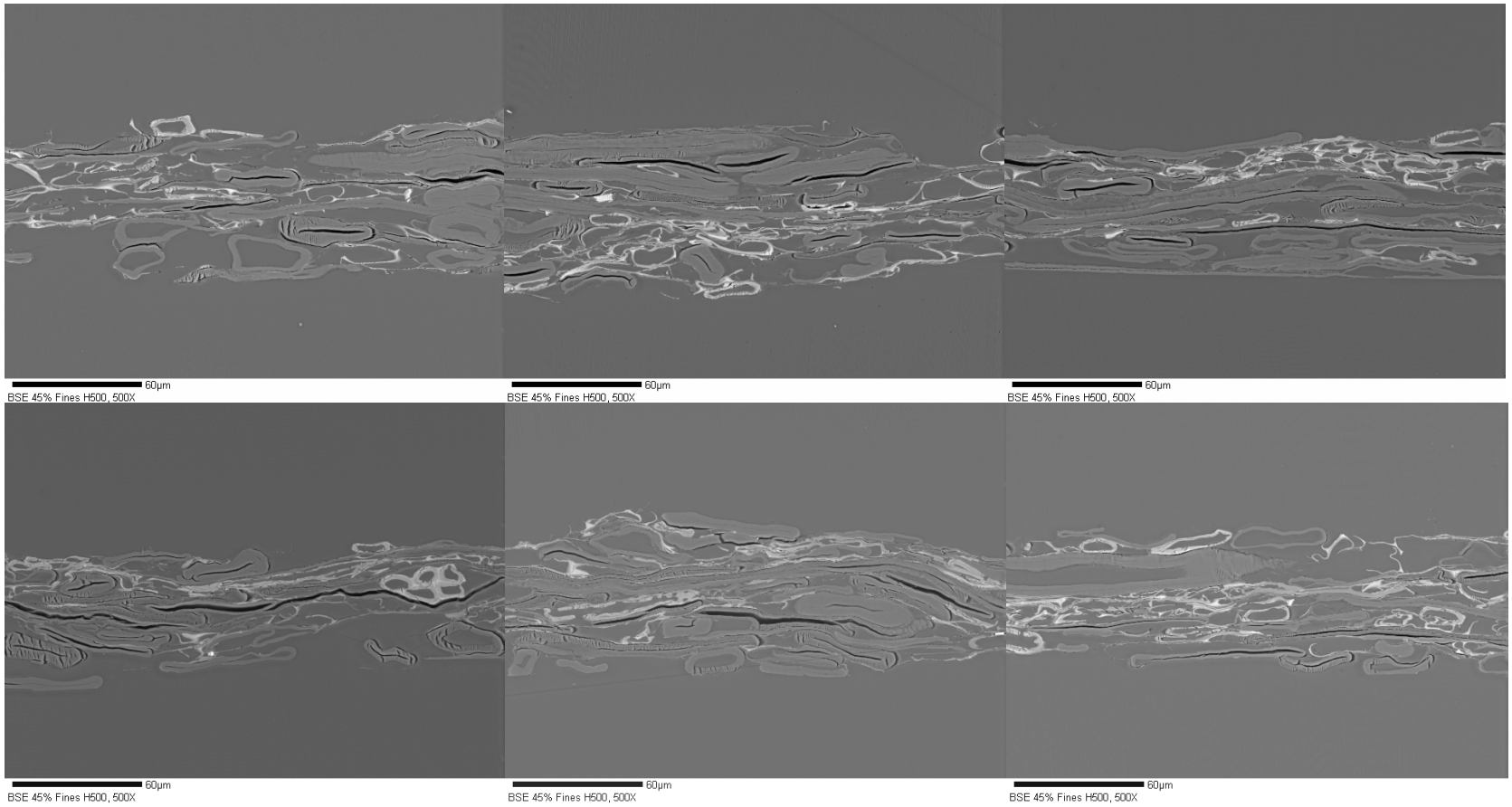

28.6% P200 fines in R48 sheet, press dried 16.9 psi (400X)

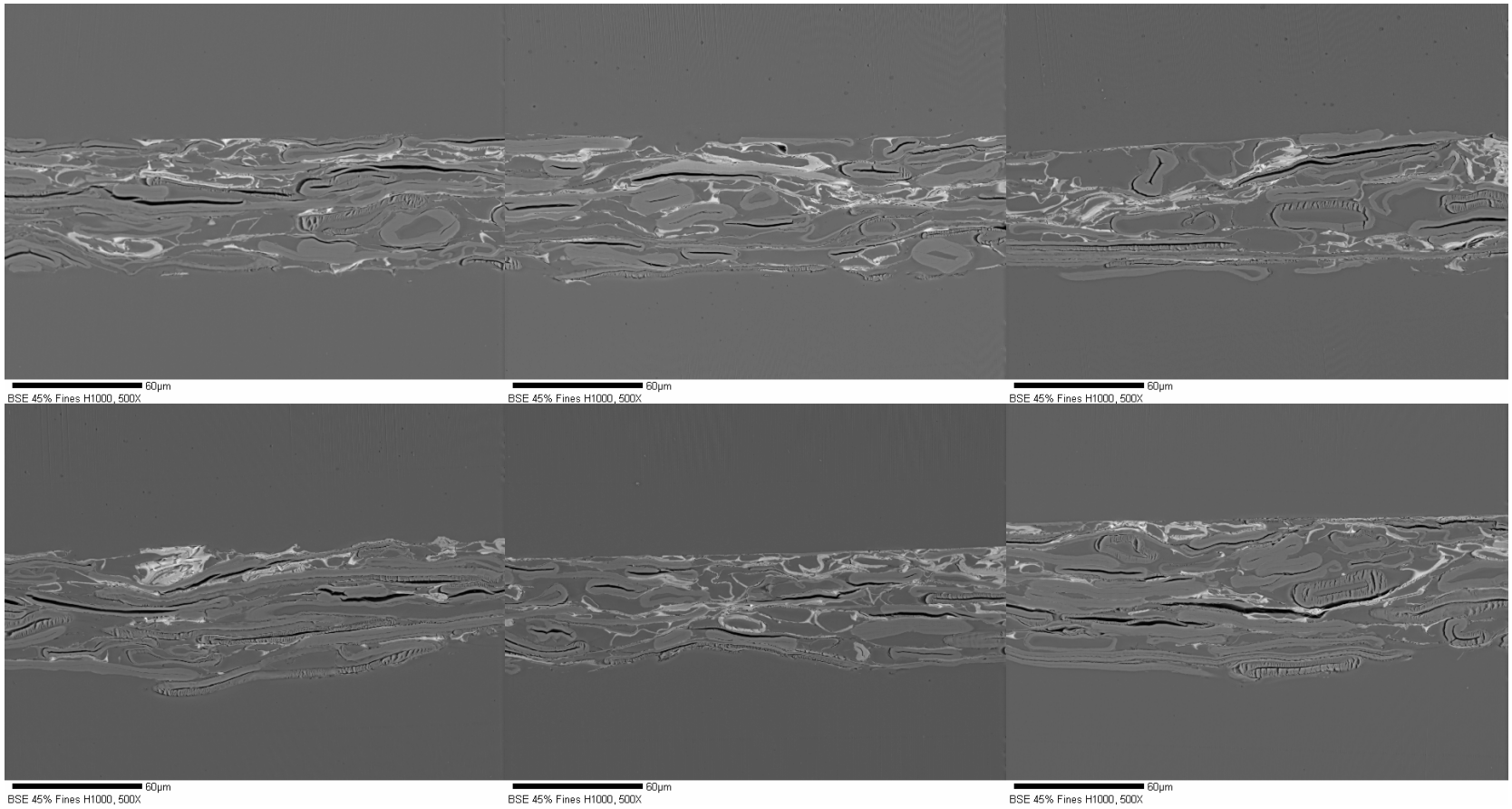

28.6% P200 fines in R48 sheet, press dried 34 psi (400X)

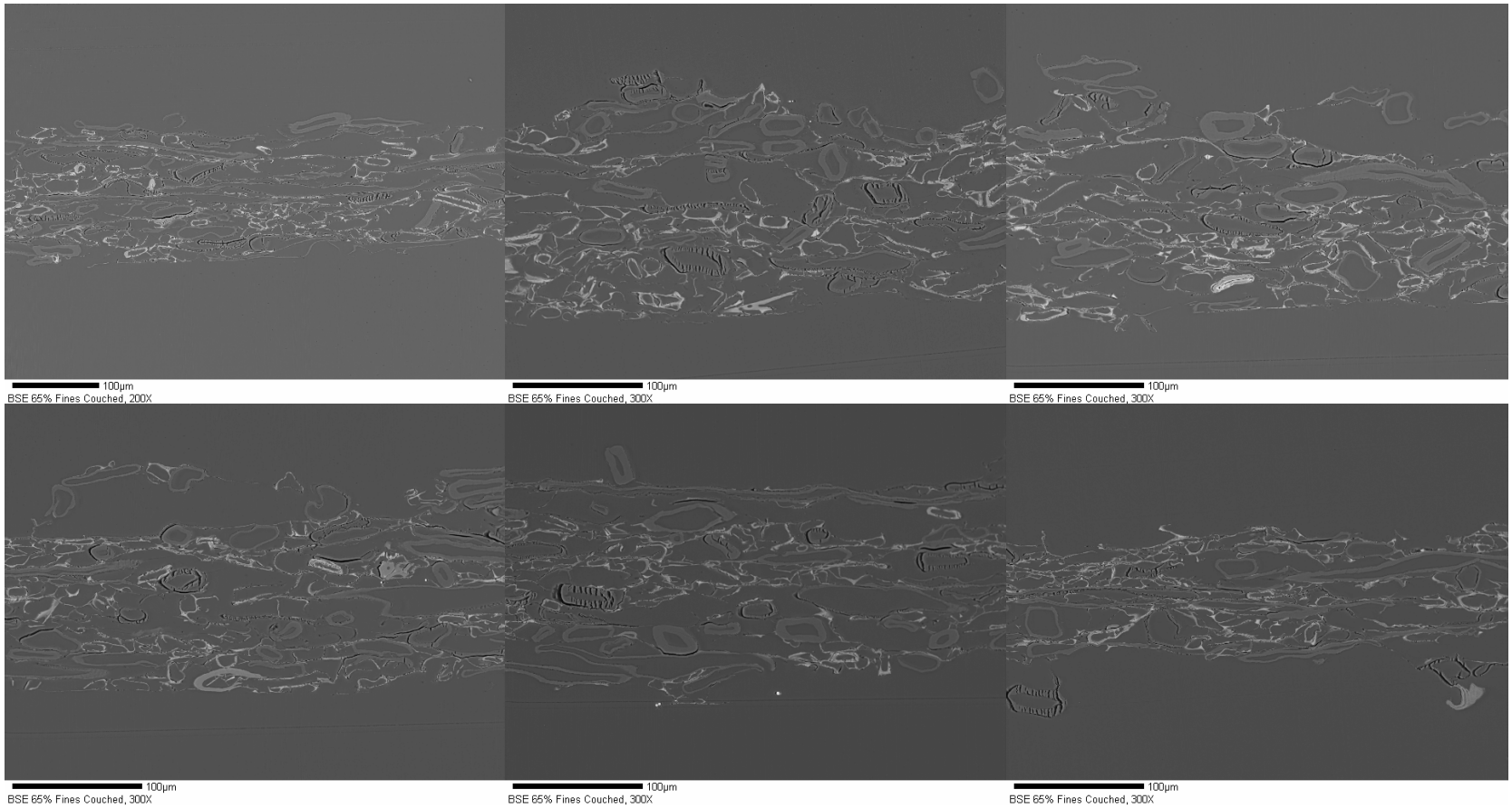

45.4% P200 fines in R48 sheet, couched (200X and 300X)

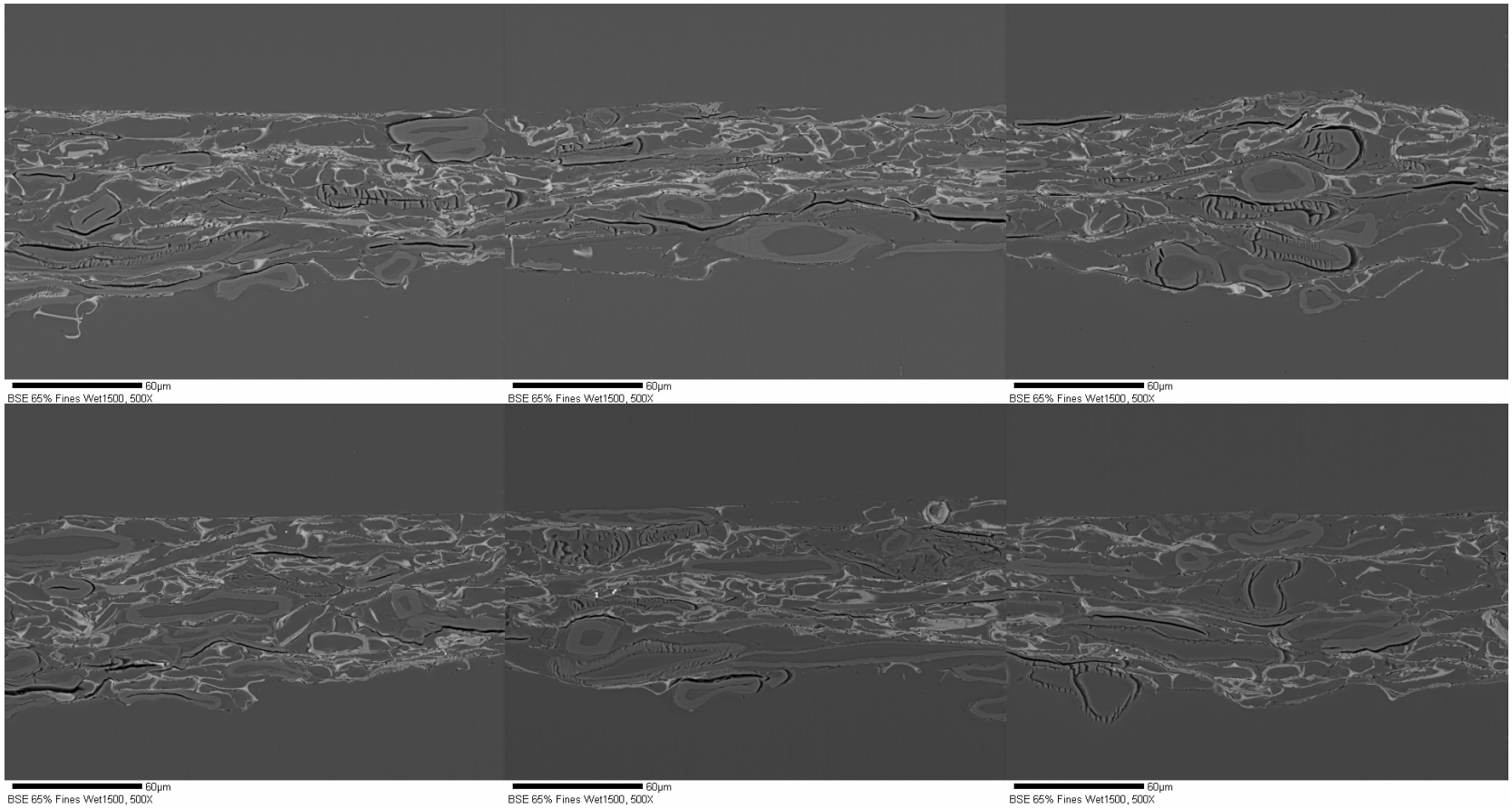

45.4% P200 fines in R48 sheet, wet pressed 65 psi (500X)

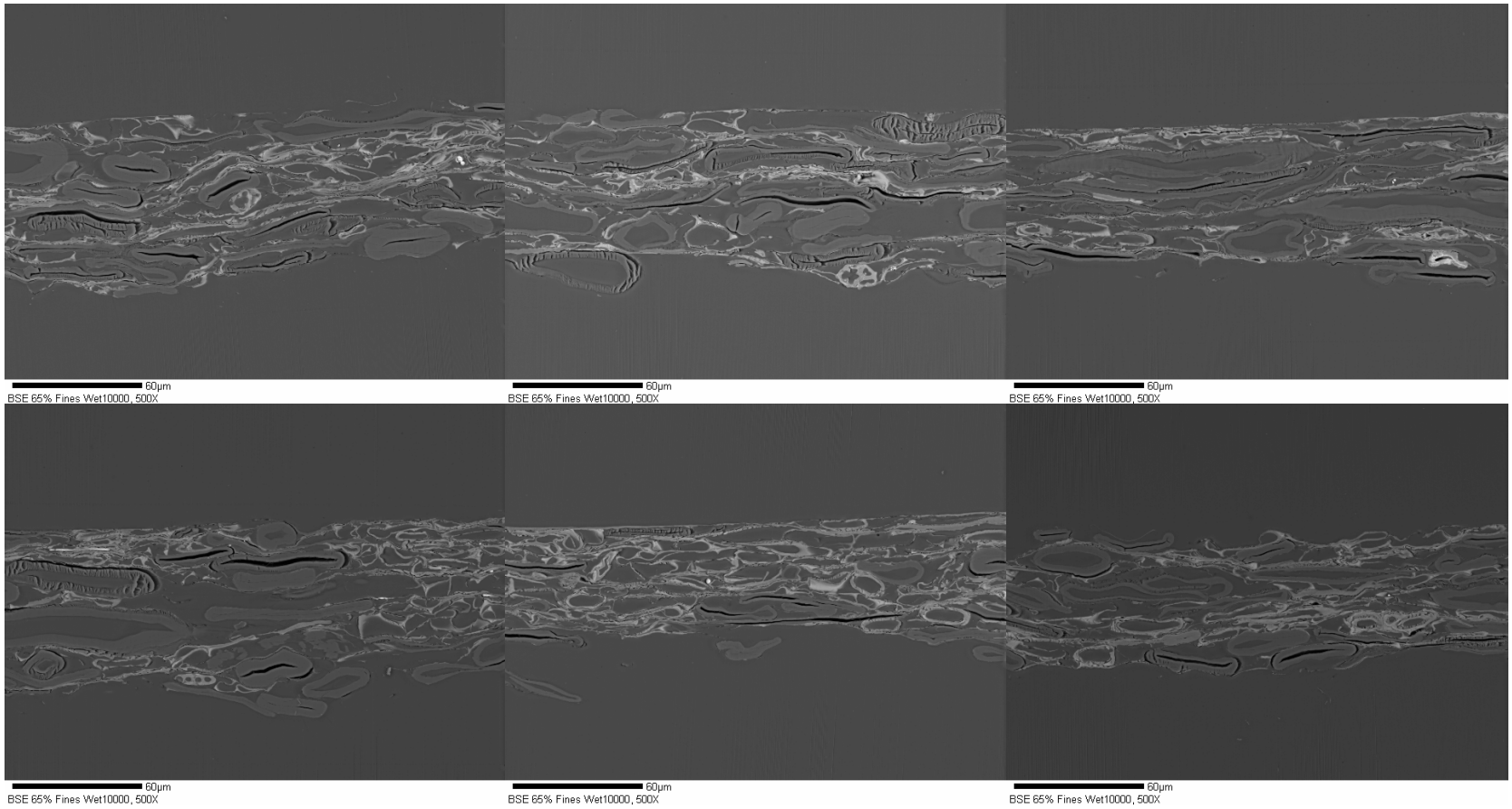

45.4% P200 fines in R48 sheet, wet pressed 340 psi (500X)

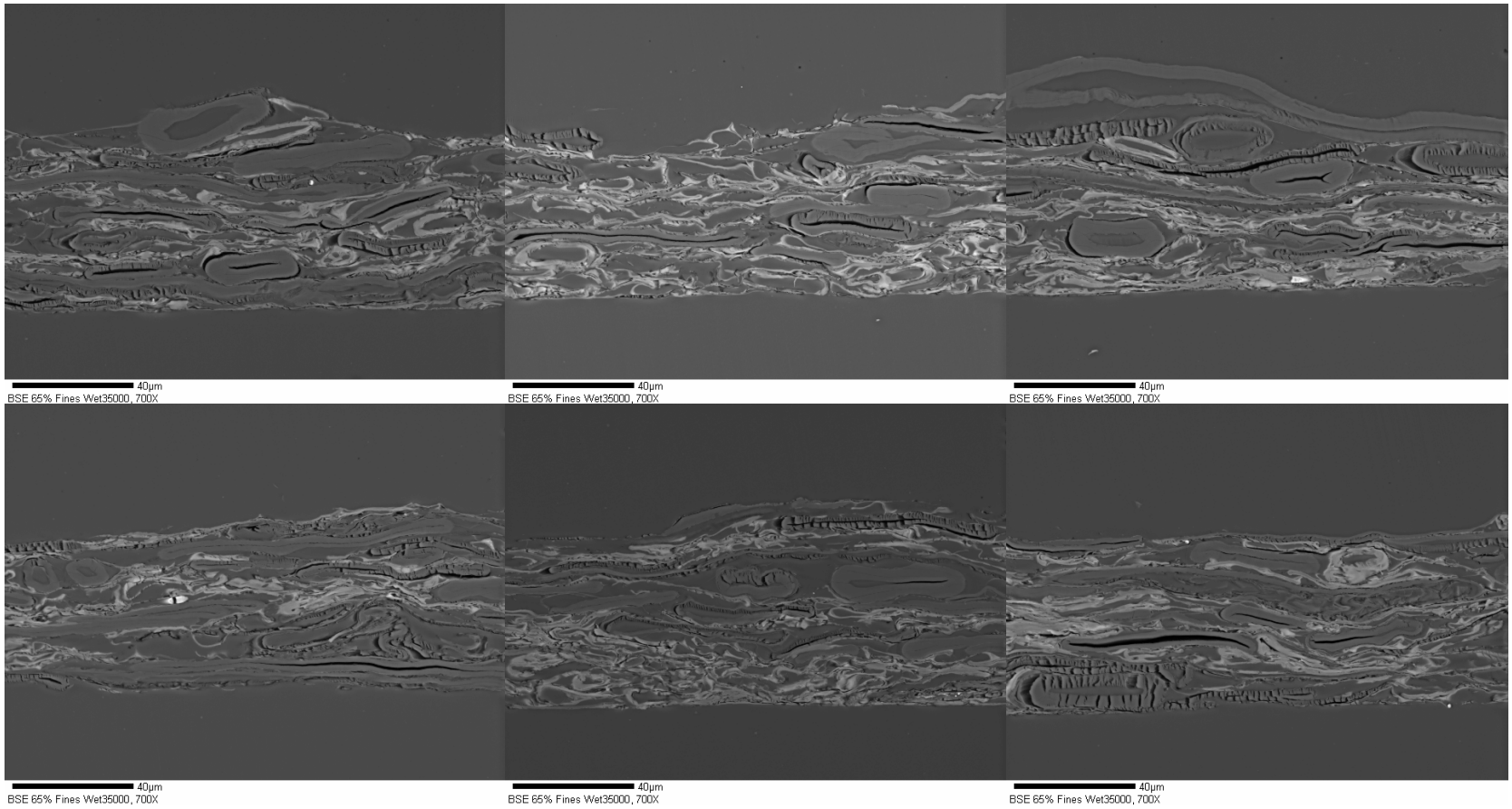

45.4% P200 fines in R48 sheet, wet pressed 1180 psi (700X)

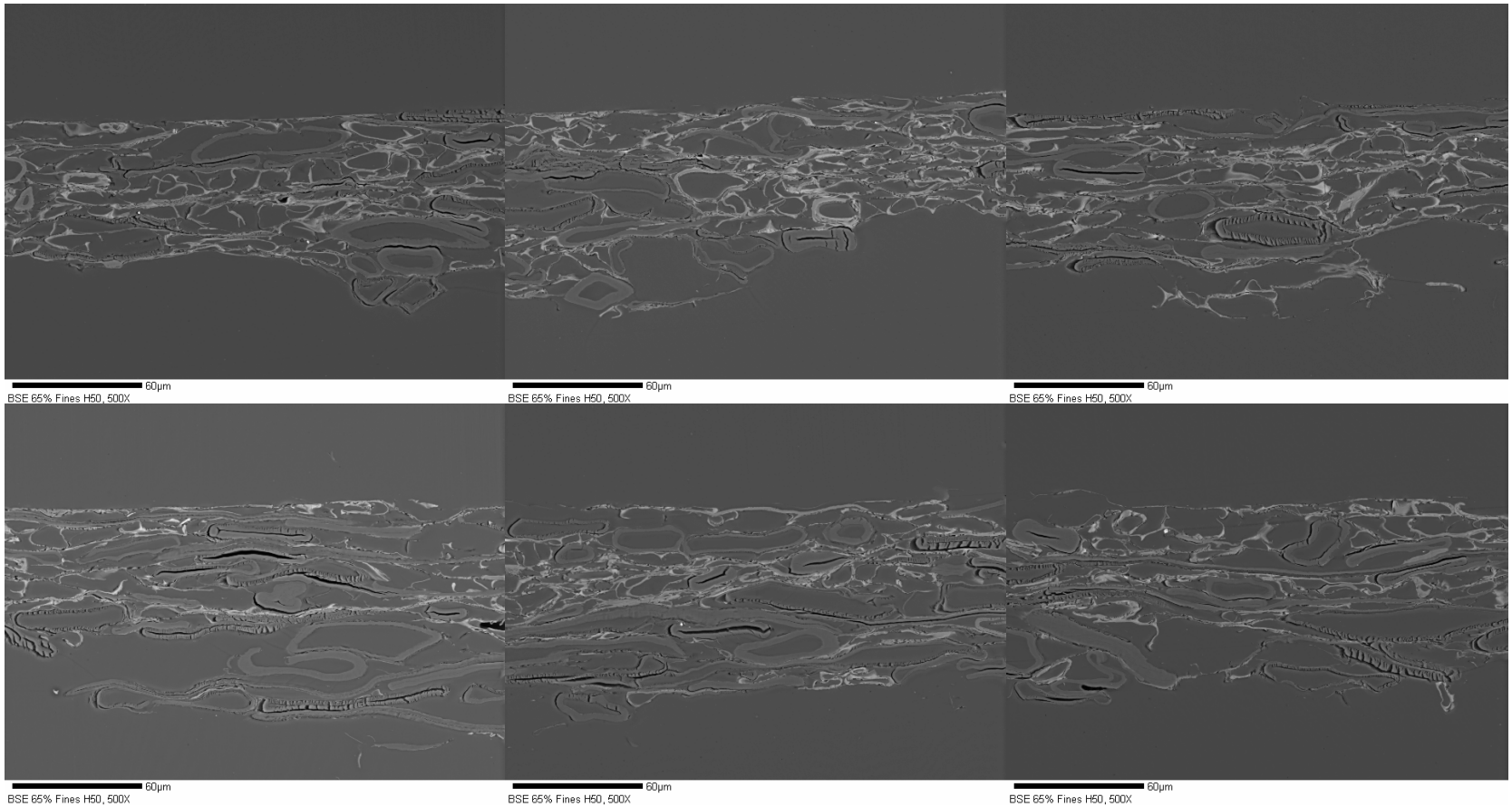

45.4% P200 fines in R48 sheet, press dried 1.7 psi (500X)

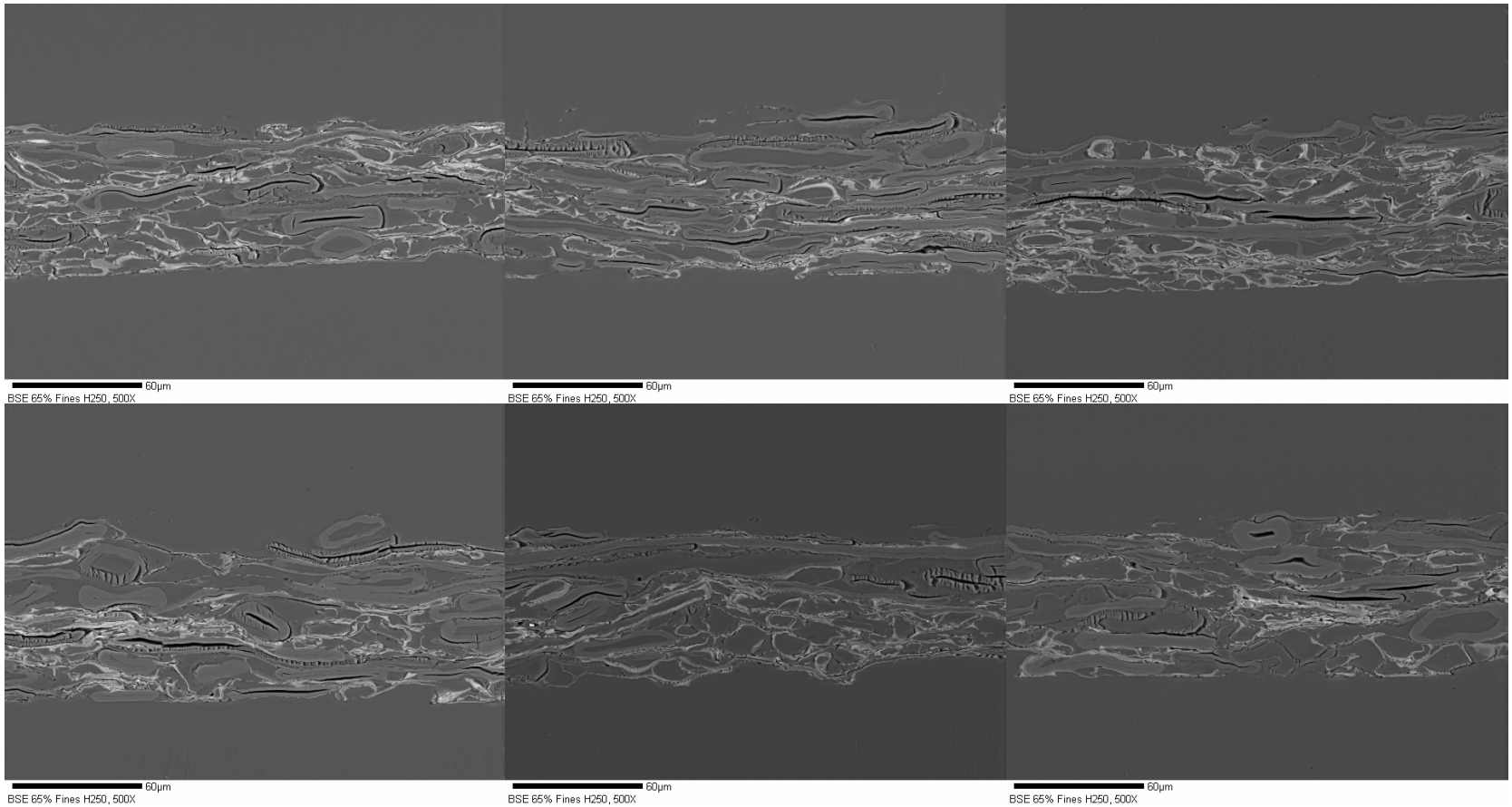

45.4% P200 fines in R48 sheet, press dried 8.5 psi (500X)

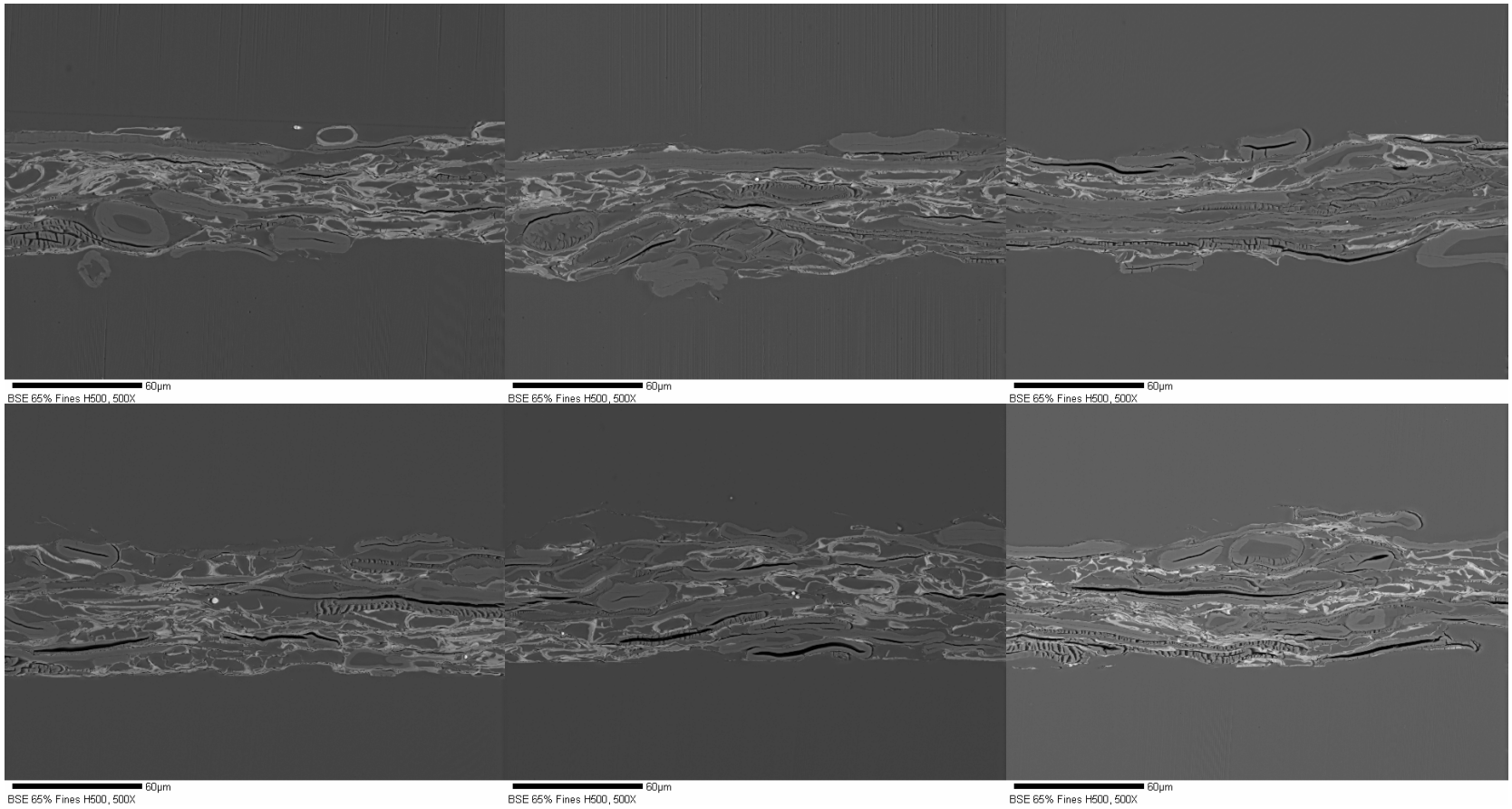

45.4% P200 fines in R48 sheet, press dried 16.9 psi (500X)

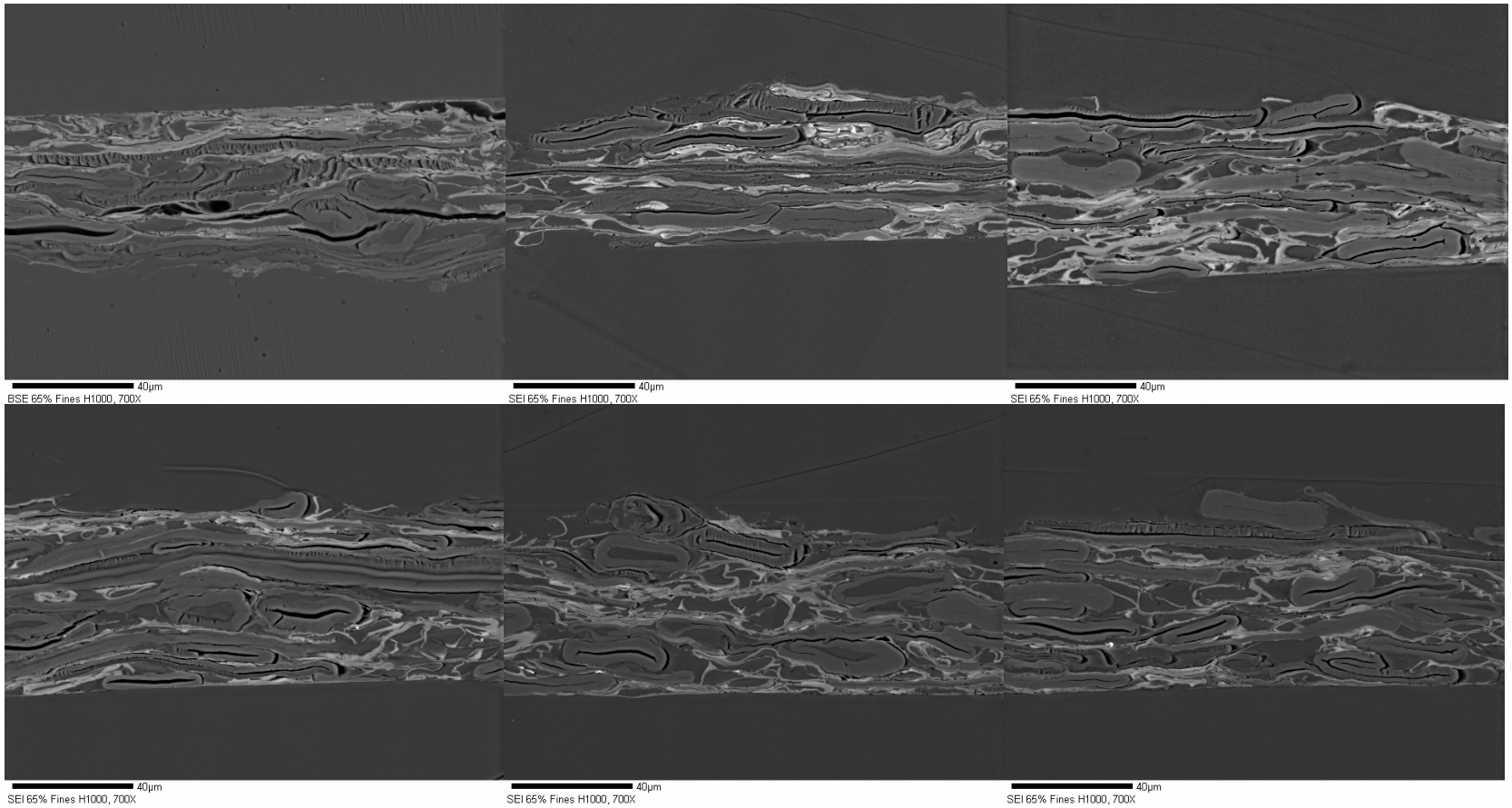

45.4% P200 fines in R48 sheet, press dried 34 psi (700X)

Physical properties of mixed sheets with brominated fines (P200)

Fines %	Pressing force, psi	Basis weight, g/m^2	Caliper mm	Density g/cc	Scattering coeff. m^2/kg	Absorption coeff. m^2/kg
13.06	0.0	64.34	0.3629	177.29	38.09	3.17
13.98	50.9	65.02	0.1691	384.52	36.87	3.60
12.85	339.4	64.18	0.1424	450.71	35.71	3.75
12.56	1187.9	63.97	0.1018	628.39	26.86	3.28
12.89	1.7	63.86	0.1503	424.92	27.39	4.71
10.00	8.5	61.81	0.1117	553.39	27.70	5.39
11.14	17.0	62.60	0.0886	706.57	24.66	5.27
10.38	33.9	62.08	0.0749	828.79	23.46	4.77
12.10	67.9	63.29	0.0713	887.60	19.33	3.76
28.14	0.0	61.60	0.2628	234.41	43.34	4.17
28.01	50.9	61.50	0.1315	467.66	34.85	4.21
28.56	339.4	61.97	0.0934	663.50	31.86	4.31
28.80	1187.9	62.18	0.0797	780.19	21.95	3.87
30.62	1.7	63.39	0.1194	530.92	26.93	5.89
31.92	8.5	64.60	0.0894	722.61	25.68	8.00
26.27	17.0	59.66	0.0749	796.48	23.46	5.62
26.60	33.9	59.92	0.0614	975.89	17.33	4.65
44.10	0.0	59.39	0.1813	327.60	41.84	6.70
44.54	50.9	59.87	0.1036	577.86	40.62	6.54
44.78	339.4	60.13	0.0744	808.20	30.02	5.53
46.06	1187.9	61.55	0.0678	907.82	27.91	5.82
45.51	1.7	60.60	0.0922	657.30	30.43	8.42
46.07	8.5	61.23	0.0759	806.78	29.12	7.87
45.46	17.0	60.55	0.0680	890.45	25.61	8.07
46.30	33.9	61.50	0.0604	1018.17	19.98	7.12